# Towards
# Novel Polymeric Contrast Agents
# for
# Magnetic Resonance Imaging

Thesis submitted in part fulfilment of the degree of
Doctor of Philosophy
by

**Jonathan Martinelli**

*Supervisors*:
Dr. Joachim H. G. Steinke
Dr. Ramon Vilar
Dr. Patrizia Ferretti

Department of Chemistry, Imperial College London
September 2008

## Declaration of Authorship

The work described in this thesis is entirely my own, unless otherwise acknowledged.

*Jonathan Martinelli*

## Abstract

This project centres on the exploration of novel contrast agents for Magnetic Resonance Imaging, with improved performances to signal specific objects in high-resolved images of the human body for medical and diagnostic purposes, and in particular for labelling and tracking stem cells after transplantation. The target agents are based on polymeric molecular architectures containing several MRI probes, thus being able to solve the sensitivity problems commonly known to affect this technique. The molecular structure was also designed to prevent those factors known to affect and limit the performances of contrast agents previously reported in the literature.

Following a thorough literature research, complexes of gadolinium(III) were chosen, in particular with 1,4,7,10-tetraazacyclododecane-1,4,7,10-tetraacetic acid (DOTA) as macrocyclic ligand due to its known ability to form highly stable (i.e. non-toxic) complexes. Furthermore, this ligand opens up the possibility for its modification and functionalisation in order to obtain a final molecular structure with desired well-defined properties.

The synthetic strategy was then planned and carried out, leading first to compounds which represent intermediate structures needed for further development. Most of them are themselves new substances not reported before.

The corresponding gadolinium(III)-complexes of some intermediates were prepared and tested on cell cultures for an evaluation of their biocompatibility and performances as contrast agents.

The prepared monomers were then used in several attempts of polymerisation exploiting different principles and techniques (radical, metathesis, "click-chemistry"); when successful, such procedures led to products which were characterised by suitable analytical methods, and eventually tested as contrast agents for MRI in terms of their relaxation performances and biological safety.

*To my parents Nicla and Giulio*
*and my brother Massimiliano*

## Acknowledgements

I have first to thank my supervisors Dr. Joachim Steinke and Dr. Ramón Vilar (Department of Chemistry, Imperial College London), and Dr. Patrizia Ferretti (Developmental Biology Unit, Institute of Child Health, University College London) for giving me the opportunity to work on such an interesting, challenging and multidisciplinary project. Joachim and Ramon chased me around the lab for 3 years, letting me develop and apply my own ideas under the fumehood but at the same time reminding me to focus-focus-focus during our meetings. Beside the chemistry aspect, I also want to thank Joachim for the great BBQs, cheese fondue parties and Christmas fire punch events that he organises so well. Patrizia gave me the chance to take some breaks from chemistry and introduced me to the different but still fascinating world of Cell Biology. Giving project update presentations to her group at ICH allowed me to see the whole project from a very different point of view.

The Marie Curie Host Fellowship for Early Stage Training in Chemical Biology at Imperial College London is gratefully acknowledged for funding this project.

I am thankful to Prof. David Gadian (Radiology and Physics Unit, Institute of Child Health, University College London) and Dr. Mark Lythgoe (Centre for Advanced Biomedical Imaging, University College London) for their interest in my project and the useful meetings.

A huge acknowledgement goes to Rachael Dobson (Developmental Biology Unit, Institute of Child Health, University College London) for her invaluable help with cell cultures and MRI scanning, as well as her patience, availability, advice, data-storing and company. I would like to express my gratitude also to Jack Wells (Radiology and Physics Unit, Institute of Child Health, University College London), who gave a big help with MRI data processing and has always been very kind and keen in trying to solve practical problems related to pulse sequences and coil sensitivity.

A big thank to Beeta Balali-Mood, Nazila Kamaly and Andrew Surman (Department of Chemistry, Imperial College London) for the enlightening exchanges of opinions about MRI contrast agents.

I am thankful to Peter Haycock (Cross-Faculty NMR Centre at Imperial College London) for his help and assistance with the NMR experiments. I would also like to thank Emilia Kot (Department of Chemical Engineering, Imperial College) for helping with the $H_2O$-GPCs, and Ms. Virginia Manch (Secretary to BBC Group, Department of

Chemistry, Imperial College London) for her great ability to efficiently overcome the inevitable bureaucratic issues.

If I managed to go through this wonderful but sometimes testing and stressing experience, I owe it mostly to the support, encouragement and company that many people constantly gave me. For sure I am going to miss mentioning someone, and I deeply apologise about that. In Italy I could always count on having great time especially with the Pokkò Band and the Bellaria Lovers Volleyball Team (past and present). And I would put my life at risk if I did not send a particular thank to Elisa (aka Filpa aka Snapurzia) for just everything. Surely the biggest hug is for my family, particularly my parents and my brother Bo to whom this thesis is dedicated. And of course my dog Kiske!

On the London-and-abroad front, my lab mates deserve a big thank for the time spent together in experimenting, commenting, complaining, gossiping, joking, etc.; among them Wayne, Chris, Michelle, Magda, Edu, Yi, Big Mike, Sally, Wei, and Shengzhong. The last three deserve a special acknowledgement for their big help with the submission of my thesis. I also had a lot of nice moments inside and outside the College thanks to Jeeason, Raymond, Gnigni, the IC Volleyball Team and especially Bieppe.

Finally, I need to reserve a special mention for five very special Friends of mine, in the chronological order of their appearance in my life:

Ilaria Anichini, who helped me to survive my first months in London and encouraged me to go on despite the big difficulties of being alone in a foreign city;

Dr. Natasha Shirshova, my constant post-doc, competent consultant about polymers and great companion during hot chocolate and cake breaks;

Dr. Christian Adelwöhrer, my "Austriac" mate with whom I shared so many experiences and had so much fun around London;

And finally Julio Jover and Ilias Pechlivanidis, who became much more than just the volleyball team-mates they were at the beginning. I simply cannot explain what a powerful force and bright light their Friendship has been and still is for me. It cannot be predicted where our respective walks of life will lead us, but with no doubt the memories of the time we spent together will remain fixed in my mind forever.

**Faith of the Heart**

*Written by* Diane Warren

*Originally performed by* Rod Stewart (1998, "Patch Adams")

*Reworked by* Russel Watson (2001, "Star Trek: Enterprise")

It's been a long road
Getting from there to here
It's been a long time
But my time is finally near

And I can feel the change in the wind right now
Nothing's in my way
And they're not gonna hold me down no more
No there not gonna hold me down

Cause I've got faith of the heart
I'm going where my heart will take me
I've got faith to believe
I can do anything
I've got strength of the soul
And no one's gonna bend or break me
I can reach any star
I've got faith
I've got faith
Faith of the heart

It's been a long night
Trying to find my way
Been through the darkness
Now I finally have my day
And I will see my dream come alive at last
I will touch the sky
And they're not gonna hold me down no more
No there not gonna change my mind

Cause I've got faith of the heart
I'm going where my heart will take me
I've got faith to believe
I can do anything
I've got strength of the soul
And no one's gonna bend or break me
I can reach any star
I've got faith
Faith of the heart

I've known a wind so cold
and seen the darkest days
But now the winds I feel
are only winds of change
I've been through the fire
and I've been through the rain
But I'll be fine

Cause I've got faith of the heart
I'm going where my heart will take me
I've got faith to believe
I can do anything
I've got strength of the soul
And no one's gonna bend or break me
I can reach any star
I've got faith

Faith of the heart

Faith of the heart
I'm going where my heart will take me
I've got faith to believe
That no one's gonna bend or break me
I can reach any star
I've got faith
I've got faith
Faith of the heart

It's been a long road…

# Contents

List of Figures ..... 11
List of Schemes ..... 15
List of Tables ..... 20
List of Abbreviations ..... 23
**1. Introduction ..... 27**
1.1 Magnetic Resonance Imaging ..... 27
1.1.1 Mechanism ..... 28
1.2 Contrast agents for magnetic resonance imaging ..... 29
1.2.1 Mechanism ..... 30
1.2.2 Relaxation theory ..... 33
1.2.3 Strategies in development of contrast agents for MRI ..... 39
1.2.4 Toxicity of metal complexes ..... 41
1.2.4.1 Stability of metal complexes *in vivo* ..... 41
1.2.4.2 Excretability ..... 42
1.2.5 *In vivo* targeting ..... 43
1.2.6 Smart contrast agents ..... 44
1.2.7 Labelling of stem cells ..... 45
1.3 Gadolinium complexes ..... 46
1.3.1 Types of gadolinium-complexes ..... 48
1.3.1.1 Macromolecular contrast agents ..... 51
1.3.2 DOTA as ligand ..... 57
1.3.2.1 Kinetics and thermodynamics ..... 60
1.3.3 Hyperbranched polymers ..... 63
1.4 AIMS AND OBJECTIVES ..... 64
1.4.1 Aim ..... 64
1.4.2 Objectives ..... 64
**2 Results and discussion I: monomers synthesis ..... 66**
2.1 Divergent synthesis of DOTA-amides ..... 67
2.1.1 Synthesis *via* ester derivatives of DOTA ..... 68
2.1.2 Synthesis *via* DOTA ..... 73
2.1.2.1 Attempted synthesis *via* acyl chlorides ..... 75
2.1.2.2 Synthesis using peptide coupling reagents ..... 77

2.2 Convergent synthesis ..... 83
2.2.1 Initial synthesis of DOTA-amides with amines or thiols as terminal groups ..... 85
2.2.2 Synthesis of DOTA-amides with halogens as terminal groups ..... 88
2.2.3 Synthesis of allyl-, propynyl- and styryl-DOTA-amides ..... 92
2.2.4 Synthesis of other DOTA-styryl-derivatives ..... 97
2.2.4.1 Attachment of **57** and **61** to cyclen ..... 103
2.3 Synthesis of monomers *via* "click chemistry" ..... 111
2.3.1 Overview ..... 111
2.3.2 Model compounds and potential "arms" ..... 115
2.3.3 Divergent synthesis *via* click chemistry ..... 121
2.3.4 Convergent synthesis following preparation of arm **67** *via* click chemistry ..... 131
**3 Results and discussion II: polymerisations ..... 134**
3.1 Polymerisation *via* metathesis ..... 134
3.1.1 Overview on metathesis reactions ..... 134
3.1.2 Attempt of polymerisation of DOTA-tetra-allyl-amide **52** *via* metathesis ..... 137
3.2 Radical polymerisations ..... 141
3.2.1 Overview on radical polymerisations ..... 141
3.2.2 Attempt of polymerisation of DOTA-tetra-allyl-amide **52** *via* radical reaction ..... 143
3.2.3 Polymerisation of 1,4,7,10-tetrakis(2-styrylcarbamoylmethyl)-1,4,7,10-tetraazacyclododecane 54 ... 144
3.2.4 Polymerisation of 1,4,7,10-tetrakis(ethoxycarbonylmethyl)-1,4,7,10-tetraazacyclododecane **63** ..... 146
3.2.5 Conclusions about radical polymerisation with tetra-styryl monomers ..... 148
3.3 Polymerisation *via* cycloaddition reactions ..... 149
3.3.1 "Click chemistry" with Zn-complex **73** ..... 150
3.3.2 "Click chemistry" with Gd-complex **85** ..... 155
3.3.3 Thermal cycloaddition with Gd-complex **85** ..... 159
3.3.4 Thermal cycloaddition with ligand **53** ..... 162

3.3.5 Cycloadditions data comparison ..... 166

**4 Results and discussion III: MRI measurements and toxicity tests ..... 170**

4.1 Synthesis of the Gd-complexes ..... 170

4.2 Determination of relaxivity ..... 174

4.3 Viability tests ..... 182

**5. Conclusions and future perspectives ..... 190**

5.1 Conclusions ..... 190

5.2 Perspectives and future work ..... 193

**6. Experimental Part ..... 194**

6.1 Synthetic Chemistry ..... 194

6.1.1 General ..... 194

6.1.2 Experimental details ..... 197

6.2 MRI measurements and biological assays ..... 229

6.2.1 Determination of relaxivity ..... 229

6.2.2 Incubation for cell viability tests ..... 232

**References ..... 234**

## List of Figures

**Figure 1.1** Sagittal MRI image of the skull. [From Radiology Regional Center, Florida; *www.radiologyregional.com/ mri.html,* accessed on September 2005]

**Figure 1.2** MR images of breast affected by cancer, before (left) and after (right) injection of a contrast agent. [From University of Liverpool website; *http://int.ch.liv.ac.uk/Lanthanide/Ln_Chemistry_folder/MRI%20folder/MRImages.html,* accessed on September 2005]

**Figure 1.3** Schematic view of the relaxation mechanisms (and the main relaxation parameters) operating in an aqueous solution containing a paramagnetic $Gd^{III}$ chelate. [From Aime, S. *et al.*; *Chem. Soc. Rev.* **1998**, *27*, 19-29]

**Figure 1.4** Simulated inner-sphere relaxivities. Left: $\tau_r = 0.1$ ns. Right: $\tau_r = 1$ ns.. [From Caravan, P. *et al.*; *Chem. Rev.* **1999**, *99*, 2293-2352]

**Figure 1.5** Inner-sphere relaxivities calculated as a function of $\tau_m$ and $\tau_r$ for various values of $\tau_{s1}$ at 0.5 T and 1.5 T, with $q = 1$ and $d = 3.1$ Å. [From Caravan, P. *et al.*; *Chem. Rev.* **1999**, *99*, 2293-2352]

**Figure 1.6** Simulated inner-sphere proton relaxivities (here indicated with $R_1$) at 20 MHz. Left: $\tau_m$=2μs, $\tau_{s0}$=850 ps, $\tau_v$=20 ps. Centre: $\tau_r$=10 ns, $\tau_{s0}$=850 ps, $\tau_v$=20 ps. Right: $\tau_m$=2μs, $\tau_r$=10 ns, $\tau_v$=20 ps. The graphs were simulated using Solomon-Bloembergen-Morgan equations (Section 1.2.2). [From Peters, J. A. *et al.*; *Prog. Nucl. Magn. Reson. Spectrosc.* **1996**, *28*, 283-350]

**Fig 1.7** Variation of water proton relaxivity (298 K, 20 MHz) with water exchange rate for the series of $GdL(OH_2)X_3$ complexes changing the anion as shown. Data obtained for two anionic complexes (circles and squares) are shown for comparison. [From Parker, D. *Chem. Soc. Rev.* **2004**, *33*, 156]

**Figure 1.8** Tricapped trigonal prism (TTP) and monocapped square antiprism (CSAP) geometries. [From Caravan, P. *et al.*; *Chem. Rev.* **1999**, *99*, 2293-2352]

**Figure 1.9** The four polyaminocarboxylic ligands of the MRI contrast agents approved for clinical use.

**Figure 1.10** Some of the most effective DTPA-derivatives. **5**, **6** and **7** have been successfully used to bind non-covalently with Human Serum Albumin (Section 1.3.1.1). Stability constants for the corresponding Gd-complexes are reported in Table 1.2. Relaxivities are reported in Table 1.1.

**Figure 1.11** Some particularly successful DOTA-derivatives, and the basic structure of Cyclen **15**. For the DOTA-derivatives, stability constants of the corresponding Gd-complexes are reported in Table 1.2. Relaxivities are reported in Table 1.1.

**Figure 1.12** DO3A and one of its derivatives, ligands for $Gd^{3+}$ where just 3 of the 4 nitrogens are functionalised with acetate arms, so allowing binding of a further water molecule. Relaxivities for the corresponding Gd-complexes are reported in Table 1.1. Stability constants are reported in Table 1.2.

**Figure 1.13** Pyridine-containing cyclen-derivatives, ligands for $Gd^{3+}$ used to test the effect on relaxivity by increased rigidity of the structure. Relaxivities of the corresponding Gd-complexes are reported in Table 1.1. Stability constants are reported in Table 1.2.

**Figure 1.14** Two acyclic ligands used to test stability of Gd-complexes, whose relaxivities are reported in Table 1.1. Stability constants are reported in Table 1.2.

**Figure 1.15** Cyclic ligands not based on the cyclen structure and used to test stability of Gd-complexes, whose relaxivities are reported in Table 1.1. Stability constants are reported in Table 1.2.

**Figure 1.16** Chemical structure of polylysine – DTTA-MA conjugate **26**. [From Caravan, P. *et al.*; *Chem. Rev.* **1999**, *99*, 2293-2352]

**Figure 1.17** Chemical structure of CMD-A2-Gd-DOTA, a modified dextran polymer.

**Figure 1.18** Schematic drawing of a generation 2 PAMAM thiourea DTPA dendrimer (left) and chemical structure of Gadomer 17 (right). Relaxivity values are reported in Table 1.1. [From Caravan, P. *et al.*; *Chem. Rev.* **1999**, *99*, 2293-2352]

**Figure 1.19** Schematic representation of the dissociation of apoferritin into subunits at pH 2, followed by its reforming at pH 7. In this way the solution components are trapped within its interior. [From Aime, S. *et al.*; *Angew. Chem. Int. Ed.* **2002**, *41*, 1017-19]

**Figure 1.20** Some reported macromolecular contrast agents, whose performances are lower than expected. Arrows show the sites endowed with rotational freedom. [Structures from Caravan, P. *et al.*; *Chem. Rev.* **1999**, *99*, 2293-2352]

**Figure 1.21** Left: equilibria between diastereomeric conformations (CSAP and twisted CSAP) for Gd-complexes of DOTA. [From Caravan, P. *et al.*; *Chem. Rev.* **1999**, *99*, 2293-2352]. Right: schematic representation of the two diastereoisomers of a Ln(III) macrocyclic complex based on the tetraazacyclododecane ring, rising from rotation of the acetate arms. [From Aime, S. *et al.*; *Acc. Chem. Res.* **1999**, *32*, 941-949]

**Figure 1.22** Stability of $Gd(DOTA)^-$ as a function of the publication year. [From Comblin, V. *et al.*; *Coord. Chem. Rev.* **1999**, *186*, 451-470]

**Figure 1.23** Schematic architecture of a hyperbranched polymer from $AB_2$ monomers. [From Jikei, M. *et al.*; *Prog. Polym. Sci.* **2001**, *26*, 1233-1285]

**Figure 2.1** The most common peptide coupling reagents and additives.

**Figure 2.2** Possible products from the reaction of cysteamine with *p*-methoxybenzyl chloride.

**Figure 2.3** *Ansa*-compound and capsule as possible by-products when trying to attach an arm functionalised at both ends.

**Figure 2.4** Main and minor products from the first synthesis of 4-vinylbenzylamine **55**, with the corresponding m/z values from $CI^+$ MS, NMR chemical shifts, and retention factors as from TLC ($SiO_2$, MeCN/MeOH/25% $NH_4OH$ 80:19.9:0.1).

**Figure 2.5** GPC eluogram (DMF) of the water-insoluble residue from the reaction between cyclen and chloroacetate carried out in the presence of $Cs_2CO_3$ and KI (Table 2.12, entry 3). MW calculations are reported in Table 2.13 and discussed in the text.

**Figure 2.6** Molecular structures of hydroquinone and 2,6-di-*tert*-butyl-4-methylphenol (TBMP). The former is a common radical inhibitor, and the second was chosen as an equivalent but having hindering *tert*-butyl groups to prevent the phenolate reacting as a nucleophile.

**Figure 2.7** A dual contrast agent is detectable by both MRI and fluorescence microscopy, and a direct overlay of both images affords identification and corroboration of the transplant of stem cells. I = injection tract; cc = corpus callosum; lv = lateral ventricle. [Image source: Modo, M. *et al.*; *Neuroimage* **2002**, *17*, 803-811]

**Figure 2.8** Comparison between the same regions of the $^1H$ NMR spectra in DMSO-$d_6$ of compounds **73** (top) and **53** (bottom).

**Figure 2.9** X-ray crystal structure of **73** showing the hexa-coordinate stereochemistry of the $Zn^{II}$-complex. Hydrogen atoms and solvent molecules have been omitted for clarity. Crystal data are reported in Chapter 6 (Table Exp.1). Selected bond lengths and angles are reported in Table 2.17.

**Figure 3.1** Comparison between Schrock and Fischer carbene complexes, and the first alkylidene carbene complex proposed by Schrock.

**Figure 3.2** The most commonly reported molybdenum-based Schrock catalyst (top), ruthenium-based Grubbs catalysts (middle) and Hoveyda catalysts (bottom).

**Figure 3.3** Comparison between the same regions of the $^1H$ NMR spectra recorded (in $CDCl_3$) for DOTA-tetra-allyl-amide **52** (bottom) and after mixing it with 2,6-dichloro-1,4-benzoquinone (top). The top structure represents schematically the product (compatible with the NMR analysis) from the hypothesised reaction between **52** and dichlorobenzoquinone.

**Figure 3.4** Comparison between the RI traces (DMF, 1% $Et_3N$, 1% AcOH) relative to click chemistry reactions with [**73**]/[**81**] ratios of (from top) 1:4, 1:2, 1:1, 1.5:1, and Zn-complex **73** itself (bottom).

**Figure 3.5** Comparison between the RI traces (DMF, 1% $Et_3N$, 1% AcOH) relative to click chemistry reactions (filtrates) with [**85**]/[**81**] ratios of (from top) 1:4, 1:2, 1:1.33, 1:1, 1.5:1 and Gd-complex **85** itself (bottom).

**Figure 3.6** Comparison between the RI traces (DMF, 1% $Et_3N$, 1% AcOH) relative to the filtrates from thermal cycloadditions between **85** and **81** in ratios of (from top) 1:6, 1:4, 1:2, 1:1, and Gd-complex **85** itself (bottom).

**Figure 3.7** Comparison between the RI traces (DMF, 1% $Et_3N$, 1% AcOH) relative to thermal cycloaddition reactions (filtrates) with [**53**]/[**81**] ratios of (from top) 1:4, 1:2, 1:1, 1.165:1, 1.33:1 and DOTA-tetra-propargyl-amide **53** itself (bottom).

**Figure 4.1** $ESI^+$ mass spectra expansions showing the multiple-peaks pattern observed for the $[L+Gd]^+$ ions for complexes **85** (left) and **86** (right).

**Figure 4.2** X-ray crystal structure of **85** showing the nona-coordinate stereochemistry of the $Gd^{III}$-complex. Hydrogen atoms, chloride anions and solvent molecules (except the coordinated water molecule) have been omitted for clarity. Crystal data are reported in the Experimental Part (Table Exp.2). Selected bond lengths and angles are reported in Table 4.2.

**Figure 4.3** Comparison between a typical representation of the capped square antiprismatic geometry (left, from Woods M. *et al.*; *Dalton Trans* **2005**, *(24)*, 3829-3837) and a perspective view of the X-ray structure of **85** (right, where the propargyl groups are omitted for clarity).

**Figure 4.4** Magnetisation intensity *vs.* time graph (normalised) for solutions of **84** at different concentrations.

**Figure 4.5** Relaxation rate *vs.* Gd-concentration plots and relative linear fits for complexes **83-85**.

**Figure 4.6** Molecular structures of DOTTA **87** (left) and DOTA-tetra-benzyl-amide **88** (right), two DOTA-amides whose relaxivities are reported in the literature.

**Figure 4.7** $R_1$ *vs.* [Gd] plots and relative linear fits for some products of the cycloaddition reactions between **85** and **81**. Data are reported in Table 4.5 and discussed in the text.

**Figure 4.8** Molecular structure of the pH indicator Phenol Red, among the components of DMEM.

**Figure 4.9** Left: dead or dying cells, with the typical round morphology, as a consequence of incubation in the presence of a 10 mM toxic concentration of **84**. Right: healthy cells (irregularly-shaped), which survived incubation with a 1 mM concentration of **84**.

**Figure 4.10** Results of the Alamar Blue assay on cell cultures of **83-85**.

**Figure 4.11** Results of the Methylene Blue assay on cell cultures of **83-85**.

## List of Schemes

**Scheme 1.1** Richman-Atkins procedure for the synthesis of cyclen **15**. i) DMF, 100 °C, 2 h, 80%; ii) 97% $H_2SO_4$, 100 °C, 48 h; 6 N HCl.

**Scheme 1.2** The Weisman-Reed procedure to synthesise cyclen **15**. [From Weisman, G. R. *et al.*; *J. Org. Chem.* **1996**, *61*, 5186-5187]

**Scheme 2.1** First retrosynthetic analysis to obtain tetra-substituted cyclens possessing polymerisable groups (Y) at the terminal position of the pendant arms. X = leaving group, Y = polymerisable moiety, Z = leaving group, ~~~ = spacer between the amine/amide moiety and the polymerisable group.

**Scheme 2.2** Second retrosynthetic analysis to obtain tetra-substituted cyclens possessing polymerisable groups (Y) at the terminal position of the pendant arms. X = leaving group, Y = polymerisable moiety, ~~~ = spacer between the amine/amide moiety and the polymerisable group.

**Scheme 2.3** Representation of a possible divergent synthesis deriving from one of the retrosynthetic analyses (Scheme 2.1) and leading to a tetra-substituted cyclen possessing moieties which can be exploited for polymerisation.

**Scheme 2.4** Synthesis of DOTA-tetra-esters **30** and **31**. Conditions and results are reported in Table 2.1 and discussed in the text.

**Scheme 2.5** General representation of the attempts of synthesis of tetra-amide derivative **32** from tetra-ester **31** and *n*-butylamine. Conditions are reported in Table 2.2.

**Scheme 2.6** Synthesis of DOTA. i) cyclen (1 mol eq), bromoacetic acid (4.4 equivalents), 5 M NaOH, $H_2O$, pH 10, 70 °C, 8 h; ii) 37% HCl, pH 2. Overall yield: 73%.

**Scheme 2.7** Mechanism for acyl chloride formation using thionyl chloride (up) or oxalyl chloride (down).

**Scheme 2.8** General representation of the attempted syntheses of tetra-amide **32** from DOTA *via* the corresponding acid chloride using either thionyl chloride or oxalyl chloride. Conditions reported in Table 2.3.

**Scheme 2.9** Mechanism of peptide bond formation through carbodiimide activation.

**Scheme 2.10** Catalytic role of DMAP **37** as additive in amide formation following activation by carbodiimides.

**Scheme 2.11** Mechanism of peptide bond formation using a carbodiimide and a benzotriazole as additives for activation of the carboxylic moiety. For a list of possible Xs and Ys see Figure 2.1.

**Scheme 2.12** Coupling procedure using onium salts as additives for activation of the carboxylic acid. $Z^+$ = uronium or phosphonium cation; for a list of possible Xs and Ys see Figure 2.1.

**Scheme 2.13** Mechanism of amidation using the reagent combination NHS/EDC.

**Scheme 2.14** Attempted synthesis of tetra-amide derivative **32** by using peptide coupling reagents. Conditions and results are reported in Table 2.4 and discussed in the text.

**Scheme 2.15** Representation of a possible convergent synthesis deriving from one of the retrosynthetic analyses (Scheme 2.2) and leading to a tetra-substituted cyclen possessing moieties which can be exploited for polymerisation.

**Scheme 2.16** Synthesis of *N*-butyl-2-chloroacetamide **39**. i) chloroacetyl chloride (1 mol eq), *n*-butylamine (1 mol eq), $Et_3N$ (1 mol eq), THF, -10 °C, 1 h, 84%.

**Scheme 2.17** Synthesis of tetra-amide derivative **32** from cyclen through a convergent synthesis procedure. i) cyclen (1 mol eq), $Cs_2CO_3$ (5 mol eq), KI (5 mol eq), **39** (5 mol eq), DMF, 70 °C, 18 h, 69%.

**Scheme 2.18** General representation of the monoprotection of ethylenediamine with BOC-group. Conditions and results are reported in Table 2.5 and discussed in the text.

**Scheme 2.19** Monoprotection of cysteamine. Conditions and results are reported in Table 2.6 and discussed in the text.

**Scheme 2.20** Synthesis of bis-haloacetamides **43** and **44**. Conditions and results are reported in Table 2.7 and discussed in the text.

**Scheme 2.21** General representation of the attempted of synthesis of compounds **45** and **46**. Conditions and results are reported in Table 2.8 and discussed in the text.

**Scheme 2.22** General representation of the synthesis of haloacetamides **47-51**. Reaction conditions and results are reported in Table 2.9.

**Scheme 2.23** Attempted syntheses of DOTA-tetra-amides **52-53**. Reaction conditions and results are reported in Table 2.10 and discussed in the text.

**Scheme 2.24** Synthesis of 4-vinylbenzylamine **55**. i) 4-vinylbenzyl chloride (1 mol eq), $NH_4OH$ (>100 mol eq), $AcONH_4$ (1 mol eq), THF, RT, 2 d, 34%. The low yield is discussed in the text.

**Scheme 2.25** Second synthesis of 4-vinylbenzylamine **55** as its hydrochloride salt **56**. i) 4-vinylbenzyl chloride (1 mol eq), $NH_4OH$ (>100 mol eq), $AcONH_4$ (1 mol eq), THF, RT, 2 d; ii) 1 M HCl, RT, 30 min, 83%.

**Scheme 2.26** Synthesis of *N*-(4-vinylbenzyl)-2-chloroacetamide **57**. i) **56** (1 mol eq), chloroacetyl chloride (1 mol eq), $Et_3N$ (2 mol eq), THF, 0 °C, 2 h, 91%.

**Scheme 2.27** Attempted reactions between cysteamine hydrochloride, ethylenediamine or mercaptoethanol and 4-vinylbenzyl chloride. Conditions and results are reported in Table 2.11 and discussed in the text.

**Scheme 2.28** Synthesis of chloroacetate **61**. i) **60** (1 mol eq), chloroacetyl chloride (5 mol eq), $Et_3N$ (1 mol eq), THF, 0 °C, 2 h, 53%.

**Scheme 2.29** Synthesis of tetra-substituted derivative **62**. i) Cyclen (1 mol eq), **57** (4.4 mol eq), $Cs_2CO_3$ (4.4 mol eq), KI (4.4 mol eq), DMF, 50 °C, 48 h. Purification problems are discussed in the text.

**Scheme 2.30** General representation of the attempts of synthesis of DOTA-tetra-ester **63**. Reaction conditions and results are reported in Table 2.12 and discussed in the text.

**Scheme 2.31** Generic representation of the Huisgen [3+2] dipolar cycloaddition reaction between an alkyne and an azide, leading to a mixture of 1,4- and 1,5-substituted triazoles.

**Scheme 2.32** Generic representation of the copper(I)-catalysed cycloaddition between alkynes and azides, also showing the first step of formation of the $Cu^I$ acetylide.

**Scheme 2.33** Binuclear catalytic mechanism proposed by Sharpless and co-workers for copper(I)-catalysed cycloaddition reactions between alkynes and azides.

**Scheme 2.34** Alternative catalytic mechanism proposed for cycloadditions between azides and internal alkynes catalysed by *N*-heterocyclic carbene-copper complexes.

**Scheme 2.35** Synthesis of 2-[2-(2-azidoethoxy)ethoxy]ethanol **64**. i) 2-[2-(2-chloroethoxy)ethoxy]ethanol (1 mol eq), $NaN_3$ (2 mol eq), DMF, 100 °C, 24 h, 99%.

**Scheme 2.36** Cu(I)-catalysed 1,3-dipolar cycloaddition between azide **64** and alkyne **49** to yield chloroacetamide **65**. i) **49** (1 mol eq), **64** (1.1 mol eq), $CuSO_4 \cdot 5H_2O$ (0.1 mol eq), Na-ascorbate (0.2 mol eq), $H_2O$/*t*-BuOH 1:1, 50 °C, 5 h, 98%.

**Scheme 2.37** Synthesis of *p*-vinylbenzyl azide **66**. i) 4-vinylbenzyl chloride (1 mol eq), $NaN_3$ (1.1 mol eq), $H_2O$/EtOH, reflux, 14 h, 60%.

**Scheme 2.38** Click chemistry reaction to prepare *N*-((1-(4-vinylbenzyl)-*1H*-1,2,3-triazol-4-yl)methyl)-2-chloroacetamide **67**. i) **49** (1 mol eq), **66** (1.1 mol eq), $CuSO_4 \cdot 5H_2O$ (0.1 mol eq), Na-ascorbate (0.2 mol eq), $H_2O$/*t*-BuOH 1:1, 50 °C, 14 h, 55%.

**Scheme 2.39** Synthesis of fluorescein-5-(2-(2-(2-azidoethoxy)ethoxy)ethyl)thiocarbamate **68**. i) FITC (1 mol eq), **64** (1 mol eq), $Et_3N$ (2 mol eq), DMF, 60 °C, 24 h, 77%.

**Scheme 2.40** Attempt of synthesis of chloroacetamide **69** *via* click-chemistry. i) **49** (1 mol eq), **68** (1 mol eq), $CuSO_4 \cdot 5H_2O$ (0.1 mol eq), Na-ascorbate (0.2 mol eq), $H_2O$/*t*-BuOH, 50 °C, 24 h. The product did not form.

**Scheme 2.41** General representation of the attempted synthesis of tetra-substituted species **70** *via* click-chemistry. Conditions and results are summarised in Table 2.15 and discussed in the text.

**Scheme 2.42** General representation of the attempted synthesis of tetra-substituted species **71** *via* click-chemistry. Conditions and results are summarised in Table 2.16 and discussed in the text.

**Scheme 2.43** Attempt of synthesis of $Gd^{III}$-complex **72** *via* click-chemistry. i) **85** (1 mol eq), **66** (4.4 mol eq), $CuSO_4 \cdot 5H_2O$ (0.4 mol eq), Na-ascorbate (0.8 mol eq), $H_2O$/DMF, 50 °C, 24 h. The NMR line broadening did not allow estimation of the crude yield or conversion.

**Scheme 2.44** Synthesis of $Zn^{II}$-complex **73**. i) **53** (1 mol eq), $Zn(ClO_4)_2$ (1.1 mol eq), $H_2O$/MeOH, 80 °C, 14 h, 87%.

**Scheme 2.45** Synthesis of $Zn^{II}$-complex **74** *via* click-chemistry. i) **73** (1 mol eq), **66** (4.4 mol eq), $CuSO_4 \cdot 5H_2O$ (0.4 mol eq), Na-ascorbate (0.8 mol eq), $H_2O$/DMF, 50 °C, 14 h. Crude yield: 46%.

**Scheme 2.46** Convergent synthesis of 1,4,7,10-tetrakis((1-(4-vinylbenzyl)-*1H*-1,2,3-triazol-4-yl)methylcarbamoylmethyl)-1,4,7,10-tetraazacyclododecane **71**. i) **15** (1 mol eq), **67** (4.4 mol eq), $Cs_2CO_3$ (4.4 mol eq), KI (4.4 mol eq), DMF, 50 °C, 48 h. Purification problems are discussed in the text.

**Scheme 3.1** Generic representation of a metathesis reaction.

**Scheme 3.2** Reaction mechanism for a generic metathesis process, involving the formation of an intermediate metallacyclobutane.

**Scheme 3.3** Generic representation of the 3 types of metathesis reaction: a) ring-opening metathesis polymerisation; b) ring-closing metathesis; c) cross-metathesis.

**Scheme 3.4** Attempt of polymerisation of DOTA-tetra-allyl-amide **52** *via* metathesis reaction. Conditions and results are reported in Table 3.1 and discussed in the text.

**Scheme 3.5** The three steps of radical polymerisations. A fourth step, *chain transfer*, is also described in the text.

**Scheme 3.6** Benzoyl peroxide and AIBN, and the free radicals obtained from them by thermal activation.

**Scheme 3.7** Attempt of radical polymerisation of DOTA-tetra-allyl-amide **52**. i) **52** (1 mol eq), AIBN (0.2 mol eq), $CHCl_3$, 40 °C, 20 hours.

**Scheme 3.8** General procedure for the attempts of polymerising DOTA-tetra-styryl-amide **54** through radical reactions. Conditions and results are reported in Table 3.2 and discussed in the text.

**Scheme 3.9** General procedure for the attempts of co-polymerisation of DOTA-tetra-ester **63** through radical reaction. Conditions and outcomes are reported in Table 3.3 and discussed in the text.

**Scheme 3.10** Synthesis of co-monomer 1,2-bis(2-azidoethoxy)ethane **81**. i) 1,2-bis(chloroethoxy)ethane (1 mol eq), $NaN_3$ (20 mol eq), DMF, 60 °C, 15 h, 91%.

**Scheme 3.11** General procedure for click chemistry polymerisations between Zn-complex **73** and diazide **81**. Reaction conditions and results for the most promising molar ratios are reported in Table 3.4 and discussed in the text.

**Scheme 3.12** General procedure for click chemistry polymerisations between Gd-complex **85** and diazide **81**. Reaction conditions and results for the most promising molar ratios are reported in Table 3.5 and discussed in the text.

**Scheme 3.13** General procedure for thermal cycloaddition polymerisations between Gd-complex **85** and diazide **81**. Reaction conditions and results for the most promising molar ratios are reported in Table 3.6 and discussed in the text.

**Scheme 3.14** General procedure for 1:x thermal cycloaddition polymerisations between ligand **53** and diazide **81**. Reaction conditions and results for the most promising molar ratios are reported in Table 3.7 and discussed in the text.

**Scheme 4.1** Synthesis of the Gd-complex of tetra-ester **31**. i) **31** (1.5 mol eq), $GdCl_3 \cdot 6H_2O$ (1 mol eq), $H_2O$, 50 °C, 4 d, 84%

**Scheme 4.2** Synthesis of Gd-complexes **83-86**. Reaction conditions and results are reported in Table 4.1 and discussed in the text.

## List of Tables

**Table 1.1** Longitudinal proton relaxivities $r_1$ ($mM^{-1}$ $s^{-1}$, 20 MHz, 37 °C) for selected gadolinium(III)-complexes.

**Table 1.2** Stability constants for various cyclic and acyclic gadolinium(III)-complexes.

**Table 2.1** Reaction conditions and results for the synthesis of DOTA-esters **30** and **31**, as shown in Scheme 2.4.

**Table 2.2** Reaction conditions and results for the synthesis of DOTA-tetra-butyl-amide **32** shown in Scheme 2.5.

**Table 2.3** Reaction conditions and results for the attempted synthesis of DOTA-amide **32** *via* the corresponding acyl chloride, as shown in Scheme 2.8.

**Table 2.4** Reaction conditions and results for the procedure shown in Scheme 2.14.

**Table 2.5** Reaction conditions and results for the synthesis of *N*-(*tert*-butoxycarbonyl)-1,2-diaminoethane **40**, as shown in Scheme 2.18.

**Table 2.6** Reaction conditions and results for the monoprotection of cysteamine, as shown in Scheme 2.19.

**Table 2.7** Reaction conditions and results for the synthesis of bis-haloacetamides **43** and **44**, as shown in Scheme 2.20.

**Table 2.8** Reaction conditions and results for the attempted synthesis of tetrasubstituted macrocycles **45** and **46**, as shown in Scheme 2.21.

**Table 2.9** Reaction conditions and results for the synthesis of haloacetamides **47-51**, as shown in Scheme 2.22.

**Table 2.10** Reaction conditions and results for the attempted syntheses of DOTA-tetra-amides **52-54**, as shown in Scheme 2.23.

**Table 2.11** Reaction conditions and results for the synthesis of styryl-derivatives **58-60**, as shown in Scheme 2.27.

**Table 2.12** Reaction conditions and results for the attempted syntheses of DOTA-tetra-ester **63**, as shown in Scheme 2.30.

**Table 2.13** Chromatographic data related to the chromatogram shown in Figure 2.5.

**Table 2.14** Attempts of purification of DOTA-tetra-ester **63**.

**Table 2.15** Reaction conditions and results for the attempted syntheses of tetra-triazole-derivative **70**, as shown in Scheme 2.41.

**Table 2.16** Reaction conditions and results for the attempted syntheses of tetra-triazole-derivative **71**, as shown in Scheme 2.42.

**Table 2.17** Selected bond lengths [Å] and bond angles [deg] for **73** (numbers in parentheses are estimated standard deviations in the least significant digits).

**Table 3.1** Reaction conditions and results for the attempted polymerisation of DOTA-tetra-allyl-amide **52**, as shown in Scheme 3.4

**Table 3.2** Reaction conditions and outcomes for the attempts of polymerisation of DOTA-tetra-styryl-amide **54** *via* radical procedures, as shown in Scheme 3.8.

**Table 3.3** Reagents and co-reagents ratios, products solubilities and swelling tests results for the attempted co-polymerisation reactions of **63**, as shown in Scheme 3.9. Reaction temperature = 80 °C; reaction time = 3 h.

**Table 3.4** Reaction conditions and characterisation data for the products of the click chemistry polymerisation between Zn-complex **73** ($A_4$) and diazide **81** ($B_2$). $CuSO_4 \cdot 5H_2O$ (10 mol% per functional group not in excess), Na-ascorbate (20 mol% per functional group not in excess), DMF, 50 °C, 14 h. The data are discussed in the text.

**Table 3.5** Reaction conditions and characterisation data for the products of the click chemistry polymerisations between Gd-complex **85** ($A_4$) and diazide **81** ($B_2$). $CuSO_4 \cdot 5H_2O$ (10 mol% per functional group not in excess), Na-ascorbate (20 mol% per functional group not in excess), DMF, 50 °C, 14 h. The data are discussed in the text.

**Table 3.6** Reaction conditions and characterisation data for the products of the thermal cycloaddition polymerisation between Gd-complex **85** ($A_4$) and diazide **81** ($B_2$). DMF, 80 °C, 14 h. The data are discussed in the text.

**Table 3.7** Reaction conditions and characterisation data for the products of the thermal cycloaddition polymerisation between ligand **53** ($A_4$) and diazide **81** ($B_2$). DMF, 80 °C, 14 h. The data are discussed in the text.

**Table 4.1** Reaction conditions and results for the synthesis of Gd-complexes **83-86**, as shown in Scheme 4.2.

**Table 4.2** Selected bond lengths [Å] and bond angles [deg] for **85** (numbers in parentheses are estimated standard deviations in the least significant digits).

**Table 4.3** Longitudinal relaxation times ($T_1$) and rates ($R_1$) calculated for solutions at different concentration of complexes **83**, **84** and **85.**

**Table 4.4** Longitudinal ($r_1$) and transversal ($r_2$) relaxivities calculated for complexes **83**, **84** and **85** following different methods and at different magnetic field strengths ($B$).

**Table 4.5** Longitudinal and transversal relaxation times ($T_1$, $T_2$), rates ($R_1$, $R_2$) and relaxivities ($r_1$, $r_2$) for some of the products obtained by cycloaddition reactions between **85** and **81**.

**Table 4.6** Summary of the properties of some the products obtained by cycloaddition reactions between **85** and **81** and used in relaxation measurements (see Tables 3.3, 3.4 and 4.6.

**Table 4.7** Typical Dulbecco's modified Eagle's medium (DMEM) formulation.

**Table 4.8** Summary of the final response (+ = positive; - = negative) about cell viability towards Gd-complexes **83-85**.

**Table 6.1** Crystallographic data and experimental details for **73** (numbers in parentheses are estimated standard deviations in the least significant digits).

**Table 6.2** Reaction conditions for click chemistry experiments between **73** and **81**.

**Table 6.3** Reaction conditions for click chemistry experiments between **85** and **81**.

**Table 6.4** Reaction conditions for thermal cycloaddition experiments between **53** and **81**.

**Table 6.5** Reaction conditions for thermal cycloaddition experiments between **85** and **81**.

**Table 6.6** Crystallographic data and experimental details for **85** (numbers in parentheses are estimated standard deviations in the least significant digits).

**Table 6.7** Longitudinal and transversal relaxation times ($T_1$, $T_2$), rates ($R_1$, $R_2$) and relaxivities ($r_1$, $r_2$) for Gd-complexes **83-85** and selected cycloaddition products. T = 25 °C.

**Table 6.8** Results of the Alamar Blue assay on cell cultures of **83-85**

**Table 6.9** Results of the Methylene Blue assay on cell cultures of **83-85**

## List of Abbreviations

| | |
|---|---|
| ADMET | Acyclic diene metathesis polymerisation |
| BOC | *tert*-Butoxycarbonyl |
| BOP | Benzotriazol-1-yloxy-tris(dimethylamino)phosphonium hexafluorophosphate |
| BOPTA | (4*RS*)-4-Carboxy-5,8,11-tris(carboxymethyl)-1-phenyl-2-oxa-5,8,11-triazatridecan-13-oic acid |
| BP2A | 3,11,17,18-Tetraazatricyclo[11.3.1.15,9]octadeca-1(17),5,7,9(18),13,15-hexaene-3,11-diacetic acid |
| BSA | Bovine serum albumin |
| BuOH | Butanol |
| CI | Chemical ionisation |
| Cis-DOTA(BOM)$_2$ | DOTA-α1,α4-bis(phenylmethyl) ester |
| Cl-HOBt | 1-Hydroxy-5-chlorobenzotriazole |
| CM | Cross-metathesis |
| CSAP | Monocapped square antiprism/antiprismatic |
| CTA | Chain transfer agent |
| Cyclen | 1,4,7,10-Tetraazacyclododecane |
| DCC | Dicyclohexylcarbodiimide |
| DCM | Dichloromethane |
| DIPEA | *N*,*N*-Diisopropylethylamine |
| DMAP | 4-Dimethylaminopyridine |
| DMEM | Dulbecco's modified Eagle's medium |
| DMF | *N*,*N*-Dimethylformamide |
| DMSO | Dimethylsulphoxide |
| DMSO-d$_6$ | Deuterated DMSO |
| DO3A | 1,4,7,10-Tetraazacyclododecane-1,4,7-triacetic acid |
| DO3MA | α,α',α''-Trimethyl-DOTA |
| DOTA | 1,4,7,10-Tetraazacyclododecane-1,4,7,10-tetraacetic acid |
| DOTA(BOM) | DOTA-mono(phenylmethyl) ester |
| DOTA(BOM)3 | DOTA-tris(phenylmethyl) ester |
| DOTAM | 1,4,7,10-Tetraazacyclododecane-1,4,7,10-tetraacetamide |
| DOTMA | α,α',α'',α'''-Tetramethyl-DOTA |

| | |
|---|---|
| DT | Dodecanethiol |
| DTMA | *N,N',N'',N'''*-Tetramethyl-DOTAM |
| DTPA | Diethylenetriaminepentaacetic acid |
| DTPA-BMA | DTPA bismethylamide |
| DTTA-MA | Diethylenetriaminetetraacetic acid monoamide |
| EBSS | Earl's Buffered Salt Solution |
| EDC | *N*-(3-Dimethylaminopropyl)-*N'*-ethylcarbodiimide |
| EDTA | Ethylenediamine-*N,N,N',N'*-tetraacetic acid |
| EPI | Echo-planar imaging |
| ESI | Electrospray ionisation |
| $Et_2O$ | Diethyl ether |
| $Et_3N$ | Triethylamine |
| EtOAc | Ethyl acetate |
| EtOH | Ethanol |
| FAB | Fast atom bombardment |
| fMRI | Functional MRI |
| FCS | Foetal calf serum |
| FT | Fourier transform |
| GPC | Gel permeation chromatography |
| HOAt | 1-Hydroxy-7-azabenzotriazole |
| HOBt | 1-Hydroxybenzotriazole |
| HPDO3A | 1,4,7,10-Tetraazacyclododecan-1-(2-hydroxypropyl)-4,7,10-triacetic acid |
| HSA | Human serum albumin |
| I | Initiator |
| ICP-AES | Inductively coupled plasma – Atomic emission spectrometry |
| IR | Infrared; inversion-recovery |
| ME | 2-Mercaptoethanol |
| MeOH | Methanol |
| M.p. | Melting point |
| MP-2269 | *N2,N2*-Bis[2-[bis(carboxymethylamino)ethyl]-*N6*-[*N*-[(4-pentylbicyclo[2.2.2]oct-1-yl)carbonyl]-*L*-α-aspartyl-*L*-α-aspartyl]-*L*-lysinato |
| MRI | Magnetic resonance imaging |

| | |
|---|---|
| MS | Mass spectrometry |
| MS-325 | (*4R*)-1-Oxidato-4-[bis[(carboxymethyl)amino]-6,9-bis[(carboxymethyl]-1-[(4,4-diphenylcyclohexyl)oxy]-1-hydroxy-2-oxa-6,9-diaza-1-phosphaundecan-11-oic acid |
| MTB | Methylthymol Blue |
| MW | Microwave |
| MWCO | Molecular weight cut-off |
| NHS | *N*-Hydroxysuccinimide |
| NMP | 1-Methyl-pyrrolidinone |
| NMR | Nuclear magnetic resonance |
| NMRD | Nuclear magnetic relaxation dispersion |
| NOTA | 1,4,7-Triazacyclononane-1,4,7-triacetic acid |
| ODOTRA | 1-Oxa-4,7,10-triazacyclododecane-4,7,10-triacetic acid |
| PAMAM | Polyamidoamine |
| PC2A | 3,6,9,15-Tetraazabicyclo[9.3.1]pentadeca-1(15),11,13-triene-3,9-diacetic acid |
| PCTA-[12] | 3,6,9,15-Tetraazabicyclo[9.3.1]pentadeca-1(15),11,13-triene-3,6,9-triacetic acid |
| PEDTA | *N*-[2-[Bis(carboxymethyl)amino]ethyl]-*N*-(2-pyridinylmethyl)-glycine |
| ppm | Parts per million |
| PRE | Proton relaxation enhancement |
| RCM | Ring-closing metathesis |
| $R_f$ | Retention factor |
| RIME | Receptor-induced magnetisation enhancement |
| ROMP | Ring-opening metathesis polymerisation |
| RT | Room temperature |
| SE | Spin-echo |
| ST14A | Embryonic striatal temperature sensitive immortalized stem cells |
| Syn-$Cy_2$DOTA | Hexadecahydrodibenzo[b,h][1,4,7,10]tetraazacyclododecane-5,8,13,16-tetraacetic acid |
| TBMP | 2,6-Di-*tert*-butyl-4-methylphenol |
| TBTU | *O*-(Benzotriazol-1-yl)-*N,N,N′,N′*-tetramethyluronium tetrafluoroborate |

| | |
|---|---|
| TETA | 1,4,8,11-Tetraazacyclotetradecane-1,4,8,11-tetraacetic acid |
| TFA | Trifluoroacetic acid |
| THF | Tetrahydrofuran |
| TLC | Thin-layer chromatography |
| TMS | Tetramethylsilane |
| TTP | Tricapped trigonal prism/prismatic |

# 1. Introduction

## 1.1 Magnetic Resonance Imaging

Magnetic Resonance Imaging (MRI) is one of the most common techniques employed in medical diagnostics, and allows us to obtain highly resolved images of the inside of the human body.[1-4] Although based on the principles of Nuclear Magnetic Resonance (NMR), it was preferred to avoid the word "nuclear" because of its negative connotations, and to prevent patients from associating the examination with radiation exposure, which is not one of the safety concerns for MRI.[5]

Magnetic resonance was discovered independently by Felix Bloch[6] and Edward Purcell[7] in 1946, and in the period between 1950 and 1970 NMR applications for chemical and physical molecular analysis were developed. The great opportunities offered by MRI were opened up in 1971, when Raymond Damadian discovered that different types of tissues have different nuclear magnetic relaxation times,[8] thus prompting the scientific community to try and exploit magnetic resonance for human body imaging and the detection of tumours and other diseases. In 1973 Paul Lauterbur applied the principles of magnetic resonance imaging for the first time by performing some scanning on tube samples.[9] In 1975 it was suggested by Richard Ernst to combine the phase and frequency encoding and the Fourier transform to magnetic resonance imaging, thus creating the basic technique for modern MRI methods.[10] Two years later, Peter Mansfield developed the Echo-Planar Imaging (EPI) technique to produce images at video rates (30 ms/image),[11] soon applied by Edelstein and co-workers to carry out imaging of the body; the acquisition of a single image took about five minutes by this technique,[12] compared with the few seconds required nowadays. In 1987, EPI was used to record a movie imaging of a single cardiac cycle;[13] in the same period Charles Dumoulin set up the magnetic resonance angiography, which allows to image the blood while flowing through arteries, veins and capillaries.[14] A technique to map the function of the different zones of the brain through EPI was developed in 1992 and named *functional MRI* (fMRI), which opened up the possibility to discover and assign the regions of the brain responsible for all cerebral activities, such as thought and motor control.[15, 16] In 2003, Lauterbur and Mansfield were awarded with the Nobel Prize in Medicine for their discoveries related to magnetic resonance imaging.[17] At that point, MRI was so commonly used in medical diagnostics that there were approximately

10,000 MRI units worldwide, and approximately 75 million MRI scans performed per year.

### 1.1.1 Mechanism

MRI is a volume imaging technique, i.e. it scans thin slices of the human body and shows on screen the distribution of the NMR signal intensity throughout them (Figure 1.1).

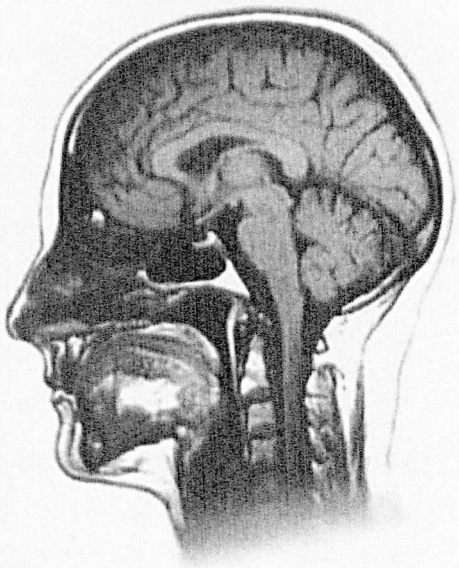


**Figure 1.1** Sagittal MRI image of the skull. [From Radiology Regional Center, Florida; *www.radiologyregional.com/ mri.html,* accessed on September 2005]

The intensity of each element of the picture (*pixel*) is proportional to the NMR signal intensity of the corresponding volume element (*voxel*) in the slice. Thus MRI allows one to obtain images of tissues and organs that are topological representations of NMR parameters, in particular of the longitudinal ($1/T_1$) and transverse ($1/T_2$) relaxation rate of water protons. Basically, the object to be scanned is entered in an external uniform magnetic field, and consequently the magnetisation (i.e. the vectorial sum of the proton spins) adopts an orientation which is parallel in respect to the direction (conventionally considered as the z-axis) of the applied. After that one or more radiofrequency pulses are applied to perturb the proton spins, the z-component of the magnetisation tends to "relax" back to its equilibrium value, according to an exponential recovery whose time constant is known as the *longitudinal* (or *spin-lattice*) *relaxation time* $T_1$. Similarly, the decay of the xy-component of the magnetisation to its equilibrium value of zero is characterised by the *transversal* (or *spin-spin*) *relaxation*

*time* $T_2$. Tissues with short $T_1$ values generally produce a higher image intensity compared to those with longer values, since the steady-state magnetisation along the $z$-axis is greater in the tissue with the fastest relaxation. On the other hand, short $T_2$ values are always associated with a low signal intensity as this decreases the net transverse magnetisation available for detection.

Therefore, MRI is basically an elaborate $^1$H NMR experiment that visualises water molecules in the human body. It is based on the generation of images obtained through the spatial localisation of the tissues' water protons. Compared to a traditional NMR experiment, the spatial information is obtained by the application of three magnetic fields (gradient fields) perpendicular to each other: one to select the slice and the other two to determine the spatial coordinates. As a result, each volume element of the scanned object is identified uniquely. The success of MRI is basically related to the fact that the proton relaxation time depends on the physico-chemical environment of a given tissue, which is modified (and then becomes visible at MRI) in the presence of a pathological state.

## 1.2 Contrast agents for magnetic resonance imaging

Among the many different imaging modalities, MRI might be thought to be that least requiring a pharmacologically-enhanced contrast because it can exploit the intrinsic tissue differences for image contrast by use of a wide variety of pulse sequences and parameters. Nonetheless, contrast agents have been developed for MRI and have found many useful applications.[1, 2, 4, 18-26]

The first usage of a paramagnetic salt (ferric nitrate) to enhance the relaxation rates of water protons was reported by Bloch,[6] and afterwards Bloembergen and Solomon[27-29] developed the standard theory that describes the correlation between the nuclear relaxation rates and the presence of a paramagnetic substance. It was also demonstrated by Eisinger, Shulman, and Blumberg[30] that when a paramagnetic metal ion is bound to a macromolecule the proton relaxation is enhanced as a consequence of the slowing down of the tumbling time, a phenomenon known as *proton relaxation enhancement* (PRE effect). Following his experiment of MR scanning of tube samples[9] (Section 1.1), Lauterbur managed to do the same with the human body in 1977.[31-33] Himself, Mendoca-Dias and Rudin first showed[34] that paramagnetic agents allow further tissue discrimination through the enhancement of water proton relaxation rates,

and their studies were later confirmed by Brady *et al.*[35, 36] The first human NMR imaging study involving a paramagnetic agent was performed by Young *et al.*,[37] while Carr and co-workers demonstrated[38] the diagnostic usefulness of paramagnetic agents by administering $Gd^{III}$-diethylenetriaminepentaacetate $[Gd(DTPA)(H_2O)]^{2-}$ intravenously to patients with cerebral tumours and obtaining a visual enhancement of the damaged region. Nowadays, about 40-50% of the MRI examinations make use of contrast agents,[39] but this percentage is predicted to increase further following the development of more effective and specific contrast media than those currently commercially available. In effect, a great number of pharmaceutical companies make a considerable investment every year in the development of new and improved MRI contrast agents.

### 1.2.1 Mechanism

The effect of such agents is based on the enhancement of the relaxation rates of water protons in the body's tissues where they distribute, thus adding relevant physiological information to the high anatomical resolution usually obtained in the uncontrasted images (Figure 1.2).[40-42] In tissue, MRI contrast agents are not visualised directly on the NMR picture but are rather detected indirectly on the basis of the changes they induce in water proton relaxation behaviour.

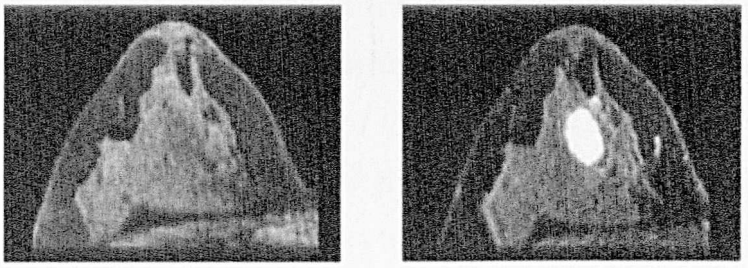


**Figure 1.2** MR images of breast affected by cancer, before (left) and after (right) injection of a contrast agent. [From University of Liverpool website; *http://int.ch.liv.ac.uk/Lanthanide/Ln_Chemistry_folder/MRI%20folder/MRImages.html,* accessed on September 2005]

Relaxation of magnetic resonance signals generally results from the presence of local fluctuating magnetic fields. If we consider a solution of pure water, the most important mechanism whereby such fields are produced is the dipole-dipole interaction between close protons. Each proton has a magnetic dipole moment which produces a small magnetic field at neighbour protons. As a result of Brownian motion of the water molecules, the magnitude of the field experienced by close protons fluctuates randomly,

and this produces relaxation. The relaxation times $T_1$ and $T_2$ are dependent not only on the magnitude of these fields, but also on the time scale (which is expressed in terms of *correlation time*, see Section 1.2.2), and this can cause differences between $T_1$ and $T_2$ under conditions where the average mobility of the water is reduced (as happens in tissues).

Paramagnetic ions have magnetic dipole moments that are of the order of 1000 times as large as that of protons. These large magnetic moments produce correspondingly large local fields and can therefore enhance the relaxation rates of the water protons that are in the proximity of the ions. The closest protons are those of the water molecules that coordinate or bind to the paramagnetic ion in aqueous solution. There is also an *outer sphere* contribution to relaxation that is a direct relaxation effect experienced by water molecules beyond the first hydration shell. In many cases, this can contribute approximately 10% of the total relaxation rate,[43] but in some cases (e.g. when exchange of bound water is very slow or when bound water is totally excluded from a complex) outer sphere effects can predominate. However, it seems likely that the most effective contrast agents will be those for which outer sphere effects will be dominated by effects involving bound water.

All MRI agents are compounds which, thanks to their magnetic moment based on unpaired electron spins (paramagnetism) or on the basis of a bulk magnetic moment of individual particles in suspension, increase longitudinal and transversal relaxation rates (i.e. decrease $T_1$ and $T_2$), but with different degrees. Signal tends to increase with increasing $1/T_1$, while they decrease with increasing $1/T_2$ (Section 1.1.1), as a consequence of the dependence of the longitudinal ($M_z$) and transversal ($M_{xy}$) magnetisation vectors on time ($t$). After a pulse turning the total magnetisation vector from parallel to perpendicular with respect to the external magnetic field, the equation describing the recovery for the component along the $z$-axis from 0 to its maximum value $M_z^0$ is:

$$M_z = M_z^0\left(1 - e^{-t/T_1}\right) \qquad \textbf{(1.1)}$$

Analogously, for the decay of the component laying on the $xy$-plane from its maximum value $M_{xy}^0$:

$$M_{xy} = M_{xy}^0 e^{-t/T_2} \qquad \textbf{(1.2)}$$

The time scale for $T_1$ is seconds, while for $T_2$ is tens to hundreds of milliseconds.

Pulse sequences that emphasise changes in $1/T_1$ are referred to as *$T_1$-weighted*, and the analogue is true for *$T_2$-weighted* scans. The phenomena involved are very complicated and dependent on the nature of the formulation of the agent (e.g., solution or suspension), on the distribution and concentration achieved in the region of interest in normal and abnormal tissues, on field strength, on sequence and on specific sequence parameters. It is evident from this that it is strictly not possible to speak of "$T_1$-" or "$T_2$-agents",[40] although that happens frequently;[2, 42, 44, 45] furthermore, though it is possible to speak of "positive contrast effects" (signal increase) and "negative contrast effects" (signal decrease), it is meaningless to speak of "positive agents" and "negative agents". However, some generalisations can be made: the most frequently used gadolinium chelate agents have predominantly $T_1$ effects in the concentrations and at the field strengths most commonly used, and behave as positive agents on $T_1$-weighted sequences;[2] the particulate superparamagnetic agents (such as iron oxide particles) have predominantly $T_2$ effects, and may be thought as negative contrast agents on $T_2$-weighted sequences.[2] $T_1$ agents usually have $r_2/r_1$ ratios (see Section 1.2.2 below) of 1-2, whereas the same ratios for $T_2$ agents are as high as 10 or more.[2] The choice between the two types of contrast agents depends on the tissue of interest, though bright changes induced by positive contrast agents are generally easier to detect on MR images. The most important consideration for relaxation enhancement is the difference between $T_1$ and $T_2$ shortening mechanisms: the process of $T_1$ shortening requires the direct interaction between protons and the magnetic parts of the contrast agent; in other words, hydrogen nuclei of water molecules must be close to the magnetic particles to obtain relaxation enhancement. The process of $T_2$ shortening, on the other hand, is a remote effect that disturbs $T_2$ relaxation with local magnetic field heterogeneity produced by $T_2$ agents.

In addition to their nuclear relaxation properties, MRI contrast agents must be biocompatible pharmaceuticals. Thus, besides the standard pharmaceutical features, such as water solubility, the requirements relevant for metal-based agents can be classified into three general categories:

1) *relaxivity*: the agent must be effective enough to induce a significant increase in the water proton relaxation rates of the target tissue, also considering that enhancements above 10-20% in $1/T_1$ can be detected by MRI;
2) *in vivo stability, excretability, and lack of toxicity*: the toxicity of a metal complex is mostly dependent on its *in vivo* stability and on the ability of the

body to eliminate it. The doses of heavy metal ions required to obtain a sufficient change in the proton relaxation rate are toxic, thus it is necessary that the complex does not dissociate significantly. The free ligand could also exhibit a certain toxicity degree in case of dissociation. Moreover, the agent should be excreted as soon as possible (ideally within hours from administration) after the image acquisition, in order to minimise the possibility of dangerous interactions with the biological system;

3) *specific in vivo distribution*: preferably, the agent should be able to target a specific tissue or body region.

### 1.2.2 Relaxation theory

The efficiency of a contrast agent is commonly evaluated in terms of its longitudinal ($r_1$) and transversal ($r_2$) relaxivities, defined as the enhancement of the relaxation rates of water proton nuclei per mM solution of metal ion (in units of $mM^{-1}s^{-1}$)

$$r_i = \frac{1/T_i^{obs} - 1/T_i^0}{[M]} \qquad (1.3)$$

where $1/T_i^{obs}$ is the observed relaxation rate, $1/T_i^0$ is the relaxation rate for the solvent, solution or plasma in the absence of the magnetic molecules, and *[M]* is the metal concentration (mM). It usually refers to the value measured at the observation frequency of 20 MHz (0.47 T) and at the temperature of 25 or 39 °C (it has been often recommended to report the value measured at 39 °C because it is much closer to the body temperature, though sometimes chemists prefer to measure this parameter close to room temperature at 25 °C).

For the experimental determination of $r_1$ and $r_2$, the observed relaxation rates $1/T_1^{obs}$ and $1/T_2^{obs}$ are measured and plotted versus the concentration of the metal, thus obtaining straight lines whose slope represents the relaxivity value:

$$\frac{1}{T_i^{obs}} = \frac{1}{T_i^0} + r_i[M] \qquad (1.4)$$

Much work has been done to understand the relationship between structure and dynamics of a paramagnetic complex and the observed relaxivity. The relaxivity results from the sum of contributions regarding the relaxation enhancement of water molecules in the inner ($r_i^{IS}$) and in the outer ($r_i^{OS}$) coordination spheres of the complex,

respectively (Figure 1.3), as a consequence of the contributions determining the observed relaxation times $T_1^{obs}$ and $T_2^{obs}$:

$$\frac{1}{T_i^{obs}} = \frac{1}{T_i^{IS}} + \frac{1}{T_i^{OS}} + \frac{1}{T_i^{0}} \qquad \textbf{(1.5)}$$

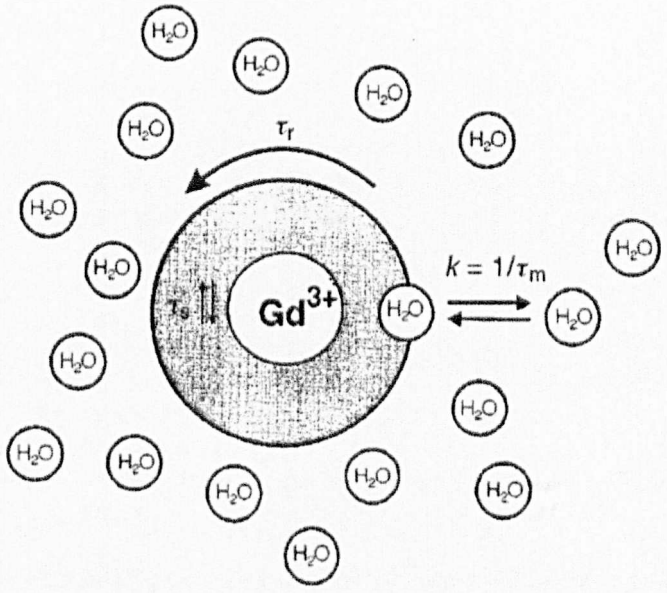



**Figure 1.3** Schematic view of the relaxation mechanisms (and the main relaxation parameters) operating in an aqueous solution containing a paramagnetic $Gd^{III}$ chelate. [From Aime, S. *et al.*; *Chem. Soc. Rev.* **1998**, *27*, 19-29]

The inner sphere contribution arises from the exchange of water directly coordinated to the paramagnetic metal ion and, according to the Solomon-Bloembergen theory,[27-29] it is given by the following equation:

$$\frac{1}{T_i^{IS}} = [M]\frac{q}{55.6}\frac{1}{T_i^{M} + \tau_m} \qquad \textbf{(1.6)}$$

where *[M]* is the metal concentration of paramagnetic ions, $q$ is the hydration number (number of bound water molecules), 55.6 is the molarity of water, $T_i^M$ is the relaxation time of the inner sphere water protons and $\tau_m$ is the exchange time between free and bound water.

Commonly, $T_1^M$ and $T_2^M$ are evaluated on the basis of the expressions developed for simple aqua-ions (Solomon-Bloembergen-Morgan equations):

$$\frac{1}{T_1^M} = \frac{2}{15}\frac{g^2\mu_B^2\gamma_H^2 S(S+1)}{d^6}\left(\frac{3\tau_{c1}}{1+\omega_H^2\tau_{c1}^2} + \frac{7\tau_{c2}}{1+\omega_S^2\tau_{c2}^2}\right) \qquad \textbf{(1.7)}$$

$$\frac{1}{T_2^M} = \frac{1}{15}\frac{g^2\mu_B^2\gamma_H^2 S(S+1)}{d^6}\left(4\tau_{c1} + \frac{3\tau_{c1}}{1+\omega_H^2\tau_{c1}^2} + \frac{13\tau_{c2}}{1+\omega_S^2\tau_{c2}^2}\right) \qquad \textbf{(1.8)}$$

where $g$ is the Landè factor for the free electron, $\mu_B$ is the Bohr magneton, $\gamma_H$ is the proton gyromagnetic ratio, $S$ is the electronic spin quantum number (7/2 for $Gd^{III}$), $d$ is the distance between the metal ion and the protons of the bound water molecules, $\omega_H$ and $\omega_S$ are the proton and electronic Larmor frequencies, respectively ($\omega_S = 658.21\omega_H$), and $\tau_{ci}$ are the correlation times that characterise the time scale of the fluctuation of the dipole-dipole magnetic interaction, and depend on the rotational tumbling time $\tau_r$, the above mentioned exchange time $\tau_m$, and the electron spin relaxation times $\tau_{s1}$ and $\tau_{s2}$ according to the equation

$$\frac{1}{\tau_{ci}} = \frac{1}{\tau_r} + \frac{1}{\tau_m} + \frac{1}{\tau_{si}} \qquad \textbf{(1.9)}$$

Thus, the shortest of the three correlation times determines $\tau_c$ and, then, $T_i^M$ and the overall relaxivity.

Interpretation of the Solomon-Bloembergen equations is complicated by the fact that $\tau_{si}$ is itself dependent on frequency; according to the expression

$$\frac{1}{\tau_{s1}} = C_1\tau_v\left(\frac{1}{1+\omega_S^2\tau_v^2} + \frac{4}{1+4\omega_S^2\tau_v^2}\right) \qquad \textbf{(1.10)}$$

$$\frac{1}{\tau_{s2}} = C_2\tau_v\left(3 + \frac{5}{1+\omega_S^2\tau_v^2} + \frac{2}{1+4\omega_S^2\tau_v^2}\right) \qquad \textbf{(1.11)}$$

where $C_i$ are constants and $\tau_v$ is a field independent correlation time that typically has a value of approximately $10^{-11}$ s.

To further simplify Equations **1.7** and **1.8**, two cases can be considered:

A) $\omega_H\tau_{c1} << 1$;

B) $\omega_H\tau_{c1} \cong 1$ or greater.

For frequencies up to 60 MHz (where $\omega_S = 3.7\cdot10^8$) the former condition holds if $\tau_{c1}$ is $10^{-10}$ s or less. From equation **1.9**, $\tau_{c1}$ will be less than $10^{-10}$ s if any of $\tau_r$, $\tau_m$ *or* $\tau_{s1}$ is less than $10^{-10}$ s. According to the Debye-Stokes theory, the rotational time can be estimated from the expression

$$\tau_r = \frac{4\pi\eta a^3}{3kT} \qquad \textbf{(1.12)}$$

where $\eta$ is the viscosity of the solution, $a$ is the radius of the molecule under consideration, $k$ is the Boltzmann constant and $T$ is the absolute temperature. For water at 20 °C, this formula gives $\tau_r \cong 3\cdot10^{-12}$ s; for free $Gd^{III}$ ions, $\tau_r$ can be calculated as

approximately $10^{-10}$ s, and it has been verified for some gadolinium-complexes that such a condition is true. Therefore, the Solomon-Bloembergen equations can be further simplified as follows

$$\frac{1}{T_1^M} = \frac{2}{15}\frac{g^2\mu_B^2\gamma_H^2 S(S+1)}{d^6}\left(3\tau_{c1} + \frac{7\tau_{c2}}{1+\omega_S^2\tau_{c2}^2}\right) \quad \textbf{(1.13)}$$

$$\frac{1}{T_2^M} = \frac{1}{15}\frac{g^2\mu_B^2\gamma_H^2 S(S+1)}{d^6}\left(7\tau_{c1} + \frac{13\tau_{c2}}{1+\omega_S^2\tau_{c2}^2}\right) \quad \textbf{(1.14)}$$

For large paramagnetic complexes, condition B) can apply, provided that not only $\tau_r$, but also $\tau_m$ and $\tau_s$ are rather long. Under these conditions, $\omega_S\tau_{c2}$ is very much greater than unity, and far greater than $\omega_H\tau_{c1}$, with the result that the Solomon-Bloembergen equations can be simplified as follows

$$\frac{1}{T_1^M} = \frac{2}{15}\frac{g^2\mu_B^2\gamma_H^2 S(S+1)}{d^6}\left(\frac{3\tau_{c1}}{1+\omega_H^2\tau_{c1}^2}\right) \quad \textbf{(1.15)}$$

$$\frac{1}{T_2^M} = \frac{1}{15}\frac{g^2\mu_B^2\gamma_H^2 S(S+1)}{d^6}\left(4\tau_{c1} + \frac{3\tau_{c1}}{1+\omega_H^2\tau_{c1}^2}\right) \quad \textbf{(1.16)}$$

Comparison of data obtained for free $Gd^{III}$ or small gadolinium-complexes and for macromolecular systems reveals two important differences that are of relevance to the use of contrast agents in imaging:

1) the relaxation becomes more efficient because $\tau_{ci}$ increase;
2) the frequency dependence differs considerably for the two conditions A) and B); this is because $\omega_S$ provides the frequency dependence in condition A), whereas $\tau_{si}$ (which through Equation **1.9** become important when $\tau_r$ is long) provide a different type of frequency dependence under condition B).

The outer-sphere term $1/T_i^{OS}$ describes the contribution arising from water molecules which diffuse around the paramagnetic complex and, according to the model developed by Hwang and Freed,[46, 47] can be related to the minimum distance between the metal and the outer-sphere water protons ($a$), the relative solute-solvent diffusion coefficient ($D$) and, again, the electronic relaxation times ($\tau_{si}$):

$$\frac{1}{T_1^{OS}} = C_{OS}\frac{[M]}{aD}\left[3\,J(\omega_H,\tau_{s2}) + 7\,J(\omega_S,\tau_{s1})\right] \quad \textbf{(1.17)}$$

$$\frac{1}{T_2^{OS}} = C_{OS}\frac{M}{aD}\left[2 + 1.5\,J(\omega_H,\tau_{s2}) + 6.5\,J(\omega_S,\tau_{s1})\right] \quad \textbf{(1.18)}$$

where $C_{OS}$ is a constant ($5.8 \cdot 10^{-13} s^{-2} M^{-1}$), *[M]* is the concentration of the complex, and the dependence on the electronic relaxation times is expressed in the non-Lorentzian spectral density functions $J(\omega_X, \tau_{si})$.[48]

As has been said above, a parameter which the Solomon-Bloembergen-Morgan equations depend on is the external magnetic field strength: for instance, in Equation **1.7** the two terms inside the last factor in brackets (the so-called *3-term* and *7-term*) have field dependence. The 3-term is a function of the nuclear precession frequency, while the 7-term is a function of the electron precession frequency. Since the gyromagnetic ratio for the electron is much greater than for a proton ($\gamma_S/\gamma_H = 658$), at high fields $\omega_S^2 \tau_{c2}^2$ will be so greater than 1 that the 7-term will tend to zero, and the overall relaxivity will be dominated by the 3-term. The measurement of relaxation rates as a function of magnetic field (called *nuclear magnetic relaxation dispersion*, *NMRD*) is widely used to characterise contrast agents. As shown in Figure 1.4, the typical profile for a slowly rotating molecule differs remarkably from a more rapidly tumbling one.

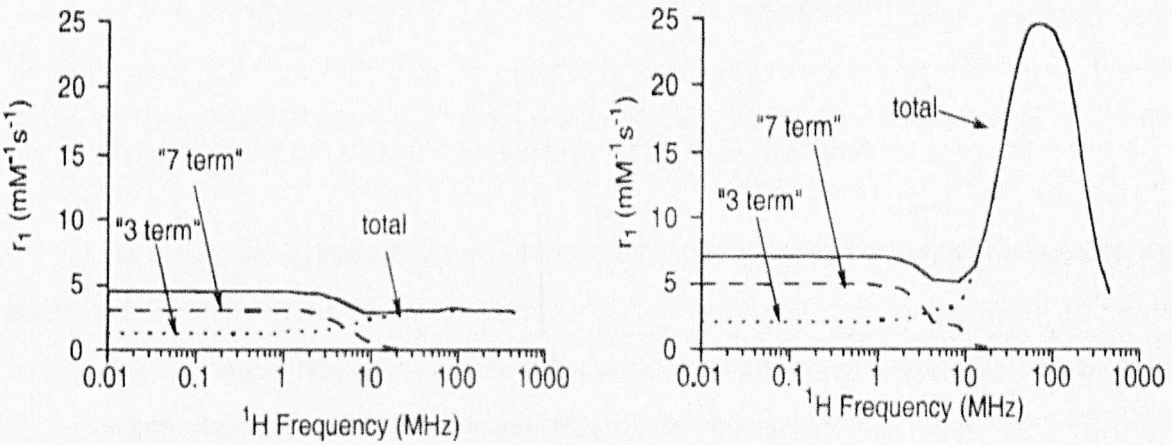



**Figure 1.4** Simulated inner-sphere relaxivities. Left: $\tau_r$ = 0.1 ns. Right: $\tau_r$ = 1 ns.. [From Caravan, P. *et al.*; *Chem. Rev.* **1999**, *99*, 2293-2352]

In fact, at ~5 MHz the only dispersion is that of the 7-term, while the 3-term does not disperse, under these conditions, until ~1000 MHz. Increasing $\tau_r$ allows the frequency dependence of $\tau_{s1}$ to be expressed (Equation **1.10**). Experimentally, the solvent relaxation rate can be measured over a wide range of magnetic fields, and the obtained data points representing the NMRD profile can be adequately fitted to yield the values of the relaxation parameters.

Relaxivity reaches a maximum when the correlation time $\tau_{c1}$ is the inverse of the proton Larmor frequency. As $\tau_m$ is present in both Equations **1.6** and **1.7**, there is a

conflict: in the basis of Equation **1.6**, it would be desirable to have $\tau_m << T_1^M$; however, if $\tau_m$ is too short, it will begin to influence $T_1^M$. The optimum value for $\tau_m$ is about $10^{-8}$ s. In Figure 1.5, the influence of $\tau_{s1}$, $\tau_r$ and $\tau_m$ on relaxivity at two common imaging fields is shown.

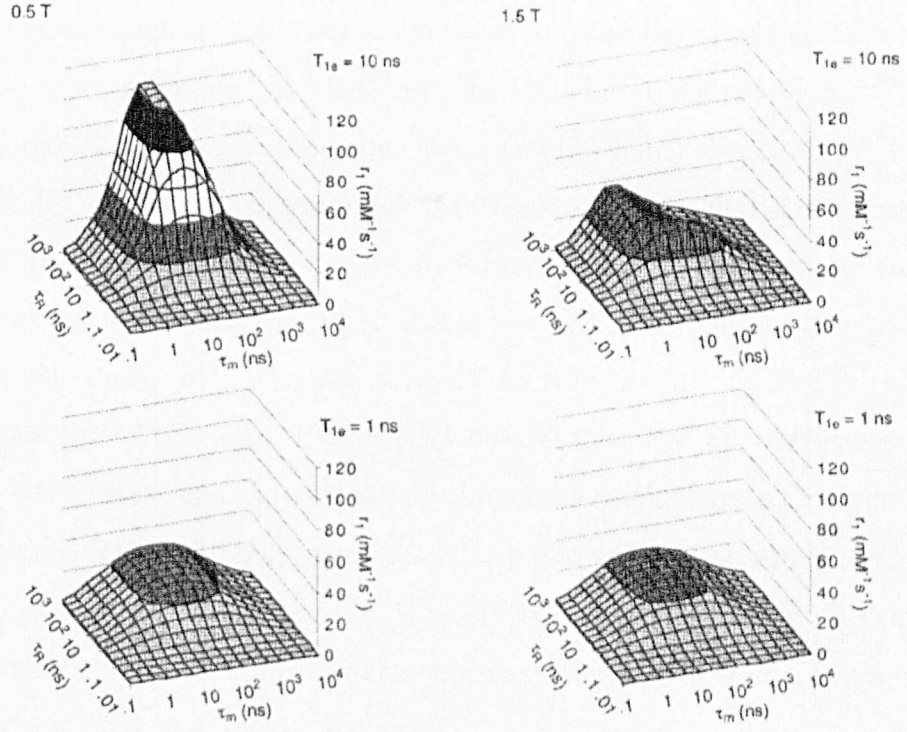



**Figure 1.5** Inner-sphere relaxivities calculated as a function of $\tau_m$ and $\tau_r$ for various values of $\tau_{s1}$ at 0.5 T and 1.5 T, with $q = 1$ and $d = 3.1$ Å. [From Caravan, P. *et al.*; *Chem. Rev.* **1999**, *99*, 2293-2352]

At these field strengths, the 7-term tends to zero and, consequently, $\tau_{s2}$ can be neglected. There are two points to note:

1) the maximum relaxivity achievable decreases with increasing the field strength;

2) when one parameter is optimised, the others become more critical.

The dependence of the relaxivity $r_1$ on different correlation times is shown in Figure 1.6.

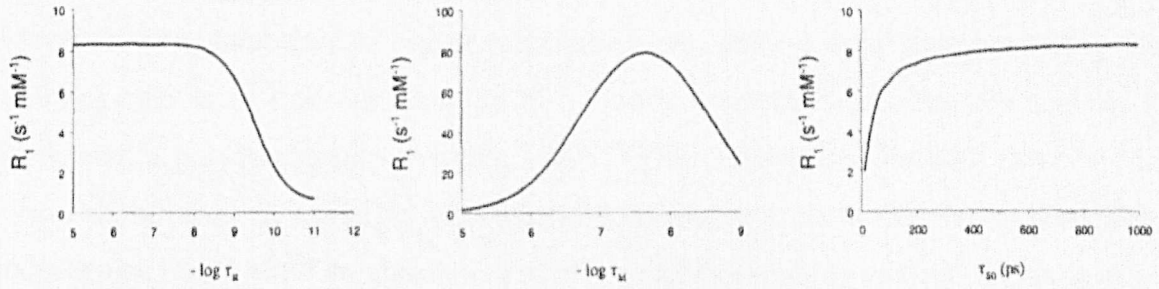



**Figure 1.6** Simulated inner-sphere proton relaxivities (here indicated with $R_1$) at 20 MHz. Left: $\tau_m$=2μs, $\tau_{s0}$=850 ps, $\tau_v$=20 ps. Centre: $\tau_r$=10 ns, $\tau_{s0}$=850 ps, $\tau_v$=20 ps. Right: $\tau_m$=2μs, $\tau_r$=10 ns, $\tau_v$=20 ps. The graphs were simulated using Solomon-Bloembergen-Morgan equations (Section 1.2.2). [From Peters, J. A. *et al.*; *Prog. Nucl. Magn. Reson. Spectrosc.* **1996**, *28*, 283-350]

### 1.2.3 Strategies in development of contrast agents for MRI

On the basis of the above discussion and equations, some factors that govern the potential value of contrast agents are to be considered.

First of all, to produce strong relaxation effects, the paramagnetic ion should preferably have a high spin number *S*. However, such an ion must also have reasonably long values of $\tau_{si}$. $\tau_{si}$ for $Mn^{II}$ and $Gd^{III}$ are longer than for most other ions.[49-51]

Moreover, the paramagnetic ion should bind directly to the water. Hypothetically it would be preferred that each ion was bound to several water molecules, because of the effect of the hydration number *q* on relaxivity (see Section 1.2.2). However it has been shown[52] that stability (and also water-exchange rate) issues can rise when coordination sites are occupied by further water molecules rather than a multi-dentate ligand (see also Section 1.3.1 below). The $1/d^6$ dependence in Equations **1.7** and **1.8** makes this a particularly important consideration; when designing paramagnetic complexes it is important to ensure that water is not totally excluded from direct access to the paramagnetic ion. If water were totally excluded, relaxation could still be produced by outer sphere effects, but the efficiency of such a relaxation would be small.

In addition to the characteristics of the metal centre and the number of water molecules in the inner coordination sphere, the relaxivity of a contrast agent is determined by several parameters. As reported above, at the magnetic field strengths used in MRI scans (0.5-1.5 T, 20-60 MHz) the relaxation times $T_i^M$ of bound water protons are dominated by electronic ($\tau_{si}$) and reorientational ($\tau_r$) correlation times, and by the exchange lifetime ($\tau_m$) of the coordinated water molecules. While the modulation of $\tau_s$ appears difficult to obtain, a number of approaches have been tried to lengthen $\tau_r$, as the slower the agent is tumbling, the longer the correlation time leading to faster relaxation rates (and thus to higher relaxivities). A common approach to slowing the tumbling rate is to link the complex to a slowly rotating macromolecule such as a dendrimer, a polysaccharide, a protein, etc.[2, 42] This linkage can consist[53] either in the formation of covalent bonds between the two systems, or in the realisation of reversible adducts as a result of the establishment of non-covalent bonds as well as of trapping the complex inside the macromolecular structure during its formation. An additional advantage of these macromolecular entities is that they have longer lifetime blood flow, a good aspect for the development of angiographic applications. However, the

relaxivities found for such systems developed so far are lower than the theoretical values expected on the basis of their reorientational times, mainly because of structures affecting the water exchange, as well as local freedom of rotation of the complexes that partially counterbalances the gain from the global molecular tumbling (see Section 1.3.1.1 below for more details).

The possibility to regulate the rate of exchange ($1/\tau_m$) of the water molecules bound to a contrast agent may seem difficult, but recently some steps have been made to understand the exchange mechanisms and permit control of this parameter. The total charge of a complex has a great effect on $1/\tau_m$, as the water on positively charged systems exchanges more slowly than with neutral complexes, and the latter exchange more slowly than if negatively charged ones are compared. $\tau_m$ also depends on the extent of second sphere hydration, which is determined by the hydrophobicity of the complex, as well as by the conformational equilibrium that every ligand undergoes, where different values of $\tau_m$ correspond to different conformers. Particular modifications of the ligand structure have been made to favour either side of such equilibrium.[54, 55] The nature of the counterions also affects the water exchange rate,[54] as it determines the outer-sphere hydration structure together with the charge density of the metal ion: more highly charged ions and higher charge densities impose strong electrostatic order, breaking relatively weak hydrogen bonds and creating a well-defined and ordered second sphere of hydration through which water molecules exchange relatively slowly. On the other hand, less charge dense ions (e.g., large ions) do not perturb the bulk water hydrogen bonding significantly, allowing water to exchange more easily with the metal centre. A rough scale for obtaining higher relaxivities is $I^-$ >$Br^-$>$AcO^-$>$CF_3COO^-$>triflate>$SO_4^{2-}$>$Cl^-$ (Figure 1.7).

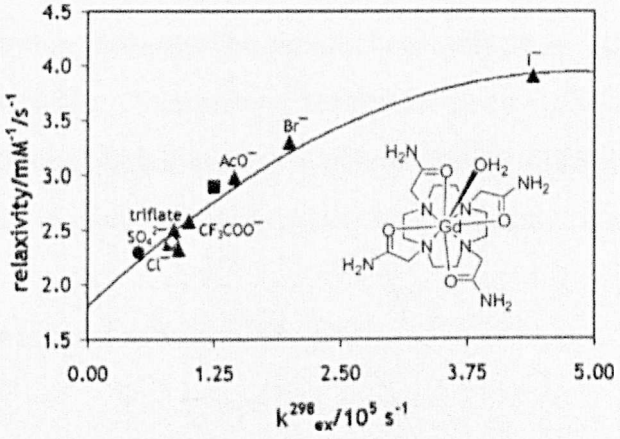



**Fig 1.7** Variation of water proton relaxivity (298 K, 20 MHz) with water exchange rate for the series of $GdL(OH_2)X_3$ complexes changing the anion as shown. Data obtained for two anionic complexes (circles and squares) are shown for comparison. [From Parker, D. *Chem. Soc. Rev.* **2004**, *33*, 156]

### 1.2.4 Toxicity of metal complexes

Toxic effects from a metal complex can arise from:

a) free metal ion, released by dissociation;

b) free ligand and its metabolites, which also arise from dissociation;

c) the intact metal complex.

The available toxicological data[1, 2, 42] show the importance of metal complex dissociation as a source of toxicity. Both metal ions and free ligands tend to be more toxic than metal chelates. This is reasonable considering that complexation itself "neutralizes" the coordinating properties of both the ligand and the metal ion, decreasing their ability to bind to proteins, enzymes, or membranes *via* intermolecular interactions, or even covalent bonds. As its simplest, the degree of toxicity of a metal chelate is related to its degree and rate of dissociation *in vivo* before excretion. The coordination of metal ions to oxygen, nitrogen, or sulphur atoms in macromolecules and membranes alters the dynamic equilibria necessary to sustain life. $Gd^{III}$, for example, can bind to $Ca^{II}$ binding sites, often with higher affinity, owing to its greater charge/radius ratio.[56] Moreover, it can be complexed by a variety of ligands, such as $OH^-$, citrate, phosphate, carbonate, dicarboxylic acids, bicarbonate, transferrin, oxalic acid, etc. The toxicity of free ligands, which is less understood, can derive from the sequestration of essential metal ions such as $Ca^{II}$, $Mg^{II}$, $Zn^{II}$ and $Cu^{II}$, in addition to "organic" toxicity.[1, 2, 42] Intact metal complexes present a wide variety of specific and nonspecific effects: a difference in osmolality between intracellular and extracellular environments is established after injection of large quantities of the ionic complexes and appropriate counter ions; water is drawn out of cells as a result of the osmotic gradient, causing cellular and circulatory damage. Other possible mechanisms of chelate toxicity include enzyme inhibition, non-specific protein conformational effects, or alteration of membrane potentials. The interactions between metal chelates and biological macromolecular structures, which are not well understood, represent an important area of investigation related to understanding toxicity on a molecular basis.

#### 1.2.4.1 Stability of metal complexes *in vivo*

The stability requirements for metal complexes are specifically kinetic, not thermodynamic, requirements.[1, 2] The agent should be efficiently eliminated from the

body within hours after its administration, and stability is thus required only during this residence time. Unfortunately, the spherical electronic distribution of $Fe^{III}$, $Mn^{II}$ and $Gd^{III}$ is detrimental to the stability of their complexes. The absence of a sufficient ligand-field stabilization energy in complexes of these ions leads, generally, to very weak metal-ligand bonds. Kinetic stability must therefore derive from the structure of a suitable multi-dentate ligand. Thermodynamic considerations are also important to establish the source of instability: a variety of coordinating species and proteins can compete for the paramagnetic metal ion, as well as other metal ions can compete for the multidentate ligand. The biological environment thus provides a very rigorous test for the stability of a metal complex. Finally, an important thermodynamic side effect for trivalent metal ions in serum is their precipitation with commonly present anions like hydroxide, carbonate or phosphate.

In the effort to design improved MRI contrast agents, synthetic methods have been developed particularly towards kinetically inert $Gd^{III}$-complexes. Some of them are flexible enough to allow specific substitutions on the complexes which are capable to modulate their properties. At the same time, an in-depth understanding of the factors affecting the kinetic stability of metal complexes is needed in serum and other physiological environments.

Although iron oxide nanoparticles are commonly used as MRI "negative" contrast agents for oral administration or cell labelling (despite their drawbacks, see Section 1.2.7 below), gadolinium remains the metal of choice to design novel CAs because of its positive contrast effect (easier to identify on a MRI scan) and magnetic properties. However, CAs based on manganese have recently attracted more and more attention especially after gadolinium has been linked to the Nephrogenic Systemic Fibrosis disorder (see Section 1.3 below).

#### 1.2.4.2 Excretability

After intravenous administration, a metal complex rapidly diffuses in the fluid compartments between blood vessels and cells, spaces that are commonly referred to as the *extracellular compartment*. Depending on its structure, the chelate can even distribute into various intracellular environments. Finally, also the excretion pathway is determined by the molecular structure. Usually, small molecular weight hydrophilic chelates that are not capable to bind to plasma proteins are filtered out in the kidneys

(*glomerular filtration*).[3, 40, 57-60] If the molecule has not a strong hydrophilic or hydrophobic character, and especially if it contains aromatic moieties, some amount of the complex is taken up by cells in the liver and eliminated *via* the bile (*hepatobiliary excretion*).[19, 61] Such molecules usually show some ability to bind to plasma proteins, particularly albumin, and this reduces the amount available for glomerular filtration. The renal and hepatobiliary pathways can thus be competitive.[1] Generally, the greater the degree of lipophilicity of a molecule, the greater the hepatobiliary excretion. Of course it is desirable that complete clearance of the agent from the body takes place by such routes in order to minimize toxicity. However, when the complex is very lipophilic it can distribute into fat tissues or membranes, or precipitate in blood vessels and be uptaken by reticuloendothelial cells in the spleen and/or in the liver.[1] These possibilities cause a long-term retention of the agent, which may be associated with chronic toxicity.[1]

### 1.2.5 *In vivo* targeting

Targeting a paramagnetic agent to a particular site within the body is one of the most challenging aspects of NMR contrast agent design.[1-3, 22, 41, 42, 62-66] The diagnostic utility of a contrast-enhanced NMR imaging examination will depend on the absolute concentration of the agent in the desired tissue and on the relative distribution in all tissues. Exclusive targeting is rarely achieved. After administration, the agent equilibrates preferentially in several body compartments prior to excretion; preferential distribution of the agent to the desired site is all that can be expected in most circumstances. However, the dependence of relaxivity on the chemical environment alters this simple view. What is directly relevant to NMR imaging is not the actual distribution of the agent but the distribution of the relaxation rate changes induced by the agent. The enhancement in relaxivity induced by binding the agent to a macromolecule (the PRE effect, Section 1.2) is of central importance.[1, 42, 67, 68] By targeting a complex to sites where binding interactions can occur, the induced increase in relaxation rate may be far higher than the one expected on the basis of the local concentration of the complex solely.

### 1.2.6 Smart contrast agents

One of the most exciting areas of research about contrast agents is that concerning responsive or "smart" contrast agents,[42, 69] whose relaxivity is modulated by changes in physiological environment such as pH, partial oxygen pressure, metal ion concentration, or enzyme activity.

Research into pH-responsive contrast agents[69-79] is driven by the fact that the pH in solid human tumours is approximately 0.4-0.6 units lower than in healthy tissues. This pH decrease is attributed to the extensive production of lactic acid within tumour cells.[80, 81] Therefore, if one can design a contrast agent that responds to such small changes in pH this can be used to highlight or to map tumours on the basis of pH itself. Usually, relaxivity is rendered a function of pH by virtue of a pH-dependent change in hydration state $q$,[71, 72, 76-78] but pH-dependence can also involve the protonation of the ligand or, for polymeric agents, the structure of the macromolecule.[70, 74]

The partial oxygen pressure ($pO_2$) is particularly significant in metabolic processes of cells, and its variation from normal values often indicates pathologies, such as ischemic diseases, strokes and tumours. Accurate and localised measurements of oxygen concentration are also desirable for differentiation between venous and arterial blood, or for cerebral mapping of task activation. $pO_2$-responsive contrast agents[26, 69, 82-85] that respond to changes in partial oxygen pressure, are currently being investigated, based on metal complexes whose central ion can change its oxidation state depending on the biological environment, with the two oxidation state forms having different relaxation properties.

Several metal ions play a crucial role in biological processes, whereas some others are toxic.[86] Alteration of the metal concentration in the body can often be correlated to disease states. For this reason, metal ion-responsive contrast agents,[22, 69, 87] that respond to different *in vivo* concentrations of certain metal ions, are currently of interest. The classic ones are $Ca^{II}$ responsive agents, as $Ca^{2+}$ is an important intracellular secondary messenger of signal transduction, and changes in the cytosolic concentration of $Ca^{2+}$ produce changes in cellular metabolism and are responsible for cell signalling and regulation. Anyway, efforts have been recently directed towards $Zn^{II}$ and $Fe^{II/III}$. The change in relaxivity is due to a change in the coordination geometry of the complex following the complexation of the metal ion, thus displacing an inner-sphere water molecule and consequently turning off the activity of the agent.

Enzymatically responsive contrast agents[69, 88, 89] are being studied to detect enzymes associated with a disease state. They are designed to be MRI silent until activated by a specific enzyme, which can "switch on" the high relaxivity.

### 1.2.7 Labelling of stem cells

Stem cells have become the centre of great attention because of their ability to turn into all the different cell types that make up complex organisms, and it seems possible to drive such differentiation by modifying the chemical and biological environment. The implications for medicine are far reaching, but practical and ethical barriers stand in the way.[90, 91]

There are complex academic definitions for "stem cells", but the basic concept is that such cells are unspecialized cells that can differentiate into specialized cell types with specific functions in the body. Cells with this ability are called *pluripotent* (*plures*, meaning several).[90, 91] Besides the development stage, stem cells can also be found in adult tissues: for instance, adult muscle stem cells can repair a muscle,[90, 91] while haematopoietic stem cells are well known to be able to produce all the different types of blood cells.[90, 91]

Early human stem cells have at least two advantages: the first consists in the fact that they allow us to have an insight of the mechanisms at the basis of the early human development; secondly, since they can differentiate into those cells that are non-reproductive in an adult human body, they offer the opportunity to investigate cell replacement processes. In other words, studying stem cells could lead to many beneficial achievements in medicine and diagnosis, ranging from repairing brain damage to learning about the molecular processes behind the development of tumours.

The possibility of an *in vivo* visualisation would allow monitoring of the fate of transplanted cells. Current MRI technology displays a very good spatial resolution, and is the technique of choice to observe a very small number of cells. However, cells have to be labelled prior to transplantation with a suitable contrast agent, through their incubation with the marker in suitable conditions.[90, 91]

So far, the labelling of cells[92] has been obtained mainly using superparamagnetic iron oxide particles (with negative or $T_2$-contrast effect).[93-96] Nevertheless, the use of such particles has some drawbacks.[66] First, their functionalisation cannot be specific in number and position of moieties introduced. Furthermore, since they act primarily as $T_2$

(negative) agents producing dark spots in the MR images, they are particularly effective for applications dealing with anatomical regions (e.g. brain) characterized by intense MR signals, and therefore problems might arise when the detection of grafted cells involves a region with a low intrinsic MR signal. Moreover, it has been shown that the distribution and morphology of endosomes filled with iron-oxide particles are highly sensitive to the effects of external static magnetic fields:[97] in fact, such magnetic compartments are deformed along the field and attract each other to form chaplets within the cytoplasm. Finally, as the tolerance towards such compounds is sometimes limited by their coating,[98] they should be administered through low infusions.

Until now, very few agents based on paramagnetic complexes have been used to label stem cells,[99-101] although with good results in terms of cellular uptake and relaxivity performance.

## 1.3 Gadolinium complexes

The $Gd^{III}$ ion has a number of properties that makes it particularly suitable for this kind of application:

1) it has a high paramagnetism (7 unpaired electrons);
2) it has a relatively long electronic relaxation time, as the symmetric S-state of $Gd^{III}$ is a more hospitable environment for electron spins leading to a much slower electronic relaxation rate;
3) it forms stable chelates, usually containing one or two water molecules in its inner coordination sphere.

Because of their large size, lanthanides tend to favour high coordination numbers in aqueous media: all gadolinium(III)-based chelates approved so far for use in MRI are nine-coordinated complexes in which a ligand occupies eight binding sites at the metal centre and the ninth coordination site is occupied by a water molecule; for nine-coordinated complexes the ideal coordination geometries are the tricapped trigonal prism (TTP) and the monocapped square antiprism (CSAP), as shown in Figure 1.8.[1,2]

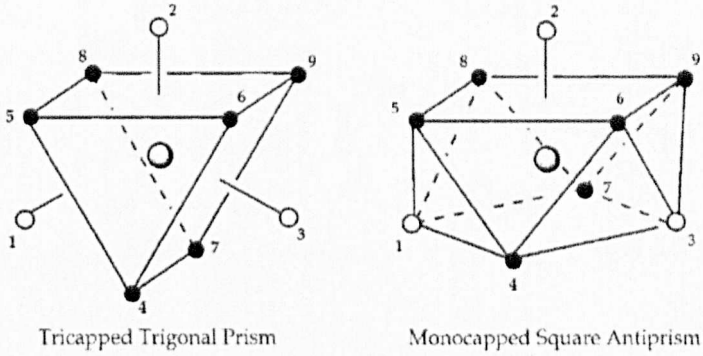



**Figure 1.8** Tricapped trigonal prism (TTP) and monocapped square antiprism (CSAP) geometries. [From Caravan, P. *et al.*; *Chem. Rev.* **1999**, *99*, 2293-2352]

The high thermodynamic stability of certain gadolinium-chelates (usual log $K_{ass}$ included between $10^{16}$ and $10^{23}$)[56] is a compulsory requirement in order to avoid the release in the body of free $Gd^{III}$ ions, which could be very toxic even at low doses[42] ($LD_{50} \cong 0.1$ mmol/Kg). It is clear that the integrity of the gadolinium-complex must be maintained *in vivo* in order to create a safe and efficacious MRI agent. Dissociation of $Gd^{III}$ from an MRI contrast agent is undesirable, as both the free metal and unchelated ligands are generally more toxic than the complex itself (Section 1.2.4). Free $Gd^{III}$ is known to bind to serum proteins such as transferrin and albumin, for instance by tyrosine residues;[102-105] eventually much of the released metal comes to reside in the bones, where it becomes tightly and irreversibly associated. Detection of significant amounts of $Gd^{III}$ in skeletal tissue is the typical consequence of $Gd^{III}$ dissociation from a chelate. Low molecular weight gadolinium chelates also accumulate in the extracellular space where blood brain barrier lesion may have occurred.

A disorder (Nephrogenic Systemic Fibrosis, NSF) known since 1997 has been associated in 2006 with the use of Gd-based MRI contrast agents.[106-111] It can occur in patients with decreased renal efficiency caused by an end-stage or chronic kidney disease or a kidney injury.

While fast kinetics are characteristic of metal complexes derived from acyclic ligands, a remarkable amount of literature has shown that macrocylic complexes tend to be significantly more inert.[2, 112-114] Currently, the search for new contrast agents for MRI is directed mainly toward the synthesis of gadolinium(III)-complexes of functionalized derivatives of DTPA (DTPA= diethylenetriaminepentaacetic acid, Figure 1.9, **1**) and DOTA (DOTA= 1,4,7,10-tetraazacyclododecan-1,4,7,10-tetraacetic acid, Figure 1.9, **2**) ligands without altering their chelating abilities.[42, 69, 115]

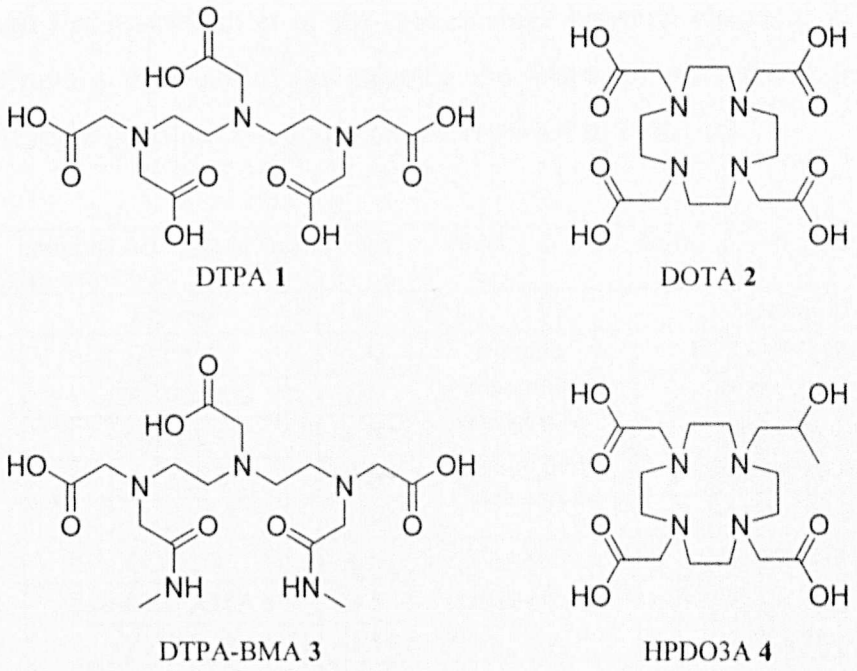



**Figure 1.9** The four polyaminocarboxylic ligands of the MRI contrast agents approved for clinical use.

Those two basic ligands are, in fact, simple and effective, commercially available or readily prepared, and in principle easy to modify to obtain the desired structure. The reason why DTPA is still used in spite of the relatively minor stability of its complexes is mainly that it is much cheaper (DTPA 99%, 100 g = £180.50, Sigma-Aldrich) than DOTA (DOTA 97%, 250 mg = £173.50, Sigma-Aldrich).

The first contrast agent approved for clinical use was Gd-DTPA[116-121] under the trade name of Magnevist™ (Schering AG, Germany). It has been followed by three other gadolinium(III)-based contrast agents whose properties are very similar to those shown by Gd-DTPA: Gd-DOTA[122-125] (Dotarem™, Guerbet SA, France), Gd-DTPA-BMA[2, 42, 126-128] (BMA = bismethylamide, Figure 1.9, **3**; Omniscan™, Amersham-Nycomed, Norway) and Gd-HPDO3A[18, 99, 129-131] (HPDO3A = 1,4,7,10-tetraazacyclododecan-1-(2-hydroxypropyl)-4,7,10-triacetic acid, Figure 1.9, **4**; Prohance™, Bracco Imaging, Italy).

All four contrast agents have similar pharmacokinetic properties, as they distribute in the extracellular fluid and are excreted *via* glomerular filtration.

### 1.3.1 Types of gadolinium-complexes

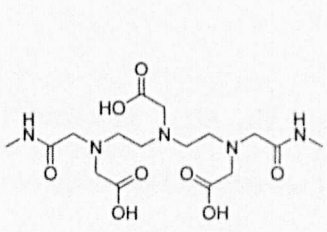
So far, gadolinium complexes have attracted the most attention and have found the most widespread practical application. In literature, hundreds of different ligands for $Gd^{III}$ have been reported, in the attempt of designing more and more effective contrast

agents through the investigation of the relationships between chemical structure and factors determining their ability to enhance the water proton relaxation rate. The relaxivities of some gadolinium-complexes are reported in Table 1.1.

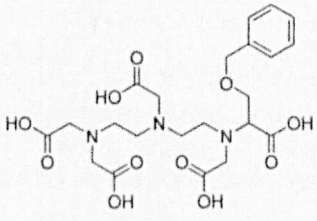
**Table 1.1** Longitudinal proton relaxivities $r_1$ ($mM^{-1}$ $s^{-1}$, 20 MHz, 37 °C) for selected gadolinium(III)-complexes.

| | *Ligand* | $r_1$ | | *Ligand* | $r_1$ |
|---|---|---|---|---|---|
| *DTPA derivatives* | DTPA **1** | 4.02 | *Pyridine containing macrocycles* | PCTA-[12] **18** | 6.9 |
| | DTPA-BMA **3** | 3.96 | | PC2A **19** | 7.5 |
| | BOPTA **5** | 4.39 | | BP2A **20** | 8.27 |
| | MS-325 **6** | 6.6 | *Other acyclic* | EDTA **21** | 6.15 |
| | MP-2269 **7** | 5.64 | | PEDTA **22** | 8.8 |
| *DOTA derivative* | DOTA **2** | 3.83 | *Other cyclic* | ODOTRA **23** | n.a. |
| | Syn-Cy2-DOTA **8** | 4.5 | | TETA **24** | n.a. |
| | DOTMA **9** | 3.8 | | NOTA **25** | n.a. |
| | DOTAM **10** | 2.5 | *Macromolecular* | DTPA-polylysine **26** | 13.1 |
| | DTMA **11** | 2.5 | | DTPA-dextran **27** | 11 |
| | DOTA(BOM) **12** | 5.4 | | DTPA-cascade-polymer | 11.9 |
| | Cis-DOTA(BOM)2 **13** | 6.8 | | G2(N[CS]N-bz-DTPA)$_{12}$ **28** | 21.3 |
| | DOTA(BOM)3 **14** | 7.5 | | Gadomer 17 **29** | 17.3 |
| *DO3A derivatives* | DO3A **16** | 4.8 | *Protein bound* | MS-325-HSA | 48.9 |
| | DO3MA **17** | 4.4 | | MP-2269-BSA | 24.5 |
| | HPDO3A **4** | 3.7 | | | |

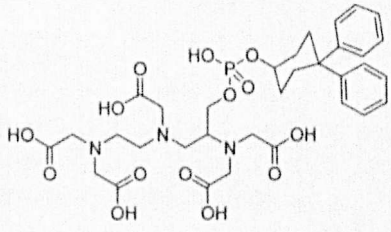
Most of the ligands proposed in the literature are derivatives of DTPA (Figure 1.10) or DOTA (Figure 1.11), where the latter can be considered a functionalised 1,4,7,10-tetraazacyclododecane, or cyclen **15**.



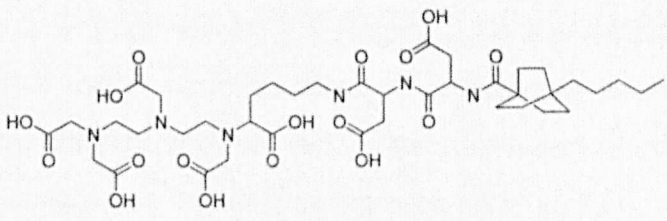
DTPA-BMA **3**



BOPTA **5**



MS-325 **6**



MP-2269 **7**

**Figure 1.10** Some of the most effective DTPA-derivatives. **5**, **6** and **7** have been successfully used to bind non-covalently with Human Serum Albumin (Section 1.3.1.1). Stability constants for the corresponding Gd-complexes are reported in Table 1.2. Relaxivities are reported in Table 1.1.

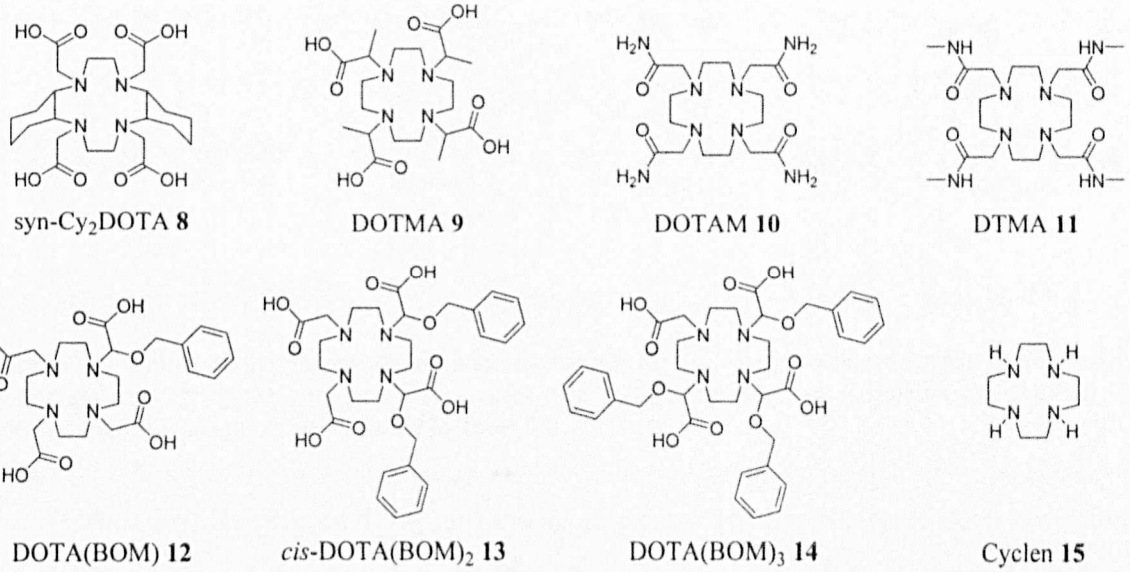



**Figure 1.11** Some particularly successful DOTA-derivatives, and the basic structure of Cyclen **15**. For the DOTA-derivatives, stability constants of the corresponding Gd-complexes are reported in Table 1.2. Relaxivities are reported in Table 1.1.

Analogously, functionalised cyclens are also 1,4,7,10-tetraazacyclododecane-1,4,7-tetraacetic acid (DO3A **16**) and its derivatives (Figure 1.12), where one of the acetate arms is missing compared to DOTA-derivatives, in order to allow a second water molecule to coordinate to the gadolinium ion, thus theoretically increasing the relaxivity ($q = 2$ in equation **1.6**; see Section 1.2.2).

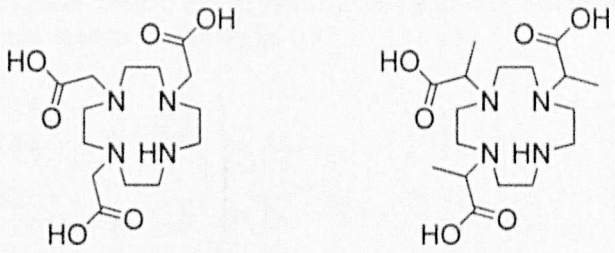
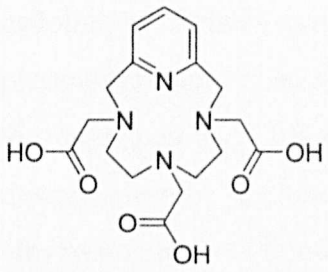
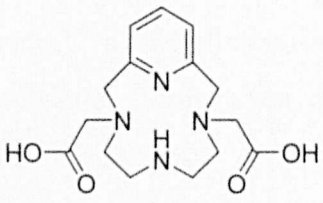



**Figure 1.12** DO3A and one of its derivatives, ligands for $Gd^{3+}$ where just 3 of the 4 nitrogens are functionalised with acetate arms, so allowing binding of a further water molecule. Relaxivities for the corresponding Gd-complexes are reported in Table 1.1. Stability constants are reported in Table 1.2.

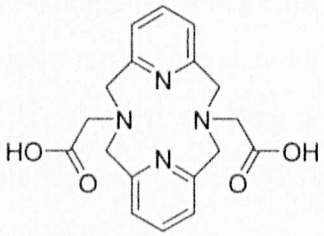
Nevertheless, such ligands form less stable complexes,[52] and the same is true for pyridine-containing cyclen-derivatives[132-136] (Figure 1.13), a particular class of chelating agents where a further cycle is condensed to the macrocycle in order to rigidify the structure. In this case, the reason of the lack of stability seems to be the asymmetry of the complex, but no satisfactory explanation has been given so far.



PCTA-[12] **18**



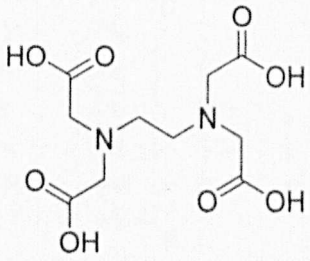
PC2A **19**



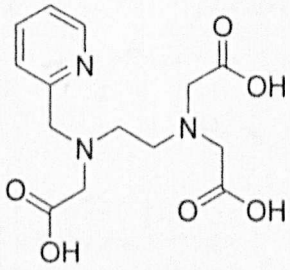
BP2A **20**

**Figure 1.13** Pyridine-containing cyclen-derivatives, ligands for $Gd^{3+}$ used to test the effect on relaxivity by increased rigidity of the structure. Relaxivities of the corresponding Gd-complexes are reported in Table 1.1. Stability constants are reported in Table 1.2.

Other acyclic (Figure 1.14) and cyclic (Figure 1.15) ligands have been tried, but their structures do not permit to bind $Gd^{III}$ with sufficient strength to allow their clinical use.

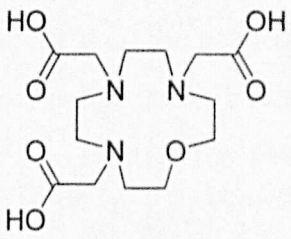


EDTA **21**

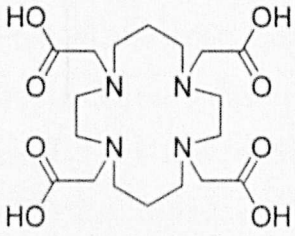


PEDTA **22**

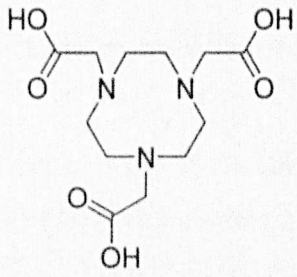
**Figure 1.14** Two acyclic ligands used to test stability of Gd-complexes, whose relaxivities are reported in Table 1.1. Stability constants are reported in Table 1.2.



ODOTRA **23**



TETA **24**



NOTA **25**

**Figure 1.15** Cyclic ligands not based on the cyclen structure and used to test stability of Gd-complexes, whose relaxivities are reported in Table 1.1. Stability constants are reported in Table 1.2.

### 1.3.1.1 Macromolecular contrast agents

As previously discussed (Section 1.2.3), an enhancement of relaxivity can be achieved by increasing the size of the complexes either by forming a covalent linkage[112] between the complex and a macromolecular substrate or by forming a non-covalent adduct between the complex and a slowly tumbling system.[2, 42] Attachment of

gadolinium-chelates to macromolecules has the further partial advantage to increase the plasma persistence (up to 15 hours),[137] as the elimination, primarily renal, first requires the degradation of the macromolecule. Conjugation methods for linking chelates to macromolecules include the functionalization of primary amines using acylation, alkylation, ureas or thiourea formation, and reductive amination.

One of the macromolecular structures that has been derivatised with gadolinium chelates is polylysine, commercially available in different molecular weight ranges (500-2000 up to 150000-300000 and more). The reactive ε-amino group of the lysine backbone is typically modified with acyclic or macrocyclic polyaminocarboxylate derivatives[2, 42, 68, 74, 137-142] (Figure 1.16).

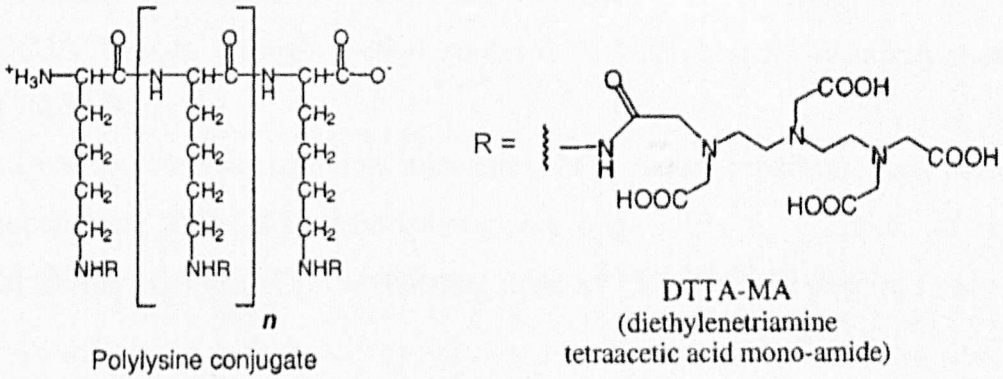



**Figure 1.16** Chemical structure of polylysine – DTTA-MA conjugate **26**. [From Caravan, P. *et al.*; *Chem. Rev.* **1999**, *99*, 2293-2352]

However, the relaxivities of these agents (Table 1.1) are much lower than expected on the basis of their increased molecular weight. This has been explained with the flexible nature of the polylysine backbone and side chains.

Dextran has also been used as a scaffold for the attachment of various chelates[2, 42, 143-150] (Figure 1.17). As for polylysine, dextrans can be sourced in various molecular weight ranges and can be linked to gadolinium complexes. Several DTPA- or DOTA-loaded carboxymethyl dextran derivatives (e.g. **27**, Figure 1.17) have been prepared, but the relaxivities reported for these compounds (Table 1.1) are, nonetheless, relatively moderate, although they can be increased by increasing the content of paramagnetic complexes, at least to a certain ratio between ligand and polysaccharide.

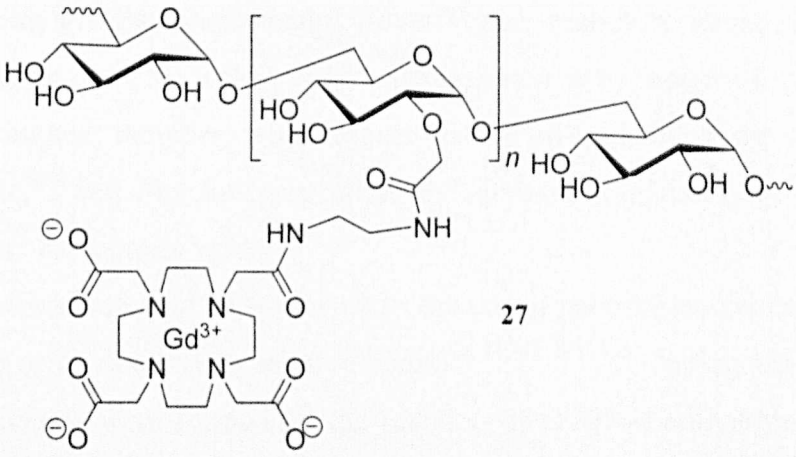



**Figure 1.17** Chemical structure of CMD-A2-Gd-DOTA, a modified dextran polymer.

Another polysaccharide, inulin, has been used[143, 151, 152] as scaffold conjugated with DO3A ligands through diethyl squarate.[138] The obtained relaxivity was 20.3 $mM^{-1}s^{-1}$ at 37 °C.

Dendrimer-based gadolinium-chelates have been reported, that consist in polyamidoamine (PAMAM) dendrimers possessing a few to hundreds of reactive terminal amines conjugated to the chelating ligands[2, 42, 58, 143, 153-163] (Figure 1.18).

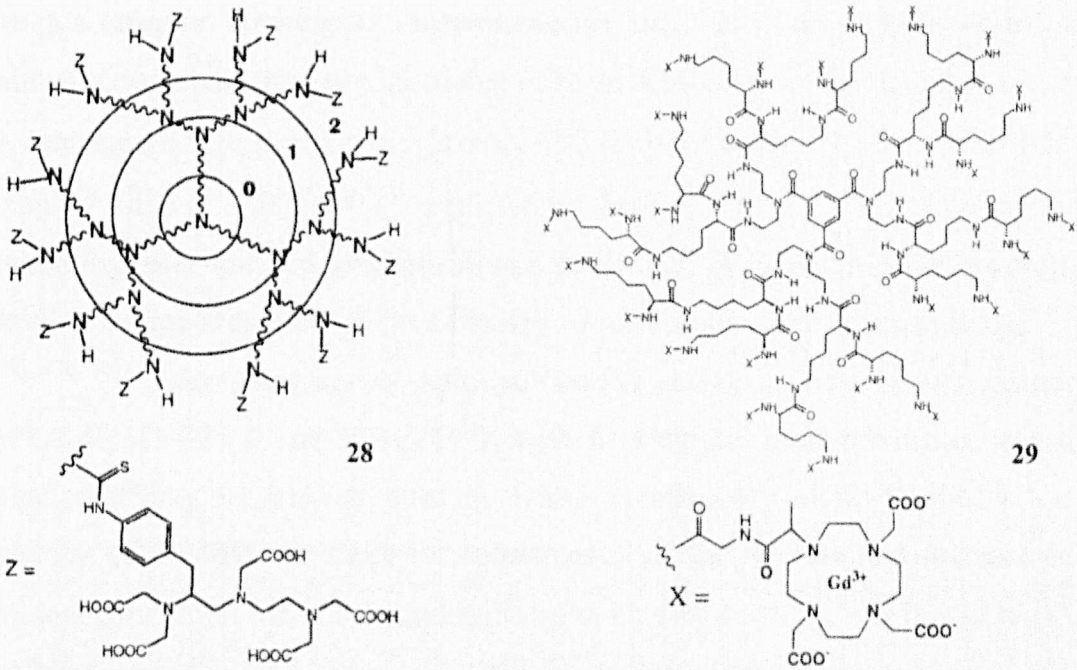



**Figure 1.18** Schematic drawing of a generation 2 PAMAM thiourea DTPA dendrimers **28** (left) and chemical structure of Gadomer-17 **29** (right). Relaxivity values are reported in Table 1.1. [From Caravan, P. *et al.*; *Chem. Rev.* **1999**, *99*, 2293-2352]

The potential of this application area is evident from the attempts of developing improved versions of agents based on a dendrimeric structure, such as 24-Gd-DTPA cascade polymer[143, 157] and Gadomer-17 **29** (Figure 1.18):[68, 158, 164] they consist of a trimesic acid central core with polylysine dendron substituents bearing 24 DTPA and 24

DO3A chelating groups, respectively. Nevertheless, relaxivity gains (Table 1.1) are once again limited by either a slow water exchange rate or by independent motion of the gadolinium-complex moieties with respect to the overall tumbling motion of the macromolecule,[164] and after few generations the increase in relaxivity generally reaches a 36-37 $mM^{-1}s^{-1}$ asymptotic value.

A significant amount of works report the use of gadolinium-chelates linked with human (HSA) or bovine (BSA) serum albumin.[2, 42, 67, 141, 165] Conjugates containing up to about 30 ligands were formed by the reaction of DTPA-dianhydride with BSA or HSA in aqueous solution. The approach developed for binding HSA has also been extended to other proteins.[68, 70] However, the development of these conjugates has been abandoned, since their synthesis was not easily controllable and there were also problems of toxicity due to the retention of gadolinium observed in bones and liver.

Gadolinium complexes that non-covalently bind to substrates have some remarkable inherent advantages from a biophysical point of view: in this approach, a contrast agent is targeted towards a particular protein or receptor site,[166-168] and this binding causes an increased concentration and retention of the $Gd^{III}$ complex in the area of such a receptor. Binding to a macromolecule also allows the complex to assume a rotational correlation time similar to that of the macromolecule itself, and this increase in $\tau_r$ can cause a high increase in relaxivity (2-3 fold, see Table 1.1), though far from the maximum value of ~100 $mM^{-1}s^{-1}$ predicted by theory (Section 1.2.2): this phenomenon is called Receptor-Induced Magnetization Enhancement (RIME).[2] Most of the work has been directed towards non-covalent binding of gadolinium-complexes to HSA,[1-3, 19, 42, 84, 135, 136, 169-175] providing agents with hydrophobic residues. Some of such ligands are BOPTA **5**, MS-325 **6** and MP-2269 **7**, with **6** being the most promising, due to its particular affinity for binding sites on HSA: its relaxivity of 42-59 $mM^{-1}s^{-1}$ at the frequency of 20 MHz is mainly a consequence of the 60-100 fold increase in the rotational correlation time of the molecule upon binding ($\tau_r$ = 10.1 ns bound *vs.* 115 ps free).[2, 42, 171, 173, 174]

β-Cyclodextrins have also been proposed[2, 132, 176-182] as a macromolecular carrier of gadolinium-chelates through non-covalent binding, but the relaxivity gain achieved is rather limited when compared to protein-bound systems; this is probably due to the small increase of $\tau_r$ for the guest-agent in spite of the binding with the cyclodextrin.

Gd-HPDO3A complexes have been trapped in apoferritin,[183, 184] the form of the protein ferritin free of iron ions. The procedure consists of dissociating the protein into

its subunits at low pH and subsequently reassembling it by increasing the pH, in the presence of the agent, thus resulting in a compartmentalisation of about 10 complexes per protein (Figure 1.19). Water exchange was permitted by channels 4 Å in diameter, where agent molecules (8-9 Å) could not diffuse through. The relaxivity shown by such systems was about 80 $mM^{-1}s^{-1}$, more than 20 times higher than the $r_1$ value of the free Gd-HPDO3A in water (3.7 $mM^{-1}s^{-1}$),[131, 185] referred as normal to a single gadolinium-complex. It is a very high value, which makes it a very good typology of agents for magnetic resonance angiography or specific tissue targeting.

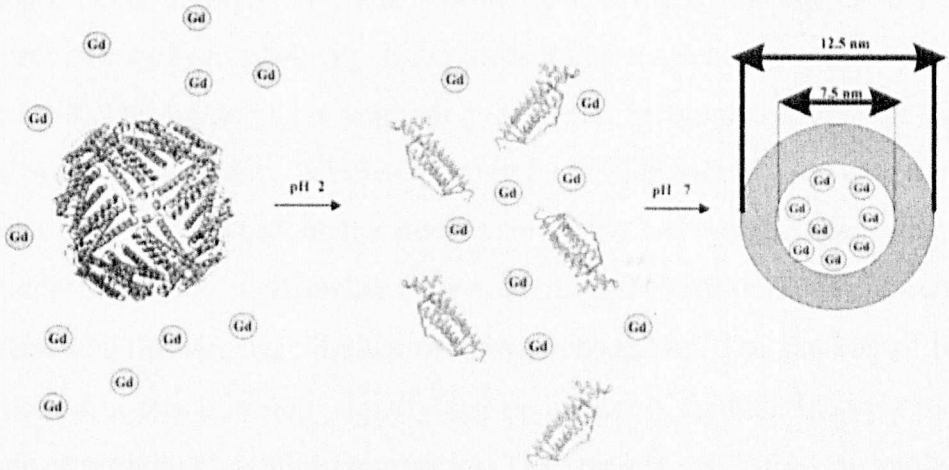



**Figure 1.19** Schematic representation of the dissociation of apoferritin into subunits at pH 2, followed by its reforming at pH 7. In this way the solution components are trapped within its interior. [From Aime, S. *et al.*; *Angew. Chem. Int. Ed.* **2002**, *41*, 1017-19]

Amphiphilic gadolinium-chelates, capable of micellar self-organization, were also investigated as potential blood pool agents.[65, 169, 172, 177] Micelle size and rigidity, both important in attaining high relaxivities for such compounds, can be regulated by the structure of the monomers: gadolinium-complexes of DOTA derivatives had relaxivities of 18-20 $mM^{-1}s^{-1}$, which are comparable to those obtained with macromolecular systems. Furthermore, with the micellar approach the problems of slow elimination from the body, often encountered with polymeric systems, are avoided: following intravenous administration, micelles have a prolonged systemic circulation time due to their small size and hydrophilic shell which minimize uptake by the mononuclear phagocyte system, and to their high molecular weight which prevents renal excretion (intact micelles have been recovered from plasma several hours after intravenous injection);[186, 187] nevertheless, their non-degradability makes them particularly safe, and such systems can be used as carriers for drugs.[187]

Liposomal contrast agents have also been reported in recent years.[2, 42, 66, 75, 130, 188-198] Different approaches exist to prepare paramagnetic liposomes: the metal chelates

can be encapsulated within the aqueous phase of the liposome, covalently attached to the liposome surface, or incorporated into the membrane. The size and membrane water permeability of the liposome are the most important factors influencing relaxivity, as both affect the rate of water exchange between the interior and exterior of the liposome. The classical procedure to prepare liposomes consists of dissolving appropriate concentrations of phospholipids in an organic solvent, evaporating it and subsequently adding water to the dry lipid layer, so leading to the spontaneous formation of multilamellar liposomes of different sizes (0.05-1 μm in diameter). Magnetic agents can be entrapped either in the internal aqueous phase, or in the lipidic bilayer, depending on their hydrophilicity/hydrophobicity. Substances that are soluble in organic solvents can be mixed with the lipids at the beginning, so being incorporated into the membrane structure of the final product, whereas water-soluble substances added with the water in the second step are trapped in the inner part of the liposomes. After sonication of multilamellar liposomes, unilamellar ones are obtained (50-100 nm in diameter) which can be separated through gel filtration or ultracentrifugation. The stability of liposomes can be altered in terms of both rigidity and permeability through incorporation in the membrane of other lipid-soluble compounds. The fate and residence time in the body of liposomes depend on their size, rigidity, charge and composition: for instance, high-density lipoproteins are the main cause of liposome instability in plasma because of the transfer of liposomal lipids to such proteins, with corresponding release of the encapsulated material. To solve this problem, cholesterol can be incorporated, causing an increase in packing of phospholipids in the membrane and thereby reducing their transfer. Recently, pH-sensitive liposomes have been proposed:[75] such vesicles become unstable under weakly acidic conditions, undergoing structural modifications that, eventually, lead to the release of the contrast agent in the external environment.

As already mentioned above (Section 1.2.3), the main problem with the macromolecular contrast agents so far reported seems to lie in the unsolved issue of effectively slowing down the complex tumbling. In fact, even if attached to large molecules such as polypeptides, polysaccharides or dendrimers, which actually do have a rather low global rotational time, single paramagnetic complexes, usually located in a periferal position, are still endowed with a relatively fast tumbling rate, possessing a certain freedom of rotation around their linker to the rest of the macromolecule (Figure 1.20).

Thus, thinking in terms of "bigger is better" has clearly shown to be substantially wrong, as the mere size of the molecule which the complex is part of does not necessarily imply a proportional increase in the rotational time of all its parts. Nevertheless, such evident consideration seems to be neglected by authors, and new agents have been continued to be proposed recently that are variations of the same conceptually "lame" ones already reported in the literature, and then leading to results that, although not negative, still miss the optimum performances expected.

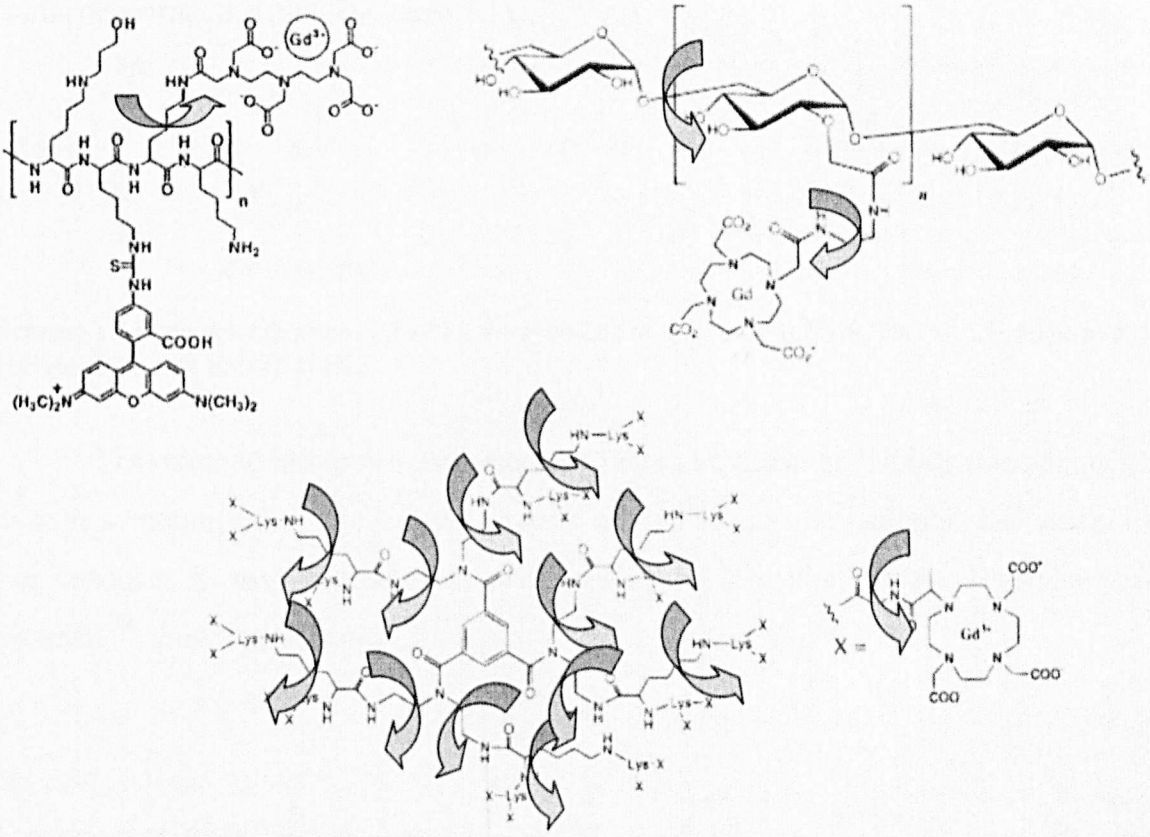


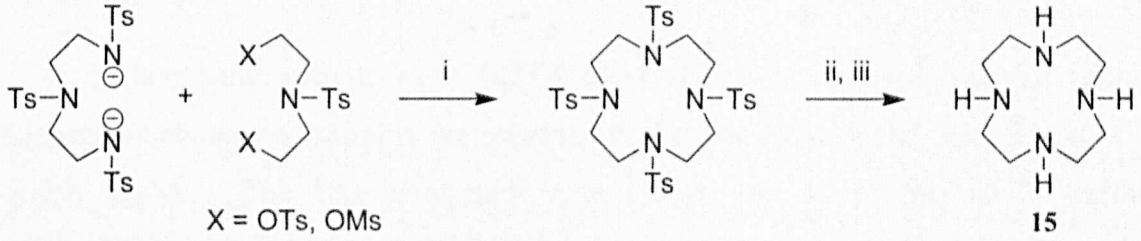
**Figure 1.20** Some reported macromolecular contrast agents, whose performances are lower than expected. Arrows show the sites endowed with rotational freedom. [Manipulation of structures from Caravan, P. *et al.*; *Chem. Rev.* **1999**, *99*, 2293-2352]

The global molecular architecture of an effective macromolecular agent needs to be thoroughly designed, from the choice of the best ligand for the paramagnetic metal (able to endow the complex with a high stability) to the design of a really rigid structure, including considerations about its external and internal hydrophilicity in order to ensure water solubility and easy access of water molecules to the metal centre.

### 1.3.2 DOTA as ligand

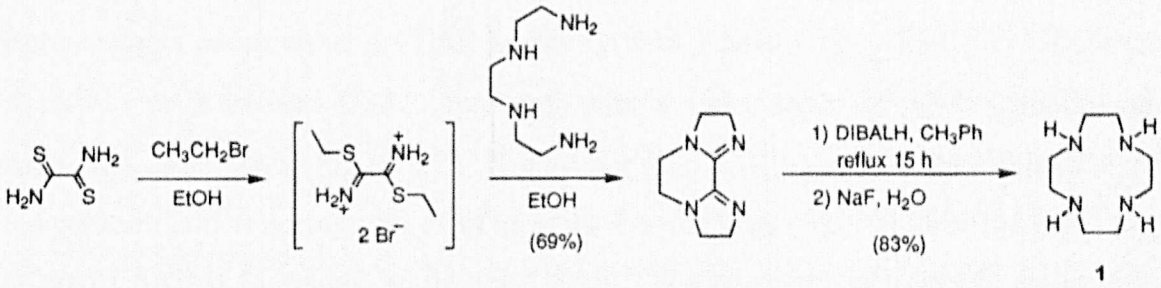
The choice of DTPA as a ligand to form stable gadolinium(III)-chelates and facilitate renal excretion was rather obvious as the properties of this ligand are well

known. It is also commercially available, although not always with a purity suitable for pharmacological applications. Despite its interesting coordination properties, the choice of DOTA was less obvious, because of the long and expensive preparation of 1,4,7,10-tetraazacyclododecane, or cyclen. The Richman-Atkins cyclisation procedure has been the most preferred synthetic method for years, involving medium-dilution macrocyclisation of the disodium salt of tritosyldiethylenetriamine with *N*-tosyldiethanolamine ditosylate to give tetratosyl cyclen, which is then detosylated with concentrated $H_2SO_4$ (Scheme 1.1).[199-203]




**Scheme 1.1** Richman-Atkins procedure for the synthesis of cyclen **15**. i) DMF, 100 °C, 2 h, 80%; ii) 97% $H_2SO_4$, 100 °C, 48 h; iii) 6 N HCl.

That method has now been superceded by more direct and efficient techniques,[22] even if sometimes they are based on rather expensive starting materials and reactants. For instance, an easy procedure to carry out in the laboratory is the Weisman-Reed protocol[204] shown in Scheme 1.2.




**Scheme 1.2** The Weisman-Reed procedure to synthesise cyclen **15**. [From Weisman, G. R. *et al.*; *J. Org. Chem.* **1996**, *61*, 5186-5187]

Cyclen is also commercially available, but quite expensive (cyclen 98%, 25 g = £254.00, Strem Chemicals). The tetraacetate arms of DOTA are typically obtained by reacting cyclen with alkyl bromoacetate or bromoacetic acid.[124, 205-207]

These efforts and many others in organic synthesis (such as procedures for alternative synthesis of monosubstituted tetraazacyclododecane rings,[208-211] with the substituent used for conjugation or sensitisation of fluorescent emission[212]) probably yielded more new chelating agents during the last few years than since the discovery of DTPA. New macrocycles derived from DOTA and substituted onto the macrocycle or

onto the acetate arms have been prepared either for linking such chelates to macromolecules, or for achieving a higher hydrophobicity.

Since there is only one water molecule in the first coordination sphere of the $Gd^{III}$ ion complexed with the tetraacetic ligands derived from cyclen, many systems have been synthesised to obtain chelates with a higher degree of hydration. For this reason, selective substitutions on one, two or three nitrogen atoms of cyclen has been carried out. In particular, the preparation of 1,7-disubstituted cyclens proved to be quite easy,[213] but with a consequent significant loss of stability.

In lanthanide complexes of DOTA or its achiral carboxamide derivatives two independent sources of chirality are present, i.e. the ring NC-CN and the arms NC-CO torsion angles. The four ethylenediamine groups can adopt two conformations indicated as λλλλ and δδδδ following Corey and Bailar's nomenclature.[214] There are also two possible arrangements for the acetate arms, in either a clockwise (Δ) or an anti-clockwise (Λ). This results in four possible stereoisomers existing as two enantiomeric pairs, which may interconvert in solution *via* rotation of the pendant arms or ring inversion.[215] Either process alone exchanges between CSAP and twisted CSAP geometries, while both processes combined in succession or concerted result in exchange between enantiomeric pairs. As mentioned above (Section 1.3) the stereoisomers adopt either a CSAP geometry with a twist angle of ~40° (Λ(δδδδ) and Δ(λλλλ)) or a twisted CSAP geometry with a twist angle of ~30° (Δ(δδδδ) and Λ(λλλλ)), as shown in Figure 1.21. The isomer ratio is dependent on the lanthanide ion, temperature and concentration of other salts. For the larger lanthanides ($La^{III}$-$Nd^{III}$) the twisted CSAP is favoured, whilst the CSAP is the predominant species observed for smaller lanthanides ($Sm^{III}$-$Er^{III}$). Ligand structure also affects the isomer ratio: for instance, tetraamides DOTAM **10** and DTMA **11** behave similarly to DOTA and exist as two diastereomeric species in aqueous solution, whereas the twisted CSAP form is favoured as the steric demand at the metal centre increases.

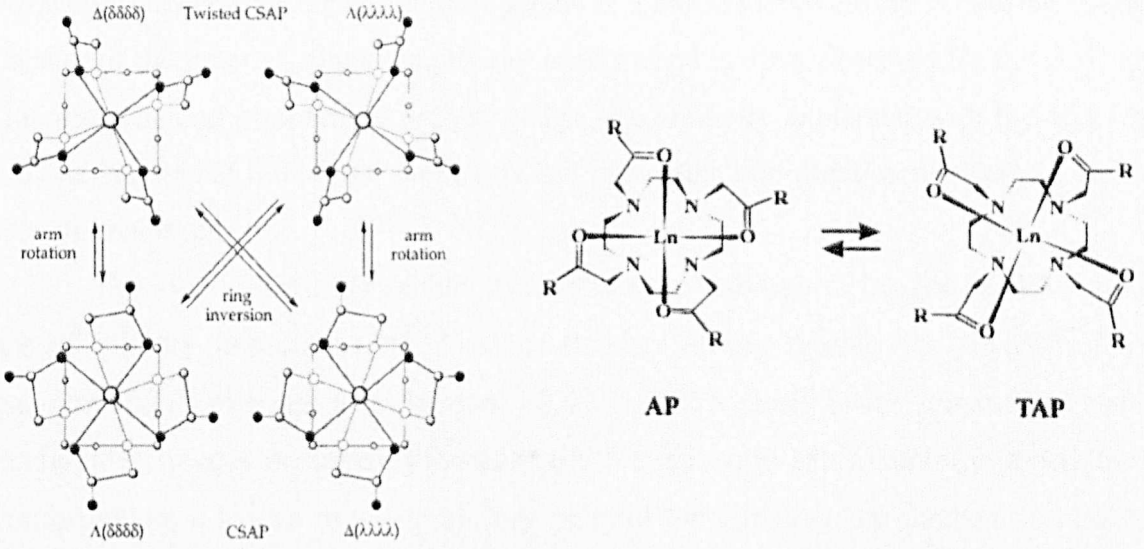



**Figure 1.21** Left: equilibria between diastereomeric conformations (CSAP and twisted CSAP) for Gd-complexes of DOTA. [From Caravan, P. *et al.*; *Chem. Rev.* **1999**, *99*, 2293-2352]. Right: schematic representation of the two diastereoisomers of a Ln(III) macrocyclic complex based on the tetraazacyclododecane ring, rising from rotation of the acetate arms. [From Aime, S. *et al.*; *Acc. Chem. Res.* **1999**, *32*, 941-949]

### 1.3.2.1 Kinetics and thermodynamics

Generally, lanthanide ions are strong Lewis acids, therefore they prefer to coordinate strong bases such as $H_2O$ and $F^-$. The external 4f orbitals do not extend out enough to interact significantly with the orbitals of the ligand (lack of directional bonding). As a consequence, the complexes are held together mainly by electrostatic interactions.

Although lanthanide ions are large because of their big radius, they are also found usually in a relatively high oxidation state (+3 and above), thus their charge density is still high. When moving along the 4f series, the ionic radius decreases uniformly (*lanthanide contraction*) leading to higher charge densities and stronger ionic bonds.

Because of their large size, lanthanide ions tend to have high coordination numbers (up to 12). In aqueous solution, a $Ln^{3+}$ ion is coordinated by eight or nine water molecules which exchange rapidly. On the contrary, thermodynamically stable complexes can be obtained by exploiting the so-called *chelate* or *macrocyclic effects*, which rely on the large increase in entropy following the displacement of multiple water molecules by a single multi-dentate ligand. The association constant of a same ligand with lanthanide ions tends to increase regularly with increasing the atomic number (i.e. decreasing the ionic radius). This can be explained with the increased electrostatic

attraction between the ligand and the metal as a consequence of the increasing charge density of the latter. A slight irregularity in this trend is often observed for the $Gd^{3+}$ ion (therefore named *gadolinium break*), and it is commonly explained with the fact that $Gd^{3+}$ is situated at the border point between two stable coordination numbers (8 and 9) in water solution.

The kinetic inertness and the thermodynamic stability of the new DOTA ligands are of primary importance,[2, 22, 42] since stability affects directly the toxicity of the gadolinium(III)-chelates (see Section 1.2.4.1). DOTA itself forms remarkably stable lanthanide chelates presumably because the tetraazacycle can assume its most stable conformation, a square in which all lone pairs of the nitrogens are directed toward the metal ion.[216]

The kinetics of formation and, more importantly, of dissociation are extremely slow ($k_{ass} = 5.9 \cdot 10^{-6}$ $M^{-1}s^{-1}$, $k_{diss} = 8.4 \cdot 10^{-6}$ $M^{-1}s^{-1}$),[112, 217, 218] a quite unusual feature in the coordination chemistry of the 4f elements. The literature covering the complexation of lanthanides with DOTA and its derivatives has proliferated particularly in the last 20 years. In the study of $Ln^{III}$-DOTA systems, many of the authors were surprised by the slowness of the formation of the thermodynamically stable complexes. At room temperature, it is necessary to wait 4-6 weeks or longer for their formation equilibria to establish. According to some authors[219-225] the formation of complexes of DOTA (and presumably of its derivatives) is a three-step mechanism. At neutral pH, the first phase involves the formation of the $[LnH_2(DOTA)]^+$ complex, in which the $Ln^{3+}$ ion is located outside the cage formed by the four nitrogen atoms and the four oxygen atoms of the carboxylic groups. The two protons bound to two diametrically opposed nitrogen atoms of the tetraaza-ring are orientated towards the inside of the cage. The $Ln^{3+}$ ion is only bound to the four oxygen atoms of the carboxylic groups and is located above the plane formed by these four atoms because of the repulsion by the protons of the tetraaza ring. The coordination number of nine for the lanthanide cation is assured by five water molecules. During the second phase, the $[LnH_2(DOTA)]^+$ complex loses a proton from a nitrogen atom to form [LnH(DOTA)] without changing the bonding modes. In phase III, there is a concerted rearrangement of the intermediate complex [LnH(DOTA)]: the $Ln^{3+}$ ion slowly penetrates the cage formed by the eight atoms (four nitrogen atoms of the ring and four oxygen atoms of the carboxylic groups) and at the same time the intermediate complex [LnH(DOTA)] loses its last proton to form the complex $[Ln(DOTA)]^-$ in which the four nitrogen atoms of the ring and the four oxygen atoms of

the carboxylic groups are bound to the $Ln^{3+}$ ion. The coordination number of nine for the lanthanide cation is completed by a water molecule. The dissociation is prevented by the tight packing of the macrocyclic cage that inhibits the protonation of the nitrogens and the resulting dissociation of the metal complex. If the macrocycle is supported with rigid groups such as cyclohexane or pyridine[133, 134, 136, 226-228] the kinetics becomes even slower. For example, the half-life of Gd-DOTA and Gd-CyDOTA are 23 h and 50 h, respectively, in 1 M HCl.[229] Such a difference ensures a lower toxicity of the contrast agent and could be important especially if the chelates are to be linked to biological macromolecules, since their residence time in the body becomes longer.

The slow complexation kinetics of DOTA derivatives with lanthanides are probably the reason why the stability constants reported in the literature often mismatch, and the results must be taken with caution. In Figure 1.22 the stability constants of Gd-DOTA published in the literature are plotted versus their date of publication, and the discordance among the data is evident. The stability constants for several gadolinium-complexes are shown in Table 1.2.

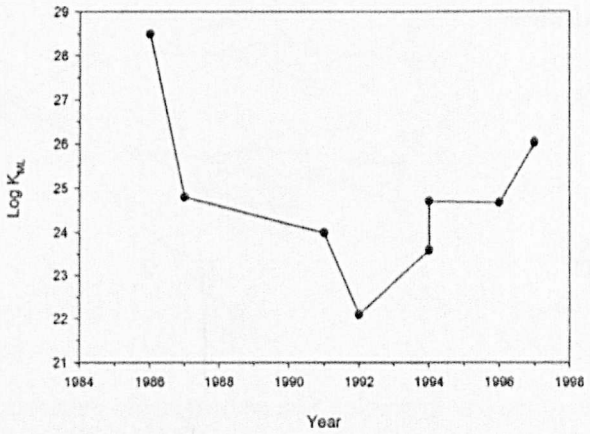



**Figure 1.22** Stability of Gd(DOTA)$^-$ as a function of the publication year. [From Comblin, V. *et al.*; *Coord. Chem. Rev.* **1999**, *186*, 451-470]

**Table 1.2** Stability constants for various cyclic and acyclic gadolinium(III)-complexes.

| ***Ligand*** | *Log K* | *Ligand* | *Log K* |
|---|---|---|---|
| DTPA **1** | 22.5 | DOTA **2** | 25.3 |
| DTPA-BMA **3** | 16.9 | HP-DO3A **4** | 23.8 |
| BOPTA **5** | 22.6 | DOTAM **10** | 10.1 |
| DTMA **11** | 12.8 | DO3A **16** | 21.1 |
| DO3MA **17** | 25.3 | PC2A **19** | 16.6 |
| BP2A **20** | 14.5 | EDTA **21** | 17.3 |
| PEDTA **22** | 15.6 | ODOTRA **23** | 21.6 |
| TETA **24** | 15.8 | NOTA **25** | 13.7 |

### 1.3.3 Hyperbranched polymers

In the early 1990s, Kim and Webster were working on dendritic polymers as rheology control agents and as spherical multifunctional initiators. The need to obtain the material rapidly and in large quantities forced them to develop a new route for a one-step synthesis of dendritic polyphenylenes. As a result, the obtained polymers were polydispersed and had defects in the form of built-in linear segments, but nonetheless they were highly branched molecules. Kim and Webster then named them *hyperbranched polymers*.[230] Since then, polymers obtained from the statistical polymerization of $AB_x$ monomers by means of condensation or addition procedures are referred to as *Hyperbranched Polymers* (HBPs) (Figure 1.23), and a new field of branched polymers has risen. Many kinds of hyperbranched polymers have been investigated as novel dendritic macromolcules.[231-237]

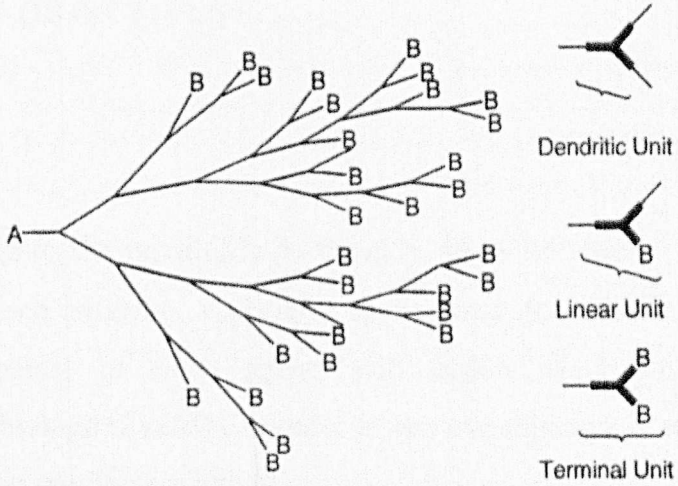



**Figure 1.23** Schematic architecture of a hyperbranched polymer from $AB_2$ monomers. [From Jikei, M. *et al.*; *Prog. Polym. Sci.* **2001**, *26*, 1233-1285]

Hyperbranched polymers are still a rapidly growing area within the field of macromolecules. They are promising materials due to their relative ease of preparation, especially when compared to dendrimers. They are also phenomenologically different from linear polymers. For example, they are endowed with a lower viscosity with respect to linear polymers of the same molecular weight, as a consequence of the more globular structure. Because of their unique properties, such as low viscosity, good solubility and multi-functionality, HBPs have already found many applications in different fields.

From the perspective of the present project, hyperbranched polymers seem to represent the ideal structure on which to base a macromolecular contrast agent, since several of their characteristics match the solutions to the encountered problems. First of all, the very rigid structure should ensure the magnetic complexes to be fixed in their position, so possessing the same rotational correlation time of the whole macromolecule with no additional (and detrimental) freedom of tumbling. Moreover, the possibility to regulate the degree of branching should permit tuning of access of water molecules to the metal centres. Their water solubility complies with one of the compulsory biological requirements. Finally, in the unlikely case of dissociation of some gadolinium ions from the complexes, it is expected that the whole macromolecular structure act as a cage to avoid release of such a toxic metal in the biological environment, thus enforcing the safety of the agent.

## 1.4 AIM AND OBJECTIVES

### 1.4.1 Aim

To investigate the possibility to develop novel polymeric contrast agents for Magnetic Resonance Imaging, especially to be used for labelling stem cells. The molecular architecture of these agents will endow them with improved MRI performance and biological safety. In order to achieve this aim, it will be necessary to tackle the following specific objectives.

### 1.4.2 Objectives

- Choice of the type of contrast agent most suitable for the project purposes. The main requirements are: stability in biological environment; lack of toxicity; possibility of selective and specific modification and functionalisation; good detectability; flexibility of use and target.
- Establishment of a chemical structure to contain the magnetic probes, able to improve performances.
- Synthesis of suitable monomers/ligands aimed at the established macromolecular architecture, also involving the synthesis of model compounds

in order to investigate realisability and best conditions for the reactions to be carried out.

- Preparation of model contrast agents from significant intermediates, in order to refine protocols for such type of synthesis. In particular, the conditions (temperature, concentration, molar ratio, etc.) necessary to incorporate paramagnetic metals with the best yields and time scales will be investigated, as well as procedures to detect toxic free metal and to avoid its presence in the final agent.
- Test of the prepared model contrast agents on cell cultures, to make practice with techniques and solve possible problems encountered in terms of biocompatibility, toxicity and performance.
- Synthesis of macromolecules based on the established molecular architecture, either 100% loaded with paramagnetic metals (from metal-containing monomers) or "empty". Both types of structure will be chemico-physically characterised as fully as possible. Various synthetic protocols will be applied, depending on the polymerisable moieties borne by the monomers used.
- Test of the final metal-containing polymeric compounds on stem cells in order to investigate their biocompatibility, and evaluation of the obtained MRI contrast effect.

## 2. Results and discussion I: monomers synthesis

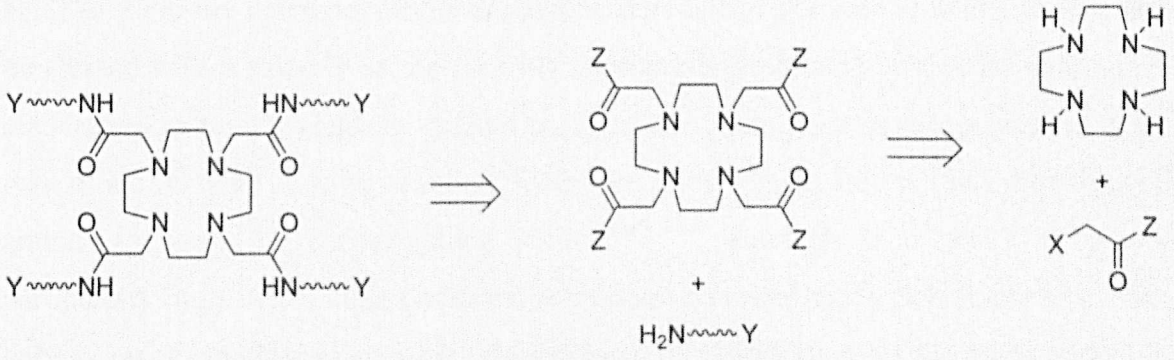
In order to obtain a hyperbranched polymeric structure containing several paramagnetic complexes based on a 1,4,7,10-tetraazacyclododecyl macrocycle, two structural characteristics are required.

The first is the presence of carbonyl groups in the substituents of the macrocycle. In order for these groups to optimally coordinate the metal, it is required that the carbonyl groups are in *beta* position with respect to the nitrogen atoms of the cycle.

The second requirement is the presence of polymerisable groups at the other end of some or all the substituent "arms".

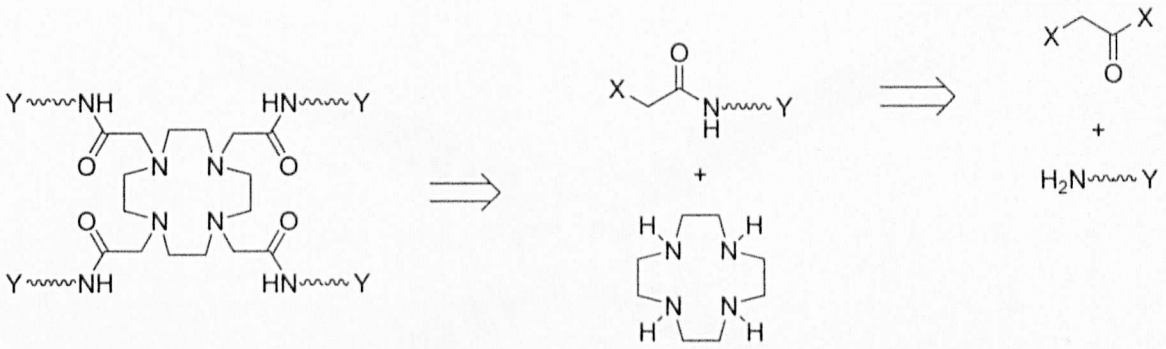
Among the different possible types of derivatives, tetra-amides seem to be simple to obtain and relatively stable in a biological environment.[238] Two possible retrosynthetic analyses can be carried out, which led to a synthesis design strategy based on readily available starting materials, a small number of steps, and reactions which are relatively easy to carry out.

According to the first retrosynthesis (Scheme 2.1), the tetra-amide derivative may be obtained from a commercially available amine (protected at the $\omega$-functional group, if any and if necessary) and a suitable reactive 1,4,7,10-tetraazacyclododecane-1,4,7,10-tetraacetyl derivative. In turn, the latter can be synthesised from 1,4,7,10-tetraazacyclododecane (cyclen, **15**) and a suitable 2-haloacetyl derivative, both commercially available.




**Scheme 2.1** First retrosynthetic analysis to obtain tetra-substituted cyclens possessing polymerisable groups (Y) at the terminal position of the pendant arms. X = leaving group, Y = polymerisable moiety, Z = leaving group, ~~~ = spacer between the amine/amide moiety and the polymerisable group.

A second possible approach (Scheme 2.2) consists of the direct attachment to cyclen of the complete arms, obtained previously from a 2-haloacetyl halide and an amine, most of which are commercially available.



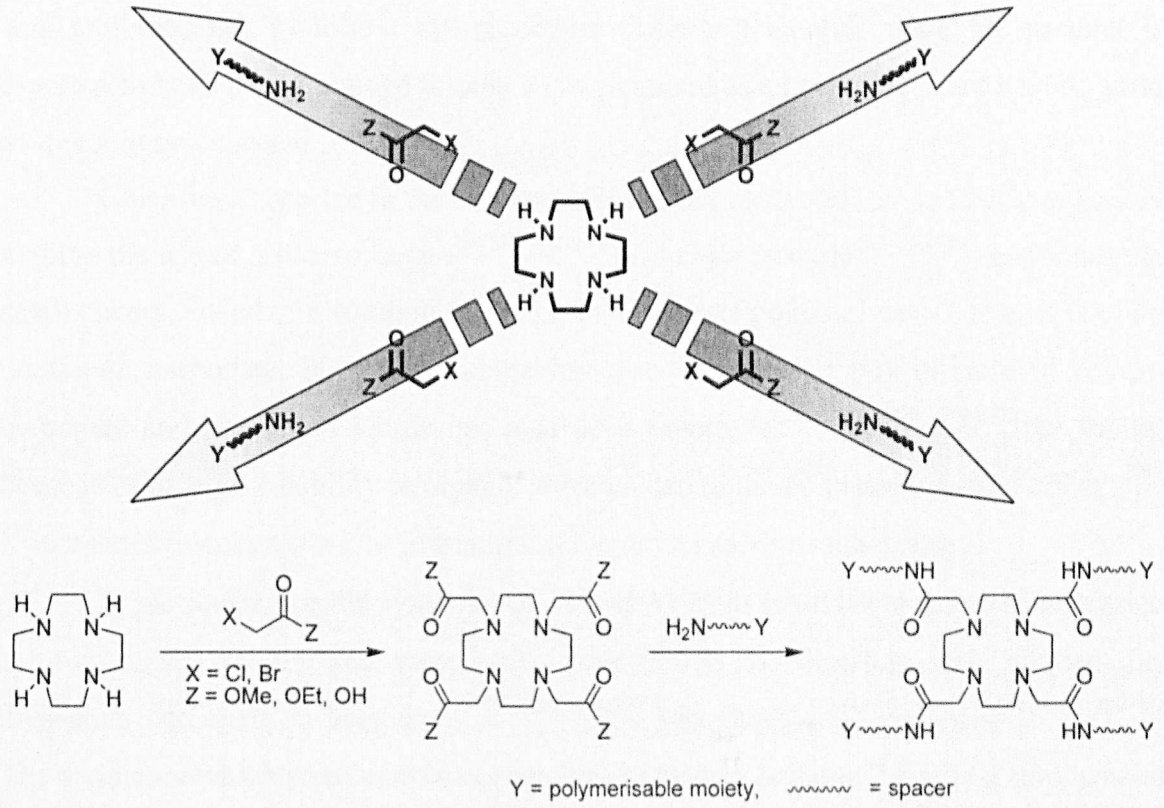
**Scheme 2.2** Second retrosynthetic analysis to obtain tetra-substituted cyclens possessing polymerisable groups (Y) at the terminal position of the pendant arms. X = leaving group, Y = polymerisable moiety, ~~~ = spacer between the amine/amide moiety and the polymerisable group.

Scheme 2.1 gives rise to a *divergent* synthesis, as it involves the tetra-substitution of cyclen with acetyl arms bearing a moiety suitable for further derivatisation. In turn, such arms will be "elongated" to have terminal functional groups which can be exploited for polymerisation.

The retrosynthetic analysis shown in Scheme 2.2 leads to a *convergent* protocol, where the complete arms are prepared before attaching them to the central core, i.e. the tetraazacyclododecane ring.

## 2.1 Divergent synthesis of DOTA-amides

The synthetic three-step sequence based on the retrosynthetic analysis shown in Scheme 2.1 is illustrated in Scheme 2.3. In this approach, cyclen is reacted with a suitable 2-haloacetyl derivative (alkyl bromo- or chloroacetate, bromo- or chloroacetic acid) to yield the corresponding macrocyclic tetra-acetyl derivative, which in turn will be reacted with a suitable amine carrying appropriate protecting groups for subsequent elaboration to finally yield the desired product. The main issue in this procedure is the type of amide bond forming reaction. Esters are known to be able to react directly with amines to form the corresponding amides,[239, 240] although their reactivity is not particularly high. Also, their synthesis, in principle, is relatively easy. Exploiting other derivatives or coupling reagents for the synthesis of amides requires the preparation of a tetra-carboxylic acid as intermediate.




**Scheme 2.3** Representation of a possible divergent synthesis deriving from one of the retrosynthetic analyses (Scheme 2.1) and leading to a tetra-substituted cyclen possessing moieties which can be exploited for polymerisation.

### 2.1.1 Synthesis *via* ester derivatives of DOTA

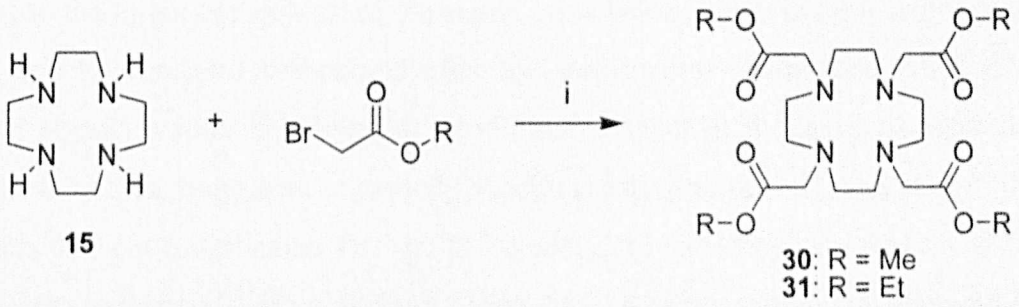
Ester derivatives of DOTA are reported in the literature,[200, 241-245] and in the first instance attempts to reproduce such protocols were carried out. In particular, methyl and ethyl esters **30** and **31** were chosen because they were expected to be reactive enough to give positive results.

The methyl ester derivative **30**, thought to be slightly more reactive in the amidation step due to the fact that the methoxy group is generally well-known to be a better leaving group than the ethoxy group,[240, 246] has not been previously reported in the literature apart from being mentioned in a patent.[247] The mono-methyl ester is mentioned in a few patents,[248-250] and the tris-methyl ester is reported in a patent[251] and a paper[252] where the esters act as protecting groups. The only reported mono-ethyl ester of DOTA (1,4,7,10-tetraazacyclododecane-1,4,7,10-tetraacetic acid, 1,4,7-tris(1,1-dimethylethyl) 10-ethyl ester) was obtained from cyclen using ethyl bromoacetate as starting material.[253-255] Functionalised tetra-ethyl ester derivatives of DOTA have been reported, prepared using triflates to attach the arms onto the ring.[256, 257] The synthesis of DOTA-tetra-ethyl ester **31** has been reported by Tsukube group[245] for stability and conformational studies about its complexes with alkali metals.[245, 258-260] However, it

was preferred not to follow the procedure described therein, since the product is reported to have been obtained in only 29% yield and as an oil rather than a white solid as it would be expected.

Conditions reported in the literature for the tetra-substitution on cyclen generally involve the use of a bromoacetate[79, 238, 261-273] or a chloroacetate[265, 273-284] and a base in small excess, added to a solution of cyclen in an aprotic polar solvent. The base is often potassium carbonate, but triethylamine has also been used.[272] A mixture of cesium carbonate and potassium iodide has also been employed:[241, 275, 276, 279-282] the former because of its high solubility in organic solvents due to the so-called "cesium effect";[285-287] the latter to achieve *in situ* formation of the more reactive iodoacetate.

In particular, for the synthesis of **30** and **31** from ethyl bromoacetate and cyclen the two most common and successful procedures in the literature were applied, i.e. potassium carbonate in acetonitrile,[79, 265, 267-270] and $Cs_2CO_3$/KI in DMF.[275, 276, 279-282] The syntheses which were carried out are represented in Scheme 2.4, and a summary of conditions and results is reported in Table 2.1.




**Scheme 2.4** Synthesis of DOTA-tetra-esters **30** and **31**. Conditions and results are reported in Table 2.1 and discussed in the text.

**Table 2.1** Reaction conditions and results for the synthesis of DOTA-esters **30** and **31**, as shown in Scheme 2.4.

| R | | Conditions | Yields |
|---|---|---|---|
| Me | 1 | cyclen (1 mol eq), methyl bromoacetate (5 mol eq), $K_2CO_3$ (7 mol eq), MeCN, reflux, 18 h. | **30** 60% (crude) |
| | 2 | cyclen (1 mol eq), methyl bromoacetate (4.4 mol eq), $Cs_2CO_3$ (5.6 mol eq), KI (5.6 mol eq), DMF, 80 °C, 18 h. | **30** 48% (crude) |
| Et | 1 | cyclen (1 mol eq), ethyl bromoacetate (5 mol eq), $K_2CO_3$ (7 mol eq), MeCN, reflux, 18 h. | **31** = 52% |
| | 2 | cyclen (1 mol eq), ethyl bromoacetate (4.4 mol eq), $Cs_2CO_3$ (5.6 mol eq), KI (5.6 mol eq), DMF, 80 °C, 18 h. | **31** = 78% |

The TLC of the crude mixture for both the methyl ester syntheses revealed the presence of at least one new species besides unreacted starting material; the spot with intermediate polarity had an irregular stretched-out shape and therefore it could be the consequence of the overlapping of several minor spots. It was not possible to find the

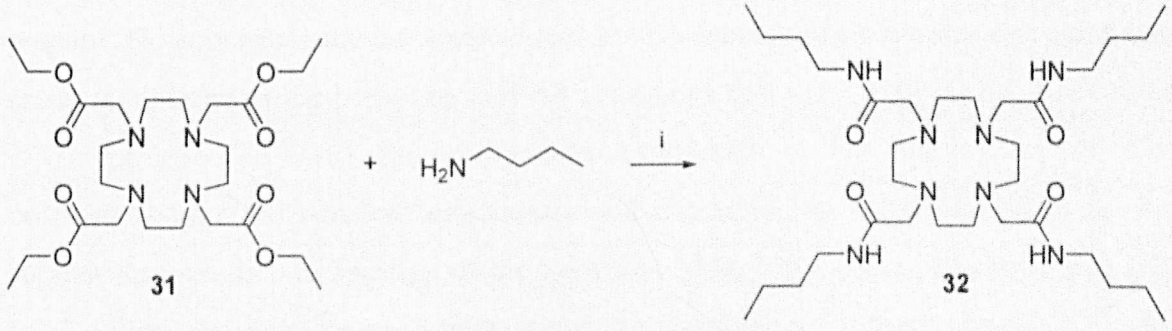
conditions for the resolution of such spot. The formation of the desired compound was assessed by NMR spectroscopy and mass spectrometry. The $^{1}H$ NMR spectrum showed the set of signals expected for the target product, with a sharp singlet at 3.74 ppm for the methyl group and two broad peaks at 3.19 and 2.35 ppm produced by the acetyl and ring protons respectively. The broadness of such signals suggests a conformational equilibrium[258, 261, 288] (Section 1.3.2), which is responsible for an analogous phenomenon in the $^{13}C$ NMR spectrum where, besides sharp signals at 173.7, 55.0 and 52.2 ppm due to the carbonyl, the methyl and the acetyl methylene groups respectively, a very broad signal centred at 51.4 ppm was observed and assigned to the macrocycle carbons. The $CI^{+}$ and $FAB^{+}$ mass spectra showed the molecular ion ($[M+H]^{+}$) peak at 461 m/z. However, a complete purification of the target compound was not achieved in spite of the several attempts carried out through extractions, chromatography with different conditions in terms of eluent and stationary phase, recrystallisation or precipitation using various solvents or combinations of solvents. Such techniques only allowed a partial removal of the impurities, as assessed by integration (normalised with respect to the target compound) of the signal areas belonging to the impurities in the $^{1}H$ NMR spectra recorded before and after the purification procedures. Also, $CI^{+}$ MS showed signals neither belonging to the desired product or the starting materials, nor assignable to their fragments or partially substituted by-products. The identity of the by-products was not investigated further. The crude yield and the purity was lower for the methyl ester obtained with $Cs_2CO_3$/KI than for the same compound prepared in the presence of $K_2CO_3$ (see Table 2.1).

On the contrary, pure ethyl ester **31** was obtained from both procedures (see Table 2.1) after chromatography followed by precipitation. The same methods were among those tried previously and unsuccessfully for the purification of **30**. The identity of the product was first determined by NMR spectroscopy, being in agreement with the literature data.[245] Besides the two sharp signals expected for the ethyl chain (a triplet at 1.27 ppm and a quartet at 4.18 ppm), the $^{1}H$ NMR spectrum of **31** showed two broad signals centred at 2.37 and 3.22 ppm, that were assigned to the protons of the macrocycle and the methylene group of each arm, respectively. Again, a broad peak was observed in the $^{13}C$ NMR spectrum at 51.5 ppm due to the ring carbon atoms. The $^{1}H$ and $^{13}C$ NMR spectroscopic results are in agreement with those reported in the literature.[241] The identity of the product was confirmed by $CI^{+}$ MS, showing a peak at 517 m/z that can be assigned to the molecular ion ($[M+H]^{+}$). The absorption band at

1723 $cm^{-1}$ in the IR spectrum is typical of the C=O stretching in an ester moiety. The final yields showed that the method with cesium carbonate and potassium iodide was more effective (78% vs. 52%), as expected on the basis of the cesium effect and the catalytic role of iodide as mentioned above.

Besides the possibility that one reaction had worked more cleanly than the other, it can be speculated that the slightly greater polar character of methyl ester **30** with respect to ethyl ester **31** may explain its different behaviour (i.e. final separation from impurities and by-products) towards the purification techniques (i.e. extractions, chromatography with different conditions in terms of eluent and stationary phase, recrystallisations, precipitations) in the presence of impurities with analogous chemical and physical properties. For instance, solubility is obviously affected, and that has an effect on the precipitation procedure, which could not be adjusted despite the several attempts. More generally, if the polarity which ester **30** is endowed with is very close to that of some of the impurities, as well as partially substituted cyclens (which however were not detected), all such species will be more difficult to separate in comparison to the ethyl ester derivative.

Because of the problems encountered with the preparation of methyl ester **30**, only ethyl ester **31** was used in the next step of the divergent synthesis of amide derivatives of DOTA. Amidation achieved through direct reaction of the ester with an amine was first tested by using a simple alkyl amine, namely *n*-butylamine. The product expected from this reaction, 1,4,7,10-tetrakis(butylcarbamoylmethyl)-1,4,7,10-tetraazacyclododecane **32**, has been reported previously[289] although synthesised according to a convergent approach (see Section 2.2 below). The attempts of synthesis were carried out with both an excess and a stoichiometric amount of amine, as shown in Scheme 2.5 and under the conditions reported in Table 2.2.




**Scheme 2.5** General representation of the attempts of synthesis of tetra-amide derivative **32** from tetra-ester **31** and *n*-butylamine. Conditions are reported in Table 2.2

| **Table 2.2** Reaction conditions and results for the synthesis of DOTA-tetra-butyl-amide **32** shown in Scheme 2.5. | | |
|---|---|---|
| | **Conditions** | **Result** |
| 1 | **31** (1 mol eq), *n*-butylamine (>100 mol eq), $CH_2Cl_2$, reflux, 18 h. | **32** = 92% |
| 2 | **31** (1 mol eq), *n*-butylamine (4 mol eq), DCM, reflux, 48 h. | The target product did not form |
| 3 | **31** (1 mol eq), *n*-butylamine (8 mol eq), MeCN, 70 °C, 48 h. | The target product did not form |
| 4 | **31** (1 mol eq), *n*-butylamine (4 mol eq), MeCN, MW, 65 °C, 1 h. | The target product did not form |
| 5 | **31** (1 mol eq), *n*-butylamine (8 mol eq), DMF, MW, 100 °C, 1 h. | The target product did not form (est. conv. = 6%) |

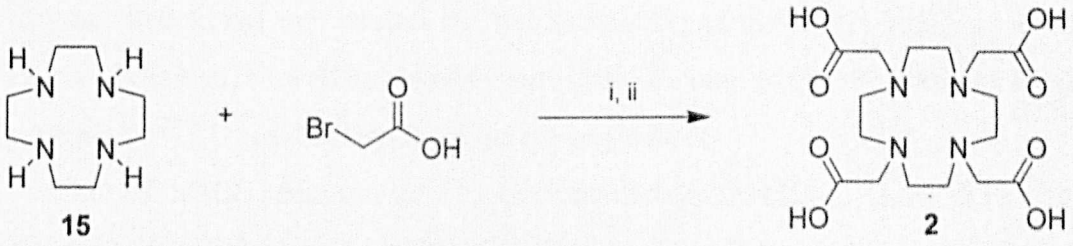
Two DOTA monoamide derivatives (a 2-aminoethylamide and a hydrazide) are reported to have been obtained from DOTA-esters by using a large excess of the suitable amine.[253, 254] Ester **31** was reacted with neat *n*-butylamine, used as both reactant and solvent (Table 2.2, entry 1). After extraction and recrystallisation, the pure target compound was obtained in 92% yield. The analytical data were consistent with those available in the literature.[289] In particular, the $^1$H NMR spectrum showed a broad singlet centred at 7.14 ppm and due to the amide moiety, two broad peaks centred at 3.07 and 2.70 ppm and produced by the acetyl and ring protons respectively, and the set of four signals typical of a butyl chain. In the $^{13}$C NMR spectrum the resonance for the carbonyl group was at 170.6 ppm, the peak due to the acetyl methylene group was observed at 59.3 ppm and the ring carbons produced a broad signal at 53.3 ppm. It was thus demonstrated for the first time that, in principle, complete amidation can be achieved from DOTA-tetra-esters.

The next step was the synthesis of the same compound using just a stoichiometric amount or a slight excess of amine, since in some cases it is not convenient to employ it as a solvent, e.g. when the amine is expensive or complicated to prepare. No procedure for the synthesis of DOTA-tetraamides from the corresponding esters is reported in the literature, and the conditions that were tried (Table 2.2, entries 2-5) were based on basic organic chemistry considerations. The solvent was varied in order to change the reaction temperature and check for an improving effect by the solvent through the stabilisation of the transition state. Microwave irradiation was also tried, following literature procedures about the synthesis of tertiary amines.[290-293] All procedures were unsuccessful, and the starting material was recovered completely unreacted. Only for the last attempt a 6% conversion of the ester groups was estimated on the basis of the NMR spectroscopic analysis, but no evidence was obtained that the

desired tetra-amide had formed. It is clear that simple alkyl esters are not reactive enough to be exploited in amide-bond-forming reactions with a stoichiometric or little excess of amines, as a high excess is required in order to achieve a good conversion. The fact that such a protocol has never been reported in the literature in spite of its apparent simplicity, combined with the failures herein, suggests that it might have always been unsuccessful, if tried in the past. This route was then abandoned, because the synthesis of DOTA-tetra-esters expected to be more reactive (such as the 4-nitrophenyl ester) required starting materials not readily available. Also, preliminary positive results were obtained at the same time for the convergent synthesis of model compound **32**, as shown in Scheme 2.17 and reported in Section 2.2 below. It was preferred to explore alternative methods for a divergent synthesis of formal tetra-amide derivatives of DOTA.

### 2.1.2 Synthesis *via* DOTA

All alternative methods that were planned for a divergent synthesis of DOTA-amides required first the preparation of DOTA itself, from which a tetra-amide could be obtained in principle through a one-pot step. Despite the fact that the gadolinium(III)-complex of DOTA is one of the few non-superparamagnetic MRI contrast agents currently approved for use in humans, only four detailed procedures for its synthesis were found in the literature.[124, 205-207] The protocol reported by Desreux[124] and Das *et al.*[205] (more straightforward, being based on the direct reaction of cyclen with chloroacetic acid) was followed. Bromoacetic acid was used because it is readily available and supposedly more reactive (Scheme 2.6).




**Scheme 2.6** Synthesis of DOTA. i) cyclen (1 mol eq), bromoacetic acid (4.4 equivalents), 5 M NaOH, $H_2O$, pH 10, 70 °C, 8 h; ii) 37% HCl, pH 2. Overall yield: 73%.

No precipitation occurred after acidification to pH 2, in contrast to what has been reported by Desreux[124] (but not mentioned in the other papers[205-207]). The solvent was removed under reduced pressure leading to a white solid. According to TLC (silica, 0.1% trifluoroacetic acid in water; atypical conditions for a TLC as reported by Das *et*

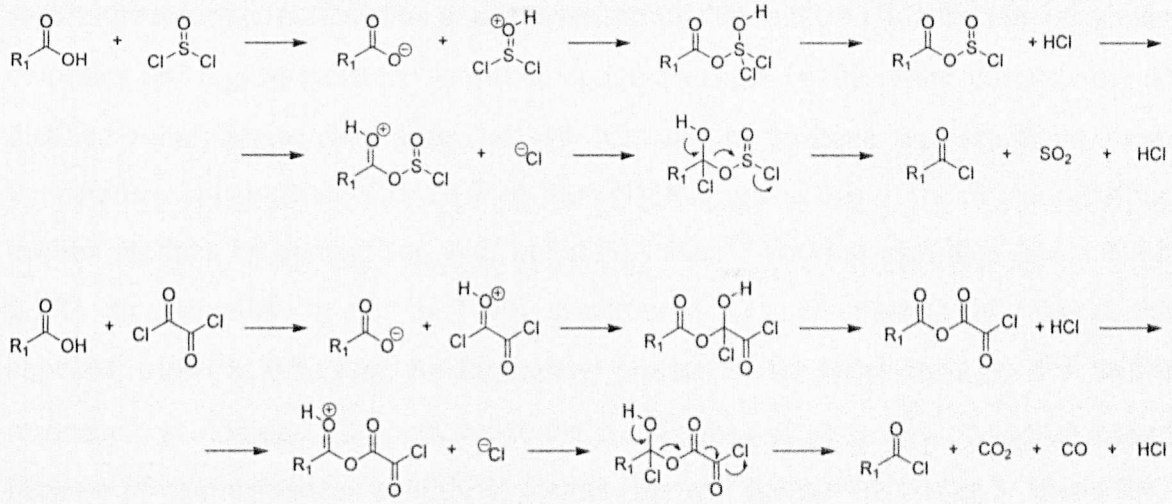
*al.*[205]) two products with $R_f$ 0.74 and 0.35 had formed. In the $^1$H NMR spectrum in $D_2O$ three resonances could be observed, assigned to DOTA (3.31 and 3.78 ppm[294-296]) and glycolic acid (4.22 ppm) formed as by-product in 0.34:1 molar ratio with respect to DOTA (i.e. basically what expected since having an excess of 0.4 molar equivalents). Following the procedure by Das,[205] the purification of **2** by column chromatography on silica gel using 0.1% TFA in water was carried out, leading to the desired compound free of glycolic acid, as shown by NMR spectroscopy. The second part of the purification according to the reported procedure[205] (chromatography with 0.1% TFA in acetonitrile) was not possible because of solubility reasons (the crude product was not soluble in such an eluent), neither was the precipitation from methanol suggested by Mease[206] (the crude product was not soluble even in hot methanol or other short-chain alcohols). Eventually, the desired compound was precipitated from water by addition of acetone. When repeating the procedure without carrying out the chromatographies, it was possible to obtain the target compound in 73% yield after precipitation. IR spectrometry also confirmed the identity of the product, the spectrum being in full agreement with the data reported by Das *et al.*[205] It is to be highlighted that in DOTA two nitrogen atoms are always protonated below pH 9, while it is necessary to go below pH 4.5 to have two protonated carboxylates and below pH 2 for total protonation.[238, 294-297] The absorption band at 1682 $cm^{-1}$ is of an intermediate value between those expected for a carboxylic acid (1715 $cm^{-1}$) and a carboxylate (1650 $cm^{-1}$), possibly as a consequence of intramolecular hydrogen bonding between the carboxylate groups themselves and the protonated nitrogen atoms (the absorption band at 2853 $cm^{-1}$ is consistent with the stretching of the N–H bond). It is possible that the differences between the data reported in the papers (regarding melting points, IR and NMR spectra, and crystal structures) are caused by the different protonation conditions in which DOTA was obtained, as well as possible formation of complexes with alkali or alkaline-earth metals[238, 295-297] used during the reaction procedures.

The $^1$H NMR spectrum of DOTA recorded in DMSO-$d_6$ showed two broad signals at 12.88 and 7.41 ppm, assigned to protonated carboxylate groups and nitrogen atoms respectively. Integration of the signal areas seemed to suggest that DOTA was in its completely protonated conditions, i.e. with four COOH groups and two $NH^+$. That could be due to the fact that $pK_a$'s of aliphatic carboxylic acids in DMSO are much higher than in water,[298, 299] whilst for aliphatic tertiary amines the values are similar.[299, 300]

### 2.1.2.1 Attempted synthesis *via* acyl chlorides

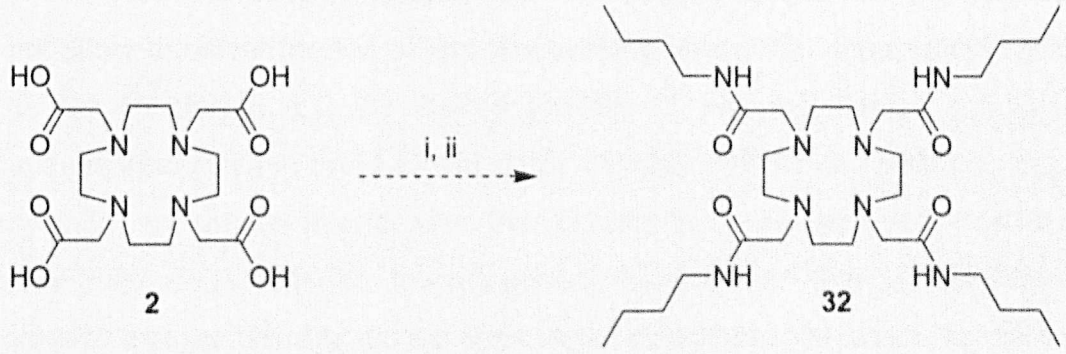
As a first method for the activation of DOTA followed by its reaction with an amine, it was tried to convert it to the corresponding acyl chloride; perhaps surprisingly such derivatives of DOTA have never been mentioned in the literature.

Acyl (or acid) chlorides are generally formed by reacting the carboxylic acid with thionyl chloride or oxalyl chloride.[240] The reaction mechanisms involved are shown in Scheme 2.7.



**Scheme 2.7** Mechanism for acyl chloride formation using thionyl chloride (up) or oxalyl chloride (down).

Both procedures were tried: **2** was dissolved in either an excess (~650 molar equivalents) of distilled thionyl chloride (used as both reagent and solvent), or a mixture of DCM and DMF (to allow dissolution of DOTA) followed by dropwise addition of oxalyl chloride (Scheme 2.8, i), according to general procedures.[301]



**Scheme 2.8** General representation of the attempted syntheses of tetra-amide **32** from DOTA *via* the corresponding acid chloride using either thionyl chloride or oxalyl chloride. Conditions reported in Table 2.3.

| **Table 2.3** Reaction conditions and results for the attempted synthesis of DOTA-amide **32** *via* the corresponding acyl chloride, as shown in Scheme 2.8. | | |
|---|---|---|
| | **Conditions** | **Result** |
| 1 | i) DOTA (1 mol eq), $SOCl_2$ (~650 mol eq), reflux, 5 h;<br>ii) *n*-butylamine (~400 mol eq), -10 °C → RT, 8 h. | **32** did not form |
| 2 | i) DOTA (1 mol eq), $(COCl)_2$ (16 mol eq), DCM/DMF, RT → reflux, 14 h;<br>ii) *n*-butylamine (~400 mol eq), -10 °C → RT, 8 h. | **32** did not form |

In both cases, after removal of solvents and some unreacted reagents under reduced pressure a brown solid residue was obtained. Such solids were used in the next step without further purification or characterisation, due to the well-known fact that acid chlorides are highly moisture sensitive. A large excess (~400 molar equivalents) of distilled *n*-butylamine was added at -10 °C, and the mixture was stirred at room temperature. No evidence was obtained from NMR spectroscopy of the formation of the desired product, by comparison with literature values[289] and our own data (see Section 2.1.1). In particular, in the $^1$H NMR spectrum it was not possible to observe the expected triplet at 0.92 ppm for the methyl protons of the butyl chain as well as the resonances at 1.33 and 1.47 ppm due to the $\beta$ and $\gamma$ methylene groups, the peaks (broad because of conformational equilibria) for the ring and acetate protons at 2.70 and 3.07 ppm respectively, the multiplet at 3.22 ppm for the methylene groups of the butyl chain in the $\alpha$ position with respect to the amide moiety, and the broad peak at 7.14 ppm due to the amide protons. Instead, complex spectra for both reaction mixtures were obtained. Although the chemical shift of some resonances was close to what was expected for the desired product, in neither case the integration was conclusive. No peak with m/z value above 200 was observed in the mass spectra of the crude products, and the data obtained did not allow the identification of any product/by-product. The spectroscopic analysis led to the conclusion that the desired product **32** had not formed, although all precautions were taken to avoid contact of the chloride with air and moisture, and both *n*-butylamine and thionyl chloride were freshly distilled. On the basis of the well-known high reactivity of acyl chlorides towards amines, it seems more than just speculation to hypothesise that the chloride did not form in the first place. That could be due to the protonation conditions of DOTA, where the absence of protons on the carboxylate groups affects the stabilisation of the tetrahedral intermediate following the nucleophilic attack of a chloride to the carbonyl moiety, as shown in Scheme 2.7. Furthermore, the formation of intra- and intermolecular hydrogen bonds, as well as complexes with

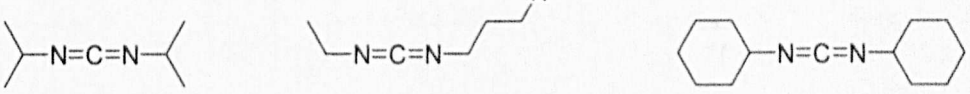
metals, could interfere with the first step of addition of the acid to the thionyl chloride (Scheme 2.7), the carboxylic/carboxylate groups being directly involved in such events.

This would be a problem also when other activating agents are used. However, since some procedures are reported in the literature about that,[302-305] it was decided to explore reagents and procedures commonly used in peptide synthesis.

### 2.1.2.2 Synthesis using peptide coupling reagents

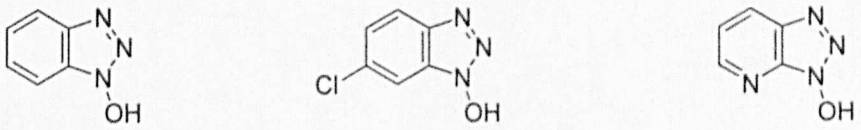
*Peptide coupling reagents* (Figure 2.1) have seen a remarkable evolution, especially in the last decade, from the carbodiimides[306-308] used at first up to the most recent *onium* (phosphonium[309, 310] and uronium[311-313]) salts.

**Carbodiimides**



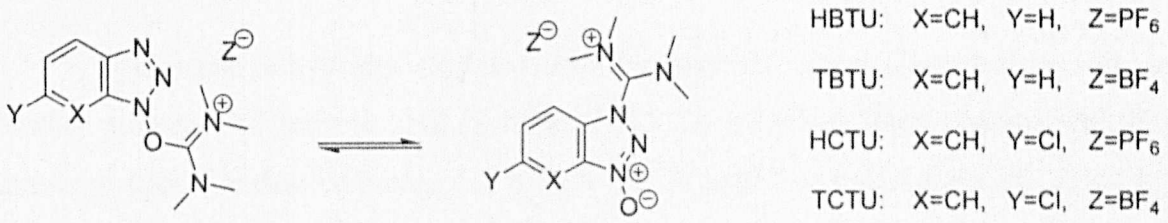
DIP (DIPCDI) EDC (EDAC, WSC, **33**) DCC (DCCI, **34**)

**Coupling additives**



HOBt (**35**) Cl-HOBt HOAt

**Aminium salts**



Uronium form Guanidinium form

HBTU: X=CH, Y=H, Z=$PF_6$

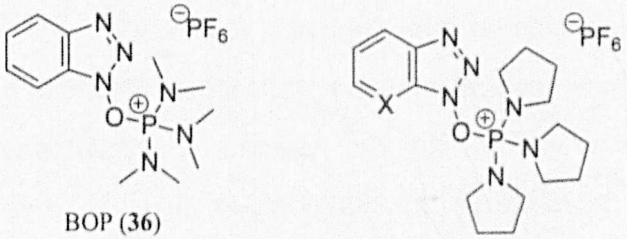
TBTU: X=CH, Y=H, Z=$BF_4$

HCTU: X=CH, Y=Cl, Z=$PF_6$

TCTU: X=CH, Y=Cl, Z=$BF_4$

HATU: X=N, Y=H, Z=$PF_6$

**Phosphonium salts**



BOP (**36**)

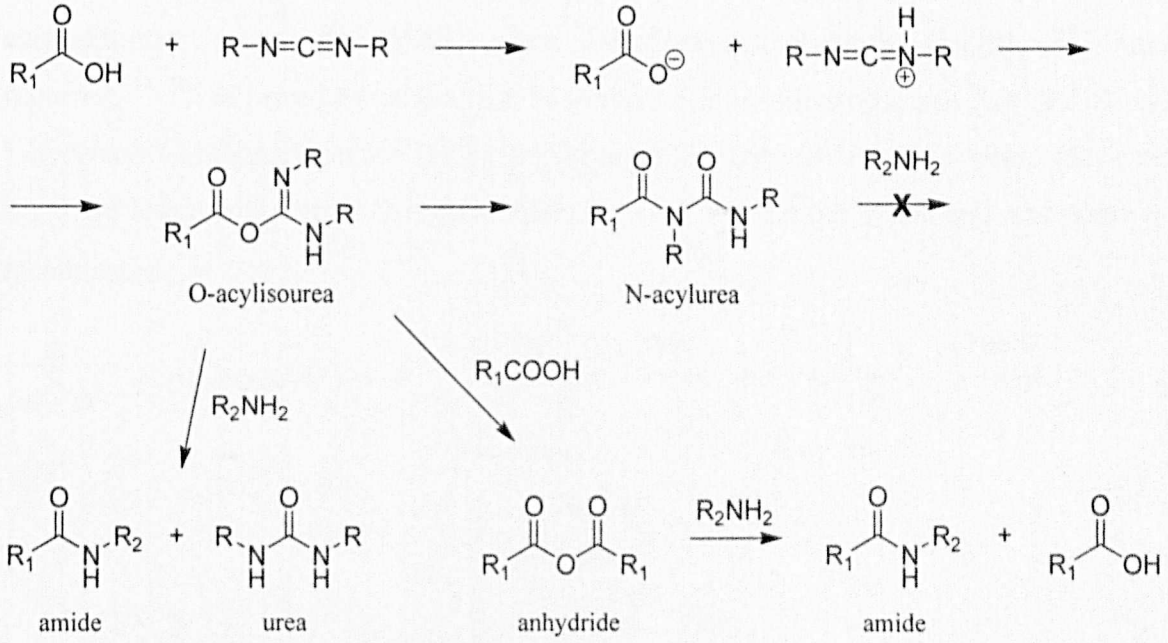
PyBOP: X=CH

PyAOP: X=N

**Figure 2.1** The most common peptide coupling reagents and additives.

The first peptide coupling agent reported was dicyclohexylcarbodiimide[308] (DCC, **34**), but because ureas in solution are usually difficult to remove, water-soluble carbodiimides (e.g., *N*-(3-dimethylaminopropyl)-*N'*-ethylcarbodiimide, EDC, **33**) have been developed and are a useful alternative.

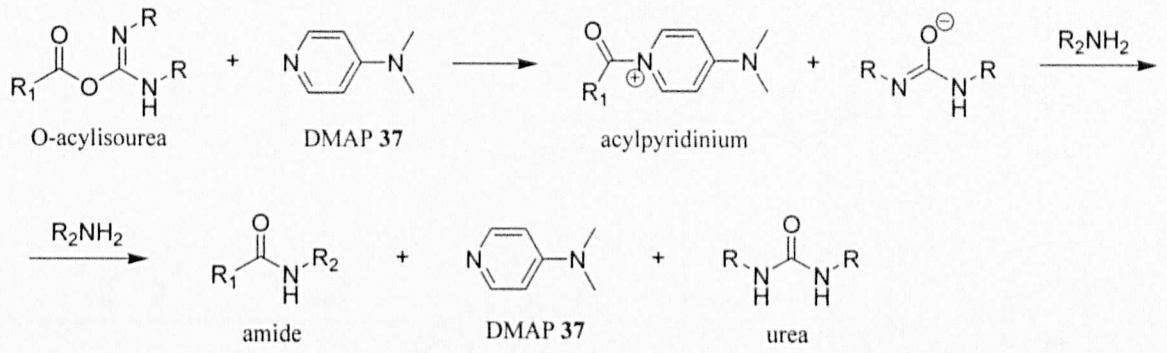
Activation of the carboxylic moiety by carbodiimides (Scheme 2.9) begins with the transfer of a proton from the acid to one of the carbodiimide nitrogen atoms, followed by formation of the *O*-acylisourea, which represents the species most able to react with the amine and form the corresponding amide. The driving force of this reaction is the formation of the urea by-product.




**Scheme 2.9** Mechanism of peptide bond formation through carbodiimide activation.

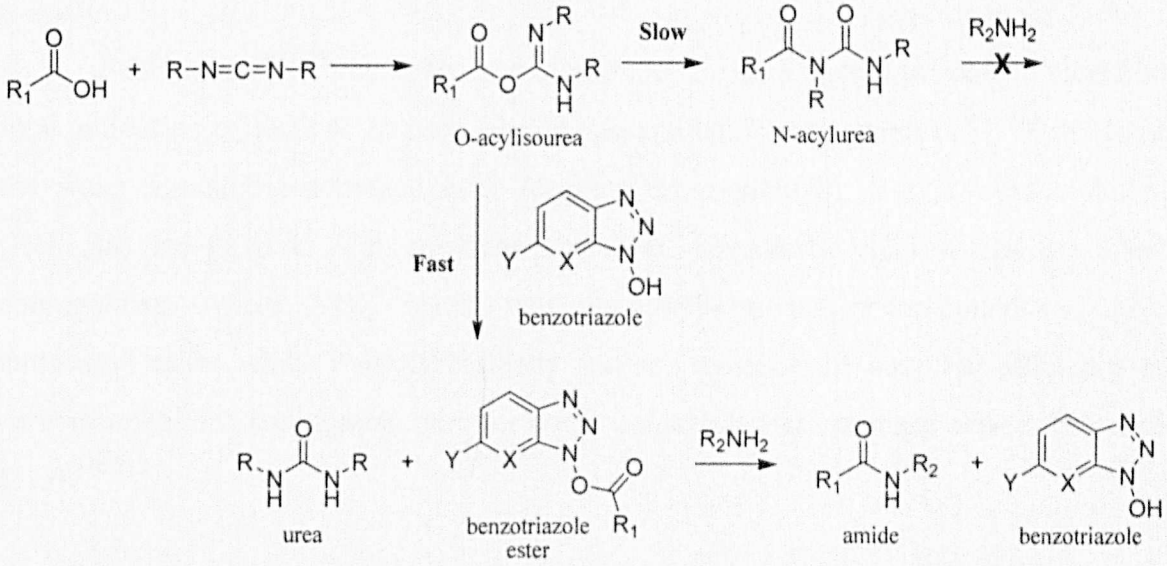
Symmetric anhydrides can also form by reaction of the *O*-acylisourea with a further molecule of starting acid (Scheme 2.9). The anhydride then couples with the amine to form the desired amide and a molecule of acid that enters the cycle again by reacting with the carbodiimide or the *O*-acylisourea. However, carbodiimides are rather reactive and inconvenient side reactions generally take place, such as the rearrangement of the *O*-acylisourea to the corresponding, inert *N*-acylurea (Scheme 2.9).

These side reactions, and especially the formation of *N*-acylisoureas, can be remarkably reduced by adding suitable nucleophiles able to react faster than the competing acyl transfer, but still forming an intermediate reactive towards the amine. One of such nucleophiles is pyridine or, better, *N*,*N*-4-(dimethylamino)pyridine (DMAP, **37**), which forms an intermediate acylpyridinium salt by reacting with *O*-acylisourea (Scheme 2.10). This species can then couple with the amine.



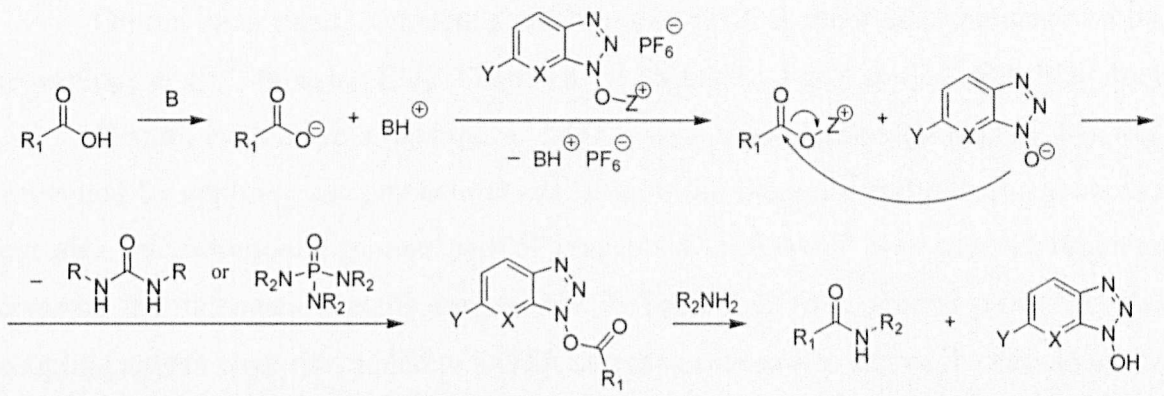

**Scheme 2.10** Catalytic role of DMAP **37** as additive in amide formation following activation by carbodiimides.

Benzotriazole derivatives (Figure 2.1) were introduced as additives to carbodiimides since the 1970s, when 1-hydroxybenzotriazole (HOBt, **35**) was reported,[314, 315] followed by others like 1-hydroxy-5-chlorobenzotriazole (Cl-HOBt) and 1-hydroxy-7-azabenzotriazole (HOAt). Although benzotriazole active esters (Scheme 2.11) are less reactive than *O*-acylisoureas, they are much more stable and less prone to racemisation.




**Scheme 2.11** Mechanism of peptide bond formation using a carbodiimide and a benzotriazole as additives for activation of the carboxylic moiety. For a list of possible Xs and Ys see Figure 2.1.

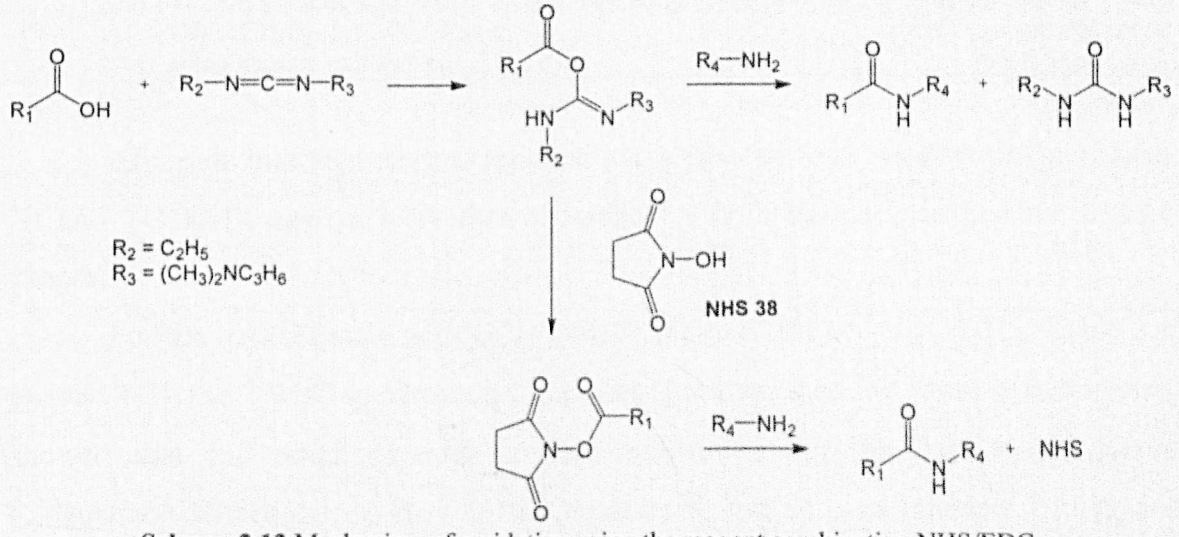
In the 1990s, onium salts of hydroxybenzotriazole derivatives have been developed,[309-313] (Figure 2.1). The amidinium salts exist in solution as an equilibrium between the uronium and the guanidinium forms. The counterion can be either tetrafluoroborate or hexafluorophosphate, and its nature has no influence on the reactivity. Instead, phosphonium salts have always $PF_6^-$ as counterion. Both react directly with carboxylates, and a minimum of one equivalent of base is then required (Scheme 2.12).



**Scheme 2.12** Coupling procedure using onium salts as additives for activation of the carboxylic acid. $Z^+$ = uronium or phosphonium cation; for a list of possible Xs and Ys see Figure 2.1.

The transitory acyloxy-phosphonium or amidinium species reacts instantaneously with the benzotriazole derivative to form the benzotriazole active ester, which in turn reacts with the amine leading to the desired amide. The driving force for reactions involving amidinium or phosphonium salts is the formation of the urea by-product or the phosphorus oxide, respectively.

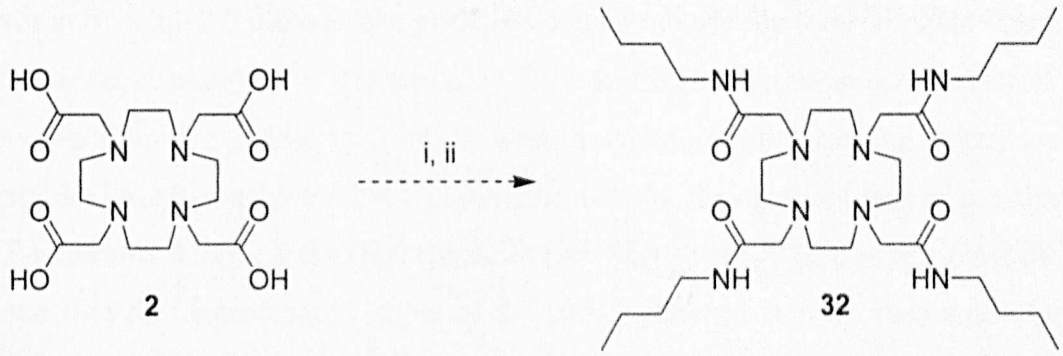
Few papers[302-305] report the use of peptide coupling agents to achieve partial or total amidation of DOTA. In particular, mono-amidation was achieved[302, 303] by using the water-compatible activated ester reagents represented by *N*-hydroxysuccinimide (NHS **38**) and EDC **33**. This protocol is used to increase the yield of EDC-mediated conjugations, where NHS reacts with carboxyl-containing compounds to give aminoacyl esters which hydrolyse slowly and can enhance the coupling efficiency of carbodiimides for conjugating carboxylated compounds with primary amines (Scheme 2.13).[316-318]



**Scheme 2.13** Mechanism of amidation using the reagent combination NHS/EDC.

On the other hand, complete amidation of DOTA is reported to be achieved by Govenlock *et al.*[305] by using EDC **33** and HOBt **35**, and by Fazal *et al.*[304] with BOP **36**.

Herein, exhaustive amidation of DOTA with *n*-butylamine (Scheme 2.14) was attempted by applying the procedures available in the literature and mentioned above, but also the commonly applied pair of reagents DCC/DMAP was tried in order to compare the outcomes. Details are reported in Table 2.4. As a general procedure, the coupling agents were first added to DOTA and the mixture was stirred in order to allow the formation of the activated intermediate; then, *n*-butylamine was added.




**Scheme 2.14** Attempted synthesis of tetra-amide derivative **32** by using peptide coupling reagents. Conditions and results are reported in Table 2.4 and discussed in the text.

**Table 2.4** Reaction conditions and results for the procedure shown in Scheme 2.14.

| | Conditions | Result |
|---|---|---|
| 1 | i) DOTA (1 mol eq), DCC (4 mol eq), DMAP (4 mol eq), $CH_2Cl_2$, RT, 10 min;<br>ii) *n*-butylamine (4.4 mol eq), reflux, 63 h. | No **32**. DOTA and DMAP unreacted. DCC converted into guanidine. |
| 2[305] | i) DOTA (1 mol eq), HOBt (5 mol eq), EDC·HCl (5 mol eq), THF/$H_2O$ 1:1, RT, 30 min; then DIPEA (10 mol eq), 0 °C, 10 min;<br>ii) *n*-butylamine (8 mol eq), RT, 63 h. | No **32**. DOTA and HOBt unreacted. EDC converted into guanidine. |
| 3[302, 303] | i) DOTA (1 mol eq), NHS (5 mol eq), EDC·HCl (5 mol eq), $H_2O$, RT, 10 min; then DIPEA (10 mol eq), RT, 30 min;<br>ii) *n*-butylamine (4.4 equivalents), RT, 72 h. | No **32**. DOTA and NHS unreacted. EDC converted into guanidine. |
| 4[304] | i) DOTA (1 mol eq), $Et_3N$ (8 mol eq), BOP (4.4 mol eq), DMF/$CH_2Cl_2$ 1:1, RT, 10 min;<br>ii) *n*-butylamine (4.4 mol eq), RT, 18 h. | **32** formed, but problems were encountered for its purification |

All crude mixtures were evaporated and extracted from water with chloroform. $^1H$ and $^{13}C$ NMR spectra were then recorded for both the aqueous and the organic phases.

For the reactions run with DCC/DMAP, EDC/HOBt and EDC/NHS (Table 2.4, entries 1-3) the NMR spectroscopic analysis (corroborated by mass spectrometry) showed that the target product or less substituted cyclens were not achieved (comparison with data reported in the literature[289] and or own [Section 2.1.1]), and DOTA was quantitatively recovered unreacted from the water phase. On the other hand,

in the organic phase the "transfer agent" (DMAP, HOBt or NHS) was present unreacted, while the carbodiimides had coupled with butylamine and converted into their guanidine forms (typical resonance observable at about 155 ppm in the $^{13}C$ NMR spectrum).[319] No unreacted carbodiimide was detected (absence of the typical resonances around 140 ppm in the $^{13}C$ NMR spectrum). The formation of *O*-acylisourea or *N*-acylurea was excluded by the absence of signals at about 174 ppm in the $^{13}C$ NMR spectrum.[320-324] These data led to conclude that the activation of the carboxylic moieties of DOTA by DCC or EDC to form the more reactive *O*-acylisourea (or *N*-acylurea) as shown in Scheme 2.9 did not take place. As a consequence the transfer agents could not accept the acyl group (see Schemes 2.10, 2.11 and 2.13) and remained unreacted. The free carbodiimides could then react with butylamine to form the corresponding guanidines. Analogously to what was hypothesised for the apparent lack of reactivity of DOTA towards thionyl and oxalyl chlorides (see Section 2.1.2.1), it seems reasonable to assume that the deprotonated status of the carboxylate groups, or their unavailability caused by the formation of hydrogen bonds or metal-complexes, makes DOTA fail to react with the carbodiimide as shown in the first step of Scheme 2.9, thus leading to no activation and consequent lack of reactivity towards the amine. The reason for the success reported by Govenlock *et al.*[305] might be the different protonation or coordination condition of the DOTA used in their experiments. However, it is to be mentioned that such paper belongs to a series[274, 275, 305, 325] where the synthesis of a further 10 similar ligands is reported: all 10 compounds were obtained from the corresponding chloroacetamides and cyclen following a convergent procedure in DMF in the presence of potassium carbonate. For each ligand a complete characterisation is reported, including elemental analysis as a proof of purity. Only in one isolated case the synthesis is reported to be carried out according to the divergent protocol involving the use of EDC and HOBt, as mentioned above. A full characterisation is not reported, and the crystallinity of the product is defined "poor". Such a synthetic method was not repeated by anyone else in the literature, including the same authors. The real success and applicability of this procedure then seem questionable.

On the contrary, NMR spectroscopic analysis and mass spectrometry revealed that when BOP was used (Table 2.4, entry 4) the desired compound formed (comparison with data reported in the literature[289] and our own [Section 2.1.1]). Some conformational restrictions caused the protons of the ring to differentiate into two types, with consequent observation of two different broad signals in the $^{1}H$ NMR spectrum

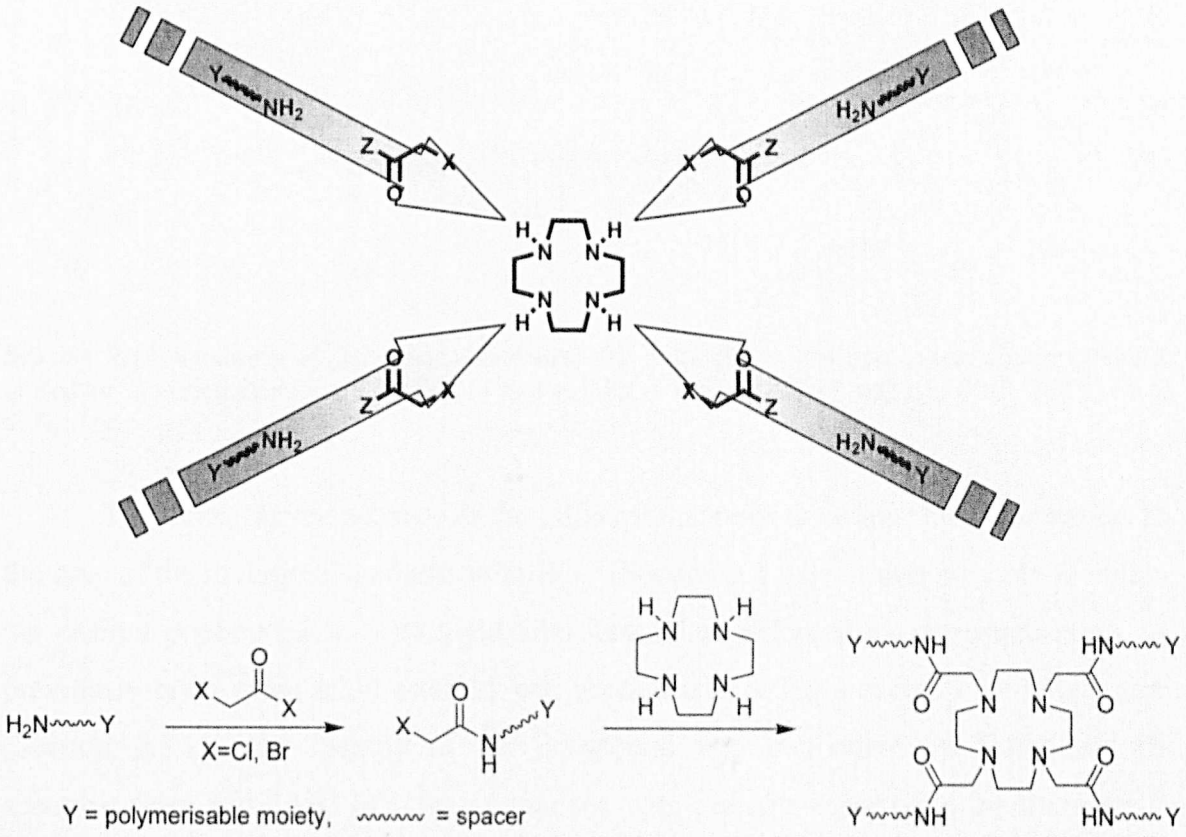
with the same integration area. The NMR spectra seemed to exclude the presence of partially substituted DOTA (MS analysis was not conclusive in this respect). This success showed the possibility of the carboxylate groups of DOTA to react with suitable reagents, and indirectly confirmed that the reason for the failures obtained with thionyl chloride, oxalyl chloride and carbodiimides was the lack of protons needed to start the activation of the carboxylic moieties as shown in Schemes 2.7 and 2.9 for these reagents.

However, purification of the target product through the techniques previously successful (Section 2.1.1) and those reported in the literature[289, 304] was not achieved. Moreover, it was not possible to find a procedure or a combination of procedures to obtain the tetra-amide derivative **32** in a pure form, after investigating eluting systems for chromatography, and solvents or combinations of solvents for recrystallisation or precipitation. The nature of the impurities formed in the presence of BOP made them apparently impossible to separate from the target compound.

In conclusion the use of BOP, although allowing the formation of the desired product, was not considered convenient with respect to other parallel procedures that led to the desired compound in a pure form (see Section 2.2 below).

## 2.2 Convergent synthesis

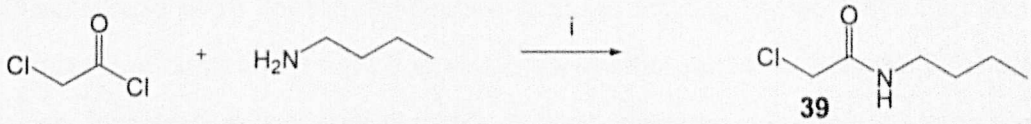
Considering the difficulties encountered in the divergent approach to prepare the targeted amide derivatives of DOTA, a different strategy was undertaken, i.e. attachment of arms already containing the amide moiety to cyclen (Scheme 2.15).




**Scheme 2.15** Representation of a possible convergent synthesis deriving from one of the retrosynthetic analyses (Scheme 2.2) and leading to a tetra-substituted cyclen possessing moieties which can be exploited for polymerisation.

According to this strategy, and to obtain **32** in the first instance, *N*-butyl-2-chloroacetamide **39** was prepared and then reacted with cyclen under conditions reported[79, 129, 261-284] to have been successful for exhaustive substitution of cyclen with different substrates.

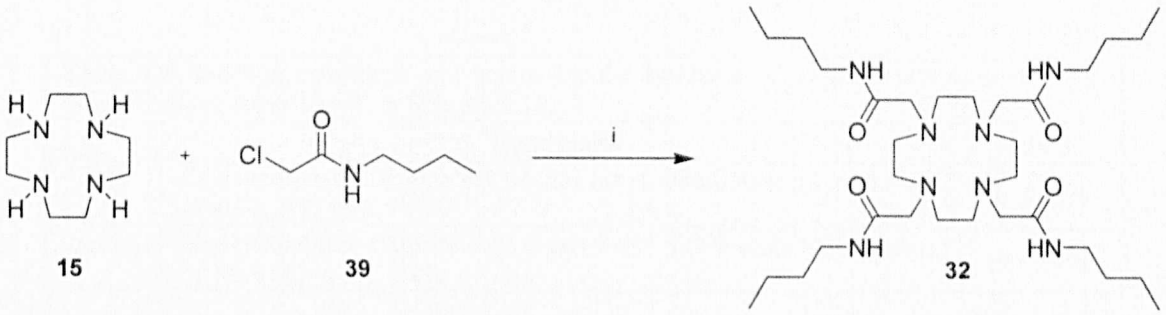
Chloroacetamide **39** was obtained in 84% yield by following a literature procedure[289] as shown in Scheme 2.16.




**Scheme 2.16** Synthesis of *N*-butyl-2-chloroacetamide **39**. i) chloroacetyl chloride (1 mol eq), *n*-butylamine (1 mol eq), $Et_3N$ (1 mol eq), THF, -10 °C, 1 h, 84%.

The identity of the product was confirmed by comparing the $^1H$ and $^{13}C$ NMR spectroscopy, $CI^+$ mass spectrometry and IR spectroscopy data with those available in the literature.[289]

In order to carry out the next step in the convergent synthesis, cyclen was mixed in DMF with cesium carbonate, potassium iodide and chloroacetamide **39** under the conditions[289] reported in Scheme 2.17.



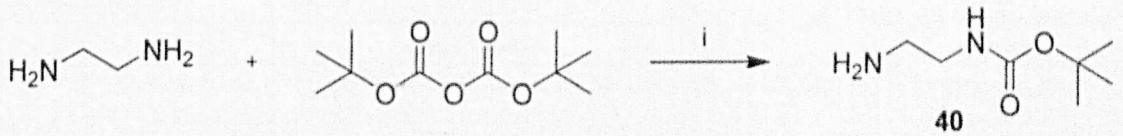

**Scheme 2.17** Synthesis of tetra-amide derivative **32** from cyclen through a convergent synthesis procedure. i) cyclen (1 mol eq), $Cs_2CO_3$ (5 mol eq), KI (5 mol eq), **39** (5 mol eq), DMF, 70 °C, 18 h, 69%.

This time, maybe because of the different nature of the impurities with respect to the case of the divergent synthesis with BOP (Section 2.1.2.2), it was possible to obtain the desired product **32** in 69% yield after extraction followed by recrystallisation, as previously done when ethyl ester **31** was reacted with a large excess of *n*-butylamine (Section 2.1.1). The identity of the compound was confirmed by NMR and IR spectroscopies and $FAB^+$ MS, by comparison with the data reported in the literature[289] and our own (Section 2.1.1).

### 2.2.1 Initial synthesis of DOTA-amides with amines or thiols as terminal groups

After this positive result in the convergent synthesis, it was tried to prepare the amide derivatives of DOTA from ethylenediamine and mercaptoethylamine, in order to introduce an amine or a thiol group for further functionalisation and/or polymerisation. This required prior protection of one of the amine groups for the ethylenediamine, and the thiol group for the mercaptoethylamine. *tert*-Butoxycarbonyl (BOC) and *p*-methoxybenzyl were chosen, respectively, as protecting groups since they are well-documented and compatible with the reaction sequence shown in Scheme 2.15; also, the protection/deprotection proceeds typically in high yield and is compatible with a variety of functional groups.[326]

Monoprotection of 1,2-diaminoethane (Scheme 2.18) was tried by following two different literature procedures,[327-330] under the conditions reported in Table 2.5.

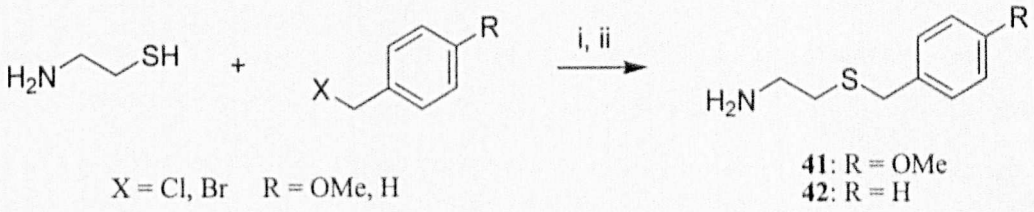



**Scheme 2.18** General representation of the monoprotection of ethylenediamine with BOC-group. Conditions and results are reported in Table 2.5 and discussed in the text.

| **Table 2.5** Reaction conditions and results for the synthesis of *N*-(*tert*-butoxycarbonyl)-1,2-diaminoethane **40**, as shown in Scheme 2.18. | | |
|---|---|---|
| | **Conditions** | **Result** |
| 1[327] | ethylenediamine (8 mol eq), di-*tert*-butyl dicarbonate (1 mol eq), dioxane, RT, 16 h. | **40** = 62% |
| 2[328-330] | ethylenediamine (10 mol eq), di-*tert*-butyl dicarbonate (1 mol eq), DCM, 0 °C → RT, 24 h. | **40** = 89% |

Both methods led to the target compound with similar purity, as assessed by elemental analysis. The NMR, MS and IR data were in full agreement with those available in the literature.[327-330] However, the yield for the second procedure was higher (89% vs. 62%; reported 50%[328] / 64%[329] / 100%[330] vs. 95%[327]), possibly because of the slightly larger excess of ethylenediamine (10 vs. 8 molar equivalents). An alternative explanation relies on the fact that solvents with different coordination abilities have a different stabilisation effect on the transition state, and in this case the use of DCM may kinetically disfavour the formation of the bis-protected by-product, and consequently increase the yield of the target monoprotected species.

Protection of the thiol moiety of 2-mercaptoethylamine (cysteamine) was attempted with either the *p*-methoxybenzyl or the benzyl groups, chosen as two of the most common and effective amine protective groups. Unclear outcomes had been obtained by other members of our group when using these reagents. Following a literature procedure,[331] the aminothiol and a halide of either protecting group were stirred in the presence of potassium carbonate as shown in Scheme 2.19 under the conditions reported in Table 2.6.




**Scheme 2.19** Monoprotection of cysteamine. Conditions and results are reported in Table 2.6 and discussed in the text.

| **Table 2.6** Reaction conditions and results for the monoprotection of cysteamine, as shown in Scheme 2.19. | | |
|---|---|---|
| | **Conditions** | **Result** |
| 1 | i) cysteamine (1 mol eq), $K_2CO_3$ (2 mol eq), MeOH, reflux, 10 min;<br>ii) 4-methoxybenzyl chloride (1 mol eq), MeOH, reflux, 15 h. | Complex mixture of products |
| 2 | i) cysteamine (1 mol eq), $K_2CO_3$ (2 mol eq), MeOH, reflux, 10 min;<br>ii) benzyl bromide (1 mol eq), MeOH, reflux, 15 h. | **42** = 54% |

In the first attempt, TLC of the crude reaction mixture revealed that many by-products had formed, unworthy to be separated. They could possibly result from multiple substitutions on cysteamine, as in principle both the amine and the thiol groups are capable of nucleophilic attack on the *p*-methoxybenzyl chloride (Figure 2.2), although the thiolate should be favoured.

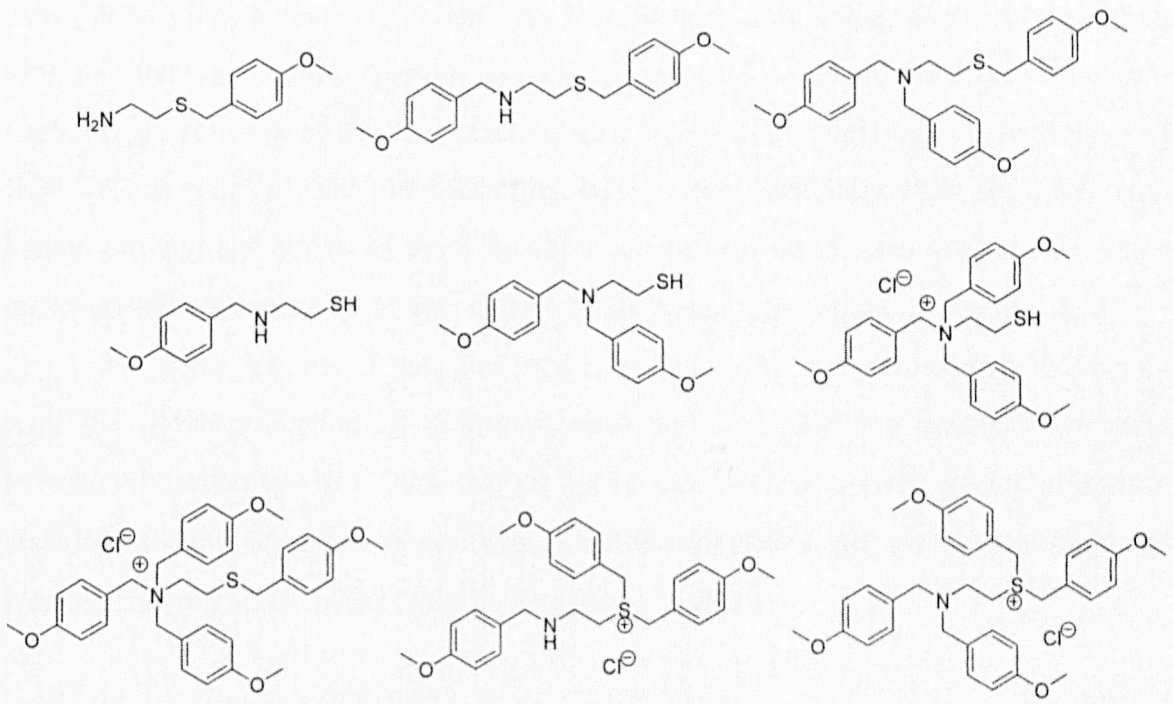


**Figure 2.2** Possible products from the reaction of cysteamine with *p*-methoxybenzyl chloride.

On the contrary, when benzyl bromide was used, compound **42** was isolated in 54% yield after extraction followed by chromatography. The spectroscopic data were in full agreement with those available in the literature.[331]

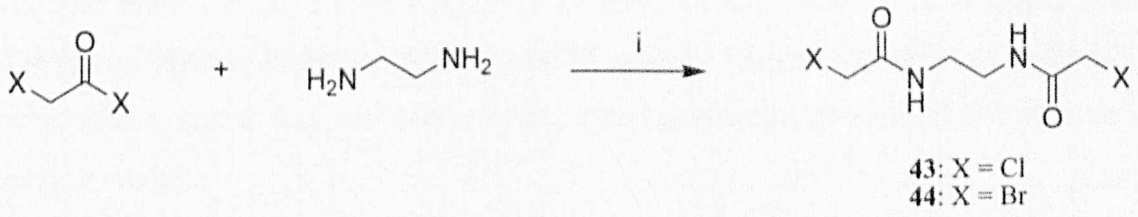
However, the relatively low yield for this reaction led to the consideration that the yield expected for the target tetra-substituted compound would be unlikely reasonable when compared to those for reactions not involving protection and deprotection steps. For instance, the overall yield in synthesising DOTA-tetra-butyl-amide **32** (see Section 2.2) was 58% (84% + 69%), attachment onto cyclen being the limiting step. When considering the 54% achieved in the protection step and hypothesising an optimistic 80% yield for the remaining reactions (i.e. formation of the chloroacetamide, tetra-substitution and final deprotection) estimated on the basis of our own results and literature data, a modest 28% is estimated. In fact, the experience gained from other people's research in our group strongly suggests that the removal of the benzyl group would be much less efficient than hypothesised. A paper published one year later[332] about exactly the same synthesis started by us (with the mono-

protection of ethylenediamine) partially confirmed the doubts reported above: the overall yield for preparing *N*-(2-amino-ethyl)-2-(4,7,10-tris-((2-amino-ethylcarbamoyl)-methyl-1,4,7,10-tetraazacyclododec-1-yl)-acetamide after synthesis of the corresponding chloroacetamide, attachment onto cyclen and deprotection was 63% (76% + 87% + 95%), which combined with the result obtained herein for the protection step (89%) gives a total 56% yield. As a conjecture, this value, apparently not bad, seems nonetheless quite suspicious, especially for the 95% yield in the deprotection step (rather high, considering the four reaction sites per molecule, although the hydrolysis of BOC groups is usually achieved with high conversions, especially when compared with benzyl groups) and above all the 87% obtained with the attachment onto cyclen, when an "orange/brown solid" (and then definitely not pure, in our opinion) was obtained.

For these reasons, it was preferred to abandon this route (including that begun with the mono-protection of diaminoethane) and focus on the synthesis of tetra-substituted derivatives of DOTA that do not require additional steps for the protection and deprotection of sensitive moieties. Terminal functional groups were chosen that were considered stable in the reaction conditions to apply.

### 2.2.2 Synthesis of DOTA-amides with halogens as terminal groups

Following the successful exhaustive attachment onto cyclen of arms bearing a *n*-butyl acetamide moiety, the tetra-substitution was attempted with arms containing functional groups to be used successively for polymerisation. The first attempts were carried out with *N,N'*-ethylenebis(2-chloro-acetamide) **43** and the corresponding bromo-analogue **44**, in order to check their different reactivities. The syntheses of these compounds have been reported in the literature,[333, 334] and they were prepared as shown in Scheme 2.20 and under the conditions reported in Table 2.7.




**43**: X = Cl
**44**: X = Br

**Scheme 2.20** Synthesis of bis-haloacetamides **43** and **44**. Conditions and results are reported in Table 2.7 and discussed in the text.

| **Table 2.7** Reaction conditions and results for the synthesis of bis-haloacetamides **43** and **44**, as shown in Scheme 2.20. | | |
|---|---|---|
| | **Conditions** | **Result** |
| 1[333] | 2-chloroacetyl chloride (2 mol eq), ethylenediamine (1 mol eq), 5 M NaOH/toluene, -10 °C, 3 h. | **43** = 58% |
| 2[333] | 2-bromoacetyl bromide (2 mol eq), ethylenediamine (1 mol eq), 5 M NaOH/toluene, -10 °C, 3 h. | **44** = 54% |
| 3[334] | 2-bromoacetyl bromide (2.5 mol eq), ethylenediamine (1 mol eq), $K_2CO_3$ (3 mol eq), $Et_2O/H_2O$/toluene, -10°C, 3 h. | **44** formed but could not be isolated |

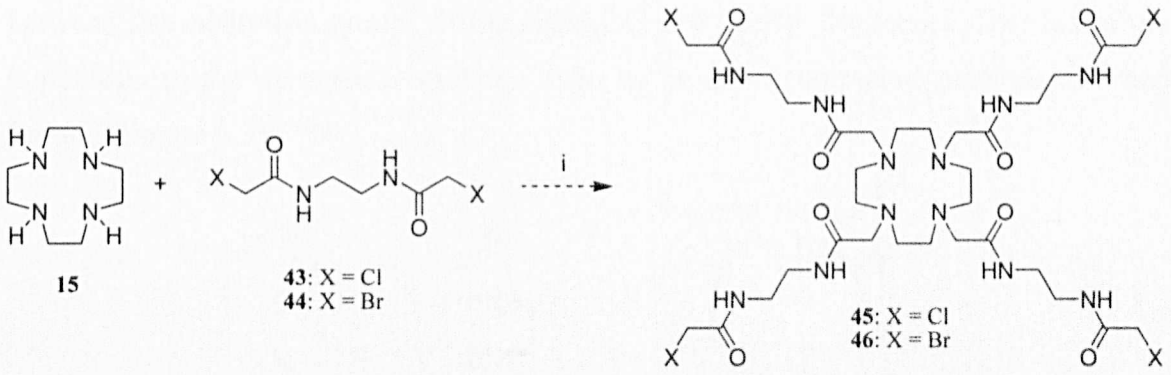
Compound **43** was isolated in 58% yield (reported[333] 85%) after washing with water and recrystallisation. The spectroscopic and spectrometric analyses were in full agreement with the literature data.[333]

Bis-bromoacetamide **44** formed with both applied methods, as established by NMR (by comparison with literature[334] data) and MS analyses of the crude reaction mixtures. However, in the second case the precipitated powder was so fine to make centrifugation ineffective and block any filtration devices (such as membrane and paper filters, and synthered funnels) from either water or organic solvents. On the contrary, there was no problem with filtering the crude mixture from the first procedure, and **44** was isolated in 54% yield (reported[334] 32%) after recrystallisation from ethanol.

As expected, the main difference between the $^1$H NMR spectra of **43** and **44** were the resonances produced by the methylene groups bound to the halogen atoms: 4.04 ppm for $ClCH_2$ and 3.84 ppm for $BrCH_2$. Consistently, the corresponding carbon atoms exhibit resonances in the $^{13}$C NMR spectra at 42.5 ppm ($ClCH_2$) and 38.4 ppm ($BrCH_2$). Because of the different force constants of the C-Cl and the C-Br bonds, the IR spectra of **43** and **44** presented different absorption bands in the 1200-1300 $cm^{-1}$ and the fingerprint regions. As a difference in the chemical behaviour between the two bis-haloacetamides, **44** was reactive towards water after a prolonged time, with formation of *N,N'*-ethylenebis-glycolamide as proved by the signals observed in the $^1$H (7.83 ppm: NH; 5.95 ppm: OH; 3.78 ppm: $C\underline{H}_2OH$; 3.18 ppm: $NHC\underline{H}_2$) and $^{13}$C (172.1 ppm: C=O; 61.4 ppm: $CH_2OH$; 39.0 ppm: $NHCH_2$) NMR spectra. This reactivity is not reported in the literature, and it was not shown by bis-chloroacetamide **43** even after refluxing in water overnight.

In order to compare the outcomes, bis-haloacetamides **43** and **44** were reacted with cyclen by trying different procedures chosen as the most promising among those reported in literature for tetrasubstitution on tetraazacyclododecane (see Section 2.1.1

and references therein). The general representation of the attempted synthesis is shown in Scheme 2.21, and the details about the applied conditions are reported in Table 2.8.




**Scheme 2.21** General representation of the attempted of synthesis of compounds **45** and **46**. Conditions and results are reported in Table 2.8 and discussed in the text.

**Table 2.8** Reaction conditions and results for the attempted synthesis of tetrasubstituted macrocycles **45** and **46**, as shown in Scheme 2.21.

| | Conditions | Result |
|---|---|---|
| 1 | Cyclen (1 mol eq), **43** (10 mol eq), $K_2CO_3$ (5 mol eq), MeCN, reflux, 48 h. | No reaction |
| 2 | Cyclen (1 mol eq), **43** (10 mol eq), $Cs_2CO_3$ (5 mol eq), KI (5 mol eq), DMF, 80 °C, 5 d. | Mixture of products. No evidence of **45**. |
| 3 | Cyclen (1 mol eq), **43** (10 mol eq), $Et_3N$ (5 mol eq), KI (5 mol eq), DMF, 80 °C, 48 h. | Mixture of products. No evidence of **45**. |
| 4 | Cyclen (1 mol eq), **44** (10 mol eq), $Cs_2CO_3$ (5 mol eq), KI (5 mol eq), DMF, 80 °C, 48 h. | Mixture of products. No evidence of **46**. |
| 5 | Cyclen (1 mol eq), **44** (10 mol eq), $Et_3N$ (5 mol eq), KI (5 mol eq), DMF, 80 °C, 48 h. | Mixture of products. No evidence of **46**. |

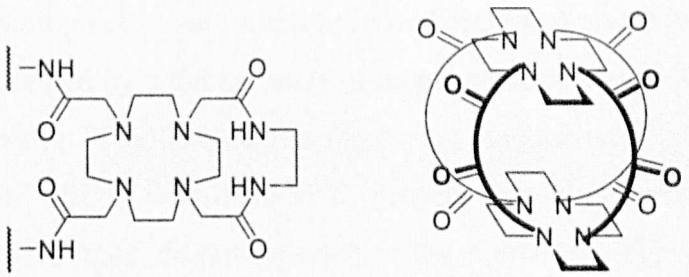
An excess of 10 molar equivalents of haloacetamide was used in all cases in order to favour tetrasubstitution rather than crosslinking.

When **43** was reacted in the presence of potassium carbonate as a base (Table 2.8, entry 1), no reaction took place and the starting materials were recovered quantitatively.

TLC and NMR analyses of the reactions with cesium carbonate (Table 2.8, entries 2 and 4) revealed that complex mixtures of products and by-products had been obtained without a predominant species. The complexity of the mixtures and the lack of evidence (from NMR spectroscopy and MS) that the target compound had been achieved led to the abandonment of this route.

When cesium carbonate was replaced by triethylamine (miscible with DMF, whilst $Cs_2CO_3$ is partially soluble; Table 2.8, entries 3 and 5), cleaner NMR spectra were obtained for the crude reaction mixtures, although several products were still detected by TLC. In particular, a set of signals looked predominant, with the resonances at 3.22 ppm in the $^1H$ NMR spectrum and at 55.9 ppm in the $^{13}C$ NMR spectrum

compatible with a hypothetical $NCH_2CO$ fragment as a result of the attachment of the arms onto cyclen. However, no differentiation was observed (as instead expected) between the methylene groups of the $NCH_2CO$ and $CH_2Br$ fragments. That led to the hypothesis that a symmetric structure such as an *ansa*-compound or a capsule had formed (Figure 2.3).




*ansa*-derivative capsule

**Figure 2.3** *Ansa*-compound and capsule as possible by-products when trying to attach an arm functionalised at both ends.

However, no evidence supporting such speculations could be obtained. Instead, several factors seemed to contradict them:

- those compounds are unlikely to form in the reaction conditions applied, since a higher dilution would be required and cyclen was added to the di-halides rather than *vice-versa*;
- the structures showed in Figure 2.3 would impose strict motional constraints to the ring, thus causing a differentiation between the resonances for pseudo-axial and pseudo-equatorial protons in the $^1H$ NMR spectrum; such differentiation was not observed;
- in fact, no signal was observed in the $^1H$ and $^{13}C$ NMR spectra which could be surely assigned to ring protons;
- no peak above 400 m/z was recorded in the MS spectra, while being 879/1056, 452 and 905 Da the molar masses of the target compound, the double-*ansa*-derivative and the capsule respectively.

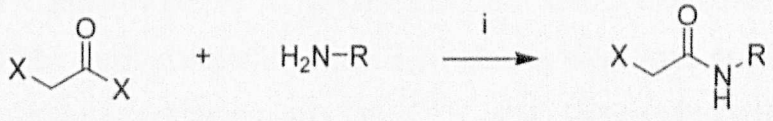
Although mass spectrometry intrinsically cannot be considered as conclusive proof to exclude the formation of the target products (or even partially substituted cyclens), the failure in isolating the main compounds in spite of the many attempted work-up procedures, and the lack of further analytical data to identify the nature of the obtained species led to the abandonment of this route. Instead, the synthesis of tetrasubstituted macrocycles was attempted, bearing moieties which could be exploited for polymerisation but not capable of reacting with cyclen itself.

### 2.2.3 Synthesis of allyl-, propynyl- and styryl-DOTA-amides

Species with terminal C-C double or triple bonds can in principle be exploited in a variety of polymerisation reactions, including metathesis, "click chemistry" (see Section 2.3.1 below) and radical additions. More importantly, in principle they can be converted methodologically into hyperbranched polymeric architectures. When the monomer is represented by a Gd-complex, a branched structure is predicted to increase the local concentration of lanthanide thus improving the relaxivity.

Because of that, it was decided to prepare the allyl-, propargyl- and styryl-amides of DOTA (compounds not reported in the literature). This required the initial syntheses of allyl-, propargyl- and styryl-haloacetamides. For allyl- and propargyl-moieties, both the bromo- and the chloroacetamides were prepared, in order to compare their reactivities in attachment onto cyclen. *N*-allyl-2-chloroacetamide **47** was first reported by Harries *et al.* in 1910,[335] and more recently by Casadei *et al.*[336] and Farkas *et al.*[337] *N*-allyl-2-bromoacetamide **48** has been recently synthesised[338, 339] on the basis of a more general procedure reported prior to it.[336] The synthesis of propargyl-chloroacetamide **49** is not reported in the literature, although it was used by Viguier *et al.*[340] to prepare a mono-propargylamide of DOTA. On the contrary, a procedure for the preparation of the corresponding bromoacetamide **50** was proposed in 1995 by Walter,[341] and it has also been very recently reported in two further independent papers.[342, 343] *N*-styryl-2-chloroacetamide **51** has never been reported in the literature.

All haloacetamides mentioned above (like butyl-chloroacetamide **39** reported in Section 2.2) were synthesised by reacting chloroacetyl chloride or bromoacetyl bromide with the suitable amine in the presence of triethylamine as a base, as generally shown in Scheme 2.22 and under the conditions reported in Table 2.9.




X = Cl, Br

**47**: X = Cl, R = allyl
**48**: X = Br, R = allyl
**49**: X = Cl, R = propargyl
**50**: X = Br, R = propargyl
**51**: X = Cl, R = styryl

**Scheme 2.22** General representation of the synthesis of haloacetamides **47-51**. Reaction conditions and results are reported in Table 2.9.

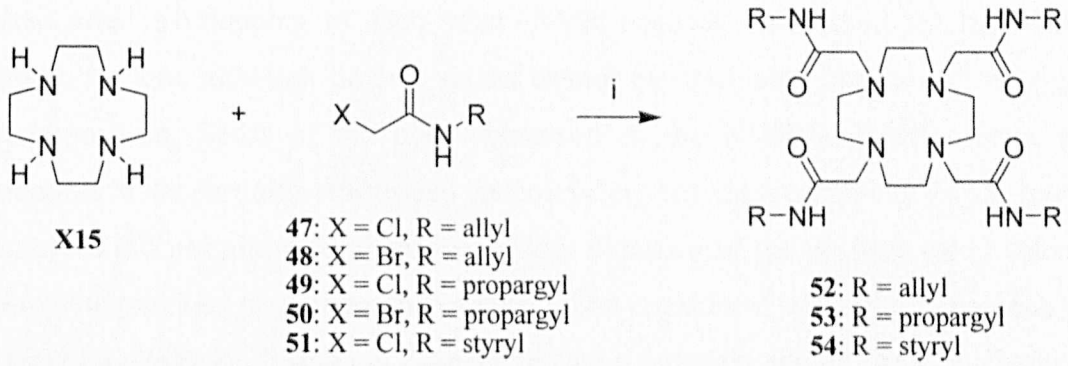
**Table 2.9** Reaction conditions and results for the synthesis of haloacetamides **47-51**, as shown in Scheme 2.22.

| | Conditions | Result |
|---|---|---|
| 1 | chloroacetyl chloride (1 mol eq), allylamine (1 mol eq), $Et_3N$ (1 mol eq), THF, -10 °C, 2 h. | **47** = 67% |
| 2 | bromoacetyl bromide (1 mol eq), allylamine (1 mol eq), $Et_3N$ (1 mol eq), THF, -10 °C, 2 h. | **48** = 69% |
| 3 | chloroacetyl chloride (1 mol eq), propargylamine (1 mol eq), $Et_3N$ (1 mol eq), THF, -10 °C, 2 h. | **49** = 49% |
| 4 | bromoacetyl bromide (1 mol eq), propargylamine (1 mol eq), $Et_3N$ (1 mol eq), THF, -10 °C, 2 h. | **50** = 59% |
| 5 | chloroacetyl chloride (1 mol eq), 4-aminostyrene (1 mol eq), $Et_3N$ (1 mol eq), THF, -10 °C, 2 h. | **51** = 55% |

The characterisation data for all synthesised haloacetamides were in full agreement with those reported in the literature (where available). Yields were slightly lower than the reported ones (**47**: not reported; **48**: 69% vs. 73%;[338] **50**: 59% vs. 67%[342]).

Haloacetamides **47-51** were then used for tetrasubstitutions on cyclen. Neither the target compounds nor partially substituted allyl- or styryl-DOTA-acetamides are reported in the literature. Only mono- and bis-propargylamides are mentioned in three papers[340, 343, 344] published contemporaneously or later than the syntheses described herein. Analogously to what was planned in this project, the authors of two of these papers exploited the C-C triple bonds in click chemistry reactions (see Section 2.3.1 below for an overview). Prasuhn *et al.*[343] introduced azide moieties onto a virus surface and successfully reacted it through a cycloaddition process with a Gd-DOTA-mono-propargylamide in order to mark it for MRI analysis. Viguier *et al.*[340] applied a click chemistry procedure to conjugate an Eu-DOTA-propargylamide with an azide-containing dye, thus preparing a lanthanide-based luminescent sensor (no yield reported).

As explained before for other exhaustive substitutions (see Sections 2.1.1, 2.2 and 2.2.2), the most successful reaction conditions were tried among those reported in the literature for attachment onto cyclen, i.e. either potassium carbonate in acetonitrile or cesium carbonate and potassium iodide in DMF. In some cases, the base was replaced with triethylamine in order to investigate whether the use of completely miscible species would favour the reaction. The general representation of these attempts is shown in Scheme 2.23, and the reaction conditions are summarised in Table 2.10.




**Scheme 2.23** Attempted syntheses of DOTA-tetra-amides **52-53**. Reaction conditions and results are reported in Table 2.10 and discussed in the text.

**Table 2.10** Reaction conditions and results for the attempted syntheses of DOTA-tetra-amides **52-54**, as shown in Scheme 2.23.

| | Conditions | Result |
|---|---|---|
| 1 | cyclen (1 mol eq), **47** (5 mol eq), $K_2CO_3$ (5 mol eq), MeCN, reflux, 18 h. | **52** = 58% |
| 2 | cyclen (1 mol eq), **47** (5 mol eq), $Cs_2CO_3$ (5 mol eq), KI (5 mol eq), MeCN, reflux, 48 h. | Complex mixture. **52** crude yield (by NMR) was low |
| 3 | cyclen (1 mol eq), **48** (5 mol eq), $K_2CO_3$ (5 mol eq), MeCN, reflux, 48 h. | Complex mixture. **52** crude yield (by NMR) was low |
| 4 | cyclen (1 mol eq), **49** (5 mol eq), $K_2CO_3$ (5 mol eq), MeCN, reflux, 48 h. | Complex mixture. **53** did not form. |
| 5 | cyclen (1 mol eq), **49** (4.1 mol eq), $Et_3N$ (4.1 mol eq), DMF/$H_2O$, 50 °C, 2 h. | **53** = 52% |
| 6 | cyclen (1 mol eq), **50** (4.1 mol eq), $Et_3N$ (4.1 mol eq), DMF/$H_2O$, 50 °C, 48 h. | **53** = 1% |
| 7 | cyclen (1 mol eq), **49** (4.4 mol eq), $Cs_2CO_3$ (4.4 mol eq), KI (4.4 mol eq), DMF, 50 °C, 48 h. | **53** = 74% |
| 8 | cyclen (1 mol eq), **51** (5 mol eq), $K_2CO_3$ (5 mol eq), MeCN, reflux, 7 d. | Complex mixture. **54** did not form. |
| 9 | cyclen (1 mol eq), **51** (4.1 mol eq), $Et_3N$ (4.1 mol eq), DMF/$H_2O$, 50 °C, 2 h. | **54** = 63% |

DOTA-allyl-amide **52** was successfully synthesised with $K_2CO_3$ as base in acetonitrile (Table 2.10, entry 1), and it was fully characterised. All analytical data were consistent with the target structure: in particular, ring and acetyl protons produce two sharp peaks in the $^1H$ NMR spectrum at 2.70 and 3.08 ppm respectively, while the corresponding carbon atoms show at 53.6 and 59.2 ppm respectively in the $^{13}C$ NMR spectrum.

The reaction with **48** (Table 2.10, entry 3) and the reaction with **47** and $Cs_2CO_3$/KI in DMF (Table 2.10, entry 2) were carried out in parallel to the previous one. By NMR analysis it was determined that they were not further progressing after two days. However, instead of clean NMR and MS spectra, complex data sets were obtained for the two crude mixtures. In particular, in the $^1H$ NMR spectra the resonances expected for compound **52** were observed, but many other signals were

present often overlapping to each other. NMR analysis established the hypothetical yields to be low, although precise values cannot be calculated because of the signals superimposition. Some of the peaks observed in the NMR and MS spectra were compatible with partially substituted macrocycles, but the complexity of the spectra themselves did not allow confirmation of this. Because of the positive result achieved through the previous procedure, in this case it was considered unworthy to proceed with the reaction work-out. It was not possible to find a rationale behind these outcomes and especially for the low reactivity of bromoacetamide **48**: the starting materials were the same as used before and the reactions were run twice to confirm the unexpected results. Moreover, although bromoacetamides always exhibited low reactivities, other tetrasubstitutions carried out later in DMF in the presence of cesium carbonate and potassium iodide (same batches) were successful (see below).

DOTA-tetra-allyl-amide was used in attempts of polymerisation *via* metathesis and radical reactions (see Chapter 3), and for the formation of the corresponding gadolinium(III)-complex to be tested for relaxivity performance and toxicity as an MRI contrast agent (see Chapter 4).

Unexpectedly, the conditions successfully applied for the synthesis of **52** ($K_2CO_3$ in acetonitrile; Table 2.10, entry 4) did not lead to compound **53** when propargyl-chloroacetamide **49** was reacted with cyclen. After two days the reaction was no longer progressing (as shown by NMR spectroscopy) and the crude mixtures were analysed by NMR and MS: complicated spectra were obtained, but among the many signals it was not possible to observe any which could be assigned to the target product. Some peaks were compatible with partially substituted rings, but neither NMR nor MS analysis were conclusive because of their complexity.

A procedure was then designed involving the use of both DMF and water as solvents (Table 2.10, entry 5) in order to favour complete solubilisation of all reagents (including triethylamine as a base) and to cause the precipitation of the target compound while forming. Effectively, a precipitate started forming after 30 minutes and reached the maximum amount after 2 hours. The precipitate was filtered and fully characterised: all analytical data were consistent with the structure of **53**, which was isolated in 52% yield. The resonances for the ring and acetyl protons appear as two broad peaks in the $^1$H NMR spectrum at 2.61 and 3.04 ppm, while the corresponding carbon atoms are

responsible for the peaks observed at 53.2 and 57.4 ppm respectively in the $^{13}C$ NMR spectrum.

A disappointing outcome was instead obtained by reacting in the same conditions propargyl-bromoacetamide **50** (Table 2.10, entry 6). Among the many unidentified by-products (as shown by NMR and TLC analysis), **53** formed and was isolated in only 1% yield. As observed for the synthesis of DOTA-tetra-allyl-amide **52**, also in this case the bromoacetamide (expected to be more reactive and then give a higher yield than the corresponding chloroacetamide **49**) exhibited instead a low reactivity.

The best result in the synthesis of **53** was achieved when chloroacetamide **49** was reacted in the presence of $Cs_2CO_3$ and KI in DMF (Table 2.10, entry 7). As previously described, these conditions did not allow the formation of tetra-allyl-amide **52** from chloroacetamide **47** with high yield and in a pure form, since a complex mixture of products formed. On the contrary, with **49** the maximum conversion was achieved after two days and the $^{1}H$ and $^{13}C$ NMR spectra of the crude mixture looked rather clean, showing a predominant set of signals consistent with the target structure. **53** was finally isolated in 74% yield, and the analytical data were in full agreement with those previously obtained.

Product **53** was used in experiments of polymerisation *via* click chemistry (see Chapter 3), and for the formation of the corresponding gadolinium(III)-complex to be tested as an MRI contrast agent in terms of relaxivity performance and toxicity towards stem cells (see Chapter 4). It was also exploited for further functionalisation through click chemistry reactions to form other species to be used as monomers (see below).

As described for the synthesis of **53**, the procedure which led to the preparation of **52** involving the use of potassium carbonate in acetonitrile was also unsuccessful for the preparation of DOTA-styryl-amide **54** from chloroacetamide **51** (Table 2.10, entry 8). In particular, it was established by TLC and NMR analysis that a very complex mixture of products had been obtained which did not include the target compound. Because of the complexity of the NMR and MS spectra, it was not possible to determine with any certainty whether partially substituted cyclens had formed, or the identity of the products.

However, the use in a parallel reaction of triethylamine as a base in a mixture of DMF and water (Table 2.10, entry 9; conditions previously applied for the synthesis of

tetra-propargyl-amide **53** with good results) led to the precipitation of a product which was isolated and fully characterised, revealed as **54**. In the $^{1}H$ NMR spectrum the resonances of the ring and acetyl protons produce two broad peaks at 2.87 and 3.27 ppm respectively, while the corresponding carbon atoms are responsible for peaks at 52.7 and 58.0 ppm respectively in the $^{13}C$ NMR spectrum.

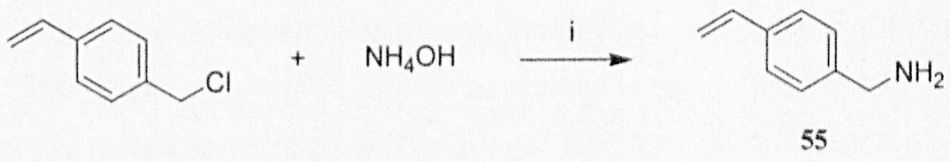
As for **53**, also the corresponding Gd-complex of **54** was prepared and tested as an MRI contrast agent in terms of relaxivity performance and toxicity towards stem cells (see Chapter 4). It was also used in radical polymerisation experiments (see Chapter 3).

### 2.2.4 Synthesis of other DOTA-styryl-derivatives

In tetra-styryl-acetamide **54** the styryl group is directly bound to the nitrogen atom of the amide moiety, and that could affect its reactivity for electronic and steric reasons. Other styryl-derivatives with spacers of various length and structure were then explored, in order to compare their chemical behaviour with **54**.

The synthesis of tetra-styryl derivatives of DOTA required first the preparation of suitable chloroacetamides or chloroacetates to be attached to the tetraazacyclododecane ring, all of which were formed starting from 4-vinylbenzyl chloride.

A first, simple way to distance the styryl group from the amide moiety is to prepare the homologous species of the previously used styrylamine, i.e. 4-vinylbenzylamine **55**. Such a compound is not commercially available, and no experimental procedure is reported in the literature for its synthesis. It was prepared from 4-vinylbenzyl chloride and ammonium hydroxide in large excess, as shown in Scheme 2.24.




**55**

**Scheme 2.24** Synthesis of 4-vinylbenzylamine **55**. i) 4-vinylbenzyl chloride (1 mol eq), $NH_4OH$ (>100 mol eq), $AcONH_4$ (1 mol eq), THF, RT, 2 d, 34%. The low yield is discussed in the text.

As shown by TLC, three products had formed. NMR and MS analysis led to the determination that the slightly predominant product was the target one (see Experimental Part and Figure 2.4), while the two by-products consisted in the di-substituted and the tri-substituted amines (Figure 2.4)

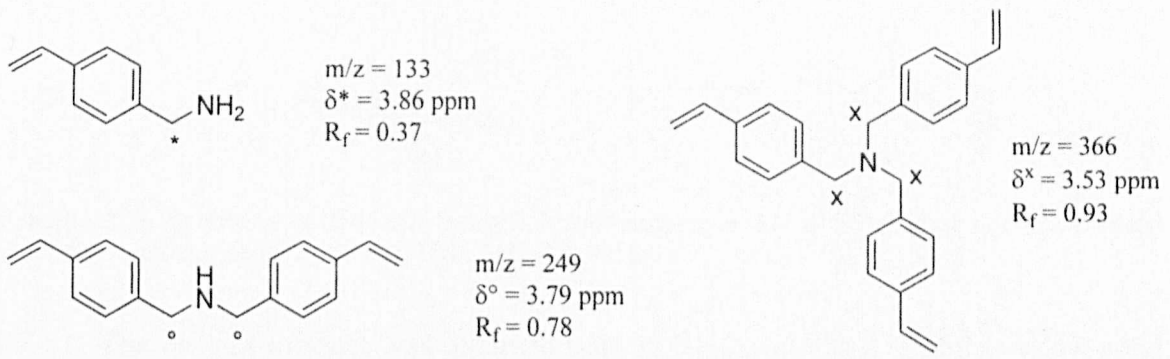
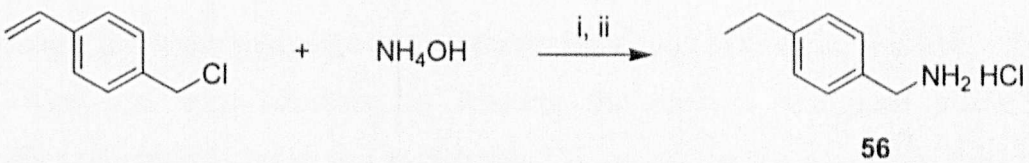



**Figure 2.4** Main and minor products from the first synthesis of 4-vinylbenzylamine **55**, with the corresponding m/z values from $CI^+$ MS, NMR chemical shifts, and retention factors as from TLC ($SiO_2$, MeCN/MeOH/25% $NH_4OH$ 80:19.9:0.1).

Column chromatography ($SiO_2$, MeCN/MeOH/25% $NH_4OH$ 80:19.9:0.1) resulted in the desired product to be isolated in 34% yield. However, it showed the tendency to easily polymerise within few minutes with formation of an insoluble gel, even when stored under nitrogen at low temperature. This behaviour was surely favoured by the fact that the compound is liquid at room temperature.

Looking for a different way to obtain the desired species, it was then thought to try and synthesise the corresponding hydrochloride salt **56**, expected to be solid and then more stable and possibly easier to purify. The reaction was carried out again under the same conditions reported above, but this time 0.1 M hydrochloric acid was added to the oil obtained after extraction with chloroform (Scheme 2.25).

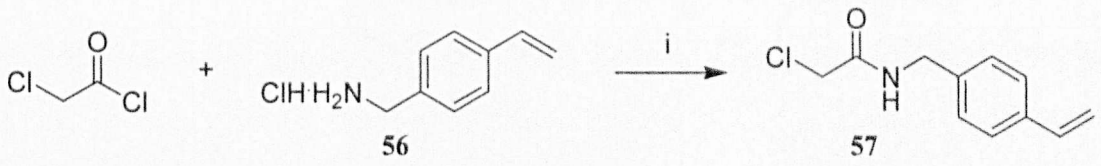



**56**

**Scheme 2.25** Second synthesis of 4-vinylbenzylamine **55** as its hydrochloride salt **56**. i) 4-vinylbenzyl chloride (1 mol eq), $NH_4OH$ (>100 mol eq), $AcONH_4$ (1 mol eq), THF, RT, 2 d; ii) 1 M HCl, RT, 30 min, 83%.

A white solid precipitated, which was freeze-dried, suspended in chloroform and filtered. The remaining white crystalline product was characterised by NMR spectroscopy, mass spectrometry and elemental analysis and formulated as the pure expected product **56**.

4-Vinylbenzylamine hydrochloride **56** was used for the synthesis of the corresponding chloroacetamide **57** through reaction with chloroacetyl chloride as shown in Scheme 2.26.

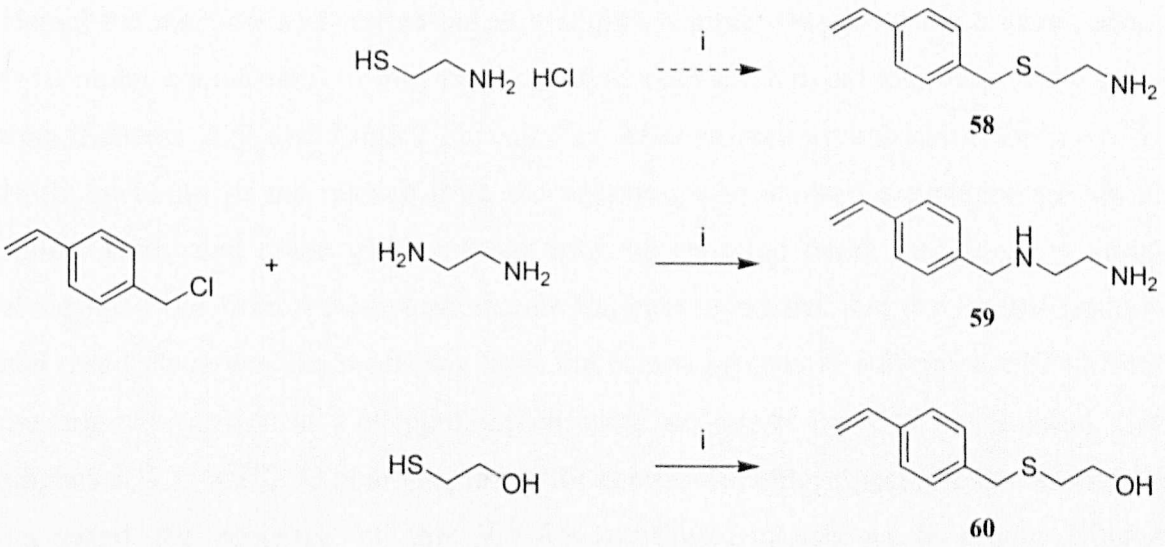



**Scheme 2.26** Synthesis of *N*-(4-vinylbenzyl)-2-chloroacetamide **57**. i) **56** (1 mol eq), chloroacetyl chloride (1 mol eq), $Et_3N$ (2 mol eq), THF, 0 °C, 2 h, 91%.

The desired product was obtained pure in 91% yield as a slightly yellow solid after filtration and extraction. The most significant data from NMR spectroscopic analysis regard the shift of the signal for the benzylic protons from 3.88 to 4.48 ppm as a consequence of the conversion of the amine group into an amide, whilst the chemical shift of the resonance due to the corresponding carbon atoms shifted from 46.1 to 43.6 ppm. With haloacetamide **57** in hand we could proceed to prepare the corresponding tetrasubstituted cyclen derivative (see Section 2.2.4.1 below).

As alternative spacers between the styryl group and the amide moiety, the fragments that could be introduced from aminoethanethiol, ethylenediamine and mercaptoethanol were chosen. Such spacers were predicted to be hydrophilic enough to favour water solubility of the hypothetical polymeric structures synthesised from the monomers bearing them. Furthermore, this hydrophilicity is also required in order to allow water molecules to reach the metal centre of the Gd-complex (once formed), thus permitting a fast water exchange rate necessary for a good MRI contrast effect.

The first step consisted in reacting the species mentioned above with 4-vinylbenzyl chloride, as shown in Scheme 2.27 and under the conditions reported in Table 2.11.




**Scheme 2.27** Attempted reactions between cysteamine hydrochloride, ethylenediamine or mercaptoethanol and 4-vinylbenzyl chloride. Conditions and results are reported in Table 2.11 and discussed in the text.

**Table 2.11** Reaction conditions and results for the synthesis of styryl-derivatives **58-60**, as shown in Scheme 2.27.

| | Conditions | Result |
|---|---|---|
| 1 | 4-vinylbenzyl chloride (1 mol eq), 2-aminoethanethiol hydrochloride (1 mol eq), $Na_2CO_3$ (3 mol eq), RT, 2 h. | Complex mixture unworthy to separate |
| 2 | 4-vinylbenzyl chloride (1 mol eq), ethylenediamine (>10 mol eq), 0 °C, 4 h. | **59** formed (crude yield = 67%), but polymerised quickly |
| 3 | 4-vinylbenzyl chloride (1 mol eq), 2-mercaptoethanol (1 mol eq), $Na_2CO_3$ (2 mol eq), MeOH, RT, 15 h. | **60** = 81% |

The synthesis of **58** (not reported in the literature) was attempted by following the same procedure applied for the attempted monoprotections of cysteamine with methoxybenzyl- and benzyl-group, and described in Section 2.2.1. Unfortunately, an analogous mixture of several products (as shown by TLC) was obtained, whose complex $^1H$ and $^{13}C$ NMR spectra showed no predominant species was present. The hypothesis that the several products were the result of single and multiple nucleophilic attacks by both the thiol and the amine groups to the chloride (as discussed in Section 2.2.1) seemed to be confirmed by the observation that the many resonances in the $^1H$ NMR spectrum were concentrated in the regions between 2.7-3.1 ppm ($SCH_2CH_2N$), around 3.7 ppm ($ArCH_2S$ and $ArCH_2N$) and at chemical shifts typical of the styryl moiety, thus suggesting similar structures with different degree of substitution (as shown in Section 2.2.1, Figure 2.2). MS analysis was not conclusive from this point of view. It was considered unworthy to proceed with further attempts of purification.

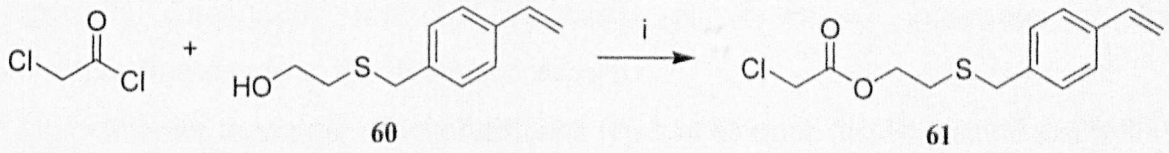
Mono-substituted diamine **59** is reported in the literature,[345] synthesised by addition of 4-vinylbenzyl chloride to a 4-fold excess of ethylenediamine in DCM.

Herein the reaction was carried out in a slightly simpler way by using a large excess (>10 molar equivalents) of ethylenediamine as reactant, solvent and base at the same time (Scheme 2.27 and Table 2.11, entry 2). After extraction with chloroform, the $^{1}H$ NMR spectrum of the residue from the organic phase showed a predominant set of signals (estimated crude yield = 67%) with the expected peaks for the styryl group alongside those from the ethylenediamine fragment; evidence that the desired reaction had taken place was the resonance from the benzyl protons at 3.80 ppm, shifted from the original position at 4.60 ppm, which could no longer be observed. Instead, two singlets at 3.77 and 2.76 ppm integrating for about 1/10 with respect to the main signals suggested the presence of the *N,N'*-bis-substituted amine as by-product, being assignable to the corresponding benzyl and ethyl protons respectively. The $^{13}C$ NMR spectrum showed the expected set of signals for the desired product, where the benzyl carbon had shifted from 46.1 (in the starting chloride) to 53.7 ppm. $CI^{+}$ MS analysis confirmed the presence of the product. However, as it had happened with 4-vinylbenzylamine **55**, within half an hour the oil had changed into a gel, which was found to be insoluble even after long stirring (and continuous extraction when possible) in all tried solvents (aqueous hydrochloric acid, dimethyl sulfoxide, DMF, NMP, water, methanol, ethanol, isopropanol, ethyl acetate, acetone, DCM, chloroform, diethyl ether, chlorobenzene, toluene, hexane). For both **55** and **59** it is not clear how the polymerisation is promoted and the cross-linking (apparently confirmed by the general insolubility of the gel) takes place. Such behaviour was also observed when storing the compounds at low temperature, either in the presence or in the absence of oxygen. Because of this tendency shown towards polymerisation, the successive planned reaction of **59** with chloroacetyl chloride was considered uncertain and unreliable in terms of the products that might actually form: the acyl chloride could react not only with **59** but also with its oligomers and polymers, cross-linked and not, which in turn could even possibly form cyclic derivatives by reaction of their amine moieties with the $CH_2Cl$ groups in a totally unpredictable way. Thus, it was decided to abandon this route in favour of a derivative less reactive and easier to handle.

A synthetic protocol for alcohol **60** is not reported in the literature, and it was therefore prepared by following the same procedure applied for the syntheses of compounds **58** and **59** (Scheme 2.27; Table 2.11, entry 3). After extraction and chromatography, the isolated product was fully characterised, and was revealed to be the target compound in

81% yield. In particular, the benzyl protons signal in the $^{1}H$ NMR spectrum shifted upfield to 3.71 ppm (being 4.58 ppm for the 4-vinylbenzyl chloride). The same was observed in the $^{13}C$ NMR spectrum for the corresponding carbon peak, which shifted to 35.4 ppm from the 46.2 ppm recorded for the starting material. The $CI^{+}$ mass spectrum showed the peak for the molecular fragment at 195 ($[M+H]^{+}$) m/z.

Compound **60** was then reacted with chloroacetyl chloride to form the corresponding ester **61** according to the procedures carried out to synthesise the chloroacetamides reported above, since a synthetic procedure for **61** is not described in the literature. At first, equimolar amounts of the reactants were used, but after a few hours a substantial quantity of unreacted alcohol was still present, which required additional purification steps resulting in a remarkable decrease of the final yield. It was then decided to use a 5-fold excess of chloroacetyl chloride, as shown in Scheme 2.28.




**60** **61**

**Scheme 2.28** Synthesis of chloroacetate **61**. i) **60** (1 mol eq), chloroacetyl chloride (5 mol eq), $Et_3N$ (1 mol eq), THF, 0 °C, 2 h, 53%.

By TLC ($Al_2O_3$, $CHCl_3$) it was established that a product was present ($R_f$ 0.45) in the crude reaction mixture, together with some more polar species. Unreacted alcohol ($R_f$ 0.26) was not detected. $^{1}H$ and $^{13}C$ NMR spectra were recorded, showing the sets of signals expected for **61**. In the $^{1}H$ NMR spectrum, the protons of the methylene group in *alpha* position with respect to the ester moiety produce a resonance at 4.28 ppm, remarkably shifted with respect to the previous position at 3.67 ppm in **60**, when the $CH_2$ group was instead directly bound to a hydroxyl group. A singlet at 4.12 ppm in the $^{1}H$ NMR spectrum was assigned to chloroacetic acid formed from the chloride in excess, which also produces two resonances in the $^{13}C$ NMR spectrum at 173.7 and 40.5 ppm, consistent with our own data for chloroacetic acid. MS analysis also confirmed that **61** had formed. Flash chromatography ($Al_2O_3$, $CHCl_3$) was carried out to purify the target compound, but surprisingly the product remained in the column and it was not managed to wash it out. The procedure was repeated several times, and only once (when the column was loaded with a relatively large amount [~3 g] of crude material) a very small amount (about 1%) of pure **61** was obtained as colourless oil. The reasons for this outcome are not clear: it might be speculated that the pure compound is very prone to polymerisation and the time necessary to elute it through the column is too long (e.g.

with respect to that necessary to run a TLC); polymerisation thus takes place and the polymer, in turn, gets stuck in the column. Varying the acidity of the stationary phase did not lead to any improvement. When alumina was replaced by silica, **61** was eluted but still impure, although TLC of the crude material showed well separated spots. Using silica with different acidity had no effect on the purification. The effect of the impurities on the $^{1}H$ NMR spectrum was to produce additional weak peaks overlapping particularly the signals due to the aromatic protons and the ethylene chain. An analogous observation could be made for the $^{13}C$ NMR spectrum. Apart from these peaks, the spectra looked clean. Other purification methods were tried. Extractions did not bring any improvement. On the other hand, after stirring the oil in DCM in the presence of neutral alumina (60w%) for 3 hours, and then filtering through a pad of Celite, the oil obtained was still slightly yellowish but the amount of impurities and especially chloroacetic acid had decreased, as shown by integration of the corresponding signals in the $^{1}H$ NMR spectrum.

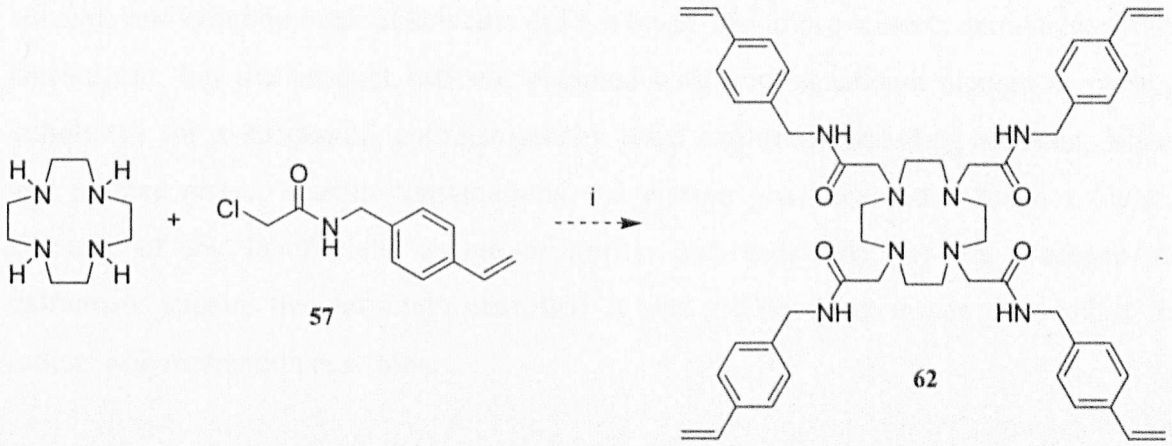
In order to test the effect of different types of alumina (acidic, neutral and basic) and solvents, several experiments were carried out, but low yields were always obtained regardless of the type of alumina and solvent employed

A gel permeation chromatography analysis of the impure product in DMF showed no evidence that a polymeric by-product had formed, since in the eluogram there were no peaks corresponding to a molecular weight higher than that of **61**. The product was then used without further purification for the next reaction of attachment onto cyclen.

### 2.2.4.1 Attachment of 57 and 61 to cyclen

The chloroacetamides and chloroacetates successfully prepared as reported in the previous Section were used in reactions for the synthesis of the corresponding derivatives of cyclen.

The attachment of **57** to cyclen was investigated by using the same procedures successfully applied for the synthesis of **32** (Section 2.2) and **53** (Section 2.2.3), i.e. by using cesium carbonate as a base and potassium iodide as catalyst (Scheme 2.29).



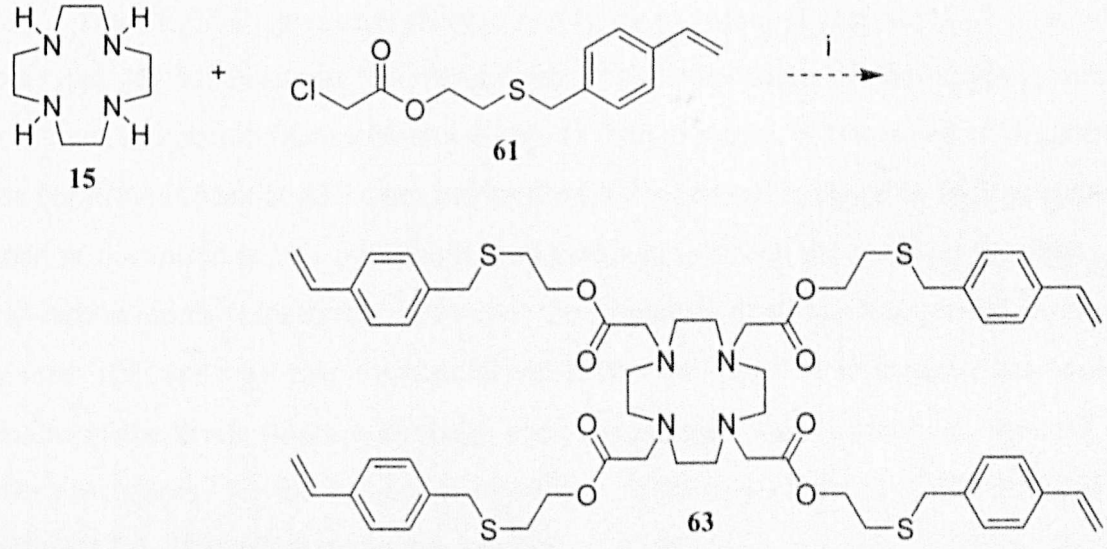

**Scheme 2.29** Synthesis of tetra-substituted derivative **62**. i) Cyclen (1 mol eq), **57** (4.4 mol eq), $Cs_2CO_3$ (4.4 mol eq), KI (4.4 mol eq), DMF, 50 °C, 48 h. Purification problems are discussed in the text.

After 2 days TLC confirmed that all chloroacetamide had been consumed. The brown water-insoluble residue obtained after filtration from water (to remove inorganic salts) was analysed by NMR spectroscopy and MS. The $ESI^+$ mass spectrum showed intense peaks at 887 ($[M+Na]^+$), 865 ($[M+H]^+$) and 433 ($[M+2H]^{2+}$) m/z. Very weak peaks could also be observed at 809, 452 ($[M+2Na]^{2+}$), 220 and 204 m/z. No peaks corresponding to partially substituted rings were recorded. In the $^{13}C$ NMR spectrum only the set of signals for one species (identified as the desired one) was observed: a peak at 170.7 ppm for the C=O, signals at 139.2 and 135.7 ppm for the quaternary aromatic carbons, resonances at 136.3 and 113.8 ppm ($CH_2$=CH-), signals at 127.4 and 126.0 ppm for the carbon atoms in *ortho* and *meta* position respectively. Furthermore, broad peaks at 57.0 and 52.7 ppm for the acetyl and the ring carbons respectively, and the benzyl carbon resonance at 41.6 ppm.

According to the above data the product was consistent with the desired species. However, the $^1H$ NMR spectrum showed many other weak signals especially close to those expected for **62**, and in particular near the peaks due to the styryl moiety. Also, the main peaks assigned to the tetra-substituted product were broad. It is not clear what the source of such additional resonances and the reasons for the line broadening could be. The formation of partially substituted rings might be excluded according to the analysis by mass spectrometry, although such technique is not conclusive from this point of view. It was hypothesised that some polymerisation had taken place, on the basis of some weak resonances appeared at about 4.5 and 3.0 ppm in the $^1H$ NMR spectrum, and of the integration of the vinyl resonances with respect to the aromatic ones, slightly lower (95%) than expected. Purification was attempted in several ways: recrystallisations and precipitations of **62** or impurities from a range of different

solvents and combinations of solvents did not bring any improvement; extractions were carried out, but the product was not obtained with any significant change in purity; conditions for a successful chromatography were explored (including alumina, silica and reverse phase, eluents combinations and elution gradients) but were not found. Because of the insufficient degree of purity, and especially for the presence of extraneous species not definitely identified, it was preferred not to use the product in radical polymerisation reactions.

The methods successful for the convergent synthesis of tetra-substituted products **32**, **52**, **53** and **54** (see Sections 2.2 and 2.2.3) were applied in reacting chloroacetate **61** and cyclen (Scheme 2.30), with different outcomes (Table 2.12).




**Scheme 2.30** General representation of the attempts of synthesis of DOTA-tetra-ester **63**. Reaction conditions and results are reported in Table 2.12 and discussed in the text.

**Table 2.12** Reaction conditions and results for the attempted syntheses of DOTA-tetra-ester **63**, as shown in Scheme 2.30.

| | Conditions | Result |
|---|---|---|
| 1 | Cyclen (1 mol eq), **61** (4.4 mol eq), $K_2CO_3$ (4.4 mol eq), MeCN, reflux, 48 h. | No evidence of **63** formation |
| 2 | Cyclen (1 mol eq), **61** (4.4 mol eq), $Et_3N$ (4.4 mol eq), DMF/$H_2O$, 50 °C, 48 h. | No evidence of **63** formation |
| 3 | Cyclen (1 mol eq), **61** (4.4 mol eq), $Cs_2CO_3$ (4.4 mol eq), KI (4.4 mol eq), DMF, 50 °C, 48 h. | **63** formed but it was not possible to isolate it |
| 4 | Cyclen (1 mol eq), **61** (4.4 mol eq), $Cs_2CO_3$ (4.4 mol eq), KI (4.4 mol eq), TBMP (0.05 mol eq), DMF, 50 °C, 48 h. | As for entry 3 |

When the reaction was carried out with potassium carbonate in acetonitrile (Table 2.12, entry 1), TLC and NMR spectroscopy confirmed that the reaction was not further progressing after 2 days. The residue from the dried crude mixture was suspended in water and filtered, in order to remove all water-soluble inorganic salts.

Both the insoluble residue and the filtrate were analysed by NMR spectroscopy. The filtrate did not contain any relevant organic product, apart from some unreacted cyclen. On the contrary, the $^{1}$H NMR spectrum recorded for the water-insoluble residue was very complex, but no evidence was obtained that the desired compound **63** had been achieved. According to the integration of suitable signals (the one for the $ClCH_2$ protons of the chloroacetate and those due to the total $CH_2$ protons of the vinyl groups) a 79% conversion was calculated, but it was not possible to determine what the starting material had converted into because of the high number of resonances and their frequent superimposition. No clear peak for the ring and acetyl protons could be identified. Multiplets could be observed next to the triplets due to the ethylene protons. It was not possible to determine whether a polymerisation process had taken place.

The $^{13}$C NMR spectrum showed two types of carbonyl groups (171.8 and 167.2 ppm) and several peaks in the regions where the resonances of the ethylene carbon atoms were expected (about 64 and 29 ppm). The presence of unreacted chloroacetate was confirmed (peak at 41.1 ppm due to the $ClCH_2$ group). A signal at 55.1 ppm and a broad peak centred at 51.1 ppm (both weak) seemed to reveal the presence of acetyl and ring carbon atoms respectively. However, the formation of **63** was not proved. Analysis by mass spectroscopy was not conclusive. It was not possible to separate the species present in the crude mixture although many techniques were applied, as reported for other procedures (see for instance the synthesis of **30** in Section 2.1.1, **32** with BOP in Section 2.1.2.2 and **62** above in this Section).

The attempt of synthesis carried out with triethylamine in DMF/$H_2O$ (Table 2.12, entry 2) led to an analogous uncertain conclusion. After 2 days the reaction was no longer progressing according to TLC and NMR spectroscopy, thus the solvents were removed and the remaining brownish oil was analysed. The $^{1}$H NMR spectrum showed a complex set of signals. The singlet at 4.40 ppm, assigned to the unreacted chloroacetate ($ClCH_2$ protons), had an integration of 0.76, while the total integration for $CH_2$ vinyl protons was 7.78, showing that a 90% conversion had taken place. Many signals were superimposed. Clear resonances assignable to the ring or acetate protons could not be identified. In place of the triplets expected for the ethylene fragments, multiplets were observed. On the other hand, many signals of various multiplicities were present, which could not be assigned. Also in the $^{13}$C NMR spectrum many signals could be observed: some of them belonged to styryl fragments (superimposed to minor

peaks), but those expected for the ethylene, ring and acetyl carbon atoms were uncertain. Both the $^{1}H$ and $^{13}C$ NMR spectra showed peaks that might indicate polymerisation of the styryl moieties from the starting material and/or substituted cyclen: around 3.5 and 2.5 ppm in the $^{1}H$ NMR spectrum, and around 45 and 43 ppm in the $^{13}C$ NMR spectrum. MS analysis was not conclusive. Separation of products, by-products and impurities was not achieved in spite of the several attempts, as also reported for other procedures (see for instance the previous reaction and the synthesis of **30**, **32** with BOP and **62**).

Instead, analytical evidence was obtained that tetra-ester **63** had formed when chloroacetate **61** was reacted with cyclen in the presence of cesium carbonate and potassium iodide in DMF (Table 2.12, entry 3). After 2 days the residue from the crude reaction mixture was filtered from water in order to remove all water-soluble inorganic salts. No relevant compound was detected in the filtrate by NMR. The water-insoluble residue was analysed, and evidence that the target compound had formed were obtained by NMR spectroscopy and MS. In particular, in the $^{1}H$ NMR spectrum the signal for the $ClCH_2$ protons of **61** was missing, while two very broad peaks could be observed in the region (2.5-3.1 ppm) where the resonances of the ring and the acetyl protons were expected. On the other hand, in the $^{13}C$ NMR spectrum the peak expected for the $ClCH_2$ carbon of **61** was missing, whilst a new peak was visible at higher frequency where the resonance of the acetyl carbon was expected. In the $ESI^{+}$ mass spectrum, peaks were recorded at m/z 555 ($[M+2H]^{2+}$), 1109 ($[M+H]^{+}$), 1131 ($[M+Na]^{+}$), 1153 ($[M-H+2Na]^{+}$) and 1175 ($[M-2H+3Na]^{+}$). Many other weak signals due to impurities were present in all spectra.

However, the crude product was partially soluble in all tried solvents (mostly in DMF and dimethyl sulfoxide), either because of the solubility properties of the main compound towards the solvents, or as a consequence of the solubilisation of just some of the species present in the crude product. Also, the NMR spectra showed additional peaks that could not be assigned unequivocally. In order to better characterise the product and assess the possible formation of polymeric species, GPC in DMF was run, leading to the eluogram shown in Figure 2.5 with MW calculations summarised in Table 2.13.

It is to be anticipated that after several GPC analyses and the impossibility to find a rationale for the obtained data, it was decided to change the elution conditions with dramatic consequences in the results, as reported and discussed below.

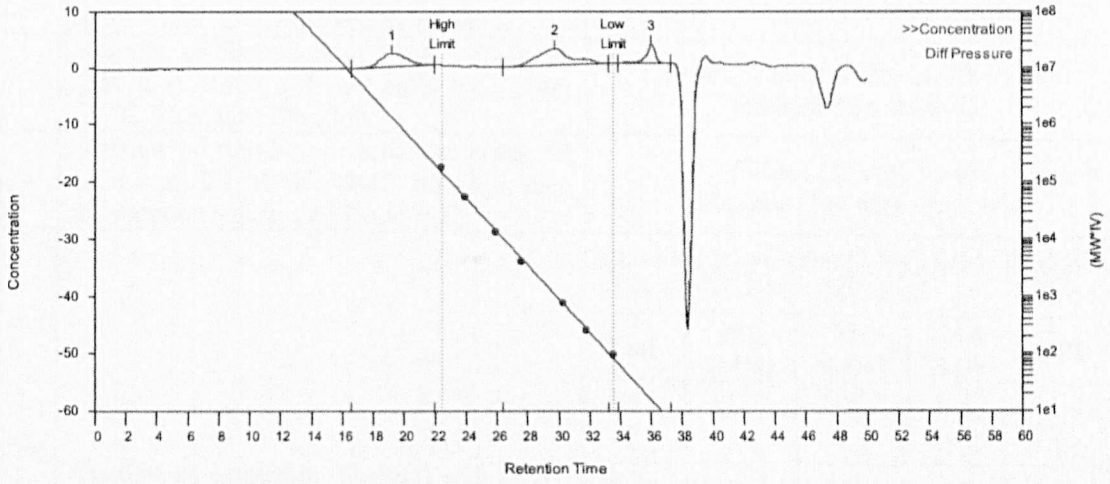



**Figure 2.5** GPC eluogram (100% DMF) of the water-insoluble residue from the reaction between cyclen and chloroacetate carried out in the presence of $Cs_2CO_3$ and KI (Table 2.12, entry 3). MW calculations are reported in Table 2.13 and discussed in the text.

**Table 2.13** Chromatographic data related to the chromatogram shown in Figure 2.5.

| Peak | $M_p$ (kDa) | $M_n$ (kDa) | $M_w$ (kDa) | PD |
|---|---|---|---|---|
| 1 | 1018.5 | 731.1 | 911.0 | 1.24 |
| 2 | 13.7 | 15.2 | 16.5 | 1.08 |
| 3 | 1.1 | 1.0 | 1.1 | 1.01 |

It was assumed that the peak identified as "3" in Figure 2.5 and Table 2.13 was due to compound **63**. The other two peaks suggest that a polymerisation occurred while the monomer was forming. That could explain the solubility behaviour observed, since the monomer and the polymeric species would show different and not coincident solubilities in different solvents (solubility tests were carried out by stirring for several hours, in order to allow dissolution of the polymeric species possibly present). Also, the extra peaks and the broad signals observed in the NMR spectra might be due to soluble fractions of polymeric species. An investigation about possible polymerisation by NMR spectroscopy was not permitted by the broadness and overlapping of the most relevant signals.

Several attempts for the purification of **63** were carried out, as summarised in Table 2.14.

**Table 2.14** Attempts of purification of DOTA-tetra-ester **63**.

| | Procedure | Result |
|---|---|---|
| 1 | Stirring in water (30-fold excess) at 50 °C for 15 h, followed by filtration. | Filtrate: no relevant species (NMR).<br>Residue: crude **63** (NMR, MS). |
| 2 | Stirring (800 mg) in DMF (30-fold excess) at 50 °C for 15 h, followed by filtration | Filtrate (585 mg): crude **63** (NMR, MS). |
| 3 | Attempt of formation of Zn-**63**: crude **63** (250 mg), $ZnCl_2$ ("1 mol eq"), $H_2O$/DMF, 50 °C, 15 h; then filtration. | Filtrate (52 mg): no Zn-**63** (NMR, MS).<br>Residue: like crude **63**. |
| 4 | Attempt of ring-N's protonation: crude **63** (250 mg), 0.1 M HCl/DMF, RT, 3 h; then evaporation and suspension in $H_2O$. | Filtrate (23 mg): no **63**.<br>Residue (244 mg): crude **63**. |
| 5 | Continuous extraction (Soxhlet) with DCM: crude **63** (4.0 g), DCM, reflux, 15 h. | DCM-soluble residue (2.5 g): crude **63** (NMR, MS). GPC (100% DMF) data: |

| Peak | Mp (kDa) | Mn (kDa) | Mw (kDa) | PD |
|---|---|---|---|---|
| 1 | 115.1 | 106.3 | 133.1 | 1.25 |
| 2 | 1.0 | 1.2 | 1.6 | 1.34 |

DCM-insoluble residue stirred in DMF at 50 °C for 15 hours and filtered. Filtrate GPC (100% DMF) data:

| Peak | Mp (kDa) | Mn (kDa) | Mw (kDa) | PD |
|---|---|---|---|---|
| 1 | 184.0 | 152.9 | 204.4 | 1.34 |
| 2 | 5.1 | 5.3 | 5.7 | 1.07 |
| 3 | 1.0 | 1.0 | 1.0 | 1.02 |

Filtrations from water (Table 2.14, entry 1) or DMF (Table 2.14, entry 2) did not allow isolation of **63** with a higher degree of purity, as established by NMR spectroscopy. Compound **63** was found to be insoluble in water but soluble in DMF. These solvents were used in an attempt of precipitation, but **63** was not obtained purer according to NMR spectroscopy.

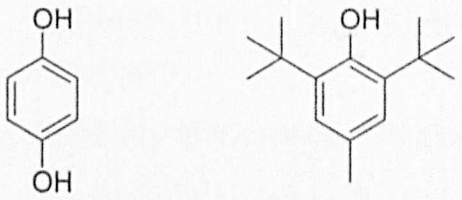
The corresponding zinc(II)-complex of **63** was expected to be easier to separate from the hypothetical polymeric species on the basis of the modified solubility. Zinc(II) was chosen instead of gadolinium because of the possibility of recording NMR spectra in the presence of this metal, whilst paramagnetic gadolinium(III) is known to produce a high line-broadening.[169, 346] However, when it was tried to form the Zn-complex of **63** (Table 2.14, entry 3) only an amount of white solid compatible with the used zinc chloride was recovered from the aqueous phase, and no evidence of the formation of Zn-**63** was obtained by NMR spectroscopy and MS.

Also the attempt of protonating the ring nitrogen atoms in order to make **63** water-soluble (Table 2.14, entry 4) was unsuccessful.

Interestingly, after continuous extraction with DCM (Table 2.14, entry 5) crude **63** was detected by NMR spectroscopy and MS in both the DCM-soluble and DCM-

insoluble residues. When analysed by GPC in 100% DMF (see Results in Table 2.14, entry 5), both samples appeared to contain high-molecular-weight polymeric products.

As already mentioned above and discussed later, a change in GPC conditions had a very important impact on the analysis results and consequent hypothesis about the presence of polymeric species. However, an attempt was first carried out to avoid polymerisation during the formation of **63** by running the reaction in the presence of an inhibitor. The most common one is hydroquinone[347] (Figure 2.6), which in this case cannot be used: since a base is required when attaching the arm to cyclen, it could also react with the hydroquinone to form the corresponding phenolate that in turn could behave as a nucleophile to attack the "arm" instead of the nitrogen atoms of the tetraazaacyclododecane ring.




hydroquinone 2,6-di-*tert*-butyl-4-methylphenol

**Figure 2.6** Molecular structures of hydroquinone and 2,6-di-*tert*-butyl-4-methylphenol (TBMP). The former is a common radical inhibitor, and the second was chosen as an equivalent but having hindering *tert*-butyl groups to prevent the phenolate reacting as a nucleophile.

Among the possible alternatives, 2,6-di-*tert*-butyl-4-methylphenol[347] (TBMP, Figure 2.6) was chosen, as the sterically hindered phenol should be much less reactive towards nucleophilic attack. The applied reaction conditions are summarised in Table 2.12 (entry 4). The analytical data obtained for the crude product and the materials recovered after the different attempts of purification (as described for crude **63** synthesised without using an inhibitor) were analogous to those reported above. In particular, the GPC chromatograms in DMF always showed peaks corresponding to high molecular weights thus apparently confirming the presence of polymeric species in spite of the use of TBMP. However, as observed with the analysis carried out during the work-up of the crude product from the previous reaction, a rationale behind the GPC data seemed to be missing, as the calculated molecular weight values for the hypothesised polymeric species were not constant.

In order to check the validity of those analytical data, it was decided to carry out the GPC measurements with a different eluting system, i.e. DMF + 1% triethylamine +

1% glacial acetic acid instead of just DMF.[348, 349] As anticipated, when using these more polar conditions to analyse the crude products and the samples from the attempts of purification, very different results were achieved, i.e. no "polymeric peaks" were observed. It was then concluded that the high molecular weights recorded through GPC analysis in DMF referred to complex aggregates forming from compound **63**. Such aggregation phenomena are clearly solvent-dependent, and as a consequence of the addition of triethylamine and acetic acid the intermolecular bonds were broken and **63** was the species with the highest molecular weight to be detected.

On the basis of this result, it was assumed that also the discussed evidences of the presence of important by-products in the crude mixture together with **63** (e.g. extra peaks in the NMR spectra and solubility problems) were in fact mainly the consequence of the formation of aggregates, although some impurities must have been present anyway (as proved by the brown colour). **63** was then used in polymerisation experiments, as described in Chapter 3.

The importance of the ability of formation of supramolecular aggregates is not limited to the analysis of compound **63**, but has to be generally extended to all complex DOTA-derivatives, since many chemical and physical properties (such as the solubility and the reactivity ) can be affected by the aggregation state.

## 2.3 Synthesis of monomers *via* "click chemistry"

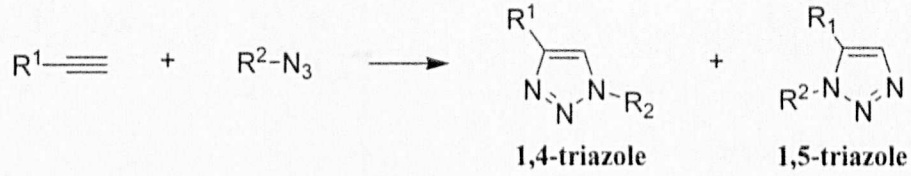
Copper(I)-catalysed cycloaddition reactions were exploited to try and synthesise further monomers for polymerisation, as well as in polymerisation reactions themselves (see Chapter 3).

### 2.3.1 Overview

The general term *click chemistry* was first used by Sharpless and co-workers in 2001[350] and refers to a wide class of reactions that, citing the authors, have to "be of wide scope, giving consistently high yields with a variety of starting materials. ... [They] must be easy to perform, be insensitive to oxygen or water, and use only readily available reagents. Reaction work-up and product isolation must be simple, without requiring chromatographic purification".[351] Among the many possible types of procedures, the requirements above may be fulfilled by some cycloadditions of

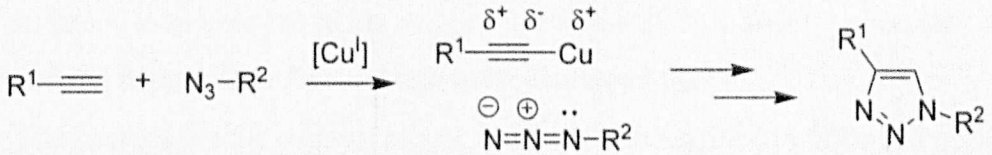
unsaturated species,[352-354] nucleophilic ring-opening reactions,[350] carbonyl reactions of the "non-aldol" type, and additions to carbon-carbon multiple bonds.[355-357]

However, it has become common to use the term *click chemistry* to improperly indicate one specific protocol, i.e. the copper(I)-catalysed version of Huisgen [3+2] dipolar cycloaddition between alkynes and azides. Huisgen additions[352, 358-360] are thermally activated and they are not regioselective, leading to mixtures of 1,4- and 1,5-triazoles (Scheme 2.31).




**Scheme 2.31** Generic representation of the Huisgen [3+2] dipolar cycloaddition reaction between an alkyne and an azide, leading to a mixture of 1,4- and 1,5-substituted triazoles.

In 2002 the Meldal[361] and Sharpless[362] groups discovered independently that in the presence of copper(I) as catalyst the reaction proceeds smoothly giving only the 1,4-substituted product in very high yields. Since it was observed that the reaction is successful only with terminal alkynes, and it is known that $Cu^{I}$ easily forms the corresponding acetylide in the presence of a base (e.g. in the Sonogashira coupling[363]), it was supposed the same as the first step in the catalytic mechanism (Scheme 2.32).



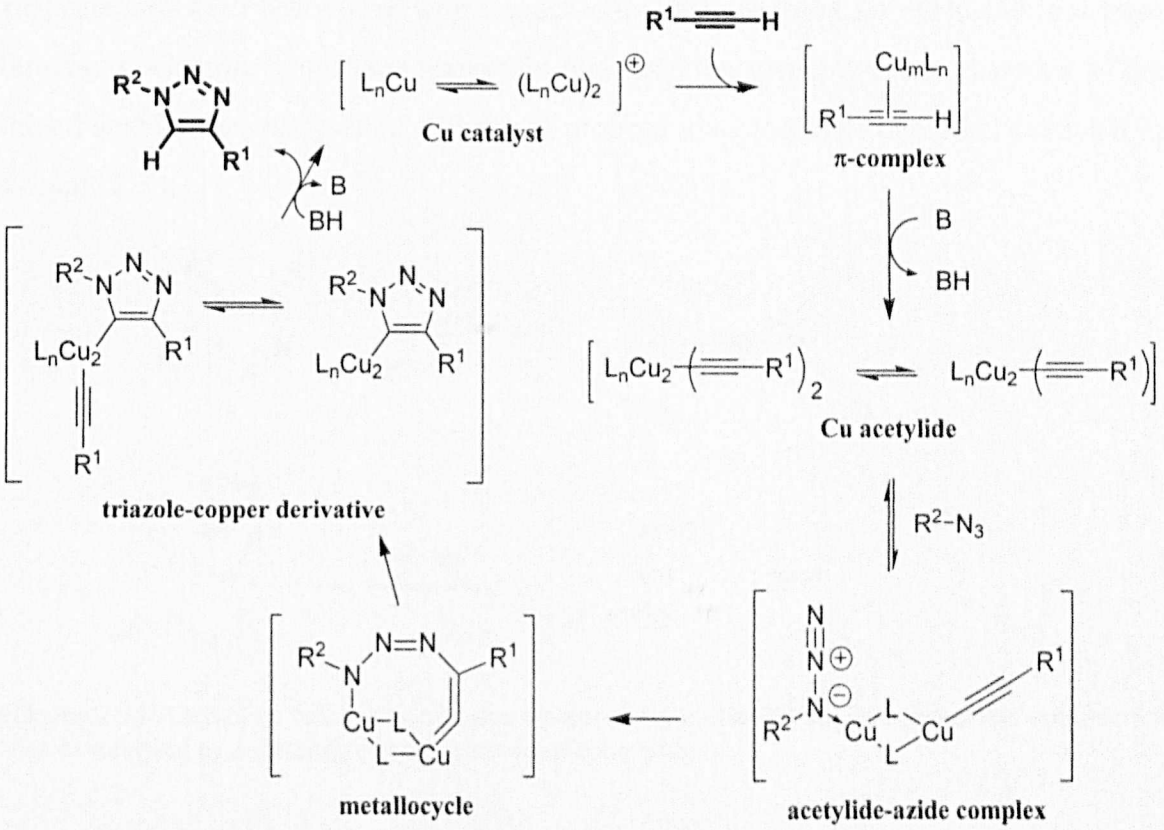

**Scheme 2.32** Generic representation of the copper(I)-catalysed cycloaddition between alkynes and azides, also showing the first step of formation of the $Cu^{I}$ acetylide.

However, the concerted mechanism proposed at first by Sharpless and co-workers[362] was retreated in favour of a binuclear system,[364] as shown in Scheme 2.33.

The main steps of this mechanism are:

- formation of a π-complex, followed by the corresponding $Cu^{I}$ acetylide;
- displacement of one of the ligands from the copper by the azide, with formation of an acetylide-azide complex;
- cycloaddition, leading to a metallocycle;
- ring contraction, with transformation of the metallocycle into a triazole-copper derivative;

- protonation of the triazole-copper derivative, with formation of the final product and regeneration of the catalyst.




**Scheme 2.33** Binuclear catalytic mechanism proposed by Sharpless and co-workers for copper(I)-catalysed cycloaddition reactions between alkynes and azides.

In order to enable the azide to bind to the metal, it is clearly necessary that the ligands around copper are labile enough to be displaced easily.

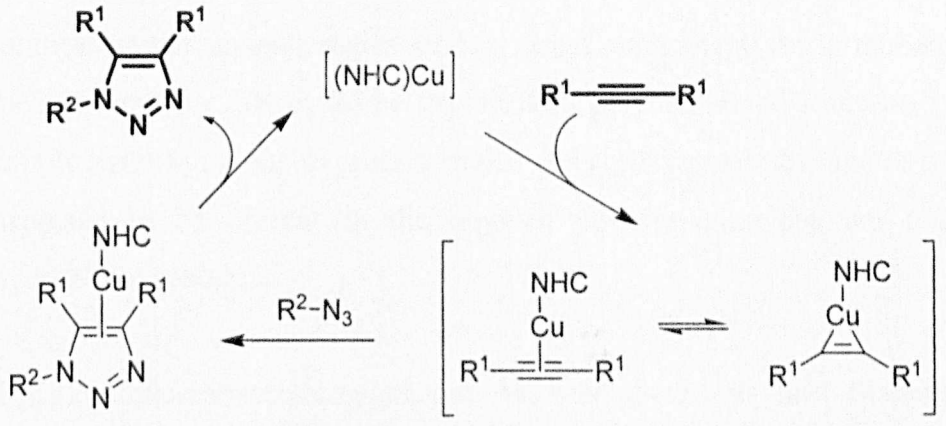
The sources for the catalyst can be basically summarised in three categories:

1) copper(I) salts, such as copper iodide;[361]
2) copper(II) salts, which are reduced in situ;[362]
3) symproportionation of copper(0) and copper(II).[365]

The second method is the most recurring one, because commercially available $Cu^{II}$ salts are cheaper and usually purer than $Cu^{I}$ salts. Copper(II) sulphate pentahydrate is by far the preferred among these types of salts. As a reductant, an excess of sodium ascorbate has proved to be a very good choice.[362]

The search for more and more efficient catalysts has led to interesting results. Recently, a heterogeneous catalyst made by copper absorbed on charcoal has also been reported.[366] According to what the authors claim, it should be possible to recover the catalyst quantitatively, with negligible or no traces of copper in the final products. That would be a very important achievement especially for biological applications.

Furthermore, a copper-catalyst containing *N*-heterocyclic carbene ligands proved to be successful even with internal alkynes.[367] A distinct mechanistic pathway has been suggested for such procedures with respect to the one proposed for cycloadditions from terminal C-C triple bonds (see above). In this case, the strong σ-donor character of the ligand enables the catalysis mechanism to proceed via a π-alkyne complex, as shown in Scheme 2.34.




**Scheme 2.34** Alternative catalytic mechanism proposed for cycloadditions between azides and internal alkynes catalysed by *N*-heterocyclic carbene-copper complexes.

$Cu^{I}$-catalysed cycloadditions have generally demonstrated to be able to go to completion in few hours even when run at room temperature. They have been carried out with excellent results in several solvents, including aqueous alcohols and also water with no organic co-solvent. Actually it is not necessary that the reagents dissolve completely, as the reaction can give high yields even for suspensions when properly stirred.[362] When water is used as a [co-]solvent, a base is not necessary since water itself acts as a base.

The wide reliability of copper(I)-catalysed cycloadditions between alkynes and azides makes it comply fully with the requirements for a reaction to be labelled as click chemistry, and actually with such an importance and applicability that, as mentioned above, the term *click chemistry* is nowadays commonly (although improperly) used to indicate such a type of protocol.

Its versatility and efficiency led it to be applied in a variety of fields ranging from drugs synthesis[351] to material science.[368-370]

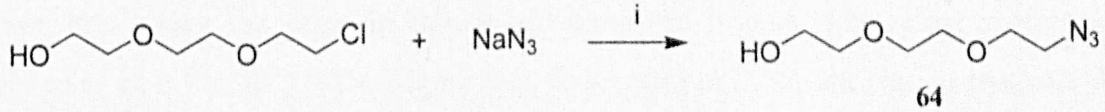
### 2.3.2 Model compounds and potential "arms"

As a first model compound to use in click chemistry reactions, a suitable azide was needed complying with the following requirements:

1) bearing only one azide moiety (a multi-azide could give partially reacted by-products or even polymeric derivatives depending on the nature of the alkyne, thus making the evaluation of the reaction and its purification more difficult);
2) mimicking the characteristics of the target monomers or co-monomers, i.e. having a moiety that could be exploited in polymerisation reactions (from the simple hydroxyl group to more complex styryl functionalities) and/or a structure expected to be present in the targeted polymeric architecture (such as a hydrophilic spacer).

2-[2-(2-Azidoethoxy)ethoxy]ethanol **64** was chosen at first because of the presence of a moiety (the hydroxyl group) to use for further functionalisation, its hydrophilicity, the commercial availability of the starting materials and the relative simplicity of the synthetic procedures available in the literature[371-377] for its preparation. The method reported by Fernandez-Megia *et al.*[373] was followed, as it seemed to be the most straightforward.

2-[2-(2-Chloroethoxy)ethoxy]ethanol was reacted with a 2-fold excess of sodium azide, as shown in Scheme 2.35.




64

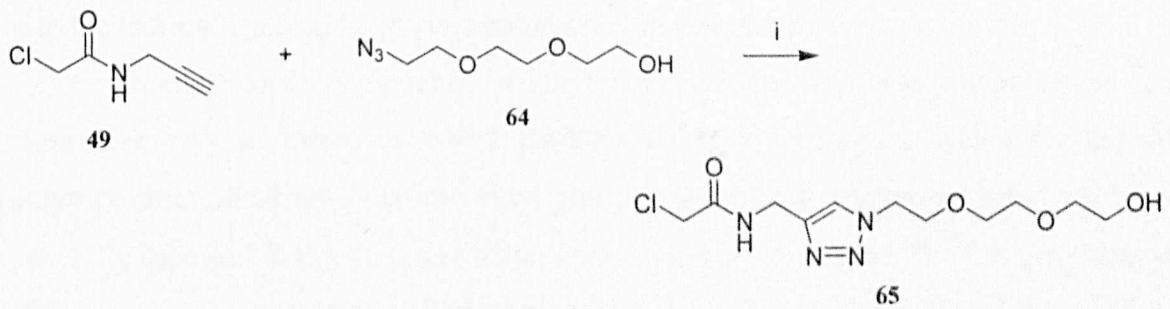
**Scheme 2.35** Synthesis of 2-[2-(2-azidoethoxy)ethoxy]ethanol **64**. i) 2-[2-(2-chloroethoxy)ethoxy]ethanol (1 mol eq), $NaN_3$ (2 mol eq), DMF, 100 °C, 24 h, 99%.

The desired compound was obtained in 99% yield (as in the literature[373]) after suspending the crude product in DCM and filtering through Celite to eliminate any inorganic salts. The identity and purity of the remaining oil was confirmed by NMR spectroscopy, mass spectrometry and elemental analysis.

The most significant change in the $^1H$ NMR spectrum ($CDCl_3$) with respect to the starting material is the slight upfield shift of the signal of the methylene protons in the *alpha* position to the azide group from 3.51 ppm to 3.38 ppm. The corresponding carbon produces a downfield shifted peak at 50.8 ppm (42.7 for the starting material) in

the $^{13}C$ NMR spectrum. Further structural evidence is provided by the strong absorption band at 2109 $cm^{-1}$ recorded in the IR spectrum and due to the azide moiety.

**64** was used in a first click chemistry reaction with *N*-propargyl-2-chloroacetamide **49**, chosen as the corresponding alkyne to form a useful intermediate for further elaboration. The reaction conditions were retrieved in the literature among those applied for azide-alkyne cycloadditions involving propargyl-amides,[378-383] in one case also with a PEG-azide.[383] **49** was reacted with a slight excess of **64** (1.1 molar equivalents) in the presence of catalytic quantities of copper(II) sulphate (10 mol%) and sodium ascorbate (20 mol%). The reaction was carried out in a 1:1 solution of water and *tert*-butanol (Scheme 2.36).



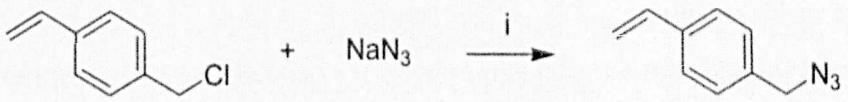

**Scheme 2.36** Cu(I)-catalysed 1,3-dipolar cycloaddition between azide **64** and alkyne **49** to yield chloroacetamide **65**. i) **49** (1 mol eq), **64** (1.1 mol eq), $CuSO_4 \cdot 5H_2O$ (0.1 mol eq), Na-ascorbate (0.2 mol eq), $H_2O$/*t*-BuOH 1:1, 50 °C, 5 h, 98%.

Analysis by TLC and NMR spectroscopy revealed the desired compound had been obtained. Attempts were made to purify the product by extraction from water with chloroform, but interestingly it was present in the final aqueous rather than organic phase, into which the azide in excess had dissolved instead. The target species was isolated as an oil in 98% yield (higher than those reported[378-383] for similar reagents: 18-96%) after column chromatography, as confirmed by NMR spectroscopy, mass spectrometry and elemental analysis. The $^{1}H$ NMR spectrum shows a peak at 7.97 ppm, where the resonance of the triazole ring proton was expected.[384, 385] The peak produced by the alkyne proton of chloroacetamide **49** at 2.28 ppm was missing. Other significant details consist in the downfield shifting of the signal due to the amide proton from 6.77 to 7.95 ppm, as well as of the peaks for the methylene groups at positions *1* and *4* on the triazole ring at 4.58 ppm (**64**: 4.11 ppm) and 4.54 ppm (**49**: 3.40 ppm), as a consequence of being directly bound to the new aromatic structure. In the $^{13}C$ NMR spectrum the peak due to the methylene carbon of the former propargyl moiety had shifted from 29.6 to 35.1 ppm, while the resonances at 78.5 and 72.2 ppm of the alkyne group were no longer present as expected. The weak signals for the carbons of the triazole ring were

observed at 144.3 (quaternary) and 123.6 (CH) ppm, consistently with literature data.[378-383] The other peaks remained basically unchanged with respect to the starting materials. The IR spectrum did not show any peak for a terminal alkyne (**49**: 2122 $cm^{-1}$) or azide (**64**: 2109 $cm^{-1}$) group.

The chemical shift values obtained in the $^{1}H$ and $^{13}C$ NMR spectra of crude **65** for the triazole proton (7.97 ppm) and carbon atoms (144.3 and 123.6 ppm) confirmed the stereoselectivity in the formation of triazole rings under $Cu^{I}$-catalysis, since there was no evidence that the 1,5-isomer had formed: in that case, a peak at lower frequency (~7.5 ppm) in the $^{1}H$ NMR spectrum and two resonances at ~137 and ~133 ppm in the $^{13}C$ NMR spectrum would have been expected according to literature data[361, 384-387] (see also the thermal cycloadditions results reported in Chapter 3).

Another azido-compound, 4-vinylbenzyl azide **66**, was prepared as an alternative way to introduce styryl moieties on tetra-substituted cyclen for radical polymerisation, assuming that the vinyl group is much less reactive according to what generally reported in the literature about click-chemistry tolerance.[350, 364] *p*-Vinylbenzyl chloride was reacted with a slight excess of sodium azide according to a protocol reported in the literature[388] for the synthesis of benzyl azide (Scheme 2.37).



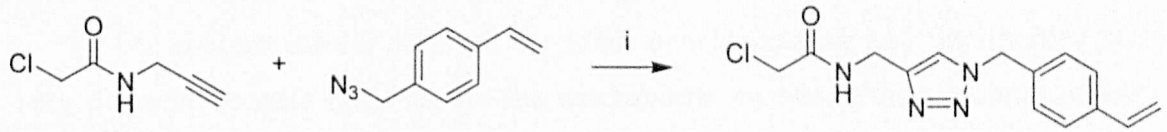

**66**

**Scheme 2.37** Synthesis of *p*-vinylbenzyl azide **66**. i) 4-vinylbenzyl chloride (1 mol eq), $NaN_3$ (1.1 mol eq), $H_2O$/EtOH, reflux, 14 h, 60%.

After purification (including column chromatography), the target compound was isolated as a colourless oil in 60% yield (reported 88%[388]). $^{1}H$ and $^{13}C$ NMR spectra were substantially consistent with those reported for benzyl azide:[388] in the $^{1}H$ NMR spectrum the signal due to the benzyl protons was slightly shifted towards higher fields from 4.58 to 4.33 ppm with respect to the starting chloride, whilst the corresponding carbon atom produces a peak at the higher frequency of 54.5 ppm (was 46.2 ppm for the chloride). The other resonances in both the $^{1}H$ and $^{13}C$ NMR spectra were basically unchanged. The IR spectrum showed a strong absorption band at 2100 $cm^{-1}$ further supporting the presence of an azide moiety.

Azide **66** was then used to carry out a click chemistry reaction with propargyl-chloroacetamide **49** by following the same procedure applied for the synthesis of

compound **65**, i.e. by reacting the chloroacetamide and the azide in the presence of catalytic amounts of copper(II) sulphate and sodium ascorbate (Scheme 2.38).




**49** **66** **67**

**Scheme 2.38** Click chemistry reaction to prepare *N*-((1-(4-vinylbenzyl)-*1H*-1,2,3-triazol-4-yl)methyl)-2-chloroacetamide **67**. i) **49** (1 mol eq), **66** (1.1 mol eq), $CuSO_4 \cdot 5H_2O$ (0.1 mol eq), Na-ascorbate (0.2 mol eq), $H_2O$/*t*-BuOH 1:1, 50 °C, 14 h, 55%.

After 14 hours TLC and NMR analysis confirmed the reaction was not progressing further. A solid product had precipitated while forming, which was filtered and analysed. NMR, IR and elemental analysis confirmed the desired triazole derivative. It was also found that the filtrate contained unreacted starting materials (about 40% of the initial amount). The yield (55%) is atypically low for a copper(I)-catalysed cycloaddition reaction, and it did not improve by increasing the amount of $CuSO_4$ and sodium ascorbate. Particularly diagnostic were, in the $^1$H NMR spectrum, the triazole proton producing a peak at 7.49 ppm, and the methylene protons (in *alpha* position with respect to the azide moiety in **66**) responsible for a signal at 5.46 ppm, i.e. shifted downfield by 1.13 ppm as a consequence of their new position between two aromatic structures. The methylene protons (belonging to the propargyl group in **49**) also produced a peak at a higher frequency, shifted from 4.11 to 4.52 ppm. The remaining resonances were basically unchanged. In the $^{13}$C NMR spectrum the signals due to the triazole ring carbons were observable at 144.3 (quaternary carbon) and 122.4 ppm (CH). There was practically no variation in the chemical shifts of the peaks for the other carbon atoms.

Following the successful outcome of the synthesis of chloroacetamides **65** and **67**, a further click chemistry model reaction was to produce another interesting functional compound. In particular, it was tried to prepare an arm to be attached to cyclen and bearing a fluorescent dye, in order to obtain a multimodal agent able to combine different spectroscopic techniques (MRI, optical imaging and fluorescence) for diagnostic purposes. In general, bifunctional contrast agents[94, 100, 101, 195, 389-396] allow exploitation of the advantages of conceptually highly different imaging techniques: *in vivo* high three-dimensional spatial resolution[140, 144, 391, 397] and simultaneous physiological and anatomical information (MRI); high sensitivity, minimal

autofluorescence[391] and improvement of the target/background ratio (optical imaging); detection at the cellular level and high sensitivity (fluorescence).

The contrast effects observed for MRI, optical imaging and fluorescence are very different because different are the mechanisms on which these techniques are based. In MRI the "probes" (i.e. water protons) are substantially everywhere in the observed sample, thus signals are detected from the whole specimen (with various intensities depending on the type of tissue) and this allows the detailed background. On the contrary, in optical imaging and fluorescence the signal is produced by specific dyes which are limited in number and localisation; detection takes place only for the regions where these dyes are present, whilst the rest appears black.

Furthermore, the limitations of each technique can potentially be compensated by the others. MRI is affected by low sensitivity[181] by at least a factor of 10-20 compared to that of light microscopy. Anatomical background information obtained with optical imaging is limited. Fluorescence microscopy provides only *ex vivo* information, and is also limited by optical aberrations and light scattering to the outer 100-300 microns of a specimen. In general, Using multimodal contrast agents, features invisible with one of these modalities can be rendered by the others, as shown in the example of Figure 2.7.

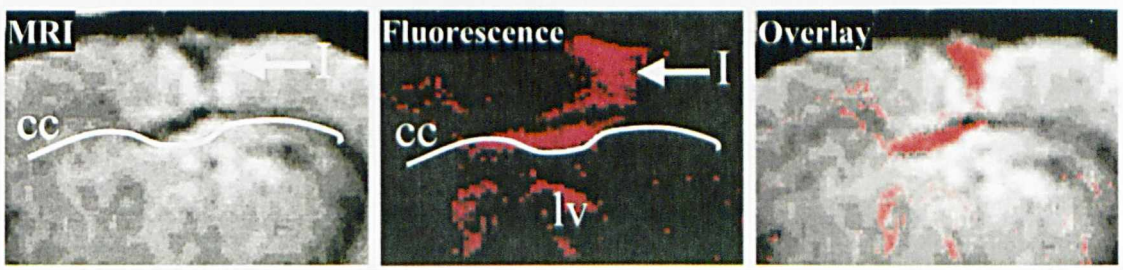
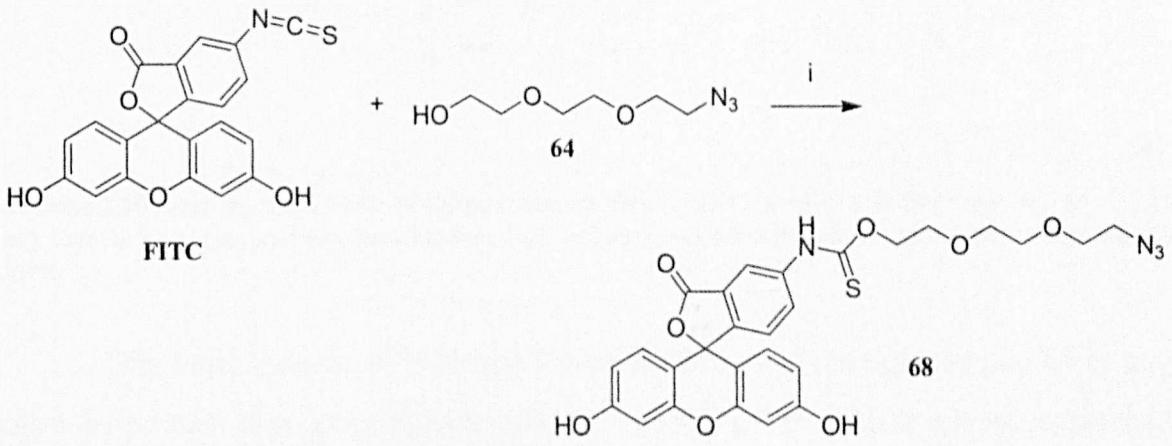



**Figure 2.7** A dual contrast agent is detectable by both MRI and fluorescence microscopy, and a direct overlay of both images affords identification and corroboration of the transplant of stem cells. I = injection tract; cc = corpus callosum; lv = lateral ventricle. [Image source: Modo, M. *et al.*; *Neuroimage* **2002**, *17*, 803-811]

Most of the reported dual agents are based on superparamagnetic iron oxide nanoparticles,[94, 389-393, 395, 396] but some drawbacks are to be considered (as mentioned in Section 1.2.7) which can make them unsuitable for certain applications, such as intravenous injection. Few proposed dual agents contain a Gd-DTPA- or Gd-DOTA-complex usually attached to a macromolecule, as well as a fluorescent dye (porphyrin derivatives,[100] tetramethylrhodamine, [101, 394] Texas Red[195]). In spite of the good results obtained with such dual agents in terms of the combination of different imaging techniques, the relaxivity values still remain low compared to the theoretically predicted

ones. As discussed before (Section 1.3.1.1) for the macromolecular agents so far reported in the literature, this is mainly due to local rotational freedom for the paramagnetic complexes, that counteracts the slow tumbling of the whole molecules.

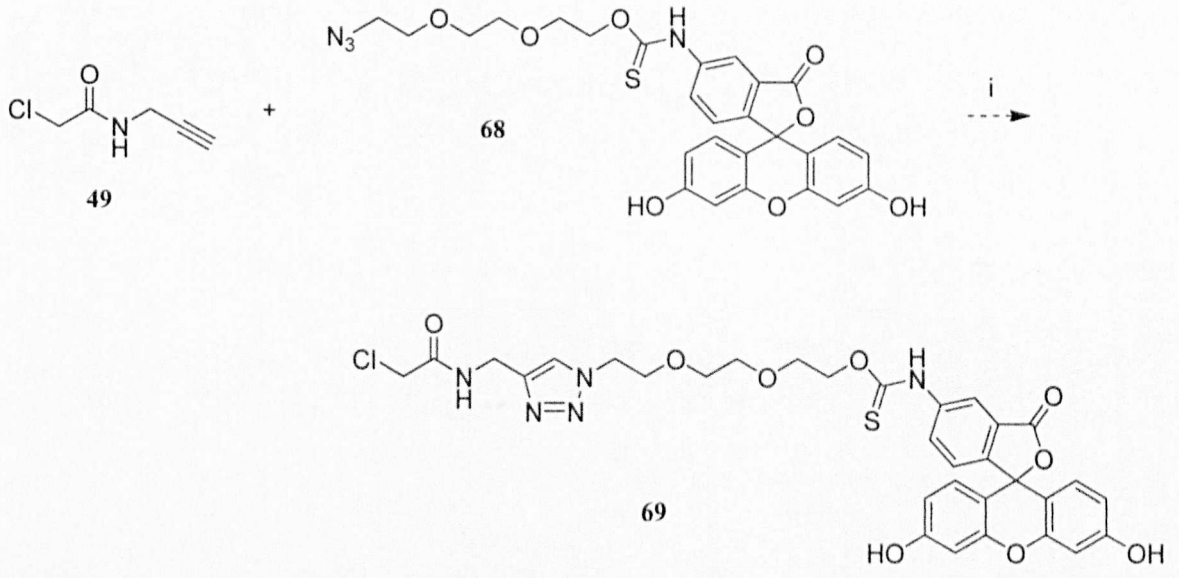
Some examples of attachment of fluorescent dyes *via* click chemistry are reported in the literature.[398-402] Herein, azido-alcohol **64** was first reacted with fluorescein 5-isothiocyanate (FITC) following the procedure reported by Llauger-Bufi *et al.*[403] for 6-(Boc-amino)-1-hexanol (Scheme 2.39).




**Scheme 2.39** Synthesis of fluorescein-5-(2-(2-(2-azidoethoxy)ethoxy)ethyl)thiocarbamate **68**. i) FITC (1 mol eq), **64** (1 mol eq), $Et_3N$ (2 mol eq), DMF, 60 °C, 24 h, 77%.

The crude product was purified by column chromatography, leading to the desired compound as an orange solid in 77% yield, as confirmed by the recorded analytical data (NMR, MS) and their comparison with those reported in the literature for fluorescein-thiocarbamates.[403, 404] No investigation was attempted on the nature of the by-products.

Azide **68** was then reacted with propargyl-chloroacetamide **49** (Scheme 2.40) according to the procedure followed previously for the preparation of triazole-derivatives **65** and **67**, as described above.



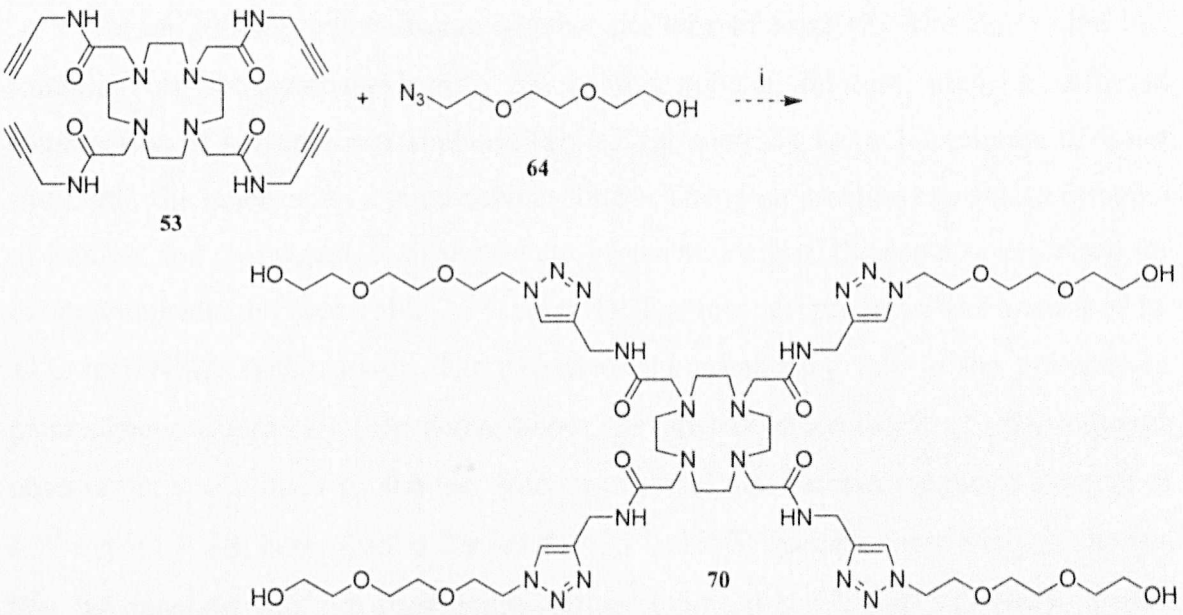

**Scheme 2.40** Attempt of synthesis of chloroacetamide **69** *via* click-chemistry. i) **49** (1 mol eq), **68** (1 mol eq), $CuSO_4 \cdot 5H_2O$ (0.1 mol eq), Na-ascorbate (0.2 mol eq), $H_2O$/*t*-BuOH, 50 °C, 24 h. The product did not form.

This time, though, no evidence for the formation of chloroacetamide **69** or any other by-product was obtained even after 24 hours. TLC and NMR spectroscopy only showed the presence of unreacted starting materials, which were actually recovered completely after removing the solvents under reduced pressure.

An identical result was obtained after running the reaction again, paying particular attention on degassing the solution before adding the catalyst and on the dissolution of the starting materials. Although the reasons for this lack of reactivity were not clear, no further effort was spent to investigate this aspect, since the reaction was not essential to the main aim. It was preferred to save time and focus on attempting the synthesis of monomers only containing polymerisable functionalities and for polymerisation purposes.

### 2.3.3 Divergent synthesis *via* click chemistry

After the success in preparing chloroacetamides **65** and **67**, hydroxy-azide **64** was reacted with DOTA-tetra-propargylamide **53**, as generally shown in Scheme 2.41.




**Scheme 2.41** General representation of the attempted synthesis of tetra-substituted species **70** *via* click-chemistry. Conditions and results are summarised in Table 2.15 and discussed in the text.

**Table 2.15** Reaction conditions and results for the attempted syntheses of tetra-triazole-derivative **70**, as shown in Scheme 2.41.

| | Conditions | Result |
|---|---|---|
| 1 | **53** (1 mol eq), **64** (4.4 mol eq), $CuSO_4 \cdot 5H_2O$ (0.4 mol eq), Na-ascorbate (0.8 mol eq), $H_2O$/*t*-BuOH, 50 °C, 14 h. | **70** did not form |
| 2 | **53** (1 mol eq), **64** (4.4 mol eq), $CuSO_4 \cdot 5H_2O$ (0.4 mol eq), Na-ascorbate (0.8 mol eq), $H_2O$/DMF, 50 °C, 20 h. | Low conversion (41%) calculated by NMR |
| 3 | **53** (1 mol eq), **64** (4.4 mol eq), $Et_3N$ (4.4 mol eq), $CuSO_4 \cdot 5H_2O$ (0.4 mol eq), Na-ascorbate (0.8 mol eq), $H_2O$/DMF, 50 °C, 20 h. | Low conversion (43%) calculated by NMR |

At first (Table 2.15, entry 1), **53** was reacted with **64** in little excess (4.4 molar equivalents) in the presence of catalytic copper(II) sulphate and sodium ascorbate, by adapting the conditions applied for the synthesis of **65** and **67** to the tetra-functionalised substrate **53**. A 1:1 mixture of water and *tert*-butanol was used as solvent system, although the solubility of compound **53** revealed it to be relatively low in this solvent mixture. After addition of the copper salt and sodium ascorbate, the colour of the mixture was at first blue-green, turning to yellow in few minutes. TLC and NMR spectroscopy did not show any evidence that a reaction had taken place even after 14 hours, since in both the $^{1}H$ and $^{13}C$ NMR spectra no signal was observable that could be assigned to a newly formed triazole ring or any other by-product, and the sets of signals from the starting materials looked essentially unchanged, albeit broadened by the presence of paramagnetic copper(II). Copper(II) (like $Cu^0$) has an odd number of electrons and therefore an unpaired electron (electronic configuration $[Ar]3d^9$) which causes paramagnetism and consequent line broadening.

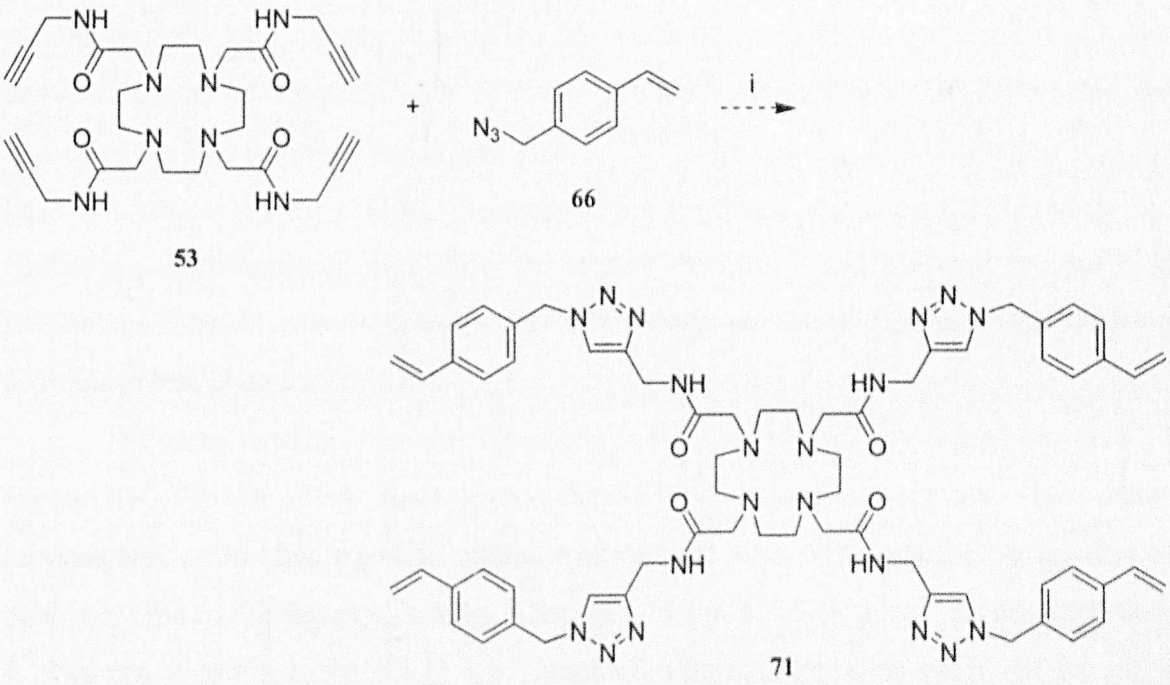
In an attempt to investigate whether the lack of reactivity was due to the low solubility of tetra-propargylamide **53** in the solvent mixture used, a different combination of solvents was applied (Table 2.15, entry 2), i.e. a 1:1 mixture of water and DMF, the latter being a good solvent for **53**. The other reaction conditions (amount of catalyst and co-reagent, temperature etc.) were maintained the same as described for the previous attempt (see Table 2.15, entry 1). The reaction progress was monitored by TLC and NMR spectroscopy. The expected line-broadening due to the presence of paramagnetic copper(II) (see above about the attempted synthesis of **70**), although observable, was limited by the low amount of metal and the low magnetic moment of $Cu^{II}$ ions (1.7 μB, compared to 7.9 μB for $Gd^{III}$). NMR spectroscopic analysis showed that the reaction was not progressing further after 20 h. $^{1}H$ and $^{13}C$ NMR spectra showed that some cycloaddition had taken place: a singlet at 7.89 ppm in the $^{1}H$ NMR spectrum and two peaks at 144.7 and 123.1 ppm in the $^{13}C$ NMR spectrum were due to the hydrogen and the carbon atoms of the triazole ring, respectively. As a consequence of the hindered rotation around the amide bond, two sets of signals were observed for the NH protons and the carbonyl carbons: on the basis of a study about configurational equilibria of peptides,[405] the peaks at 8.56 ppm in the $^{1}H$ NMR spectrum and at 171.2 ppm in the $^{13}C$ NMR spectrum were assigned to the amide groups in a *cis* configuration, while resonances at 8.43 and 170.5 ppm belonged to the *trans* isomers, in a ratio of *cis*/*trans* of 44:56 (integration of NH protons).

By comparison between the total integration for the amide protons and the integral of the triazole ring proton, a conversion of 41% was calculated. The same value was calculated on the basis of integration of the methylene protons *alpha* to the amide nitrogens ($NHC\underline{H}_2$) in the product (4.33 ppm) *versus* unreacted arms (3.89 ppm). The corresponding carbon atoms resonances appeared at 34.1 and 27.8 ppm in the $^{13}C$ NMR spectrum respectively. The signal from the alkyne protons could not be used because it overlapped with the methylene signal due to the acetyl group. As a further confirmation that some alkyne groups had not reacted, the relative peaks were observed at 81.2 and 72.8 ppm in the $^{13}C$ NMR spectrum. In spite of the significant improvement achieved with respect to the same reaction carried out in water/*tert*-butanol (previous attempt; see Table 2.15, entry 1), the relatively low conversion achieved for this reaction was surprising, when considering the almost-quantitative yields usually recorded for click-chemistry reactions, including that obtained when synthesising compound **65** from hydroxy-azide **64** (see above). Furthermore, it seemed that the acetyl protons produced

two different signals: one at 3.04 ppm as in the starting material, and a new one centred around 3.4 ppm (overlapping the signals from the PEG chain). Similarly, the peak at 2.61 ppm arising from the ring protons of compound **53** seemed to have split into two peaks at 3.04 and 2.62 ppm. At this stage, such differentiation was attributed to restricted conformational and configurational equilibria involving the whole structure and possibly due to steric hindering, although a different explanation will be proposed later.

The reaction was carried out again in exactly the same conditions but with the addition of triethylamine (see Table 2.15, entry 3) as a base (as sometimes suggested in the literature),[362] in an attempt of improving the conversion by favouring the deprotonation of the terminal alkynes and consequently their binding to copper(I) to enter the catalytic cycle (see Scheme 2.33). After 20 h the estimated conversion was still 43% (by NMR). Also in this case a splitting of the signals for the acetyl and ring protons was observed, still thought to be due to conformational restrictions.

In order to test the reactivity and also to try and form a further species to be used as a monomer in polymerisation reactions, tetra-propargyl-amide **53** was reacted with previously synthesised (see Section 2.3.2) *p*-vinylbenzylazide **66** as generally shown in Scheme 2.42. A mixture of water and DMF was used to dissolve both **53** and the catalytic system, as reported in Table 2.15 (entries 2 and 3) for the attempts of synthesis of **70**.




**Scheme 2.42** General representation of the attempted synthesis of tetra-substituted species **71** *via* click-chemistry. Conditions and results are summarised in Table 2.16 and discussed in the text.

| **Table 2.16** Reaction conditions and results for the attempted syntheses of tetra-triazole-derivative **71**, as shown in Scheme 2.42. | | |
|---|---|---|
| | **Conditions** | **Result** |
| 1 | **53** (1 mol eq), **66** (4.4 mol eq), $CuSO_4 \cdot 5H_2O$ (0.4 mol eq), Na-ascorbate (0.8 mol eq), $H_2O$/DMF, 50 °C, 48 h. | Low conversion (19%) calculated by NMR |
| 2 | **53** (1 mol eq), **66** (4.4 mol eq), $CuSO_4 \cdot 5H_2O$ (1.4 mol eq), Na-ascorbate (2.8 mol eq), $H_2O$/DMF, 50 °C, 48 h. | Apparent higher conversion than in entry 1, but not quantifiable because of NMR line broadening |

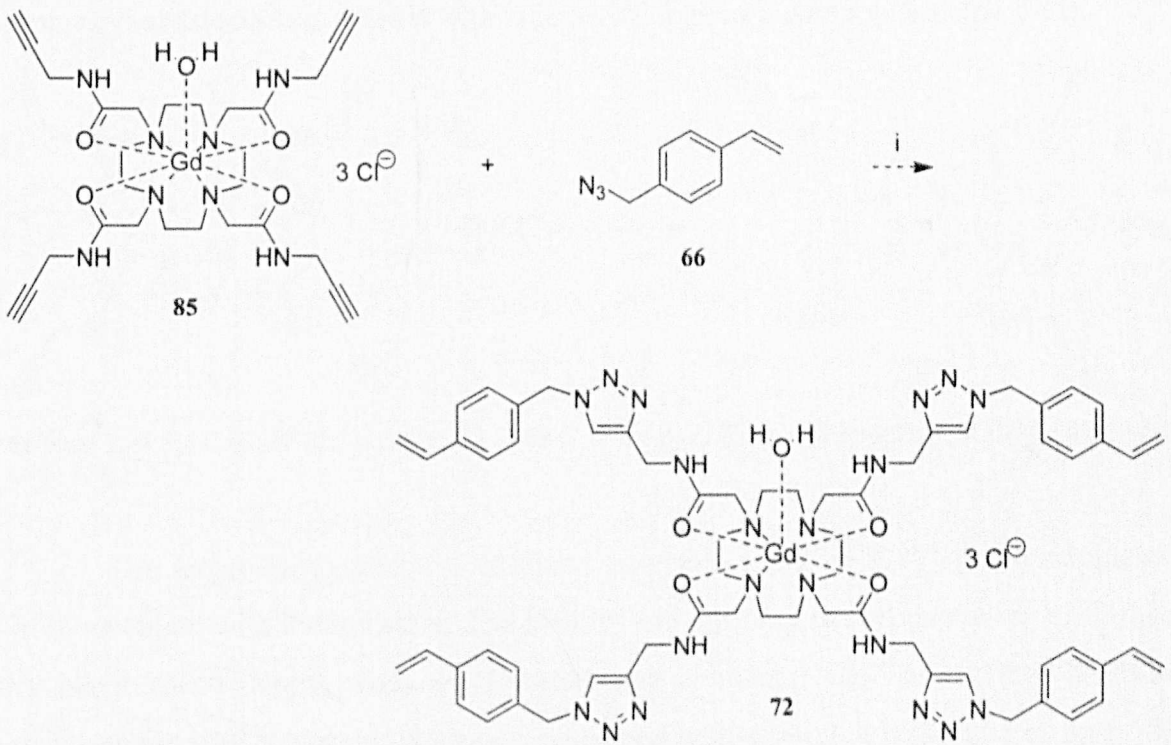
At first (Table 2.16, entry 1), a 10 mol% amount per alkyne of copper(II) sulphate and a 20 mol% amount of sodium ascorbate were once more considered as appropriate after their successful application in the click chemistry reactions leading to triazole derivatives **65** and **67** (see Section 2.3.2). After 2 days a conversion of only 19% was calculated by comparing the integrations of suitable signals in the $^1$H NMR spectrum (as described for the conversion estimates in the attempts of synthesis of **70**). Also in this case (as explained for the NMR spectra relative to the attempted synthesis of **70**) the expected line-broadening due to the presence of paramagnetic copper(II), although observable, was limited and allowed a good analysis of the spectra. As observed for the reaction attempts between **53** and hydroxyazide **64**, it looked like part of the resonance due to the acetyl protons had shifted from 3.04 to 3.36 ppm, and the peak for the ring protons had split into two peaks at 3.05 and 2.68 ppm from the original chemical shift of 2.61 ppm.

These observations led to the hypothesis of the complexation of the copper cations by the cyclic system, causing the inhibition of the catalytic cycle and then a low conversion and an apparent lack of reactivity. $Cu^{II}$-complexes of DOTA-amides are known in the literature and are indeed stable,[238, 406] with log $K_{ass}$ at 25 °C being 16.3 for DOTMA and 14.12 for DTMA. Because of the rigidity induced on the ligand by the chelation, conformational equilibria are strictly restrained and the ring protons find themselves fixed in either a pseudo-axial or a pseudo-equatorial position, thus showing different NMR chemical shifts.

The same reaction was now repeated (Table 2.16, entry 2) by using an excess of copper(II) sulphate (1.4 molar equivalents) and sodium ascorbate (2.8 molar equivalents), so to have free $Cu^I$ available as catalyst even with quantitative ligation of copper by the tetra-propargyl-amide. After 48 hours a $^1$H NMR spectrum was recorded. It was not possible to calculate the actual conversion rate with sufficient accuracy because of the line-broadening produced by the consistent presence of paramagnetic $Cu^{II}$ (see above about the attempted synthesis of **70**). However, by a rough visual

estimate based on the apparent signal areas it seemed that a higher conversion had been achieved with respect to the same reaction carried out with just a catalytic amount of copper(II) sulphate.

It was also tried to carry out a cycloaddition reaction between azide **66** and Gd-complex **85** from tetra-propargylamide **53** (whose synthesis is described in Chapter 4). Although gadolinium(III) is highly paramagnetic and produces a large broadening of the NMR signals[169, 346] with consequent loss of resolution, we hoped to obtain a $^1$H NMR spectrum clear enough to analyse the reaction outcome. This procedure would have then led to a useful Gd-complex to be used both as a monomer for the preparation of polymers already loaded with $Gd^{III}$, and as a contrast agent to be tested for performance and toxicity on cell cultures. The well-known high thermodynamic and especially kinetic stability of Gd-complexes of DOTA (see Chapter 1) are expected to ensure that no significant exchange between gadolinium and copper takes place. This is in spite of the fact that the stability constants for Gd-DOTA-amides DOTAM and DTMA are reported to be lower than those for copper(II), being log $K_{ass}$ for $Cu^{II}$-DOTAM 16.3 compared with 10.1 for $Gd^{III}$-DOTAM,[406] and 14.1 for $Cu^{II}$-DTMA compared with 12.8 for $Gd^{III}$-DTMA[238] (see Table 1.2). Thus, compound **85** was reacted with 4-vinylbenzylazide **66** (4.4 molar equivalents) as shown in Scheme 2.43.

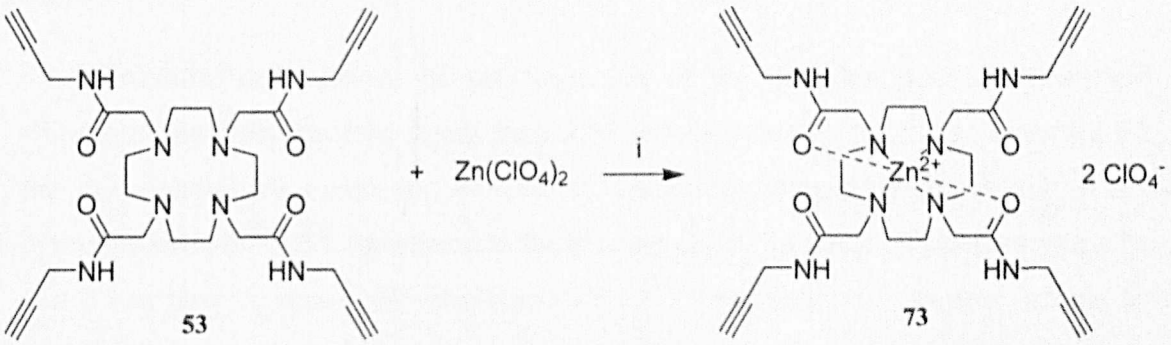



**Scheme 2.43** Attempt of synthesis of $Gd^{III}$-complex **72** *via* click-chemistry. i) **85** (1 mol eq), **66** (4.4 mol eq), $CuSO_4 \cdot 5H_2O$ (0.4 mol eq), Na-ascorbate (0.8 mol eq), $H_2O$/DMF, 50 °C, 24 h. The NMR line broadening did not allow estimation of the crude yield or conversion.

Unfortunately, as it could be expected because of the presence of copper(II) and gadolinium(III) which are both paramagnetic, the $^{1}H$ and $^{13}C$ NMR spectra were heavily affected by line broadening,[169, 346] and no information was obtained about the formation of the target product.

Rather than looking for alternative ways to analyse qualitatively and quantitatively the outcome of the reaction just described, it was considered worth to replace gadolinium with a diamagnetic metal in order to form the corresponding complex with the cyclic ligand and avoid the complexation of the copper catalyst, and also be able to analyse the progress of the reaction by NMR spectroscopy. Among the several possible choices, zinc was chosen because readily available. The formation of a zinc(II)-complex of a DOTA-tetra-amide (DOTAM) by using zinc perchlorate is reported in the literature.[406] The stability constant for such a complex is relatively high (log $K_{ass}$ = 10.5), an intermediate value between those for copper(II) and gadolinium(III) (see above). The stability constant reported in the literature for $Zn^{II}$-DTMA is even higher (log $K_{ass}$ = 13.0).[238] It has to be mentioned that the Cd-complex of **53** has been prepared as an alternative to zinc by other people[407] for the same purpose, with similar results.

Following a procedure analogous to that reported in the literature,[406] DOTA-propargyl-amide **53** was reacted with zinc perchlorate in methanol (Scheme 2.44).




**Scheme 2.44** Synthesis of $Zn^{II}$-complex **73**. i) **53** (1 mol eq), $Zn(ClO_4)_2$ (1.1 mol eq), $H_2O$/MeOH, 80 °C, 14 h, 87%.

The target compound was obtained pure in a yield of 87% after precipitation from methanol with diethyl ether. The identity and purity of the product were confirmed by NMR spectroscopy, mass spectrometry and elemental analysis. In the $^{1}H$ NMR spectrum the ring protons produce two broad and well-separated peaks at 2.67 and 3.02 ppm (Figure 2.8), as also previously observed when ligand **53** was reacted in the presence of copper (the chemical shifts of the peaks were 2.68 and 3.05, see above). This is due to the locked conformation and the consequent differentiation between

pseudo-axial and pseudo-equatorial protons, as confirmed by literature data about other Zn-DOTA-amides.[406]

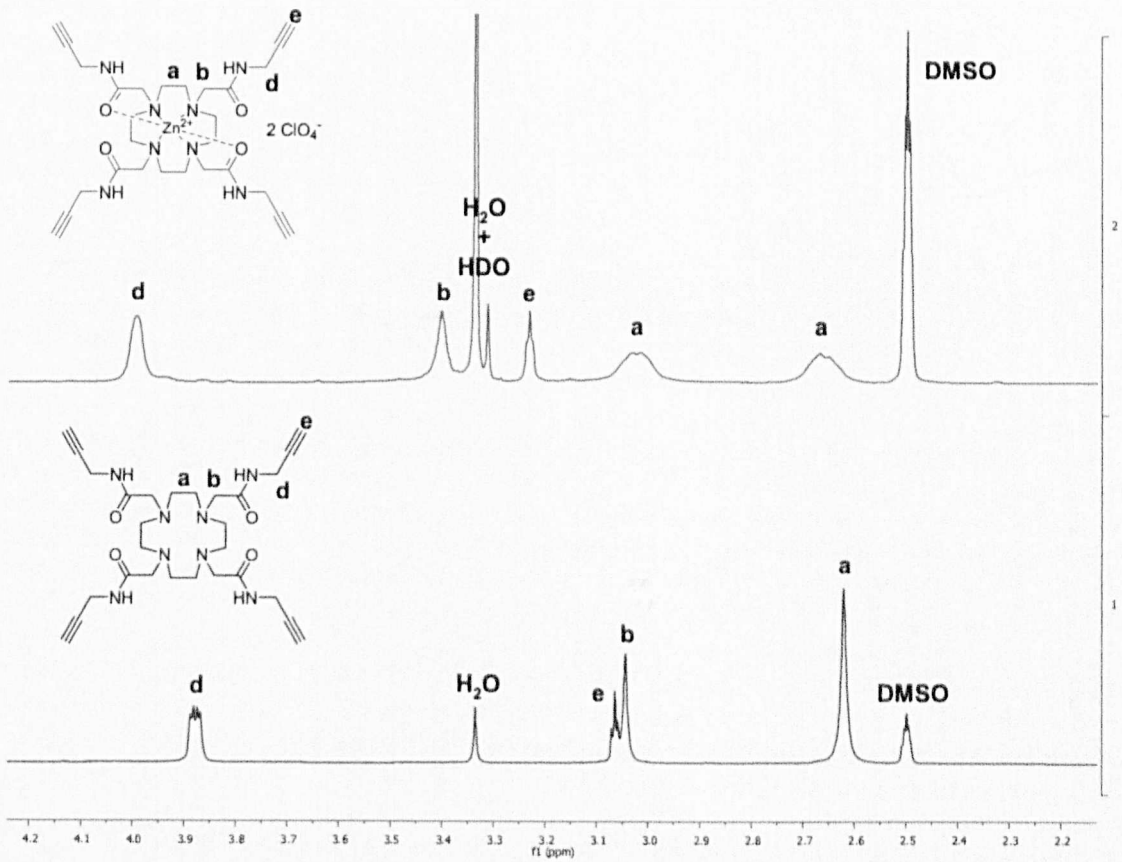



**Figure 2.8** Comparison between the same regions of the $^{1}$H NMR spectra in DMSO-$d_6$ of compounds **73** (top) and **53** (bottom).

Another consequence of the formation of the complex was the downfield shifting of the acetyl protons signal from 3.04 to 3.40 ppm. That was also observed for the click chemistry reactions between DOTA-tetra-propargyl-amide **53** and either hydroxyl-azide **64** or **53**, the chemical shifts being about 3.4 and 3.36 ppm respectively, and it can now be reasonably explained with the complexation of copper cations by some of the macrocycle derivative.

Because of the hexacoordination of $Zn^{II}$ ($Zn^{II}$ ionic radius = 0.74 Å; $Gd^{III}$ ionic radius = 0.94 Å)[406, 408] it was predicted that only two of the carbonyl groups (probably in *trans* position with respect to the ring substitution positions) and no water were coordinated to the metal centre, besides the four nitrogen atoms of the ring. The absence of any coordinated water molecule was first confirmed by elemental analysis. For further characterisation, crystals of **73** were grown[407] and analysed by X-ray crystallography. The obtained X-ray structure is shown in Figure 2.9.

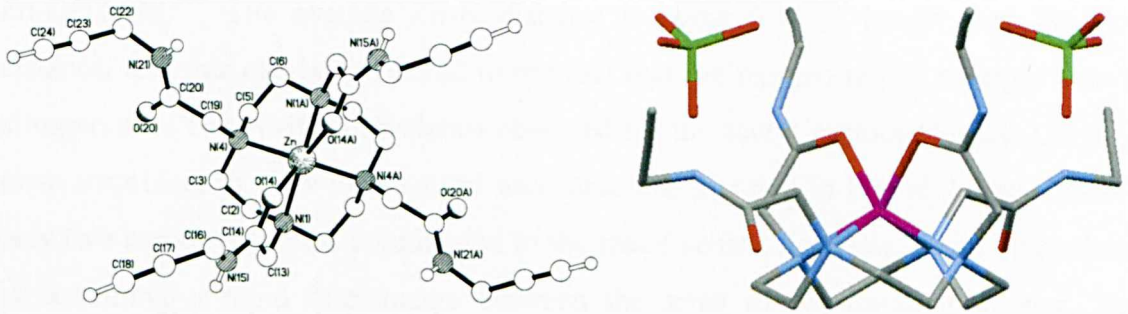


**Figure 2.9** X-ray crystal structure[407] of **73** showing the hexa-coordinate stereochemistry of the $Zn^{II}$-complex. Hydrogen atoms and solvent molecules have been omitted for clarity. Crystal data are reported in Chapter 6 (Table 6.1). Selected bond lengths and angles are reported in Table 2.17.

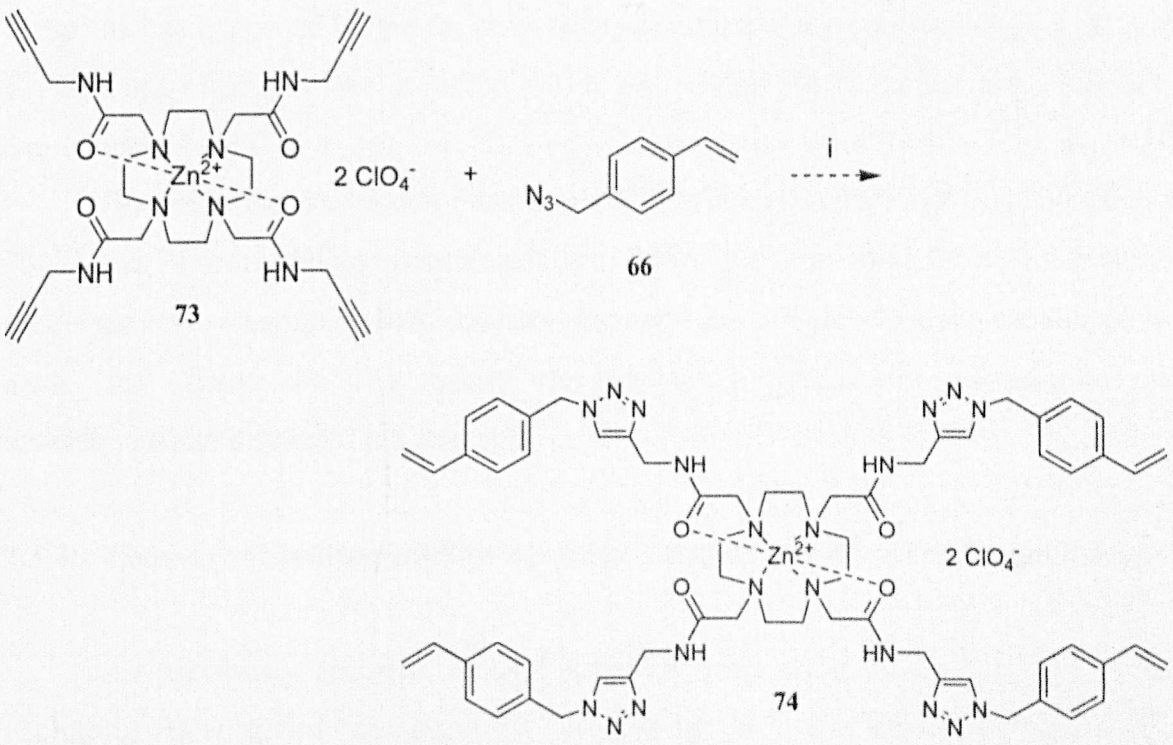
**Table 2.17** Selected bond lengths [Å] and bond angles [deg] for **73** (numbers in parentheses are estimated standard deviations in the least significant digits).[407]

| **Bond lengths** | | | |
|---|---|---|---|
| Zn – O(14A) | 2.0911(19) | N(1) – C(6A) | 1.525(5) |
| Zn – O(14) | 2.0911(19) | C(2) – C(3) | 1.486(6) |
| Zn – N(4A) | 2.182(3) | C(3) – N(4) | 1.506(5) |
| Zn – N(4) | 2.182(3) | N(4) – C(19) | 1.457(5) |
| Zn – N(1) | 2.231(3) | N(4) – C(5) | 1.502(5) |
| Zn – N(1A) | 2.231(3) | C(5) – C(6) | 1.514(6) |
| N(1) – C(2) | 1.455(5) | C(6) – N(1A) | 1.525(5) |
| N(1) – C(13) | 1.470(4) | C(13) – C(14) | 1.490(4) |
| **Bond angles** | | | |
| O(14A) – Zn – O(14) | 82.91(10) | C(13)-N(1)-Zn | 109.49(19) |
| O(14A) – Zn – N(4A) | 92.17(9) | C(6A) – N(1) – Zn | 109.0(2) |
| O(14) – Zn – N(4A) | 119.03(10) | N(1) – C(2) – C(3) | 111.4(3) |
| O(14A) – Zn – N(4) | 119.03(10) | C(2) – C(3) – N(4) | 112.0(3) |
| O(14) – Zn – N(4) | 92.17(9) | C(19) – N(4) – C(5) | 121.1(3) |
| N(4A) – Zn – N(4) | 139.15(16) | C(19) – N(4) – C(3) | 111.5(3) |
| O(14A) – Zn – N(1) | 152.28(10) | C(5) – N(4) – C(3) | 104.3(3) |
| O(14) – Zn – N(1) | 78.16(9) | C(19) – N(4) – Zn | 106.4(2) |
| N(4A) – Zn – N(1) | 79.76(9) | C(5) – N(4) – Zn | 106.3(2) |
| N(4) – Zn – N(1) | 82.02(11) | C(3) – N(4) – Zn | 106.2(2) |
| O(14A) – Zn – N(1A) | 78.16(9) | N(4) – C(5) – C(6) | 108.3(3) |
| O(14) – Zn – N(1A) | 152.28(10) | C(5) – C(6) – N(1A) | 108.8(4) |
| N(4A) – Zn – N(1A) | 82.02(11) | N(1) – C(13) – C(14) | 110.9(2) |
| N(4) – Zn – N(1A) | 79.76(9) | O(14) – C(14) – C(13) | 122.0(3) |
| N(1) – Zn – N(1A) | 126.04(16) | N(15) – C(14) – C(13) | 116.3(3) |
| C(2) – N(1) – C(13) | 111.7(3) | C(14) – O(14) – Zn | 116.48(18) |
| C(2) – N(1) – C(6A) | 118.0(3) | N(4) – C(19) – C(20) | 115.9(3) |
| C(13) – N(1) – C(6A) | 104.2(3) | O(20) – C(20) – C(19) | 121.7(3) |
| C(2) – N(1) – Zn | 104.4(2) | N(21) – C(20) – C(19) | 113.8(3) |

The crystallographic structure confirms the expected hexa-coordination, with two arms binding to the zinc centre and pointing towards the upper side of the molecule, whilst the other two arms are stretched laterally and free to rotate. The two perchlorate anions belonging to the crystalline structure are also visible. The average Zn-N and Zn-

O bond lengths of complex **73** (see Table 2.17) are consistent with those reported for Zn-DOTAM.[406] The average Zn-N distance is about 0.11 Å longer than the Zn-O distance, and this can be attributed to the fact that the oxygen radius is larger than the nitrogen one. The NMR equivalence observed for the acetyl protons (Figure 2.8) might seem surprising in view of the solid state structure reported in Figure 2.9 and showing only two carbonyl groups coordinated to the metal centre; however, it can be explained by assuming a rapid interchange between the arms in coordinating to zinc. Such exchange takes place rapidly enough to be not detected by NMR spectroscopy.

Zinc-complex **73** was reacted in a click chemistry reaction with 4-vinylbenzylazide **66** (Scheme 2.45) by employing the conditions used for the synthesis of **65**, **67**, **70** (Table 2.15, entry 2) and **71** (Table 2.16, entry 1), since under such conditions high yields (**65** and **67**) or at least the highest conversion rates (**70**) were obtained.




**Scheme 2.45** Synthesis of $Zn^{II}$-complex **74** *via* click-chemistry. i) **73** (1 mol eq), **66** (4.4 mol eq), $CuSO_4 \cdot 5H_2O$ (0.4 mol eq), Na-ascorbate (0.8 mol eq), $H_2O$/DMF, 50 °C, 14 h. Crude yield: 46%.

Analysis of the crude mixture by TLC and NMR spectroscopy showed that the end of conversion had been reached after 14 hours. The formation of the desired product was confirmed by the $ESI^+$ mass spectrum of the crude mixture, where the peaks corresponding to the $[ligand + Zn]^{2+}$, $[ligand + Zn]^+$ and $[ligand + Zn + Na]^+$ fragments at 626, 1252 and 1274 m/z respectively were observed, as well as their combinations with one perchlorate unit. Some peaks possibly due to mono-, di- or tri-substituted by-

products were present. The $^{1}$H NMR spectrum showed a set of signals consistent with the desired product, but an estimate of the conversion was not possible because of the signal superimposition combined to the line broadening due to the presence of paramagnetic $Cu^{II}$. A set of signals was observed in the $^{13}$C NMR spectrum consistent with that expected for **74**, on the basis of the spectra previously recorded for similar species such as **67** and **71**. Signals at 80.1, 72.9 and 28.7 ppm were compatible with the typical resonances for propargyl carbon atoms, thus suggesting that some unreacted C-C triple bonds were still present. After washing with diethyl ether to remove the excess of azide (about 23% of the initial amount) and Soxhlet extraction with water, **74** was obtained with a crude yield of 46%. Although the product looked quite clean by NMR spectroscopy and mass spectrometry, weak peaks in the $^{1}$H NMR spectrum as well as the yellowish colour of the solid confirmed the presence of impurities. Unfortunately, after several attempts it was not possible to find a procedure to isolate the target compound, as happened before for other tetra-substituted cyclen derivatives, e.g. **62** and **63**. Because of this, it was preferred not to use product **74** in radical polymerisation experiments.

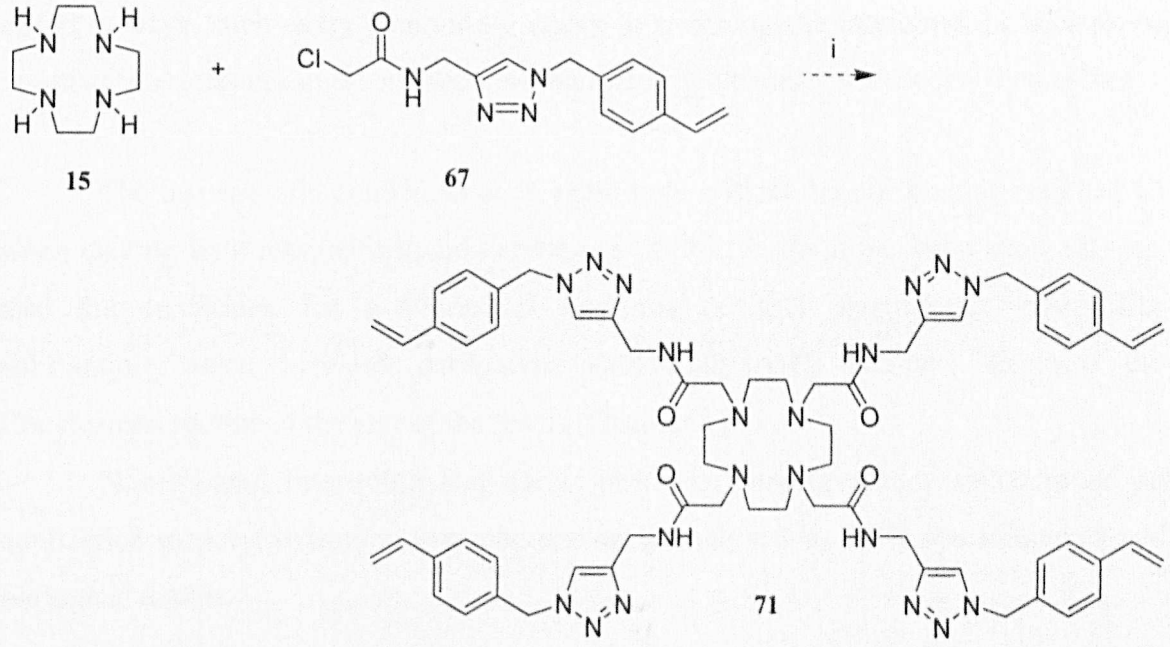
However, the conversion rates obtained in click chemistry synthesis of species **70**, **71** and **74** prompted and encouraged us to follow the same route for polymerisation processes *via* cycloaddition between tetra-propargyl Zn-complex **73** and a suitable poly-azide (see Chapter 3). The reasons for the lack of quantitative conversions are investigated and discussed in Chapter 3.

### 2.3.4 Convergent synthesis following preparation of arm 67 *via* click chemistry

As previously reported, several types of arms were attached to cyclen by exploiting the so-called "cesium effect" brought by the use of cesium carbonate as a base, together with the advantages of adding potassium iodide. The same procedure was followed to synthesise 1,4,7,10-tetrakis((1-(4-vinylbenzyl)-*1H*-1,2,3-triazol-4-yl)methylcarbamoylmethyl)-1,4,7,10-tetraazacyclododecane **71**, whose divergent synthesis was carried out as described in Section 2.3.3 with arguable success.

As shown in Scheme 2.46, cyclen was reacted with *N*-((1-(4-vinylbenzyl)-*1H*-1,2,3-triazol-4-yl)methyl)-2-chloroacetamide **67** under the conditions ($Cs_2CO_3$/KI in DMF) successfully applied for the synthesis of **31** (see Section 2.1.1), **32** (see Section

2.2), **53** (see Section 2.2.3), **62** and **63** (see Section 2.2.4.1), although the latter two products were not isolated in a pure form.




**Scheme 2.46** Convergent synthesis of 1,4,7,10-tetrakis((1-(4-vinylbenzyl)-*1H*-1,2,3-triazol-4-yl)methylcarbamoylmethyl)-1,4,7,10-tetraazacyclododecane **71**. i) **15** (1 mol eq), **67** (4.4 mol eq), $Cs_2CO_3$ (4.4 mol eq), KI (4.4 mol eq), DMF, 50 °C, 48 h. Purification problems are discussed in the text.

The brownish solid obtained after 2 days was checked by NMR spectroscopy and mass spectrometry, showing that the desired compound had formed. The $^1$H NMR spectrum looked very clean, with only the set of signals expected for the target species observable. According to this data, the conversion should be quantitative. The $^{13}$C NMR spectrum also showed the set of signals expected for the targeted compound only, thus confirming the apparent 100% conversion established on the basis of the $^1$H NMR spectrum. In the ESI$^+$ mass spectrum the main observed peaks were assigned to the desired product, at m/z 595 ($[M+2H]^{2+}$), 617 ($[M+2Na]^{2+}$), 1189 ($[M+H]^+$) and 1211 ($[M+Na]^+$). Two isolated signals were also recorded at 935 and 957 m/z, which might belong to a tri-substituted species; however, it is also possible that it comes from the fragmentation of the molecular ion, as another weak peak at 997 m/z seems to suggest. As mentioned above, the presence of partially substituted derivatives can be excluded according to NMR analysis, since there is no differentiation for any ring or arm atom.

In spite of what has been described so far, the brownish colour of the product indicated that impurities were present; this was confirmed by elemental analysis. Several purification attempts were carried out unsuccessfully, from simple washing with water through to chromatography.

Because of the presence of impurities it was doubtful if the obtained product was to be used in radical polymerisation reactions, which might be affected in many different ways, such as by committing errors in weighing the monomer, or because of negative interferences in the reaction mechanisms by the unknown species themselves.

The last reaction confirmed once again how critical the purification step can be when dealing with tetra-substituted derivatives of DOTA. As it has been shown so far, also the conditions for a successful synthesis of such compounds may differ substantially even between derivatives structurally very similar. See also the Conclusions section at the end of the thesis (Chapter 5).

Nonetheless, interesting and useful products were prepared, which found an application in polymerisation attempts, and were analysed by MRI measurements and biological assays.

# 3. Results and discussion II: polymerisations

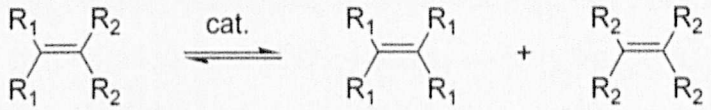
The monomers synthesised as described in Chapter 2 were used in attempts of polymerisations following different procedures, depending on the structure and the functional groups present in each monomer.

## 3.1 Polymerisation *via* metathesis

Metathesis reactions are widely reported in the literature as a means to obtain polymeric species from suitable monomers containing unsaturations.[409-414] This methodology was also applied in this context in an attempt to achieve polymeric structures for the target MRI contrast agents.

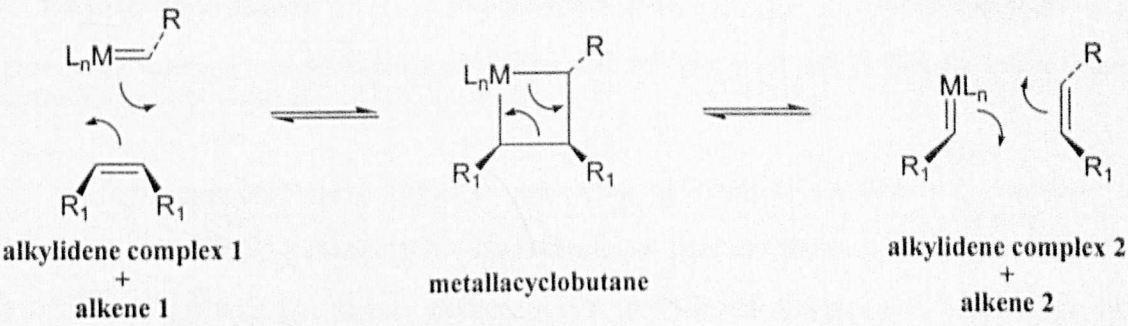
### 3.1.1 Overview on metathesis reactions

Alkene metathesis corresponds to a reaction where C-C double bonds are broken and then rearranged in a statistical way[415-419] (Scheme 3.1).




**Scheme 3.1** Generic representation of a metathesis reaction.

The commonly accepted mechanism was suggested by Chauvin[420] and includes a [2+2] cycloaddition between an alkylidene complex of a transition metal and an alkene, with formation of a metallacyclobutane. Such metal-cycle then breaks leading to the formation of a new alkylidene complex and a new alkene (Scheme 3.2).



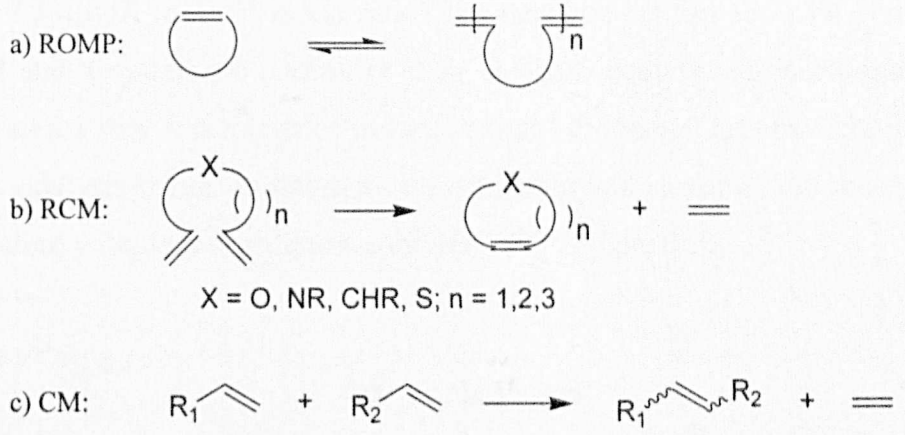

**Scheme 3.2** Reaction mechanism for a generic metathesis process, involving the formation of an intermediate metallacyclobutane.

Three types of metathesis reactions, very close to each other, can be distinguished (Scheme 3.3):

a) ring-opening metathesis polymerisation (ROMP);

b) ring-closing metathesis (RCM);

c) cross-metathesis (CM), which leads to polymer formation whenever carried out with dialkenes (acyclic diene metathesis polymerisation, ADMET).




**Scheme 3.3** Generic representation of the 3 types of metathesis reaction: a) ring-opening metathesis polymerisation; b) ring-closing metathesis; c) cross-metathesis.

Metal-alkylidene complexes possess a carbon-metal double bond and are closely related with Fischer carbene complexes.[421] Metal-carbene (or alkylidene) complexes usually have one or two alkyl or aryl substituents directly bound to the *alpha* carbon atom, differently than Fischer carbene complexes where an heteroatom is bound to the *alpha* carbon (Figure 3.1).

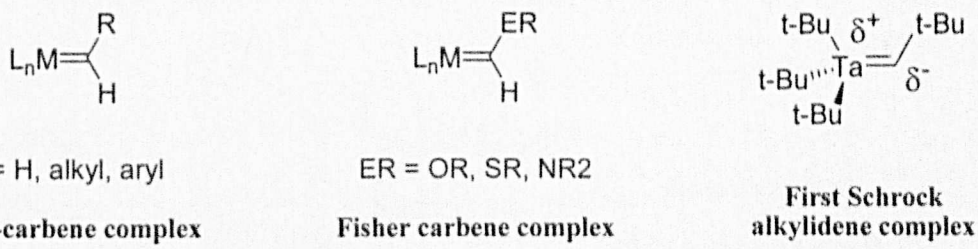



**Figure 3.1** Comparison between Schrock and Fischer carbene complexes, and the first alkylidene carbene complex proposed by Schrock.

Alkylidene carbene complexes are often referred to as *Schrock carbenes* or *alkylidenes*, after R.R. Schrock who discovered the first example of such compounds in the 70s[422] (Figure 3.1). Fisher carbenes are complexes between a middle or late transition metal with low oxidation state (e.g. $Fe^0$, $Mo^0$, $Cr^0$, $W^0$) and a π-acceptor ligand with a πp-donor substituent (e.g. alkoxy, sulphide or amino groups) on the methylene group. On the other hand, Schrock alkylidenes[355] are typically complexes

between an early transition metal with high oxidation state (e.g. $Ti^{IV}$, $Ta^{V}$) and a non-π-acceptor ligand lacking π-donor substituents. The metal-carbon double bond is highly polarised, so that the *alpha* carbon atom acts as a nucleophile.

The first catalytic systems consisted of mixtures of transition metals chlorides, oxides or oxichlorides, co-catalysts like ethylalluminium chloride or tetramethyltin, and promoters like oxygen, ethanol or phenol.[423-425] A typical example is the mixture $WCl_6/EtAlCl_2/EtOH$ in 1:4:1 molar ratio. The catalytic centres for such systems were ill-defined and a systematic control of their catalytic activity was not possible. They also possessed a very low tolerance towards several functional groups. Schrock found a variety of catalysts based on tungsten, molybdenum and rhenium, the most important being the alkoxy imido molybdenum complex **75**[426] (Figure 3.2).

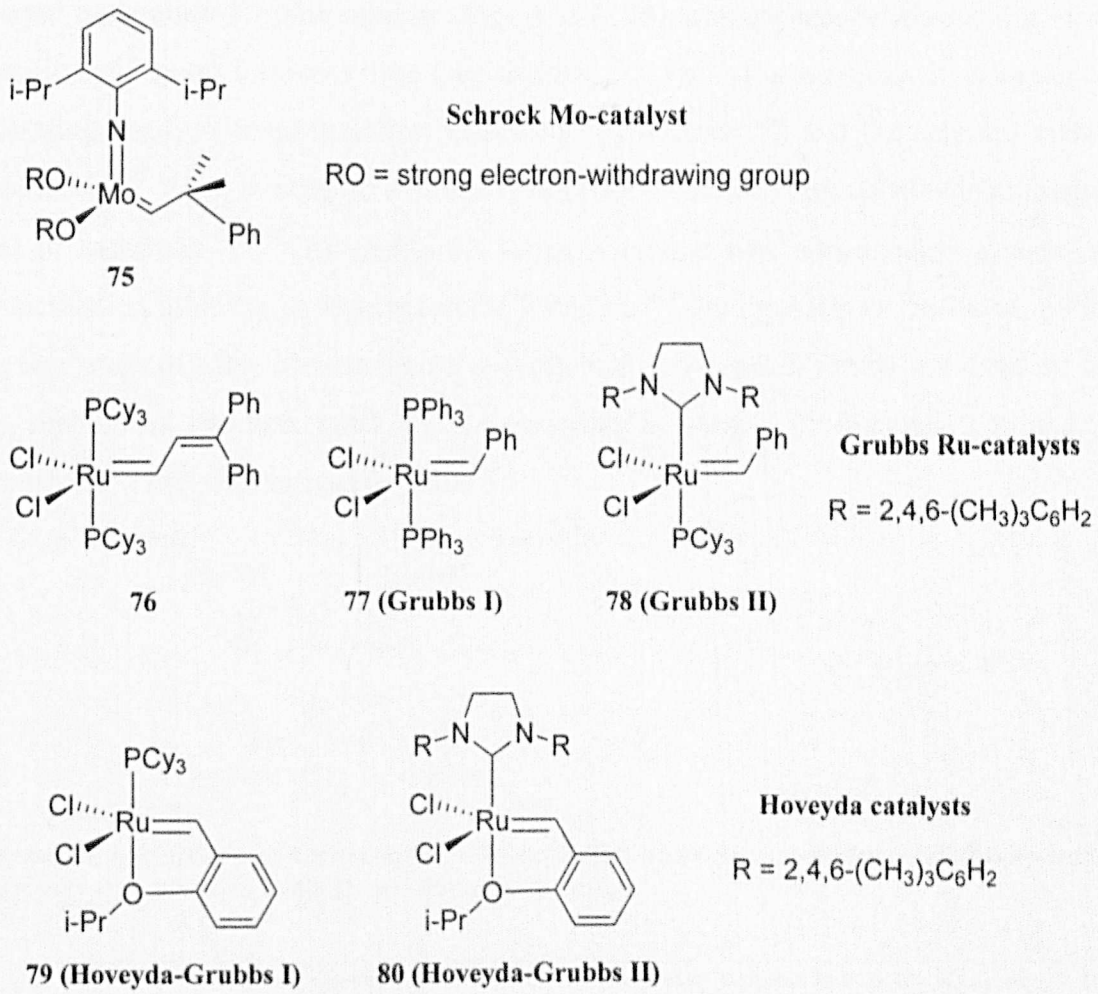


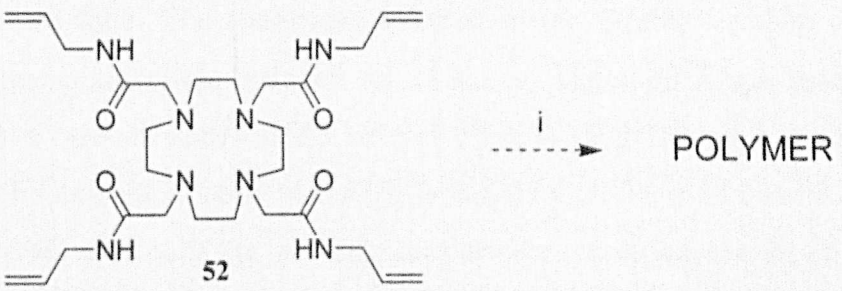

**Figure 3.2** The most commonly reported molybdenum-based Schrock catalyst (top), ruthenium-based Grubbs catalysts (middle) and Hoveyda catalysts (bottom).

Such catalysts have a good functional group tolerance and turn over activity. Their reactivity can be modified by varying the alkoxy groups. However, they are air- and moisture-sensitive, differently than most Fischer carbene complexes which are stable to air, water and even diluted acids and bases.

In the 90s Grubbs and co-workers[427-431] and Hoveyda and co-workers[432] developed a series of ruthenium-based catalysts (**76-80**, Figure 3.2) which differ from the earlier ones in many aspects. For instance, the metal is not in its higher oxidation state and it is coordinated with phosphine ligands. Moreover, these new catalysts are extremely tolerant towards many different moieties. Such tolerance, though, is counterbalanced by a lower metathesis rate with respect to Schrock catalysts.

### 3.1.2 Attempt of polymerisation of DOTA-tetra-allyl-amide 52 *via* metathesis

In an attempt of polymerising 1,4,7,10-tetrakis(allylcarbamoylmethyl)-1,4,7,10-tetraazacyclo-dodecane **52** *via* cross-metathesis (see Section 3.1.1, Scheme 3.3c), the second generation Grubbs catalyst (Figure 3.2, **78**) was chosen because of its known stability and good turn-over rate (see Section 3.1.1).[433] Furthermore, it is capable of tolerating the functional moieties possessed by substrate **52** and the selected reaction conditions.[433] Also, in order to avoid isomerisation of the allyl moieties with consequent loss of reactivity,[434-438] 2,6-dichloro-1,4-benzoquinone was added being a successful isomerisation inhibitor as reported in the literature.[439] On the basis of the literature data, the formation of some corresponding hydroquinone by-product should not interfere with the metathesis reaction itself.[439] The reaction is shown in Scheme 3.4, and the conditions[433] are summarised in Table 3.1.




**Scheme 3.4** Attempt of polymerisation of DOTA-tetra-allyl-amide **52** *via* metathesis reaction. Conditions and results are reported in Table 3.1 and discussed in the text.

**Table 3.1** Reaction conditions and results for the attempted polymerisation of DOTA-tetra-allyl-amide **52**, as shown in Scheme 3.4

| | Conditions | Result |
|---|---|---|
| 1 | **52** (1 mol eq), Grubbs II (0.2 mol eq), 2,6-dichloro-1,4-benzoquinone (2 mol eq), DCM, reflux, 15 h. | No polymerisation. Adduct between **52** and the additive (by NMR). |
| 2 | **52** (1 mol eq), Grubbs II (0.4 mol eq), 2,6-dichloro-1,4-benzoquinone (2 mol eq), DCM, reflux, 15 h. | No polymerisation. Adduct between **52** and the additive (by NMR). |

Using flame-dried glassware, the catalyst (0.05 molar equivalents per C-C double bond) and the benzoquinone (0.5 molar equivalents per C-C double bond) were weighed under inert atmosphere. The benzoquinone was dissolved in the minimum amount of dry and degassed DCM and transferred into the flask containing the catalyst. The obtained solution was then transferred into the reaction flask containing DOTA-allyl-amide **52**. The blue mixture was heated to reflux (Table 3.1, entry 1). After 2 hours the formation of a precipitate was observed. The mixture was stirred at reflux for 15 hours and then filtered. The recovered solid (~40% w/w with respect to the starting materials) was checked by NMR spectroscopy, but no useful information was deduced because of the too low signal-to-noise ratio due to the low concentration of the sample and the broadness of the peaks. The analysis of the filtrate showed that it contained a by-product whose NMR set of signals suggested a structure similar to the starting material, but with no evidence that any polymerisation had taken place. Instead, a differentiation of the ring and acetyl protons was observed.

The reaction was repeated (Table 3.1, entry 2) by using a two-fold amount of catalyst (0.10 molar equivalents per C-C double bond) in order to improve the conversion. Following a slightly different protocol, the catalyst and benzoquinone were weighed separately, the additive was dissolved in the minimum amount of dry and degassed DCM and the yellow solution was transferred into the flask containing the substrate. The colour of the solution became blue. This apparent evidence of reactivity was investigated later. The red-brown solution of the Grubbs catalyst in DCM was added, and the mixture was refluxed for 15 hours. The solid which precipitated was filtered with a cannula and washed several times with DCM until the solution was colourless. The amount of solid was slightly higher than the used quantity of catalyst. $^{1}H$ and $^{13}C$ NMR spectra of the insoluble residue were recorded, but the complex series of signals did not include the resonances expected for the desired product. $^{1}H$ NMR analysis of the filtrate showed that it contained a by-product with an NMR profile similar to the substrate, but no evidence of polymeric products was obtained. The differentiation previously observed for ring and acetyl protons was again evident. In the $^{13}C$ NMR spectrum multiple peaks for ring and acetyl carbon atoms were also observed, as well as a weak signal at 122.1 ppm that might suggest the formation of some internal alkenes. However, isomerisation of the allyl moieties can be excluded since no peaks were observed in both $^{1}H$ and $^{13}C$ NMR spectra that could be assigned to methyl groups. As a confirmation, no molecular fragment was detected by $ESI^{+}$ MS that could

be assigned to polymeric or oligomeric products; only a series of peaks below 600 m/z were recorded, among which those surely assignable (561, 519, 480, 463, 366 m/z) were related with the structure of **52**. If metathesis reactions had actually taken place, the conversion must have been very low according to the intensity of the signal at 122.1 ppm, and an estimate was not possible because no suitable resonance was identified in the $^{1}$H NMR spectrum.

Tests of reactivity between DOTA-amide **52** and the benzoquinone were carried out following the unexpected change in colour obtained when mixing the two species in the absence of catalyst. It is reported in the literature that primary, secondary and even tertiary amines can react with benzoquinones through radical processes,[440-443] yielding addition products and possibly the quinone's anion that would deactivate the catalyst. Herein, if some of the nitrogen atoms of the ring had reacted with the benzoquinone, there would be ring and acetyl protons next to a quaternary ammonium ion, and other ring and acetyl protons still bound to a tertiary amine. The obtained NMR data were consistent with this, showing that the DOTA-derivative had reacted in a way involving (at least from a spectroscopic point of view) the methylene groups directly bound to the nitrogen atoms of the ring but leaving the C-C double bonds unreacted (Figure 3.3).

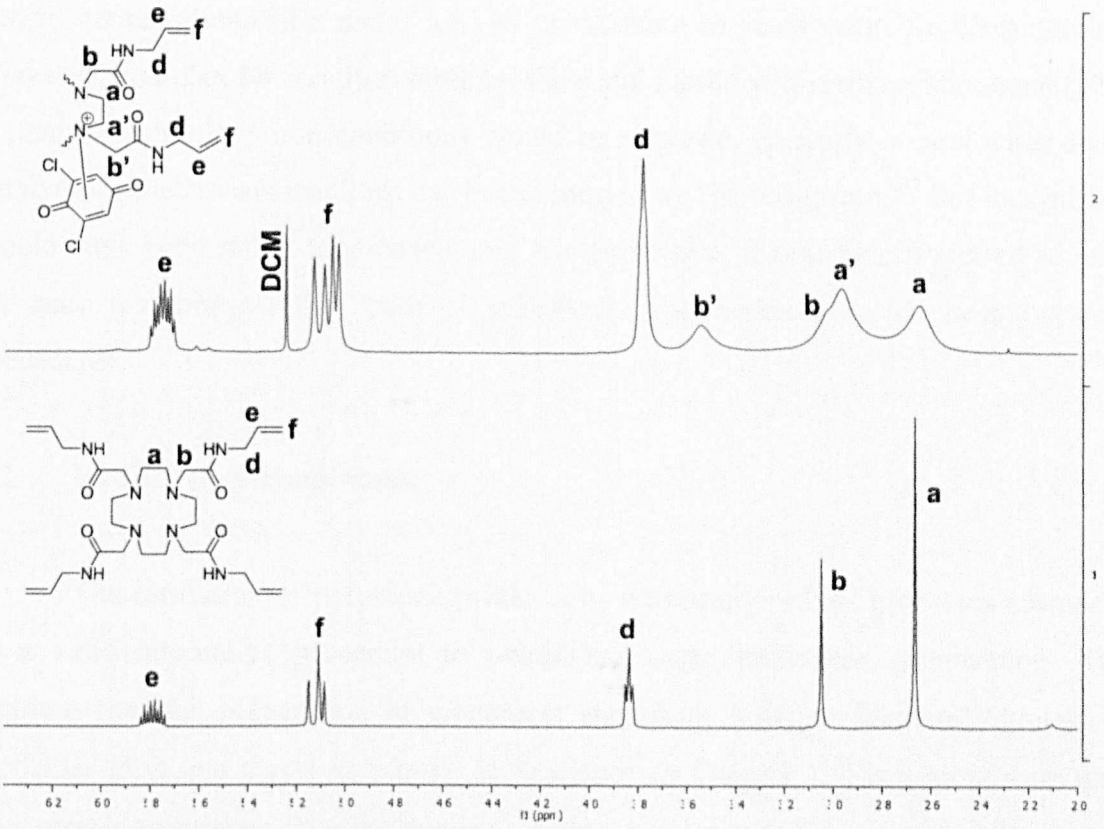



**Figure 3.3** Comparison between the same regions of the $^1$H NMR spectra recorded (in $CDCl_3$) for DOTA-tetra-allyl-amide **52** (bottom) and after mixing it with 2,6-dichloro-1,4-benzoquinone (top). The top structure represents schematically the product (compatible with the NMR analysis) from the hypothesised reaction between **52** and dichlorobenzoquinone.

The peaks for the ring and acetyl protons had split. Broad signals were observed at 2.67, ~3.0 and 3.57 ppm (the second one as a contribution of two peaks), and the integration of such signals was that expected for the ring and acetyl protons. Besides the separation of the doublets due to the vinyl methylene protons (Figure 3.3), a slight differentiation was also observed for the amide and the benzoquinone hydrogen atoms. By integration of the signals that had split, it was possible to determine that the differentiation involved about half of the total sites, consistently with the amount of additive used (2 molar equivalents with respect to a tetra-functionalised substrate).

Looking for alternative procedures, many different additives to suppress isomerisation and consequent loss of reactivity of C-C double bonds towards the metathesis reaction were taken into consideration, such as phosphine oxides,[444] acetic acid,[444] phenols,[445] iron(II)- and tin(II)-halides,[446] phosphoesters and phosphoric acids.[433] Unfortunately, negative drawbacks were found for all of them, mainly dealing with incompatibility towards the structure of amide **52**. A further option was the metathesis reaction carried out with the corresponding Gd-complex **84** (see Chapter 4)

of tetra-amide **52**. In that case the nitrogen atoms of the macrocycle ring would be too "busy" to coordinate the metal ion, so unavailable to react with the benzoquinone. However, complex **84** is only soluble in water and partially in methanol or ethanol, thus a catalyst stable in protic conditions would be required. Recently, a new water-stable catalyst for metathesis reactions has been reported by Grubbs group,[447] but its synthesis would have been rather time-consuming and expensive. It was then preferred to leave (at least temporarily) the route of metathesis polymerisation and focus on other procedures.

## 3.2 Radical polymerisations

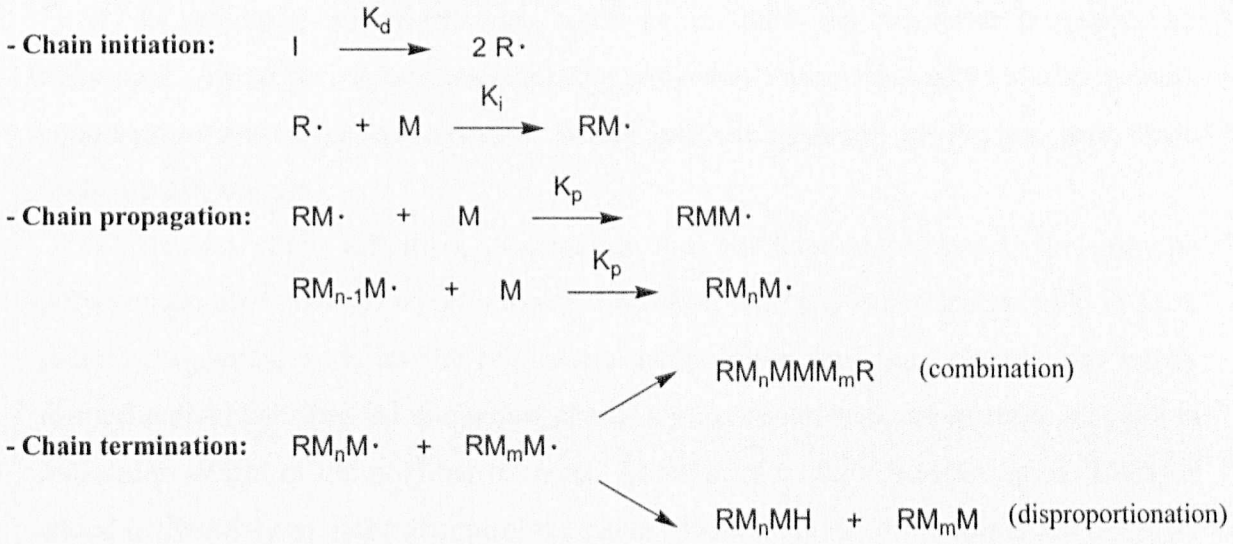
The formation of polymeric products by exploiting radical processes seemed to be a valid alternative procedure to obtain the target molecular architectures. That required first the preparation of monomers containing suitable functional groups (in particular allyl and styryl moieties), as described in Chapter 2. Such monomers were then used in reactions following common protocols relative to this type of synthesis.

### 3.2.1 Overview on radical polymerisations

Radical polymerisations[448, 449] belong to the wider class of *addition polymerisations*,[450] which are thermodynamically favoured ($\pi$-bonds are converted into $\sigma$-bonds) but need to be started. Such reactions are not explosive, as the number of reactive species remains constant.

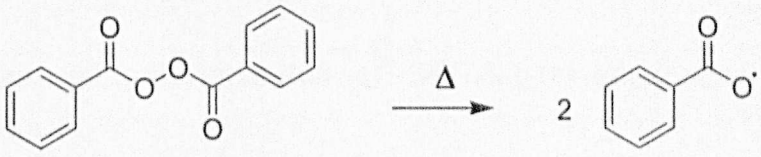
Three steps can be identified in this type of polymerisation (Scheme 3.5):

- initiation;
- propagation;
- termination.

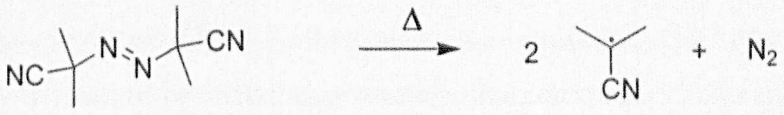



**Scheme 3.5** The three steps of radical polymerisations. A fourth step, *chain transfer*, is also described in the text.

The *chain initiation* is usually achieved by introducing an *initiator*, i.e. a species with a labile atomic bond which can break homolytically, like in the case of peroxides, hydroperoxides, disulfides or azo-groups. Very common initiators for radical polymerisations are benzoyl peroxide and 2,2′-azobis(isobutyronitrile) (AIBN), shown in Scheme 3.6.




**Benzoyl peroxide**




**AIBN**

**Scheme 3.6** Benzoyl peroxide and AIBN, and the free radicals obtained from them by thermal activation.

The initial free radical can then react with the monomer, producing a primary radical (Scheme 3.5, top).

The *chain propagation* is a consequence of the reaction between the primary radical and the monomer, where the product is still a radical that can further react with the monomer with consequent growth of the polymer chain (Scheme 3.5, middle). It is generally assumed that the rate of the reaction between the monomer and any polymer chain is approximately constant, i.e. the radicals reactivity is not affected by their length.

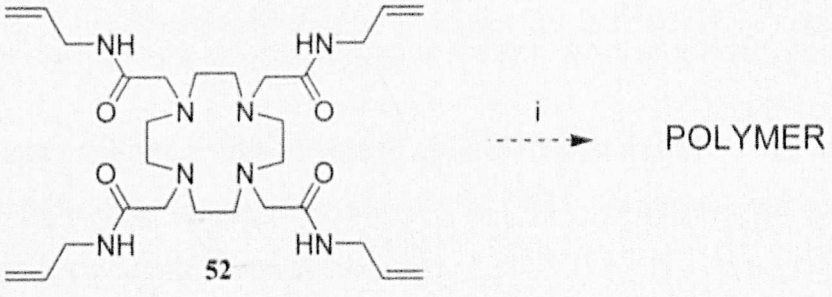
In principle, this mechanism could go on until the monomer is completely consumed. However, *chain termination* processes normally take place, namely *combination* and *disproportionation*, which end the growing of the polymer chain (Scheme 3.5, bottom).

Besides chain initiation, propagation and termination processes, the growing polymer can also undergo a *chain transfer* reaction with any other species able to form radical fragments, such as the monomer, the polymer and the solvent. The newly formed radical can then initiate a new chain. As a consequence, the average length and molecular weight of the polymer decrease. Sometimes a *chain transfer agent* (CTA) is added deliberately in order to control the chain growth and avoid the formation of cross-linked polymers. Very often these agents consist in thiols, such as dodecanethiol or mercaptoethanol, and their transfer constants are much higher than those for the monomer, polymer or solvent. The polymerisation rate is not affected by the presence of a CTA, as the total number of radical species stays unchanged.

The ability of the monomer to polymerise depends on the stability of the radical formed; so, acrylic and styryl monomers polymerise better than allyl species, which in turn are better monomers with respect to vinyl compounds.

### 3.2.2 Attempt of polymerisation of DOTA-tetra-allyl-amide 52 *via* radical reaction

As a first attempt it was tried to polymerise 1,4,7,10-tetrakis(allylcarbamoylmethyl)-1,4,7,10-tetraazacyclo-dodecane **52**, already used in attempts of polymerisation by metathesis reactions (see Section 3.1.2). The substrate (1 molar equivalent) and AIBN (0.2 molar equivalents, 0.05 molar equivalents per C-C double bond) were dissolved in dry chloroform, the solution was degassed and then refluxed for 20 hours (Scheme 3.7).



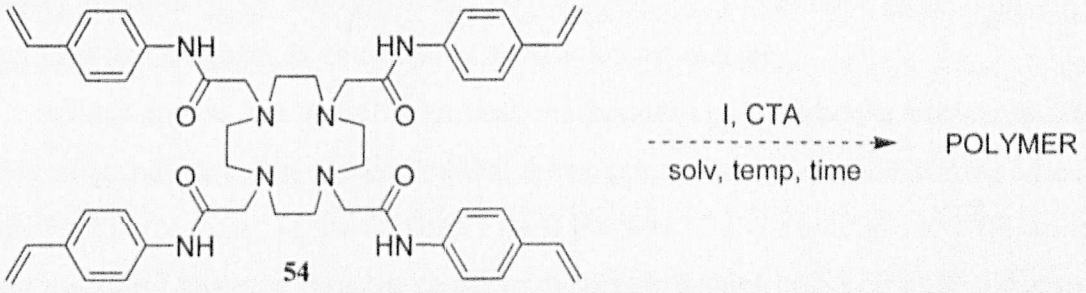

**Scheme 3.7** Attempt of radical polymerisation of DOTA-tetra-allyl-amide **52**. i) **52** (1 mol eq), AIBN (0.2 mol eq), $CHCl_3$, 40 °C, 20 hours.

The yellow solution was then added dropwise at room temperature to a 50-fold excess of methanol, but no precipitation was observed. The solvents were removed under reduced pressure, and the remaining solid residue was analysed by NMR spectroscopy and MS, and shown to consist of unreacted starting material only, which was recovered quantitatively.

This total lack of reactivity was very surprising, as allyl groups have been widely used in radical polymerisation. The only reasonable explanation that was found referred to a general deactivation because of steric hindering and/or formation of non-covalent adducts in solution, and it was possibly related to the failed formation of polymeric products from **52** *via* metathesis as described in Section 3.1.2: the low or no reactivity of the allyl moieties of **52** might allow the ring nitrogen atoms reacting with the isomerisation inhibitor. Following this unexpected outcome and in the absence of a clear rationale behind it, it was preferred to use different substrates.

### 3.2.3 Polymerisation of 1,4,7,10-tetrakis(2-styrylcarbamoylmethyl)-1,4,7,10-tetraazacyclododecane 54

Previously synthesised DOTA-tetra-styryl-amide **54** (see Chapter 2) was used as a substrate in attempts of radical polymerisation. As a general procedure (Scheme 3.8) the monomer was reacted in the presence of an initiator, and a chain transfer agent was also added in order to control chain growth and especially limit cross-linking (expected to be very likely in this case, being the substrate a tetra-functionalised monomer).




**Scheme 3.8** General procedure for the attempts of polymerising DOTA-tetra-styryl-amide **54** through radical reactions. Conditions and results are reported in Table 3.2 and discussed in the text.

Different conditions such as type of solvent, temperature and reaction time were applied, also depending on the reactants in use. Those conditions are summarised in Table 3.2, together with the reaction outcomes.

**Table 3.2** Reaction conditions and outcomes for the attempts of polymerisation of DOTA-tetra-styryl-amide **54** *via* radical procedures, as shown in Scheme 3.8.

| | **Initiator (mol eq)** | **CTA[a] (mol eq)** | **Solvent (w/w% sltn)** | **Temp Time** | **Results** |
|---|---|---|---|---|---|
| 1 | AIBN (0.02) | ME (2) | DMF (20%) | 80 °C 24 h | Solid precipitated in THF (4%). No polymer detected by GPC. |
| 2 | AIBN (0.02) | ME (1) | DMF (20%) | 80 °C 24 h | Solid precipitated in THF (50%). No polymer detected by GPC. |
| 3 | AIBN (0.04) | ME (1) | DMF (20%) | 80 °C 24 h | Formation of a gel. |
| 4 | AIBN (0.02) | ME (1) | THF (20%) | 50 °C 24 h | Monomer partially insoluble. No further precipitation. No polymer detected by GPC. |
| 5 | AIBN (0.02) | DT (1) | THF (9%) | 50 °C 48 h | Monomer dissolved completely. Formation of a gel. |
| 6 | AIBN (0.04) | ME (2) | DMF (20%) | 80 °C 24 h | Solid precipitated in THF (13%). No polymer detected by GPC. |
| 7 | AIBN (0.04) | DT (2) | DMF (20%) | 80 °C 24 h | No precipitation in THF. No polymer detected by GPC. |
| 8 | AIBN (0.06) | ME (2) | DMF (20%) | 80 °C 24 h | Solid precipitated in THF (34%). No polymer detected by GPC. |

[a] ME = 2-mercaptoethanol, DT = dodecanethiol

After stirring for 24 hours, the reaction solutions in DMF were added dropwise to a 30-fold excess of THF. When precipitation occurred (Table 3.2, entries 1, 2, 6 and 8) the suspension was centrifugated and separated. The residues and the solutions were then analysed for polymeric products by GPC, always leading to negative responses. Only in two cases (when a relatively low amount of CTA was used; Table 3.2, entries 3 and 5) a gel formed, which was insoluble in a wide range of solvents (aqueous hydrochloric acid, water, DMSO, DMF, methanol, ethanol, isopropanol, ethyl acetate, acetonitrile, acetone, chloroform, DCM, dimethoxyethane, diethyl ether, chlorobenzene, toluene, hexane) even after stirring for 15 hours or continuous extraction. It was concluded that the product consisted of a cross-linked species.

Since it was not possible to find the conditions to obtain a non-cross-linked polymeric product, it was considered that the structure of DOTA-styryl-amide **54** might influence the reactivity of the monomer itself because of electronic and sterical reasons, being the styryl moieties directly bound to the amide groups and then quite close to the macrocycle ring. With this in mind, substrates with a modified structure were designed and prepared (see Chapter 2) and then applied in radical polymerisation processes.

### 3.2.4 Polymerisation of 1,4,7,10-tetrakis(ethoxycarbonylmethyl)-1,4,7,10-tetraazacyclododecane 63

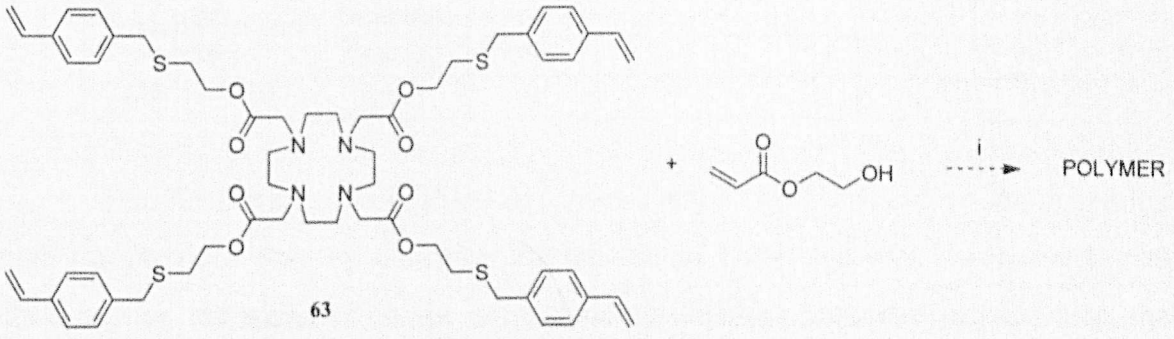
According to a paper by Slark *et al.*[451] hyperbranched co-polymers were synthesised using also a tetra-functional monomer together with methyl methacrylate (MMA) as co-monomer, dodecanethiol as CTA, AIBN as initiator and toluene (which may act as CTA itself, although less efficiently than ME) as solvent.

Following the reported procedure, previously synthesised (see Chapter 2) DOTA-tetra-ester **63** (the tetra-functional monomer herein) was used in polymerisation attempts. Because of solubility reasons and in order to endow the aimed co-polymer with higher hydrophilicity, it was necessary to apply the following modifications to the procedure.

- hydroxyethyl methacrylate (HEMA) instead of MMA as co-monomer;
- 2-mercaptoethanol (ME) instead of dodecanethiol as CTA;
- DMF instead of toluene as solvent.

The differences in chain transfer constants[452-454] were taken into consideration.

It was also necessary to increase the amount of DMF in order to favour the dissolution of **63**, and as a consequence the quantity of CTA had to be reduced according to the respective transfer constants[452-454] in order to counterbalance the chain transfer effect (see Section 3.2.1) by the solvent. The tetra-functional monomer was weighed in a reaction vial, freshly distilled HEMA was added, followed by solutions of AIBN and ME in dry DMF. The total volume of solvent was adjusted by adding the necessary amount of dry DMF, the vial was sealed, the mixture was degassed and then heated to 80 °C (Scheme 3.9).




**Scheme 3.9** General procedure for the attempts of co-polymerisation of DOTA-tetra-ester **63** through radical reaction. Conditions and outcomes are reported in Table 3.3 and discussed in the text.

In the first attempt (Table 3.3, entry 1) a gel quantitatively formed in 3 hours. This gel was stirred for several hours with DMF and then water, afterwards it was

extracted repeatedly with ethanol and acetone. Every time it was checked if some soluble product had passed into solution. Only after washing with DMF and $H_2O$ a little amount of residue was recovered (6.1% and 3.4% respectively compared with the total weight of the co-polymers that had been introduced). Such products did not reveal any polymeric structure after NMR and GPC analyses, and looked more similar to unreacted starting material. No residue was recovered after washing with ethanol and acetone.

**Table 3.3** Reagents and co-reagents ratios, products solubilities and swelling tests results for the attempted co-polymerisation reactions of **63**, as shown in Scheme 3.9. Reaction temperature = 80 °C; reaction time = 3 h.

| | | 1 | 2 | 3 | 4 | 5 |
|---|---|---|---|---|---|---|
| ***63* (mol eq)** | | 1.00 | 1.00 | 1.00 | 1.00 | 1.00 |
| ***HEMA* (mol eq)** | | 4.00 | 4.00 | 4.00 | 4.00 | 4.00 |
| ***AIBN* (mol eq)** | | 0.0244 | 0.0244 | 0.0244 | 0.0244 | 0.0244 |
| ***ME* (mol eq)** | | 0.04 | 0.04 | 0.013 | 0.06 | 0.10 |
| ***DMF* (mol eq)** | | 88 | 29 | 88 | 88 | 88 |
| **Result** | | Gel | Gel | Gel | Gel | Gel |
| **Insoluble residue in $H_2O$ (50 °C, 15 h)** | **Solubility** | No | - | - | No | No |
| | **Swelling** | No | - | - | No | No |
| | **Other** | - | - | - | - | - |
| **Insoluble residue in 1 M HCl (50 °C, 15 h)** | **Solubility** | No | - | - | No | No |
| | **Swelling** | No | - | - | No | No |
| | **Other** | Solid became brown | - | - | Solid became brown | Solid became brown |
| **Insoluble residue in NMP (50 °C, 15 h)** | **Solubility** | No | - | - | No | No |
| | **Swelling** | Yes | - | - | Yes | Yes |
| | **Other** | Yellow liquid phase | - | - | Yellow liquid phase | Yellow liquid phase |
| **Insoluble residue in IPA (50 °C, 15 h)** | **Solubility** | No | - | - | No | No |
| | **Swelling** | Yes | - | - | Yes | Yes |
| | **Other** | - | - | - | - | - |

Two further attempts (Table 3.3, entries 2 and 3) were also carried out in parallel with the previous one, by changing the amount of DMF and ME, respectively, and checking for the variation in the corresponding obtained products. In particular, the CTA was decreased in order to favour the formation of structures with high molecular weight. As it was expected after the outcome from the first reaction, gels were obtained also in these cases, which were treated as described above for the first attempt leading to

analogous results (~90% w/w gel with no trend *vs.* reactants modifications, the rest just unreacted starting material).

With the aim of avoiding or at least reducing the cross-linking degree, two more experiments were carried out with higher amounts of CTA, respectively 1.5 (Table 3.3 above, entry 4) and 2.5 (Table 3.3 above, entry 5) times. However, the results were very similar to those obtained in the previous three attempts, with a maximum of residue recovered after washing with DMF and a minimum recovered from water obtained for the last attempt (8.9% and 2.7%, respectively).

Solubility and swelling tests were carried out on the gels obtained from the first, the fourth and the fifth attempts, by stirring a small amount (2-3 mg) of each gel in 3 ml of a certain solvent for several hours at 50 °C. The used solvents were water (for swelling test), aqueous hydrochloric acid, NMP and IPA, chosen for their polarity or their ability to break possible intermolecular interactions. The results of such tests are shown in Table 3.3 above. The residues resulted to be insoluble in all tried solvents, leading to the conclusion that cross-linking had taken place.

### 3.2.5 Conclusions about radical polymerisation with tetra-styryl monomers

The reactions described in Sections 3.2.3 and 3.2.4 and involving the use of $A_4$ monomers with styryl groups as polymerisable units seem to suggest that, when the applied conditions allow such substrates to react, cross-linking always takes place of a remarkable rate. As described in those sections, when a polymerisation took place gels formed almost quantitatively, the remaining material being just unreacted reagents. Attempts to tune the amount of initiator, chain transfer agent and solvent in order to avoid or at least reduce the cross-linking rate but still obtaining polymeric products were all unsuccessful. That seems to be the consequence of the combination of the generally high reactivity of the styryl group itself towards radical reactions (unless proper inhibiting conditions are used), with the fact that $A_4$ monomers are intrinsically prone to cross-linking because of their structure (in effect, their application for the formation of branched polymers is rather rare in the literature). Since the problem appeared to lay with the $A_4$ monomer, it was considered not helpful to try different co-monomers. For this reason the radical polymerisation route was abandoned, and different procedures were looked for with monomers bearing less reactive moieties,

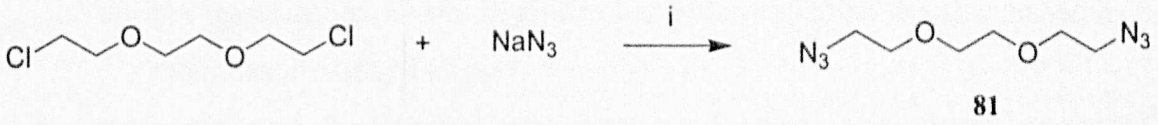
easier to handle, and by following procedures allowing (at least in theory) for more control on the characteristics of the product.

See also the Conclusions section (Chapter 5) at the end of the thesis.

## 3.3 Polymerisation *via* cycloaddition reactions

A big effort was spent in trying to produce polymers through cycloaddition reactions between alkynes and azides, either in the presence of copper(I) as catalyst ("click chemistry") or by thermal activation. For an overview about click chemistry see Section 2.3.1.

As a co-monomer 1,2-bis(2-azidoethoxy)ethane **81** was chosen, because of its relative hydrophilicity that should improve solubility in water and access of water molecules to the metal centres of the corresponding Gd-contrast agent, once formed. Diazide **81** was prepared from commercially available 1,2-bis(2-chloroethoxy)ethane and sodium azide. In a first attempt, 3 molar equivalents of $NaN_3$ were used (by following the procedure applied in Section 2.3.2 for the synthesis of mono-azide **64** and adapted to the double substitution required in this case), but a mixture of mono- and di-substituted products was obtained, which was difficult to separate. The dichloro-compound was then reacted with a much larger excess (20 molar equivalents) of sodium azide in DMF (Scheme 3.10).




**81**

**Scheme 3.10** Synthesis of co-monomer 1,2-bis(2-azidoethoxy)ethane **81**. i) 1,2-bis(chloroethoxy)ethane (1 mol eq), $NaN_3$ (20 mol eq), DMF, 60 °C, 15 h, 91%.

In this case no formation of by-products was observed and the desired compound was obtained pure after chromatography in 91% yield.

This compound was then used for all successive polymerisation reactions *via* cycloaddition (either $Cu^I$-mediated or thermal).

In order to obtain a hyperbranched polymer, a formula reported in a patent by Dvornic *et al.*[455] was used to calculate the ratio between tetra-propargyl-derivative and diazide. Under some assumptions, it is possible to select the ratio $r$ of A- to B-groups so to achieve complete conversion of the minor component without gelation (cross-linking) if:

$$\frac{1}{(x-1)(y-1)} \geq r \geq (x-1)(y-1) \qquad \textbf{(3.1)}$$

where $x$ is the number of A-groups in either co-monomer and $y$ is the number of B-groups in the other. In our case being $x = 4$ and $y = 2$ ($A_4 + B_2$ system), the previous formula gives:

$$\frac{1}{3} \geq r \geq 3 \qquad \textbf{(3.2)}$$

That means the ratio between triple bonds and azide groups has to be higher than 3 or lower than 0.33 in order to obtain a hyperbranched polymer.

It is preferred that the polymer have alkynes as terminal groups, so that they can be used to calculate the degree of branching by NMR spectroscopy; triple bonds can also be exploited for further functionalisation. That implies a value of $r$ higher than 3 has to be chosen. As a consequence:

$$r = \frac{\text{A}-\text{groups}}{\text{B}-\text{groups}} = \frac{\text{C}\equiv\text{C}}{\text{N}_3} \geq 3 \Rightarrow \frac{4 \cdot N_A \cdot \text{mol}_{A_4}}{2 \cdot N_A \cdot \text{mol}_{B_2}} \geq 3 \Rightarrow \frac{\text{mol}_{A_4}}{\text{mol}_{B_2}} \geq \frac{3}{2} \Rightarrow$$

$$\Rightarrow \quad \text{mol}_{A_4} \geq 1.5 \cdot \text{mol}_{B_2} \qquad \textbf{(3.3)}$$

The assumptions under which Dvornic's model is applicable are:

1) A-groups react only with B-groups and vice versa;
2) cyclisation reactions do not take place;
3) the reactivity of A- and B-groups is not dependent on the size and shape of the molecules they belong to.

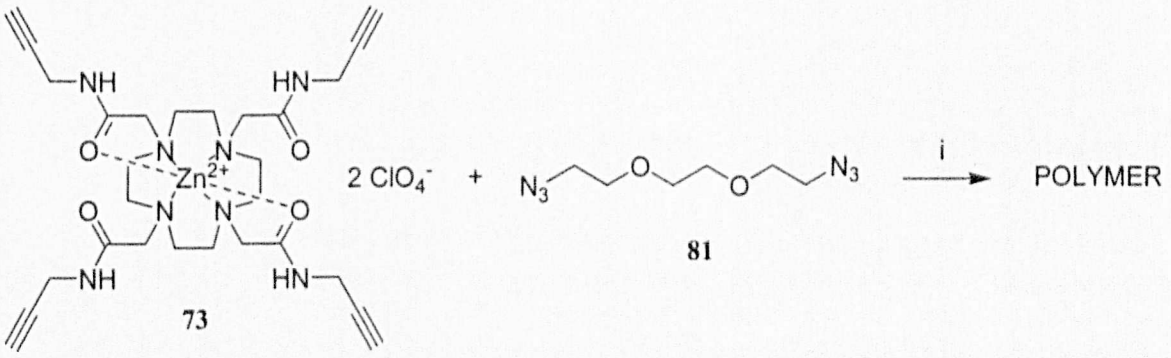
Assumption n°. 2 was initially taken for valid, although the formation of cyclic di-triazole structures might be possible. This issue is discussed furter in Section 3.3.5 below.

### 3.3.1 "Click chemistry" with Zn-complex 73

As reported in Section 2.3.3, the synthesis of zinc(II)-complex **73** from DOTA-tetra-propargyl-amide **53** was successfully carried out, in order to use such a compound in attempts of forming further monomers and as a co-monomer for polymerisations *via* click chemistry. As mentioned in Section 2.3.3, the Cd-complex of **53** has been prepared by other people[407] as an alternative to zinc for the same purpose, with analogous results. A procedure reported in a paper by Maumela *et al.*[406] was applied

(being successful for the preparation of a similar Zn-DOTA-derivative) and led to **73**, which was fully characterised. Polymerisation experiments were then carried out by using Zn-complex **73** and diazide **81** as co-monomers.

Since according to the calculations above the moles of DOTA-tetra-propargyl-amide have to be at least 1.5 times the moles of diazide to avoid cross-linking and obtain polymers with alkynes as terminal groups, molar ratios of 2:1, 3:1, 5:1 7:1 and 10:1 were initially chosen to run preliminary polymerisation experiments. For all of them the same procedure and reaction conditions were applied, which gave high yields or the highest conversion rates in the cycloaddition reactions reported in Sections 2.3.2 and 2.3.3: **73** (1 molar equivalent) and **81** were dissolved in DMF, the mixtures were degassed and copper(II) sulphate (10 mol% per azide moiety) and sodium ascorbate (20 mol% per azide moiety) were added. The mixtures were stirred at 50 °C for 14 hours. A general representation of these reactions is shown in Scheme 3.11.




**Scheme 3.11** General procedure for click chemistry polymerisations between Zn-complex **73** and diazide **81**. Reaction conditions and results for the most promising molar ratios are reported in Table 3.4 and discussed in the text.

In all cases yellow opalescent mixtures were obtained, which were evaporated under reduced pressure and analysed first by GPC to determine immediately if polymeric products had formed.

At first, just DMF was used as eluent, and the eluograms showed peaks at short retention times, thus apparently suggesting the presence of high-molecular weight polymeric species. However, there was no trend in the $M_w$ values *versus* the co-monomers ratio. Furthermore, the peaks showed atypical shapes. Finally, no polymer was isolated by dialysis. All these factors prompted us to investigate whether the use of a different eluting system would bring different results from the GPC analyses. As mentioned in Section 2.2.4.1, when a mixture of triethylamine (1%) and glacial acetic acid (1%) in DMF was used as eluting system,[348, 349] the eluograms of the same samples did not show any longer the peaks at retention times corresponding to polymeric

compounds. In fact, only starting materials and sometimes small oligomers were detected. That confirmed the tendency (also observed for compound **63**, Section 2.2.4.1) to form non-covalent aggregates through intermolecular interactions favoured by the presence of H-bond donors and acceptors, dipolar moieties, π-systems etc.

As mentioned above, when the polar DMF eluting system (from now on indicated just as "DMF") was used, no polymeric product was detected and the only peak corresponded to a molecular weight of about 1.3 kDa which can be assigned to the Zn-complex, in accordance to what was measured for a solution containing the substrate only. Analysis by NMR spectroscopy confirmed the absence of triazole rings and the presence of unreacted starting materials. The same response was obtained from MS.

The reaction was then run with [**73**]/[**81**] ratios of 1.75:1, 1.5:1, and (beyond the gelation-limit) at 1:1, 1:2, 1:4 and 1:6. Although no polymer was detected for the 1.75:1 and 1:6 reactions, partially positive results from the preliminary analysis were obtained for the other experiments, which were then run again in larger scale and worked up and analysed more thoroughly. All mixtures were filtered from DMF. The solid residues were tested for solubility in other solvents (especially water and aqueous TFA) and analysed when possible by aqueous GPC (0.3 M $NaNO_3$ + 0.01 M $NaH_2PO_4$, pH 3) and NMR spectroscopy. The residues from the filtrates were analysed by DMF-GPC and aqueous GPC, when possible, and also by NMR spectroscopy. The relative results are reported in Table 3.4.

**Table 3.4** Reaction conditions and characterisation data for the products of the click chemistry polymerisation between Zn-complex **73** ($A_4$) and diazide **81** ($B_2$). $CuSO_4 \cdot 5H_2O$ (10 mol% per functional group not in excess), Na-ascorbate (20 mol% per functional group not in excess), DMF, 50 °C, 14 h. The data are discussed in the text.

| | $[A_4]/[B_2]$ $(n_{\equiv}/n_{N3})$ | 1.5:1 (3:1) | | 1:1 (2:1) | | 1:2 (1:1) | | 1:4 (1:2) | | |
|---|---|---|---|---|---|---|---|---|---|---|
| *Filtrate from DMF* | *w%* | 91% | | 87% | | 76% | | 82% | | |
| | *Solubility[a] in $H_2O$* | P | | P | | Y | | Y | | |
| | *Solubility[a] in 0.1% TFA* | P | | P | | Y | | Y | | |
| | *Content (by NMR)* | Unknown (with triazole) | | Unknown (with triazole) | | Unknown (with triazole) | | Unknown (with triazole) | | |
| | *1,4-/1,5-[b]* | 100:0 | | 100:0 | | 100:0 | | 100:0 | | |
| | *Tr-H / ≡-H[c]* | N/A[d] | | N/A[d] | | N/A[d] | | N/A[d] | | |
| | *$M_p$ (kDa)* | 1.3 | 1.0 | 1.3 | 1.0 | 1.5 | 1.3 | 2.1 | 1.5 | 1.2 |
| | *$M_n$ (kDa)* | 1.3 | 0.9 | 1.3 | 0.9 | 1.6 | 1.1 | 2.2 | 1.6 | 1.1 |
| | *$M_w$ (kDa)* | 1.3 | 0.9 | 1.3 | 0.9 | 1.7 | 1.2 | 2.3 | 1.6 | 1.1 |
| | *$M_w/M_n$* | 1.01 | 1.02 | 1.01 | 1.03 | 1.02 | 1.02 | 1.02 | 1.01 | 1.02 |
| | *% area* | 64.2 | 35.8 | 52.1 | 47.9 | 63.5 | 36.5 | 25.5 | 43.1 | 31.4 |
| *Insoluble residue from DMF* | *w%* | 9% | | 13% | | 24% | | 18% | | |
| | *Solubility in $H_2O$* | Y | | Y | | Y | | Y | | |
| | *Solubility in 0.1% TFA* | Y | | Y | | Y | | Y | | |
| | *Content (by NMR)* | None organic | | None organic | | Na-ASC | | None organic | | |
| | *1,4-/1,5-[b]* | - | | - | | - | | - | | |
| | *Tr-H / ≡-H[c]* | - | | - | | - | | - | | |
| | *$M_p$[e] (kDa)* | N/A[f] | | N/A[f] | | N/A[f] | | N/A[f] | | |

a) Y = soluble; P = partially soluble; N = insoluble
b) Estimated by comparing the integrations of the triazole protons NMR peaks
c) Estimated by comparing the integrations of the NMR peaks due to triazole protons and terminal alkyne protons
d) Not possible to calculate because of the overlapping resonances that can not be deconvoluted with any certainty
e) The aqueous GPC analysis service Company did not provide results for $M_n$, $M_w$, PD and %area
f) No refractive index detector response

According to NMR, the solid residues did not contain unreacted co-monomers or polymeric products. The high signal-to-noise ratios and the absence of clear resonances led to the conclusion that the residues mainly consisted of inorganic salts. In one case only sodium ascorbate was detected. This conclusion was confirmed by the

results obtained from GPC analysis in $H_2O$ (no peak recorded in the eluogram that could be assigned to **73** or species with similar/higher MW).

The DMF-GPC analysis (refractive index traces supported by differential pressure) of the residues from the filtered fractions showed small differences with respect to the eluogram recorded for Zn-complex **73** (Figure 3.4 and Table 3.4). The peak at ~1.0 kDa remains basically constant (in terms of retention time) in all eluograms. The only significant difference can be observed for **$ZnC_{1:4}$**, where the peak at lower retention time corresponds to a calculated $M_w$ about double with respect to the substrate (2.3 *vs.* 1.3 kDa).

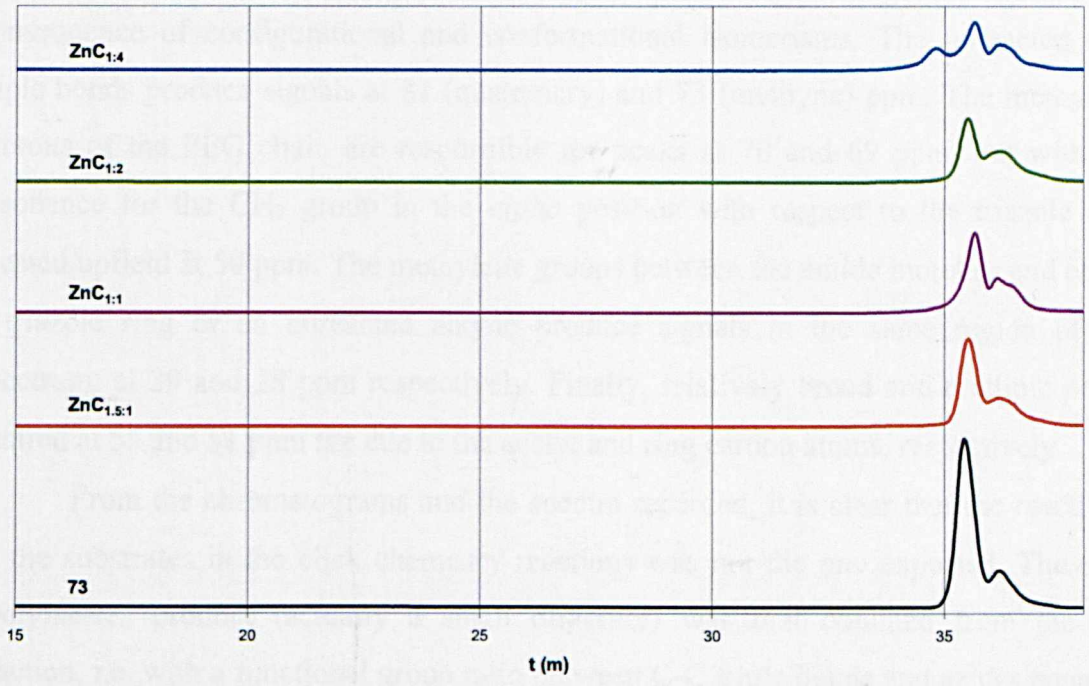



**Figure 3.4** Comparison between the RI traces (DMF, 1% $Et_3N$, 1% AcOH) relative to click chemistry reactions with [**73**]/[**81**] ratios of (from top) 1:4, 1:2, 1:1, 1.5:1, and Zn-complex **73** itself (bottom).

That led to the conclusion that some short oligomers had formed, instead of the target high-molecular weight polymers. The NMR spectra recorded for the DMF-soluble products confirmed the formation of some triazole rings, whose resonances produced signals at 7.9 and 7.8 ppm: this was due to the presence of different conformers and also a consequence of the co-existence of amide groups in *trans* and *cis* configurations, as established by the observation of multiple signals centred at 9.2 ppm and assigned to non-equivalent amide protons (for a discussion about the effect of *cis*/*trans* conformational equilibria on NMR spectra, see Section 2.3.3). The methylene group directly bound to the *N1* of the triazole ring produces a peak at 4.5 ppm, whilst the $CH_2$ between the amide group and the triazole is responsible for a signal at 4.2 ppm.

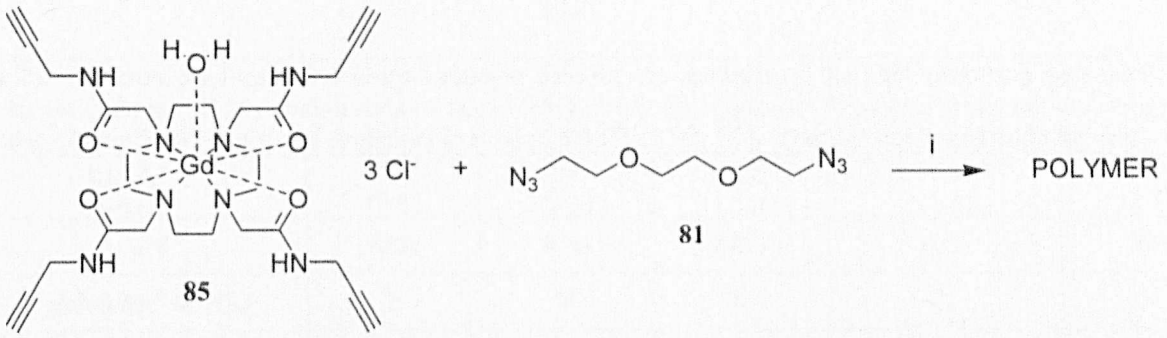
The methylene protons in the *beta* position with respect to the triazole ring give a peak at 3.7 ppm, and the resonances centred at 3.4 ppm are due to the rest of the PEG chain protons. The unreacted propargyl groups produce two peaks at 4.4 (methylene) and 3.3 (methyne) ppm. Finally, the acetyl and ring protons are responsible for signals at 3.7 and 3.0-2.6 ppm respectively. The broadness and overlapping of most signals did not allow an estimate of the conversion rates, but from the peak intensity it was clear that most of the propargyl groups had not reacted, with a minimum of the unreacted/reacted ratio apparently observable for reaction 1:4, in accordance with the results from GPC.

The conclusions above were confirmed by $^{13}C$ NMR, showing multiple peaks for the carbonyl (170-169 ppm) and triazole (144-143 and 124-123 ppm) carbons as a consequence of configurational and conformational isomerisms. The unreacted C-C triple bonds produce signals at 81 (quaternary) and 73 (methyne) ppm. The methylene protons of the PEG chain are responsible for peaks at 70 and 69 ppm, but with the resonance for the $CH_2$ group in the *alpha* position with respect to the triazole ring located upfield at 50 ppm. The methylene groups between the amide moieties and either a triazole ring or an unreacted alkyne produce signals in the same region of the spectrum, at 29 and 28 ppm respectively. Finally, relatively broad and multiple peaks centred at 56 and 51 ppm are due to the acetyl and ring carbon atoms, respectively.

From the chromatograms and the spectra recorded, it is clear that the reactivity of the substrates in the click chemistry reactions was not the one expected. The only "polymeric" product (actually a small oligomer) was that obtained from the 1:4 reaction, i.e. with a functional group ratio between C-C triple bonds and azides equal to 1:2. The excess of the latter leads to a hypothesis of a low availability of the alkynes to react, maybe because of conformational reasons, although more complex explanations can be speculated about, involving the presence of charged species ($Zn^{2+}$ and $ClO_4^-$) and/or the inactivation of the copper-catalyst by multiple coordination from the alkyne or the azide. The low reactivity issue is discussed more thoroughly in Section 3.3.5 below.

### 3.3.2 "Click chemistry" with Gd-complex 85

The same type of procedure was carried out using Gd-complex **85** as a substrate. Preliminary reactions and analyses led to focus on the interval between **[85]**/**[81]** ratios of 1.5:1 and 1:4. The general protocol is shown in Scheme 3.12.




**Scheme 3.12** General procedure for click chemistry polymerisations between Gd-complex **85** and diazide **81**. Reaction conditions and results for the most promising molar ratios are reported in Table 3.5 and discussed in the text.

After 14 hours the reaction mixtures were filtered and both residues and filtrates were checked for solubility in other solvents and analysed by NMR spectroscopy and GPC, as described for the reactions discussed in Section 3.3.1. The analytical data are reported in Table 3.5.

**Table 3.5** Reaction conditions and characterisation data for the products of the click chemistry polymerisations between Gd-complex **85** ($A_4$) and diazide **81** ($B_2$). $CuSO_4 \cdot 5H_2O$ (10 mol% per functional group not in excess), Na-ascorbate (20 mol% per functional group not in excess), DMF, 50 °C, 14 h. The data are discussed in the text.

| | $[A_4]/[B_2]$ ($n_{\equiv}/n_{N3}$) | 1.5:1 (3:1) | | 1:1 (2:1) | | 1:1.33 (1.5:1) | | 1:2 (1:1) | | | 1:4 (1:2) | |
|---|---|---|---|---|---|---|---|---|---|---|---|---|
| *Filtrate from DMF* | *w%* | 38% | | 43% | | 66% | | 63% | | | 76% | |
| | *Solubility[a] in $H_2O$* | P | | N | | N | | N | | | N | |
| | *Solubility[a] in 0.1% TFA* | P | | N | | N | | N | | | N | |
| | *Content (by NMR)* | Not determinable | | Not determinable | | Not determinable | | Not determinable | | | Not determinable | |
| | *1,4-/1,5-[b]* | N/A[d] | | N/A[d] | | N/A[d] | | N/A[d] | | | N/A[d] | |
| | *Tr-H / ≡-H[c]* | N/A[d] | | N/A[d] | | N/A[d] | | N/A[d] | | | N/A[d] | |
| | *$M_p$ (kDa)* | 1.8 | 0.9 | 1.7 | 1.0 | 1.4 | 0.8 | 2.2 | 1.7 | 0.9 | 1.6 | 0.8 |
| | *$M_n$ (kDa)* | 1.8 | 0.9 | 1.8 | 0.9 | 1.6 | 0.7 | 2.3 | 1.6 | 0.9 | 1.6 | 0.8 |
| | *$M_w$ (kDa)* | 1.9 | 1.0 | 1.9 | 1.0 | 1.6 | 0.8 | 2.4 | 1.6 | 0.9 | 1.7 | 0.8 |
| | *$M_w/M_n$* | 1.03 | 1.02 | 1.04 | 1.04 | 1.05 | 1.03 | 1.03 | 1.01 | 1.03 | 1.04 | 1.03 |
| | *% area* | 56.6 | 43.4 | 55.4 | 44.6 | 71.9 | 28.1 | 24.1 | 16.6 | 59.3 | 77.9 | 22.1 |
| *Insoluble residue from DMF* | *w%* | 62% | | 57% | | 34% | | 37% | | | 24% | |
| | *Solubility[a] in $H_2O$* | P | | P | | P | | P | | | P | |
| | *Solubility[a] in 0.1% TFA* | P | | P | | P | | P | | | P | |
| | *Content (by NMR)* | Not determinable | | Not determinable | | Not determinable | | Not determinable | | | Not determinable | |
| | *1,4-/1,5-[b]* | - | | - | | - | | - | | | - | |
| | *Tr-H / ≡-H[c]* | - | | - | | - | | - | | | - | |
| | *$M_p$[e] (kDa)* | N/A[f] | | 3.8 | 2.1 | Not run | | 3.8 | | 2.1 | 3.8 | 2.1 |

a) Y = soluble; P = partially soluble; N = insoluble
b) Estimated by comparing the integrations of the triazole protons NMR peaks
c) Estimated by comparing the integrations of the NMR peaks due to triazole protons and terminal alkyne protons
d) Due to Gd line broadening and the polymeric nature of the products, an estimate is not possible
e) The aqueous GPC analysis service Company did not provide results for $M_n$, $M_w$, PD and %area
f) No refractive index detector response

All residues insoluble in DMF were also insoluble in all other tried solvents (aqueous hydrochloric acid, dimethyl sulfoxide, DMF, NMP, water, methanol, ethanol, isopropanol, ethyl acetate, acetone, DCM, chloroform, diethyl ether, chlorobenzene, toluene, hexane), with the exception of water and aqueous TFA in which the residues were partially soluble. The NMR spectra recorded in $D_2O$ (and then regarding the water-soluble fractions) were affected by line broadening due to the presence of paramagnetic gadolinium(III)[169, 346] and copper(II), and useful information could not be

deduced from their analysis. However, the GPC eluograms in $H_2O$ for **irGdC$_{1:1}$**, **irGdC$_{1:2}$** and **irGdC$_{1:4}$** revealed the presence of oligomers with constant $M_p$ values of 3.8 and 2.1 kDa (Table 3.5).

NMR spectroscopic analysis of the residues from the filtrates was also not possible because of the line broadening effect caused by the paramagnetic environment.[169, 346] The filtered fractions were then analysed by DMF-GPC, and the corresponding RI traces (supported by differential pressure data in the original eluograms) are shown in Figure 3.5.

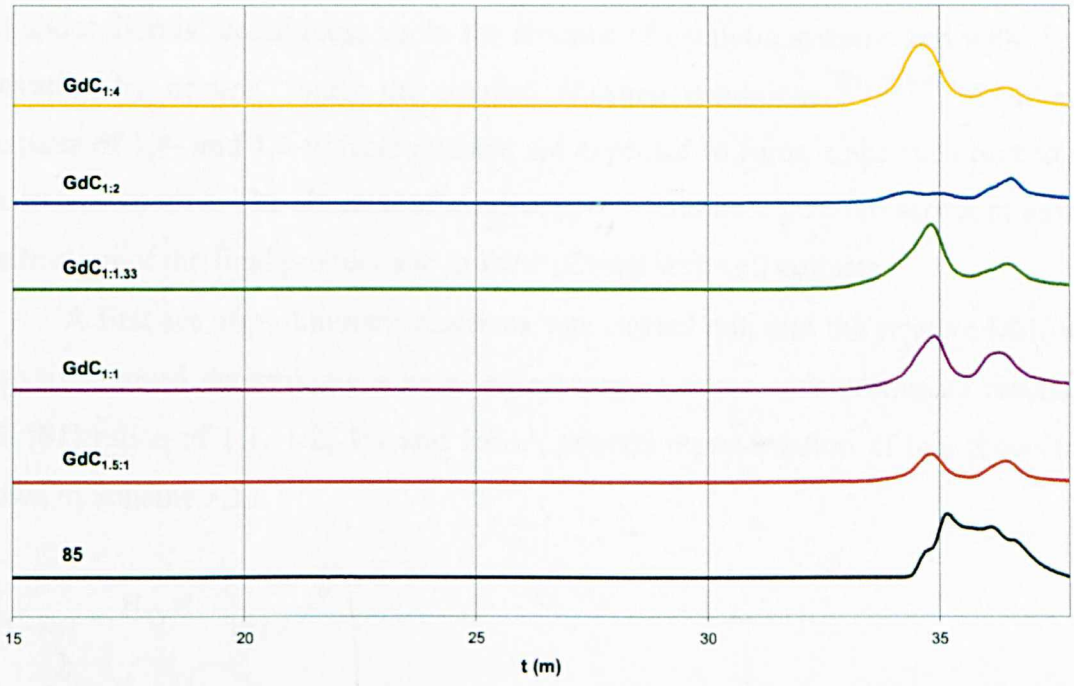



**Figure 3.5** Comparison between the RI traces (DMF, 1% $Et_3N$, 1% AcOH) relative to the click chemistry reactions (filtrates) with [**85**]/[**81**] ratios of (from top) 1:4, 1:2, 1:1.33, 1:1, 1.5:1 and Gd-complex **85** itself (bottom).

Although the measured retention times were shorter than those observed for the Gd-complex, they did not represent a significant improvement with respect to the substrate in terms of $M_w$: the calculated values lay in a range between 1.6 and 2.4 kDa, the highest corresponding, as could be expected, to **GdC$_{1:2}$**, i.e. to the experiment carried out in the presence of equimolar amounts of alkyne and azide functional groups and then more likely to undergo a cross-linking. As mentioned in Section 3.3.1, the peak corresponding to a $M_w$ value of about 1.0 kDa stays constant (in terms of retention time) through the eluograms. The value recorded for compound **85** is 1.2 kDa.

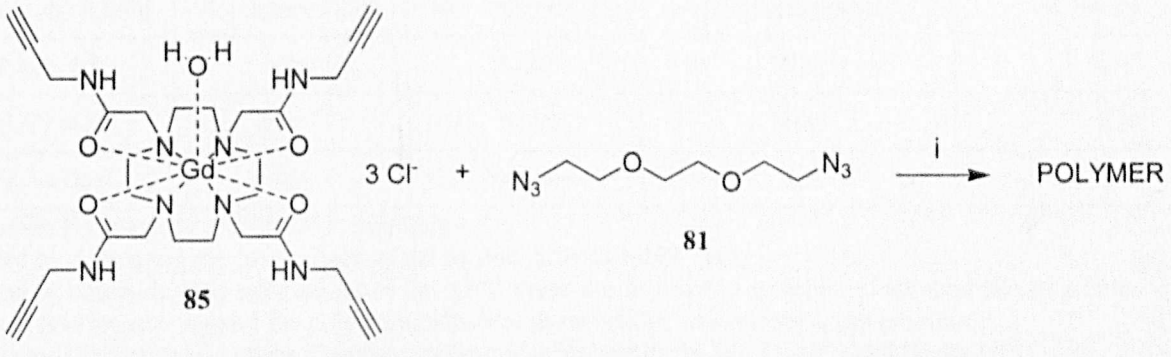
The relatively low $M_w$ values obtained for both the DMF-soluble and the DMF-insoluble products added to those obtained for click chemistry polymerisation experiments with Zn-complex **73** (see Section 3.3.1) reinforced the conclusion that a

problem or a combination of unfavourable factors occurred with those reactions. For a comparison and discussion of the data obtained with different cycloaddition mechanisms see Section 3.3.5 below.

### 3.3.3 Thermal cycloaddition with Gd-complex 85

In order to establish whether the presence of the catalyst had an influence on the results obtained from the click chemistry polymerisations described in Sections 3.3.1 and 3.3.2, cycloaddition reactions between Gd-complex **85** and diazide **81** were carried out under thermal conditions, i.e. in the absence of catalytic systems and with the sole activation by heating, under the original Huisgen conditions.[352, 358-360] That means mixtures of 1,4- and 1,5-triazole isomers are expected to form, since such procedure is not stereoselective. The absence of toxic copper would be a positive aspect in terms of purification of the final product and in view of tests with cell cultures.

A first set of preliminary reactions was carried out, and the relative DMF-GPC analysis allowed determining a range of monomers ratios with promising results, i.e. [**85**]/[**81**] ratios of 1:1, 1:2, 1:4 and 1:6. A general representation of this procedure is shown in Scheme 3.13.




**Scheme 3.13** General procedure for thermal cycloaddition polymerisations between Gd-complex **85** and diazide **81**. Reaction conditions and results for the most promising molar ratios are reported in Table 3.6 and discussed in the text.

After filtering the reaction mixtures, both insoluble residues and filtrates were tested for solubility in other solvents (aqueous hydrochloric acid, dimethyl sulfoxide, DMF, NMP, water, methanol, ethanol, isopropanol, ethyl acetate, acetone, DCM, chloroform, diethyl ether, chlorobenzene, toluene, hexane) and thoroughly analysed by NMR spectroscopy and GPC, as described for the attempts of click chemistry polymerisation discussed in Sections 3.3.1 and 3.3.2. The obtained analytical data are reported in Table 3.6.

**Table 3.6** Reaction conditions and characterisation data for the products of the thermal cycloaddition polymerisation between Gd-complex **85** ($A_4$) and diazide **81** ($B_2$). DMF, 80 °C, 14 h. The data are discussed in the text.

| | $[A_4]/[B_2]$ ($n_{\equiv}/n_{N3}$) | 1:1 (2:1) | | | 1:2 (1:1) | | | 1:4 (1:2) | | | | 1:6 (1:3) | | | |
|---|---|---|---|---|---|---|---|---|---|---|---|---|---|---|---|
| *Filtrate from DMF* | *w%* | 23% | | | 41% | | | 58% | | | | 63% | | | |
| | *Solubility[a] in $H_2O$* | Y | | | P | | | Y | | | | Y | | | |
| | *Solubility[a] in 0.1% TFA* | Y | | | P | | | Y | | | | Y | | | |
| | *Content (by NMR)* | Not determinable | | | Not determinable | | | Not determinable | | | | Not determinable | | | |
| | *1,4-/1,5-[b]* | N/A[d] | | | N/A[d] | | | N/A[d] | | | | N/A[d] | | | |
| | *Tr-H / ≡-H[c]* | N/A[d] | | | N/A[d] | | | N/A[d] | | | | N/A[d] | | | |
| | *$M_p$ (kDa)* | 2.0 | 1.6 | 1.0 | 3.3 | 2.0 | 1.0 | 2.8 | 1.9 | 1.6 | 1.0 | 2.6 | 1.9 | 1.6 | 1.0 |
| | *$M_n$ (kDa)* | 2.1 | 1.6 | 0.9 | 3.2 | 1.8 | 0.9 | 3.1 | 2.0 | 1.5 | 0.9 | 3.0 | 2.0 | 1.5 | 0.9 |
| | *$M_w$ (kDa)* | 2.1 | 1.6 | 1.0 | 3.2 | 1.8 | 0.9 | 3.1 | 2.1 | 1.5 | 0.9 | 3.0 | 2.0 | 1.5 | 0.9 |
| | *$M_w/M_n$* | 1.01 | 1.01 | 1.02 | 1.01 | 1.03 | 1.02 | 1.00 | 1.01 | 1.01 | 1.02 | 1.01 | 1.01 | 1.01 | 1.02 |
| | *% area* | 21.9 | 55.6 | 22.5 | 9.6 | 73.8 | 16.6 | 1.4 | 32.1 | 44.9 | 21.6 | 2.7 | 37.0 | 40.1 | 20.2 |
| *Insoluble residue from DMF* | *w%* | 77% | | | 59% | | | 42% | | | | 37% | | | |
| | *Solubility[a] in $H_2O$* | Y | | | P | | | P | | | | P | | | |
| | *Solubility[a] in 0.1% TFA* | Y | | | P | | | P | | | | P | | | |
| | *Content (by NMR)* | Not determinable | | | Not determinable | | | Not determinable | | | | Not determinable | | | |
| | *1,4-/1,5-[b]* | N/A[d] | | | N/A[d] | | | N/A[d] | | | | N/A[d] | | | |
| | *Tr-H / ≡-H[c]* | N/A[d] | | | N/A[d] | | | N/A[d] | | | | N/A[d] | | | |
| | *$M_p$[e] (kDa)* | 2.1 | | | Not run | | | 2.1 | | | | N/A[f] | | | |

a) Y = soluble; P = partially soluble; N = insoluble
b) Estimated by comparing the integrations of the triazole protons NMR peaks
c) Estimated by comparing the integrations of the NMR peaks due to triazole protons and terminal alkyne protons
d) Due to Gd line broadening and the polymeric nature of the products, an estimate is not possible
e) The aqueous GPC analysis service Company did not provide results for $M_n$, $M_w$, PD and %area
f) No refractive index detector response

All DMF-insoluble residues were only partially soluble in both water and aqueous TFA, apart from **irGdT$_{1:1}$**, which was completely soluble. NMR spectra in $D_2O$ were recorded, but it was not possible to determine the samples content because of the line broadening caused by the presence of paramagnetic gadolinium(III).[169, 346] GPC analysis in $H_2O$ did not show relevant polymeric or oligomeric products (Table 3.6).

All residues from the filtered fractions were soluble in water, with the exception of **GdT$_{1:2}$**, which was only partially soluble both in water and in aqueous TFA. This could be expected since such reaction is the one for which the highest cross-linking rate

would be hypothesised, being the functional groups ratio equal to 1:1. As obtained for the corresponding DMF-insoluble residues and for crude products from click chemistry reactions between the same substrates, also the NMR spectra for these filtrates were useless, as the line broadening[169, 346] was such that no assignment and estimate could be achieved. The residues from the filtered fractions were then analysed by DMF-GPC, showing some interesting results. The RI traces (supported in the chromatograms by differential pressure measurements) are shown in Figure 3.6.

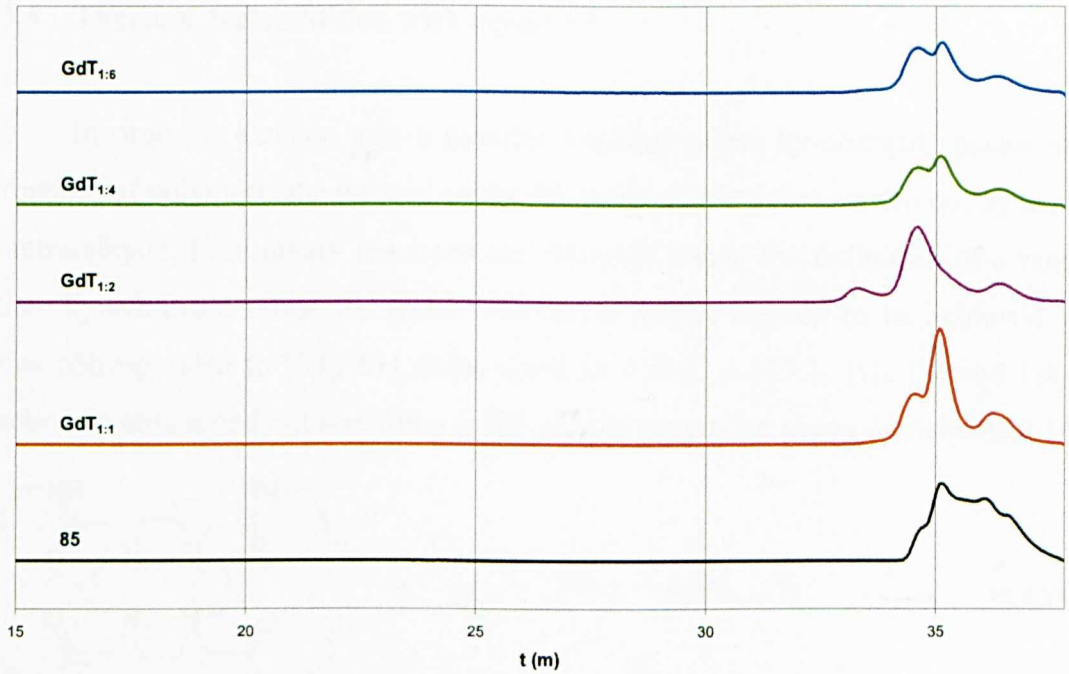


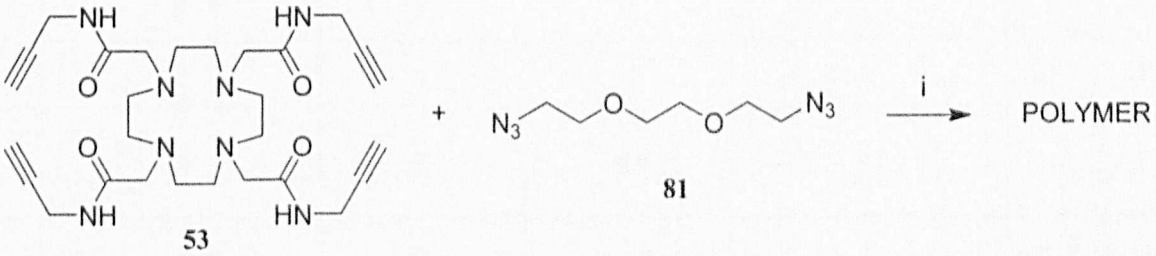

**Figure 3.6** Comparison between the RI traces (DMF, 1% $Et_3N$, 1% AcOH) relative to the filtrates from thermal cycloadditions between **85** and **81** in ratios of (from top) 1:6, 1:4, 1:2, 1:1, and Gd-complex **85** itself (bottom).

With respect to the retention time range recorded for substrate **85**, all products were eluted earlier. The calculated $M_w$ values led in a range between 2.1 and 3.2 kDa (Table 3.6), compared with the 1.2 kDa determined for the Gd-complex. In particular, decreasing the alkyne/azide ratio led to a progressive shifting of the highest $M_w$ peak towards lower retention times with a maximum in separation corresponding to **$GdT_{1:2}$** (i.e. the one obtained with equimolar amounts of alkyne and azide moieties and thus hypothetically more probable to undergo cross-linking). With the **85/81** ratio decreasing further, the first peak shifted back to overlap the ~2.0 kDa peak, which appears basically constant (in terms of retention time) in the different eluograms, as well as the peaks at ~1.5 and ~1.0 kDa.

According to the above analysis, small oligomers instead of high-molecular weight polymeric products were obtained also through this procedure. The relatively higher $M_w$ values suggest that a certain negative effect was avoided by removing the catalytic system from the reaction conditions. Such effect, though, is clearly not the only one responsible for the substantially low polymerisation degree that was achieved also with this procedure. The outcomes are compared and further discussed in Section 3.3.5 below.

### 3.3.4 Thermal cycloaddition with ligand 53

In order to exclude also a possible negative effect by charged species on the formation of polymers, the thermal cycloaddition procedure was carried out by using **53** as tetra-alkyne. Preliminary reactions and analyses led to the definition of a range of tetra-alkyne/diazide ratios for which interesting results seemed to be achieved. Such ratios corresponded to [**53**]/[**81**] ratios equal to 1.33:1, 1.165:1, 1:1, 1:2 and 1:4. The reactions were carried out according to the general procedure shown in Scheme 3.14.




**Scheme 3.14** General procedure for thermal cycloaddition polymerisations between ligand **53** and diazide **81**. Reaction conditions and results for the most promising molar ratios are reported in Table 3.7 and discussed in the text.

After filtration of the reaction mixtures, both DMF-insoluble residues and filtrates were treated as described for the cycloaddition reactions discussed in Sections 3.3.1, 3.3.2 and 3.3.3, i.e. they were tested for solubility in other solvents and thoroughly analysed by NMR spectroscopy and GPC. The obtained data are reported in Table 3.7.

**Table 3.7** Reaction conditions and characterisation data for the products of the thermal cycloaddition polymerisation between ligand **53** ($A_4$) and diazide **81** ($B_2$). DMF, 80 °C, 14 h. The data are discussed in the text.

| | $[A_4]/[B_2]$ ($n_{\equiv}/n_{N3}$) | 1.33:1 (2.66:1) | | | | 1.165:1 (2.33:1) | | | 1:1 (2:1) | | | 1:2 (1:1) | | | | 1:4 (1:2) | | | |
|---|---|---|---|---|---|---|---|---|---|---|---|---|---|---|---|---|---|---|---|
| *Filtrate from DMF* | *w%* | 18% | | | | 25% | | | 30% | | | 36% | | | | 64% | | | |
| | *Solubility[a] in $H_2O$* | Y | | | | Y | | | Y | | | P | | | | Y | | | |
| | *Solubility[a] in 0.1% TFA* | Y | | | | Y | | | Y | | | P | | | | Y | | | |
| | *Content (by NMR)* | **81** + UNKNOWN (with triazole) | | | | **81** + UNKNOWN (with triazole) | | | **81** + UNKNOWN (with triazole) | | | **81** + UNKNOWN (with triazole) | | | | **81** + UNKNOWN (with triazole) | | | |
| | *1,4-/1,5-[b]* | 58 : 42 | | | | 62 : 38 | | | 63 : 37 | | | 62 : 38 | | | | 61:39 | | | |
| | *Tr-H / ≡-H[c]* | 36 : 64 | | | | N/A[d] | | | 47 : 53 | | | 60 : 40 | | | | N/A[d] | | | |
| | *$M_p$ (kDa)* | 3.5 | 2.1 | 1.6 | 1.0 | 3.5 | 1.6 | 1.0 | 3.1 | 1.9 | 1.0 | 3.5 | 2.1 | 1.6 | 1.0 | 3.2 | 2.0 | 1.6 | 1.0 |
| | *$M_n$ (kDa)* | 3.5 | 2.2 | 1.6 | 1.0 | 3.5 | 1.7 | 0.9 | 3.5 | 1.8 | 0.9 | 3.5 | 2.1 | 1.6 | 0.9 | 3.5 | 2.1 | 1.6 | 0.9 |
| | *$M_w$ (kDa)* | 3.5 | 2.2 | 1.6 | 1.0 | 3.5 | 1.7 | 0.9 | 3.6 | 1.9 | 0.9 | 3.6 | 2.2 | 1.6 | 0.9 | 3.6 | 2.2 | 1.6 | 1.0 |
| | *$M_w/M_n$* | 1.02 | 1.01 | 1.01 | 1.01 | 1.02 | 1.02 | 1.01 | 1.04 | 1.02 | 1.02 | 1.02 | 1.01 | 1.01 | 1.01 | 1.03 | 1.01 | 1.01 | 1.01 |
| | *% area* | 9.3 | 19.9 | 65.4 | 5.4 | 16.1 | 78.9 | 5.0 | 5.7 | 87.0 | 7.3 | 11.5 | 41.9 | 41.1 | 5.4 | 9.9 | 30.7 | 50.3 | 9.1 |
| *Insoluble residue from DMF* | *w%* | 82% | | | | 75% | | | 70% | | | 64% | | | | 36% | | | |
| | *Solubility[a] in $H_2O$* | P | | | | P | | | P | | | P | | | | P | | | |
| | *Solubility[a] in 0.1% TFA* | Y | | | | Y | | | Y | | | Y | | | | Y | | | |
| | *Content (by NMR)* | **53** | | | | **53** | | | **53** | | | **53** | | | | **53** | | | |
| | *1,4-/1,5-[b]* | - | | | | - | | | - | | | - | | | | - | | | |
| | *Tr-H / ≡-H[c]* | - | | | | - | | | - | | | - | | | | - | | | |
| | *$M_p$[e] (kDa)* | N/A[f] | | | | N/A[f] | | | 2.1 | | | 2.1 | | | | 2.1 | | | |

a) Y = soluble; P = partially soluble; N = insoluble
b) Estimated by comparing the integrations of the triazole protons NMR peaks
c) Estimated by comparing the integrations of the NMR peaks due to triazole protons and terminal alkyne protons
d) Not possible to calculate because of the overlapping resonances that can not be deconvoluted with any certainty
e) The aqueous GPC analysis service Company did not provide results for $M_n$, $M_w$, PD and %area
f) No refractive index detector response

All residues insoluble in DMF were partially soluble in water but completely soluble in aqueous TFA. This is probably due to the absence of a metal centre forcing the ligand in a certain conformation, so that the structure is free to rearrange in a way allowing the formation of intermolecular interactions (hydrogen bonds, dipolar attractions, etc.) which can be broken in the presence of a strong polar environment. The NMR spectra only showed the sets of signals belonging to tetra-alkyne **53**. GPC analysis in $H_2O$ led to a partial confirmation of the NMR data: no polymeric or

oligomeric species was detected for the DMF-insoluble residues **irLigT**$_{1.33:1}$ and **irLigT**$_{1.165:1}$; an $M_p$ value of 2.1 kDa was instead calculated for **irLigT**$_{1:1}$, **irLigT**$_{1:2}$ and **irLigT**$_{1:4}$, and that was thought to be due to either an oligomeric species not observed by NMR (maybe because of low concentration) or to **53** itself. Actually, $M_p$ values around 2.0 are ubiquitous in the GPC analyses carried out for all products from all experiments (see Tables 3.4-3.7), thus leading to assignment of such peaks to the tetra-propargyl species used respectively in those experiments or to their common derivatives (e.g. dimers).

The residues obtained after evaporation of the filtrates were all soluble in water, except **LigT**$_{1:2}$, which was partially soluble in both water and aqueous trifluoroacetic acid (as also observed for the products from the cycloaddition experiments discussed in Section 3.3.3). Since this molar ratio corresponds to a functional groups ratio equal to 1:1, such a solubility result was expected, as this is the condition for which hypothetically the highest cross-linking rate is predicted (assuming 100% conversion and no reactivity dependencies on molecular weight). By NMR it was observed that both 1,4- and 1,5-triazole isomers had formed, as expected for thermal cycloadditions. The ratio between the two species is about constant at 60:40, in accordance with the fact that the formation of the 1,4-isomer is favoured because of sterical reasons. The conversion of alkyne groups into triazole rings was estimated by comparing the integrations of the peaks produced by the resonances of the triazole protons and the methyne groups. Such conversion reached a maximum with the 1:2 reaction, although the 1:4 experiment (favoured because of statistical reasons) could not be evaluated from this point of view as a consequence of the signals overlapping. The main difference between the $^1$H NMR spectra recorded for products of thermal cycloadditions with respect to what has been observed for click chemistry reactions was the presence of an additional peak at 7.51 ppm, due to the 1,5-triazole isomer[361, 384-387] which formed alongside the 1,4-isomer, responsible for a signal at 7.86 ppm. Integration of the areas of such peaks allowed calculation of the isomers ratio, which stayed approximately constant (at 1,4-/1,5- 60:40) throughout the different reactions as mentioned above. The group of peaks centred at 8.48 ppm is due to the amide protons, as confirmed by their disappearance following addition of deuterium oxide. As mentioned before, such differentiation is caused by conformational and configurational isomerisms.[405] The methylene protons directly bound to the nitrogen atom of the triazole ring produce a signal at 4.47 ppm, while the $CH_2$ group in the *beta* position gives a peak at 3.79 ppm.

The protons of the ethylene fragment between the two oxygen atoms are responsible for a resonance at 3.52 ppm, and the signal from the methylene protons in the *alpha* position with respect to unreacted azide moieties can be found at 3.46 ppm. The $CH_2$ group located between the triazole ring and the amide moiety is responsible for the peak observed at 4.32 ppm. Unreacted propargyl moieties produce peaks at 3.88 (methylene) and 3.07 (methyne) ppm, and integration of such elements followed by comparison with other significant signals allowed estimation of the conversion rate for each reaction. Finally, broad signals centred at 3.0 and 2.6 ppm were observed, due to acetyl and ring protons respectively.

In the $^{13}C$ NMR spectra the main characteristic of note was the presence of two additional signals at 136.9 and 133.2 ppm, produced by the quaternary and the CH carbon atoms of the 1,5-triazole isomer respectively.[361, 384-387]

DMF-GPC analyses (Table 3.7) revealed that the thermal cycloadditions carried out with ligand **53** as substrate afforded the products with the highest $M_w$ values (around 3.5-3.6 kDa in all cases). The relative RI traces are shown in Figure 3.7.

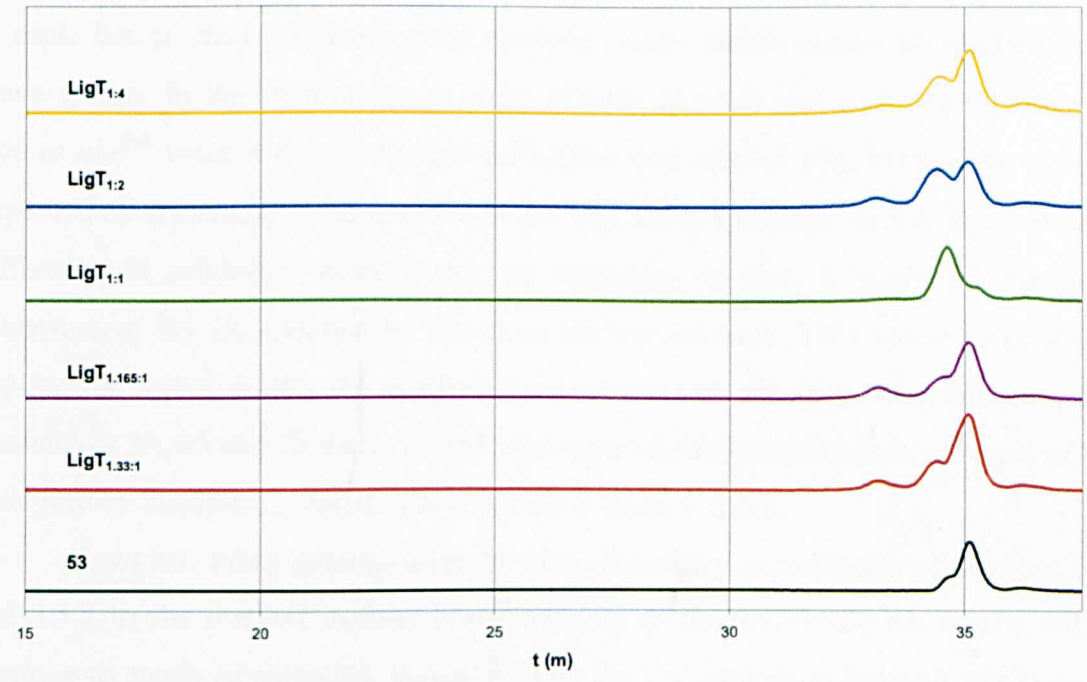



**Figure 3.7** Comparison between the RI traces (DMF, 1% $Et_3N$, 1% AcOH) relative to thermal cycloaddition reactions (filtrates) with [**53**]/[**81**] ratios of (from top) 1:4, 1:2, 1:1, 1.165:1, 1.33:1 and DOTA-tetra-propargyl-amide **53** itself (bottom).

In detail, a well defined peak is clearly observed at relatively low retention times for products **LigT$_{1.33:1}$**, **LigT$_{1.165:1}$**, **LigT$_{1:2}$** and **LigT$_{1:4}$**, while it is detected with only a 5% area percentage for **LigT$_{1:1}$**. For all reactions a peak corresponding to a calculated

2.1 kDa $M_w$ appears rather like a shoulder with respect to the more intense peak corresponding to an Mw of 1.6 kDa, with the exception of the **LigT$_{1:1}$** where the two peaks coalesce into one corresponding to 1.8 kDa. The best result appears to be that achieved from the 1:2 reaction (equimolar functional groups), with the 3.6 kDa product corresponding to 12% of the total and the 2.2 kDa product in 42%. These results are discussed and compared in Section 3.3.5 below.

### 3.3.5 Cycloadditions data comparison

In order to explain the relatively low-molecular weights obtained for the products from the click chemistry reactions described in Sections 3.3.1 and 3.3.2, a saturation phenomenon had been hypothesised. As a consequence of the complexation of $Zn^{II}$ in **73** and $Gd^{III}$ in **85**, the alkyne moieties find themselves close to each other in the upper part of the molecule, and when one of them forms the corresponding copper-acetylide species in the catalytic cycle shown in Scheme 2.33 (Section 2.3.1) this proximity might lead to coordinative saturation of the $Cu^{I}$ atom by the neighbouring C-C triple bonds, thus inactivating the catalytic centre which cannot be reached by the azide groups. In the literature an example of such an event can be found in a paper by Ryu *et al.*:[456] when a tetra-propargyl-calixarene was reacted with azidoacetic acid, the expected click chemistry did not take place. The authors explain such a failure with the difference in solubility between the two reactants; in fact, it might be due to the saturation of the $Cu^{I}$-catalyst by the close alkyne moieties. This seems to be a good explanation also to justify the relatively low conversions obtained when tetra-propargyl derivatives **53**, **85** and **73** were reacted with mono-azide compounds in attempts of $Cu^{I}$-catalysed cycloaddition reactions as reported in Section 2.3.3.

However, when passing from the click chemistry experiments of Sections 3.3.1 and 3.3.2 to the thermal cycloaddition attempts of Section 3.3.3, the results did not improve as much as expected, indicating that the $Cu^{I}$-saturation issue (if any) was not the main problem affecting the reactions under investigation. It was then hypothesised that the presence of charged species ($Gd^{3+}$, $Zn^{2+}$, $Cl^{-}$, $ClO_4^{-}$ ions) might have a general negative effect on the cycloaddition step, both in the copper(I)-catalysed reactions and in the thermal ones. This might be caused by the formation in solution of little aggregates (e.g. dimers, trimers) possibly held together by intermolecular Coulomb forces and with such a structure (possibly similar to an ionic crystal lattice) that access

to the reaction centres results limited. A sort of interference of the charged species with the reaction transition state is another possible explanation for the low reactivity shown by Zn-complex **73** and Gd-complex **85**. On the other hand, it is possible that the conformational restrictions caused by the coordination of the tetra-propargyl-structure to the metal centre ($Zn^{II}$, $Gd^{III}$) affect the availability of the terminal alkynes to react, especially those stretched towards the same side of the ring and then almost facing each other. It is reasonable to imagine that after the transformation of one of them, not enough space remains available to allow the other moieties to react as well. In such a situation it seems even likely to obtain macrocycles by reaction of two complexes and two diazide molecules. The formation of such species might be very difficult to prove on the basis of their size or chemical behaviour or nuclear and bond properties. However, some of the oligomeric species detected by GPC (see Figures 3.4-3.7 and Tables 3.4-3.7) might well belong to such sort of *ansa*-compounds or capsules. The structural restrictions could explain in particular the limited conversion observed when the Gd-complex **85** was used, since all the four arms face the upper side of the tetraazadodecane ring, as shown (for solid state) by the obtained X-ray structure (Section 4.1, Figure 4.2). As observed in the structure obtained (in solid state) for Zn-complex **73** (Section 2.3.3, Figure 2.10), such a compound has only two arms bound to the metal centre, whilst the remaining two (in *trans* position with respect to the macrocycle) have the chance to spread laterally. In this case the formation of at least a relatively long chain would be expected, but experimentally it did not happen. However, NMR analysis proved that in solution the arms are continuously and rapidly interchanging in coordinating to Zn, thus they could assume an all-up conformation resembling that of the corresponding Gd-complex **85** with consequent difficulty in polymerising and ability to form macrocycle structures as discussed above.

The reactions with ligand **53** have none of the limitations mentioned so far (presence of copper, charged species, conformational restrictions), and trying to rationalise the relatively low-molecular weight species obtained from the thermal cycloadditions between **53** and diazide **81** proves rather complicated. Under these conditions the best results were achieved, which nonetheless were still far from the target high-molecular weight structures. The reason for this must be the main one affecting also the other procedures and leading to the formation of oligomers instead of polymers. The first hypothesis deals with the steric hindering related to the size and structure of the $A_4$ monomers. When one of the alkyne groups reacts by forming a

triazole ring, the increased steric hindrance inhibits further cycloadditions. On the other hand, a second hypothesis can be formulated, related to the tendency of complex DOTA-derivatives to form aggregates by intermolecular interactions, as proved by GPC analysis (Section 2.2.4.1). This solvent-dependent aggregation phenomena could deactivate the alkyne groups (by simply hindering or "hiding" them) towards cycloaddition, with consequent loss of reactivity and low observed conversion rates.

On the basis of the obtained results, also the application of Dvornic's model needs to be discussed, since in the protocols herein it did not lead to the expected outcomes. In particular, no gelation was achieved with the calculated $[A_4]/[B_2]$ ratios for which the model predicts it should happen. The reasons for that might be a generic bug in the model, but also some of the assumptions could be not applicable in this case. In particular, for the click chemistry reactions the exclusive reactivity of A-groups with B-groups and *vice versa* does not strictly include the participation of the two moieties to an intermediate in which also copper(I) atoms and their ligands are involved. Moreover, cyclisation reactions could be occurring, possibly favoured by the geometry of the metal-complexes as discussed above. In that case, the reacted alkyne and azide groups would not participate or contribute to the formation of a polymeric species, with a consequent modification of the actual stoichiometry. Moreover, the hindering of such macrocycle structures on the remaining polymerisable groups might affect their reactivity. Finally, the reactivity of alkyne groups close to each other is partially dependent on the steric bulk presented by those already reacted. Such conditions could explain why Dvornic's model failed with the attempted cycloadditions, and such failure might constitute an indirect proof for some of the hypotheses made previously, such as that about the formation of macrocycles.

It is to be reminded that the molecular weights calculated for the obtained products are only indicative, since they are an approximation based on their hydrodynamic radius and estimated from data of refractive index and differential pressure through a calibration carried out with poly(methyl methacrylate) (DMF-GPC) or poly(ethylene oxide) (aqueous GPC) standards. The actual values of MW could be rather different, although it is still valid that oligomers instead of polymers had formed. With this in mind, the most relevant products were used in experiments to calculate their average relaxivities and to test their viability towards stem cells cultures. The same was done with the corresponding Gd-complexes of some ligands previously synthesised, in order to evaluate them as MRI contrast agents themselves in respect to

analogous compounds reported in the literature, and to compare the results with those achieved for the "macromolecular" products.

See also the Conclusion section (Chapter 5) at the end of the thesis.

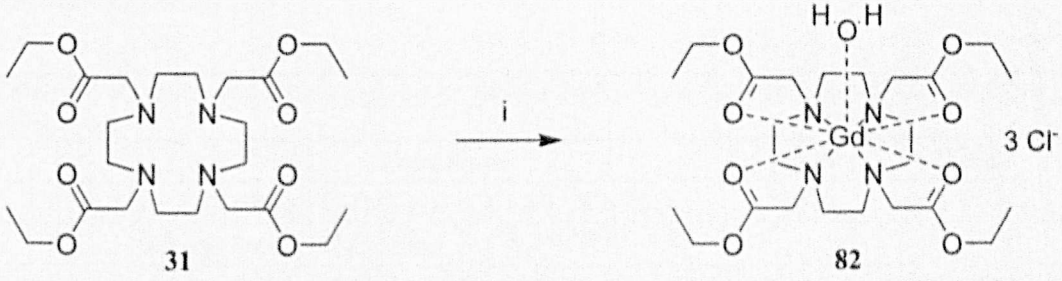
# 4. Results and discussion III: MRI measurements and toxicity tests

Following the synthesis of DOTA-amides **52**, **53** and **54** (see Section 2.2.3), the corresponding $Gd^{III}$-complexes were prepared in order to evaluate their relaxivity performance and toxicity towards stem cells and compare this performance with the measurements carried out on their oligomeric derivatives (see Chapter 3) and the data reported in the literature for other DOTA-tetra-amides. The Gd-complexes of DOTA-tetra-ethyl ester **31** and DOTA-tetra-butyl-amide **32** were first synthesised to test the reaction conditions and prepare model compounds.

## 4.1 Synthesis of the Gd-complexes

Most of the literature procedures for the complexation of gadolinium(III) with DOTA-derivatives involve the reaction of the ligand with an equimolar amount or an excess of a lanthanide salt followed by purification for the removal of unreacted $Gd^{3+}$ by filtration through Amberlite,[457] Chelex[44] or Sephadex,[193, 394] chromatography,[278, 288] dialysis[458] or precipitation[70, 74, 138, 151, 264, 459, 460] at pH 9 as $Gd(OH)_3$. It seemed to us more simple to just avoid the presence of free $Gd^{3+}$ at the end of the reaction by reacting the ligand in slight excess with $GdCl_3$, and exploiting the expected difference in solubility between the complex and the unreacted ligand to purify the target compound by filtration or extraction.

This protocol was first tested by synthesising the new Gd-complex **82**. Ligand **31** (1.5 molar equivalents) was mixed with 1 molar equivalent of $GdCl_3$ hexa-hydrate in water at 50 °C (Scheme 4.1).



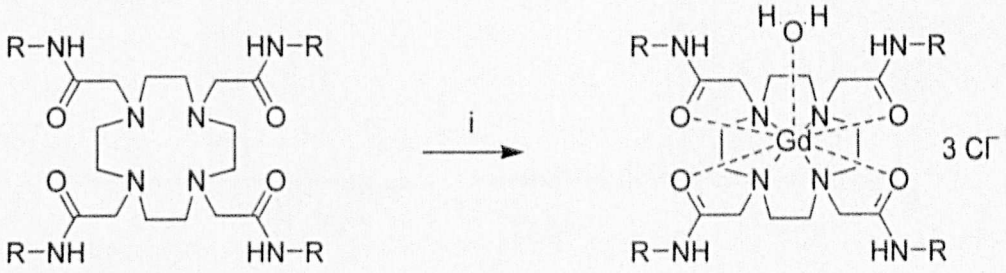

31 82

**Scheme 4.1** Synthesis of the Gd-complex of tetra-ester **31**. i) **31** (1.5 mol eq), $GdCl_3 \cdot 6H_2O$ (1 mol eq), $H_2O$, 50 °C, 4 d, 84%

The presence of free $Gd^{3+}$ in solution was checked by using MTB as an indicator[461-463] (see Section 6.1.1 for details) until the test was negative (4 days). The

crude solid obtained after removal of the solvent was washed with DCM in order to separate the unreacted ligand, and a white crystalline compound was isolated, which was characterised as fully as possible. NMR spectroscopy was not useful from this point of view, because of the line broadening due to the presence of paramagnetic $Gd^{III}$. In the IR spectrum an absorption band was observed at 1615 $cm^{-1}$, a much lower frequency with respect to the 1723 $cm^{-1}$ recorded for the ligand and justified with the electronic delocalisation and consequent weakening of the strength constant for the C=O group following the chelation of $Gd^{3+}$. The $FAB^+$ mass spectrum showed a set of peaks centred at 774 m/z which was assigned to a fragment formed by the ligand, Gd and two chlorides. Elemental analysis confirmed the identity of the compound, including the presence of one molar equivalent of water, due to the molecule of water directly bound to each metal centre in the first coordination sphere, as expected on the basis of the common nona-coordination of $Gd^{III}$.

Since the planned protocol was successful, the Gd-complexes of tetra-amides **32**, **52**, **53** and **54** (not reported in the literature) were prepared in the same way, as shown in Scheme 4.2 and summarised in Table 4.1.




**32:** R = *n*-butyl
**52:** R = allyl
**53:** R = propargyl
**54:** R = styryl

**83:** R = *n*-butyl
**84:** R = allyl
**85:** R = propargyl
**86:** R = styryl

**Scheme 4.2** Synthesis of Gd-complexes **83-86**. Reaction conditions and results are reported in Table 4.1 and discussed in the text.

**Table 4.1** Reaction conditions and results for the synthesis of Gd-complexes **83-86**, as shown in Scheme 4.2.

| | Conditions | Result |
|---|---|---|
| 1 | **32** (1.5 mol eq), $GdCl_3 \cdot 6H_2O$ (1 mol eq), $H_2O$, 50 °C, 5 h. | **83** = 72% |
| 2 | **52** (1.5 mol eq), $GdCl_3 \cdot 6H_2O$ (1 mol eq), $H_2O$, 50 °C, 5 h. | **84** = 80% |
| 3 | **53** (1.5 mol eq), $GdCl_3 \cdot 6H_2O$ (1 mol eq), $H_2O$, 50 °C, 4 h. | **85** = 86% |
| 4 | **54** (1.5 mol eq), $GdCl_3 \cdot 6H_2O$ (1 mol eq), $H_2O$/DMF, 50 °C, 3 h. | **86** = 86% |

The reactions required much less time (3-5 hours) to go to completion with respect to the ester **31** complexation, thus implying kinetic differences in the association mechanisms (which are not mentioned in the literature to the best of our knowledge). As

a comparison, it is well-known that the formation of Gd-DOTA takes weeks to go to completion,[219-225] because two ring nitrogens are always protonated below pH 9 (see Chapter 1); above such pH value $Gd^{3+}$ precipitates as the corresponding insoluble hydroxyde. Good yields were obtained for all compounds, although the starting ligands were not soluble in water. Only with styryl-amide **54** was it necessary to use a 1:1 $H_2O$/DMF mixture in order to favour the dissolution of both the ligand and the product. Washing with DCM was sufficient to remove unreacted ligands **32** and **52** and isolate complexes **83** and **84**. Continuous (Soxhlet) extraction for two days with DCM or THF was required instead to separate ligands **53** and **54**, respectively, because of their low solubility in these solvents (preferred to other solvents because of the relative solubility of the target complexes). For all products the typical multiple-peaks pattern was observed in the $FAB^+$ or $ESI^+$ mass spectra at m/z values corresponding to the Gd-ligand fragment, as shown in Figure 4.1 for **85** and **86**.

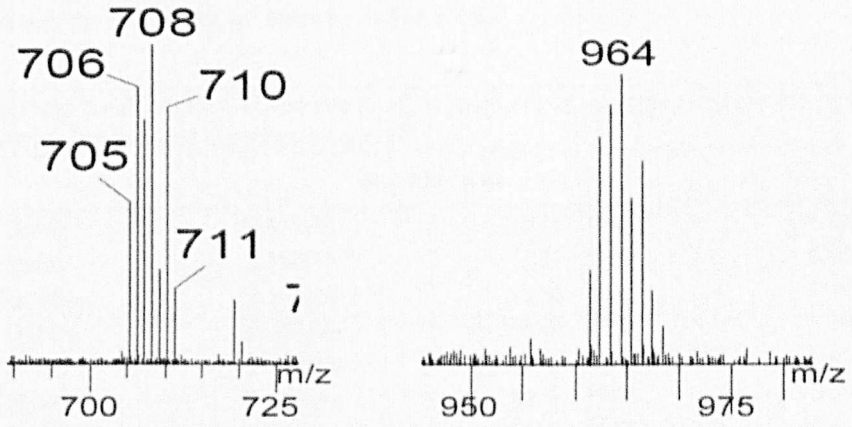



**Figure 4.1** $ESI^+$ mass spectra expansions showing the multiple-peaks pattern observed for the $[L+Gd]^+$ ions for complexes **85** (left) and **86** (right).

For **83** and **85** the $[L+GdCl]^+$ fragments were also detected by MS. As a consequence of the involvement of the amide C=O groups in binding the metal centre and similarly to what was observed in the IR spectrum of **82** for the ester C=O groups, in the IR spectra of all compounds the amide I and II bands were observed at lower frequencies in respect to those recorded for the free ligands. In particular, amide I bands were located at 1621-1631 $cm^{-1}$ (it was 1657-1674 $cm^{-1}$ for the ligands). Analogously amide II bands were observed at 1458-1485 $cm^{-1}$, compared with 1514-1553 $cm^{-1}$ for the ligands. All elemental analysis indirectly confirmed the presence of one water molecule coordinated to gadolinium.

For a comparison with the X-ray structure of Zn-complex **73** (see Figure 2.10 in Section 2.3.3) synthesised[407] from tetra-propargyl-amide **53**, crystals of Gd-complex **85**

were grown[407] and the relative X-ray structure was determined and is shown in Figure 4.2.

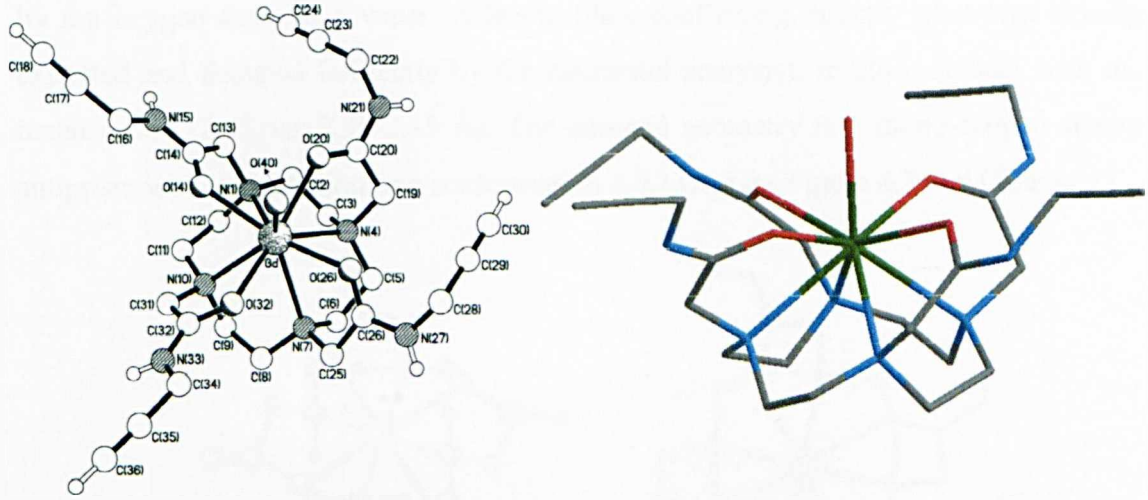



**Figure 4.2** X-ray crystal structure[407] of **85** showing the nona-coordinate stereochemistry of the $Gd^{III}$-complex. Hydrogen atoms, chloride anions and solvent molecules (except the coordinated water molecule) have been omitted for clarity. Crystal data are reported in the Experimental Part (Table Exp.2). Selected bond lengths and angles are reported in Table 4.2.

**Table 4.2** Selected bond lengths [Å] and bond angles [deg] for **85** (numbers in parentheses are estimated standard deviations in the least significant digits).[407]

| **Bond lengths** | | | |
|---|---|---|---|
| Gd – O(40) | 2.417(7) | N(1) – C(2) | 1.504(14) |
| Gd – O(26) | 2.390(7) | C(2) – C(3) | 1.496(16) |
| Gd – O(20) | 2.393(6) | C(3) – N(4) | 1.494(12) |
| Gd – O(14) | 2.401(9) | N(4) – C(5) | 1.483(14) |
| Gd – O(32) | 2.427(6) | C(5) – C(6) | 1.527(15) |
| Gd – N(10) | 2.633(9) | C(6) – N(7) | 1.490(15) |
| Gd – N(1) | 2.648(8) | N(1) – C(13) | 1.482(16) |
| Gd – N(7) | 2.654(9) | N(7) – C(25) | 1.471(13) |
| Gd – N(4) | 2.664(10) | C(14) – O(14) | 1.233(11) |
| **Bond angles** | | | |
| O(26) – Gd – O(40) | 71.4(3) | O(20) – Gd – N(1) | 72.2(2) |
| O(20) – Gd – O(40) | 71.9(2) | N(1) – Gd – N(4) | 68.2(3) |
| O(14) – Gd – O(40) | 72.5(3) | O(26) – Gd – N(7) | 65.9(3) |
| O(40) – Gd – O(32) | 73.5(2) | O(26) – Gd – N(4) | 73.8(3) |
| O(40) – Gd – N(10) | 128.6(3) | N(7) – Gd – N(4) | 67.8(3) |
| O(40) – Gd – N(1) | 127.1(3) | O(32) – Gd – N(10) | 67.0(2) |
| O(40) – Gd – N(7) | 127.9(2) | O(32) – Gd – N(7) | 72.6(3) |
| O(40) – Gd – N(4) | 126.0(3) | N(10) – Gd – N(7) | 68.8(3) |
| O(14) – Gd – N(1) | 66.2(3) | C(13) – N(1) – Gd | 106.6(6) |
| O(14) – Gd – N(10) | 73.8(3) | C(19) – N(4) – Gd | 106.6(7) |
| N(10) – Gd – N(1) | 68.6(3) | C(25) – N(7) – Gd | 107.4(6) |
| O(20) – Gd – N(4) | 65.4(3) | C(31) – N(10) – Gd | 106.9(6) |

By comparing the structure of the Gd-complex with the one previously described (Section 2.3.3) for the Zn-complex, it is clear how the contribution of the four arms in binding the metal make them all point towards the upper side of the molecule.

Eight coordination sites of the $Gd^{3+}$ ion are occupied by the four nitrogen atoms of the macrocycle and the four oxygen atoms of the amide moieties. The ninth site is occupied by the oxygen atom of a water molecule (thus confirming directly what was already expected and deduced indirectly by the elemental analysis), in close contact with the metal centre (2.42 vs. 2.39-2.43 Å). The adopted geometry is a mono-capped square antiprism with the enantiomeric conformation Δ(λλλλ) (see Figure 4.3 and Chapter 1).

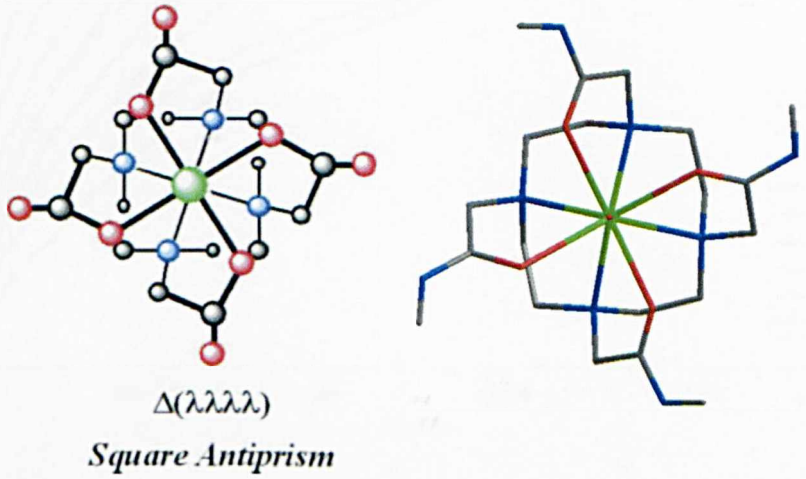



**Figure 4.3** Comparison between a typical representation of the capped square antiprismatic geometry (left, from Woods M. *et al.*; *Dalton Trans* **2005**, *(24)*, 3829-3837) and a perspective view of the X-ray structure of **85** (right, where the propargyl groups are omitted for clarity).

## 4.2 Determination of relaxivity

The longitudinal relaxivity values $r_1$ were calculated by using equation 1.4 (see Chapter 1), reported again below:

$$\frac{1}{T_1^{obs}} = \frac{1}{T_1^0} + r_1[Gd] \qquad \textbf{(1.4)}$$

where $1/T_1^{obs}$ and $1/T_1^0$ are the relaxation rates of the sample and the matrix, respectively, and [Gd] is the concentration of $Gd^{III}$.

Longitudinal water proton relaxation rates were measured at 37 °C and 2.35 T (corresponding to a proton Larmor frequency of 100 MHz) by a spin-echo pulse sequence with an echo-time *TE* of 28 ms and an array of repetition-times *TR* ranging from 100 to 2500 ms. 300 μl solutions of complexes **83**, **84**, **85** and **86** at 0.1-2.5 mM concentration range in double distilled water were prepared. **86** showed solubility problems even at the lowest concentrations and therefore it was preferred not to use it for further experiments because of the relatively wide range of concentrations needed for the measurements. For the other compounds the recovery of the magnetisation

against time was followed. As an example, the normalised graph of the concentration-dependent magnetisation recovery *versus* time for **84** is shown in Figure 4.4

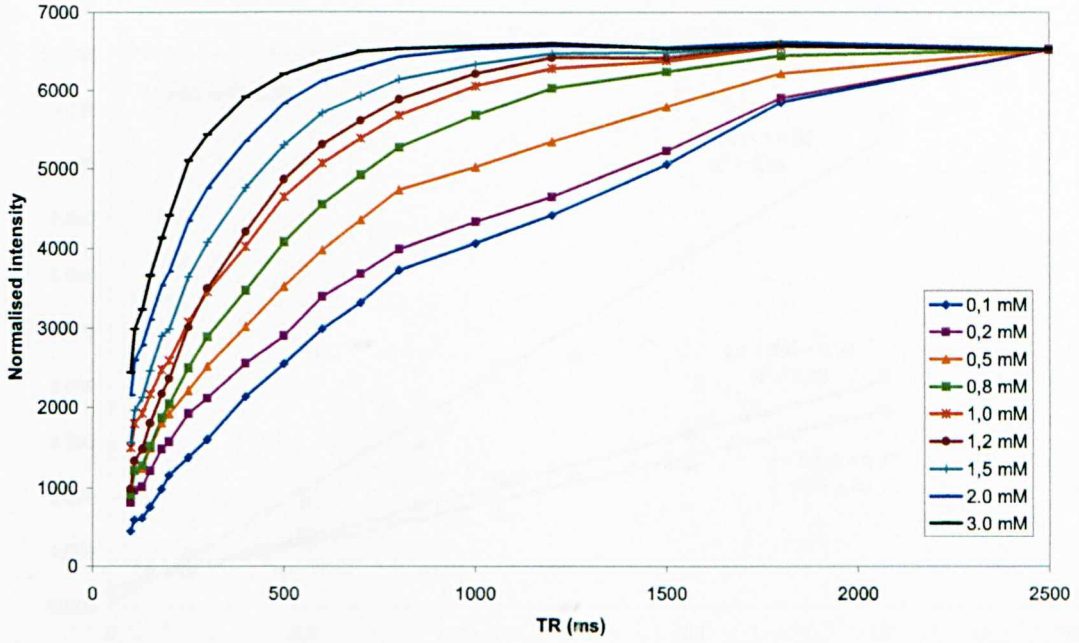



**Figure 4.4** Magnetisation intensity *vs.* time graph (normalised) for solutions of **84** at different concentrations.

It is clear that the more concentrated the solution, the shorter the time necessary for the magnetisation to recover to the maximum value corresponding to the equilibrium state. Graphs like that shown in Figure 4.4 were plotted also for complexes **83** and **85**. From them, the relaxation time for each concentration was extrapolated leading to the data sets reported in Table 4.3.

**Table 4.3** Longitudinal relaxation times ($T_1$) and rates ($R_1$) calculated for solutions at different concentration of complexes **83**, **84** and **85.**

| [Gd] (mM) | **83** | | **84** | | **85** | |
|---|---|---|---|---|---|---|
| | $T_1$ (s) | $R_1$ ($s^{-1}$) | $T_1$ (s) | $R_1$ ($s^{-1}$) | $T_1$ (s) | $R_1$ ($s^{-1}$) |
| 0 | 2.761 | 0.362 | 3.105 | 0.322 | 2.761 | 0.362 |
| 0.1 | 1.469 | 0.681 | 1.753 | 0.570 | 1.913 | 0.523 |
| 0.2 | 1.056 | 0.947 | 1.463 | 0.684 | 1.577 | 0.634 |
| 0.5 | 0.525 | 1.905 | 0.757 | 1.321 | 0.785 | 1.274 |
| 0.8 | 0.339 | 2.950 | 0.539 | 1.855 | 0.593 | 1.686 |
| 1.0 | 0.225 | 4.444 | 0.424 | 2.358 | 0.558 | 1.792 |
| 1.2 | 0.219 | 4.566 | 0.429 | 2.331 | 0.409 | 2.445 |
| 1.5 | 0.154 | 6.494 | 0.319 | 3.135 | 0.382 | 2.618 |
| 2.0 | 0.113 | 8.850 | 0.238 | 4.202 | 0.279 | 3.584 |

The relaxation rates data were finally plotted against the concentration of gadolinium, and the relaxivity for each complex was calculated as the slope of each linear fit according to Equation 1.4, as shown in Figure 4.5.

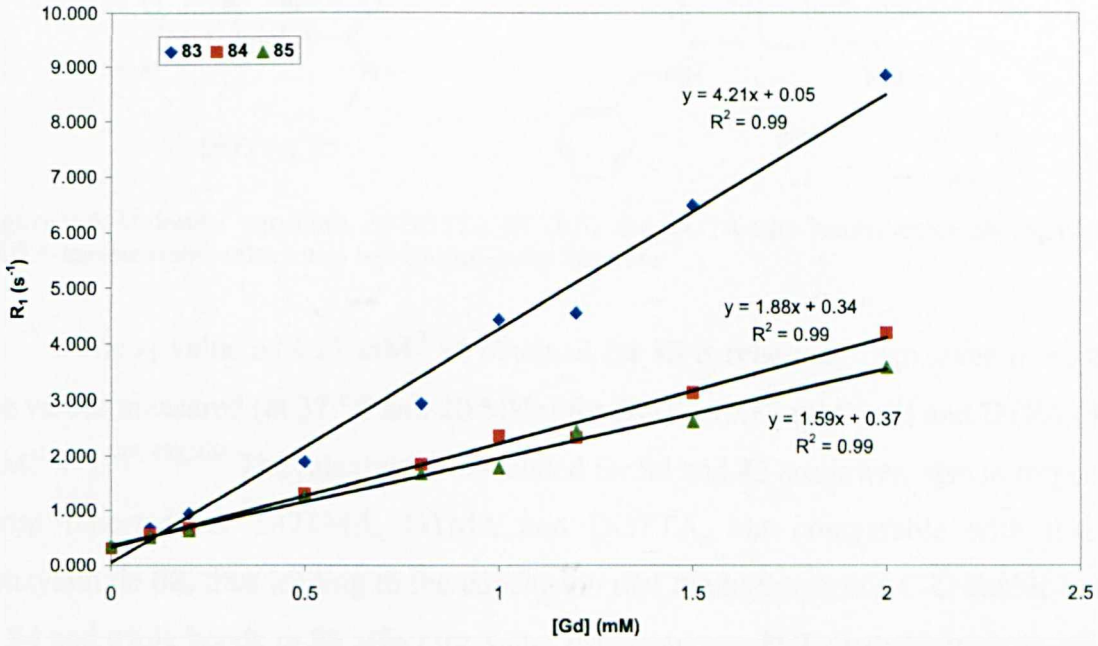
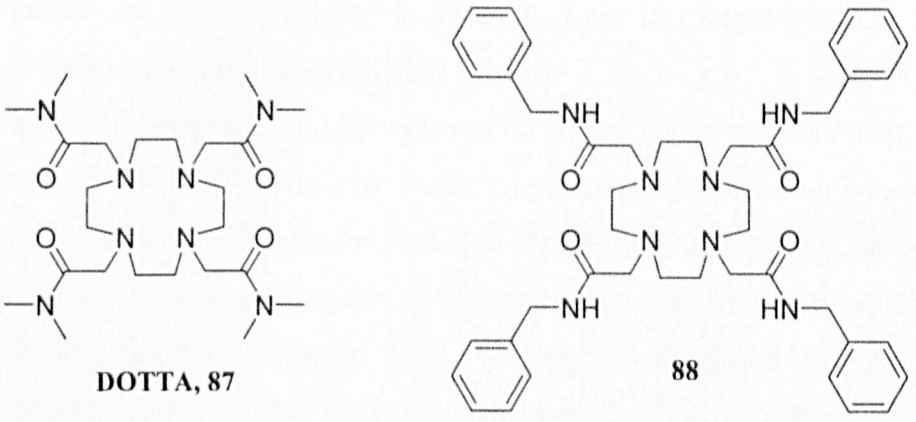



**Figure 4.5** Relaxation rate *vs.* Gd-concentration plots and relative linear fits for complexes **83-85**.

Relaxivity values of 4.21, 1.88 and 1.59 $mM^{-1}$ $s^{-1}$ were obtained for **83**, **84** and **85** respectively (see Table 4.4 below). Not much data has been reported about Gd-complexes of DOTA-amides. Among them, relaxivities of 2.5 $mM^{-1}$ $s^{-1}$ have been calculated for both DOTAM[284] **10** and DTMA[284] **11**, 3.0 $mM^{-1}$ $s^{-1}$ for Gd-DOTTA[284] **87** (Figure 4.6), and 1.88 $mM^{-1}$ $s^{-1}$ for DOTA-benzyl-amide[273] **88** (Figure 4.6). The lower values that DOTA-tetra-amides generally show in respect to DOTA reflect the slower water exchange rate which characterises them[464] and is a direct consequence of having less hydrophilic peptide groups around the metal centre compared to carboxylates.



DOTTA, 87 88

**Figure 4.6** Molecular structures of DOTTA **87** (left) and DOTA-tetra-benzyl-amide **88** (right), two DOTA-amides whose relaxivities are reported in the literature.

The $r_1$ value of 4.21 $mM^{-1}$ $s^{-1}$ obtained for **83** is relatively high, even more than the values measured (at 37 °C and 20 MHz) for DOTA (3.83 $mM^{-1}$ $s^{-1}$) and DTPA (4.02 $mM^{-1}$ $s^{-1}$).[127, 465, 466] The relaxivities calculated for **84** and **85** are lower, also in respect to those reported for DOTMA, DTMA and DOTTA, but comparable with that of benzylamide **88**, thus leading to the conclusion that the hydrophobic C-C double bonds in **84** and triple bonds in **85** affect the water exchange rate at the metal centre. In effect, the coordination of the amide carbonyl groups to the Gd-ion takes the arms to the upper side of the molecule (as discussed in Section 4.1 and shown by the structure in Figure 4.2), so the propargyl groups find themselves in proximity of the ninth coordination site where the water exchange takes place, thus possibly interfering with that.

**Table 4.4** Longitudinal ($r_1$) and transversal ($r_2$) relaxivities calculated for complexes **83**, **84** and **85** following different methods and at different magnetic field strengths ($B$).

| Method | $B$ | $r_1$ ($mM^{-1}$ $s^{-1}$) | | | $r_2$ ($mM^{-1}$ $s^{-1}$) | | |
|---|---|---|---|---|---|---|---|
| | | **83** | **84** | **85** | **83** | **84** | **85** |
| Spin-echo | 2.35 T (100 MHz) | 4.21 | 1.88 | 1.59 | 2.80 | 3.73 | 2.53 |
| Inversion-recovery | 2.35 T (100 MHz) | 4.49 | 1.92 | 1.71 | - | - | - |
| Spin-echo | 9.4 T (400 MHz) | 4.38 | 2.83 | 1.62 | 4.77 | 2.60 | 3.63 |

The longitudinal water proton relaxation rates for complexes **83-85** were also measured with an inversion-recovery technique, in order to compare the results with those obtained by spin-echo. Inversion times τ of 100 to 2800 ms were used. Analogously to what is described for the spin-echo method, the relaxation rates at the same concentrations were measured and then plotted against the concentration values themselves, and the relaxivities determined as the slopes of the corresponding linear

fits. The calculated values (reported in Table 4.4) are just slightly higher than those obtained already and seem to confirm their validity.

Finally, the longitudinal relaxivities of **83-85** were also calculated at a magnetic field strength of 9.4 T (400 MHz) by means of the same spin-echo technique used for the measurements at 2.35 T. It was expected to obtain little or no difference on the basis of the practically independent nature of the relaxation rate of low-molecular weight species on the external magnetic field strength, as derivated by the Solomon-Bloembergen-Morgan equation[2] (**1.7**) (see Chapter 1). That is actually the case for complexes **83** (4.38 vs. average 4.35 $mM^{-1}$ $s^{-1}$) and **85** (1.62 vs. average 1.65 $mM^{-1}$ $s^{-1}$). A surprising 2.83 $mM^{-1}$ $s^{-1}$ ($R^2$ = 1.00) was instead obtained for **84** (2.35 T average: 1.90 $mM^{-1}$ $s^{-1}$). The measurements were carried out again with the same result, and an explanation for that could not be found. However, it is to be noted that this value is very close to those reported for Gd-DOTMA, Gd-DTMA and Gd-DOTTA (2.5-3.0 $mM^{-1}$ $s^{-1}$; see above).

For further characterisation, transversal relaxivities $r_2$ were also calculated for **83-85** by using a spin-echo technique with a fixed *TR* of 1000 ms and an array of *TE* of 28, 30, 40, 50, 60, 80 and 100 ms. The results obtained are reported in Table 4.4. Such a parameter is very rarely reported for Gd-based contrast agents, since those compounds (belonging to the class of $T_1$-agents) act by improving the longitudinal relaxation processes and have a very limited effect on the transversal ones[2, 113] (see Chapter 1). For a comparison, the most commonly reported[2, 467, 468] $r_2$ value for DOTA is 4.75 $mM^{-1}$ $s^{-1}$ (in one case[469] also 4.9 $mM^{-1}$ $s^{-1}$). No transversal relaxivity values are available in the literature for DOTA-amides.

Longitudinal and transversal relaxation measurements at 2.35 T were finally carried out on a selection of products from the cycloaddition polymerisation attempts involving Gd-DOTA-propargyl-amide **85** and diazide **81** as co-monomers (see Sections 3.3.2 and 3.3.3). The product from the 1.5:1 click chemistry reaction $\mathbf{GdC_{1.5:1}}$ (see Table 3.5) was chosen for solubility reasons, being the only one partially soluble in water. All products from the thermal cycloaddition experiments (see Table 3.6) were suitable for $T_1$ and $T_2$ measurements, but that from 1:1 reagents ratio was not used because of it having the lower maximum $M_w$ value.

First, stock solutions were prepared for each product by stirring it thoroughly for 15 hours in double distilled water. When partial solubility occurred, the suspension was filtered and the remaining solid was weighed in order to establish the actual amount

used for the preparation of the stock solution. The actual $Gd^{III}$ concentrations of the stock solutions were determined by ICP-AES: in the products the species with different $M_w$ could not be separated by dialysis (because of their close hydrodynamic radii) or precipitation (because of their similar solubilities), and the ratio between the co-monomers which had reacted was not possible to be established by the employed analytical techniques. The ICP-determined concentration values were also useful to estimate the rough molar ratio between **85** and **81** in each product. If the catalytic amounts of copper catalyst (when present) are neglected, such ratio can be expressed as:

$$\frac{[\mathbf{85}]}{[\mathbf{81}]} = \frac{[\mathrm{Gd}]_{\mathrm{STOCK}} V^0}{M^0 - [\mathrm{Gd}]_{\mathrm{STOCK}} V^0} \qquad (\mathbf{4.1})$$

where $[\mathrm{Gd}]_{\mathrm{STOCK}}$ is the concentration of gadolinium measured by ICP, and $M^0$ and $V^0$ are the amount of product and the volume of water, respectively, that were used to prepare the stock solution. For the employed products the following ratios were calculated:

- $\mathbf{GdC}_{1.5:1}$ = 1 / 3.8;
- $\mathbf{GdT}_{1:2}$ = 1 / 2.3;
- $\mathbf{GdT}_{1:4}$ = 1 / 2.9;
- $\mathbf{GdT}_{1:6}$ = 1 / 1.5.

Such values are difficult to comment, as a trend seems to be missing. Also, the product for which the highest azide/alkyne ratio was expected (i.e. the one obtained using the highest **81**/**85** ratio) is actually that showing the lowest value.

Samples for relaxation measurements were then obtained by dilution of suitable amounts of stock solution. Longitudinal and transversal relaxation rates were measured as described above for complexes **83-85**. As an example, the $R_1$-*vs.*-[Gd] plots are shown in Figure 4.7. All results are reported in Table 4.5.

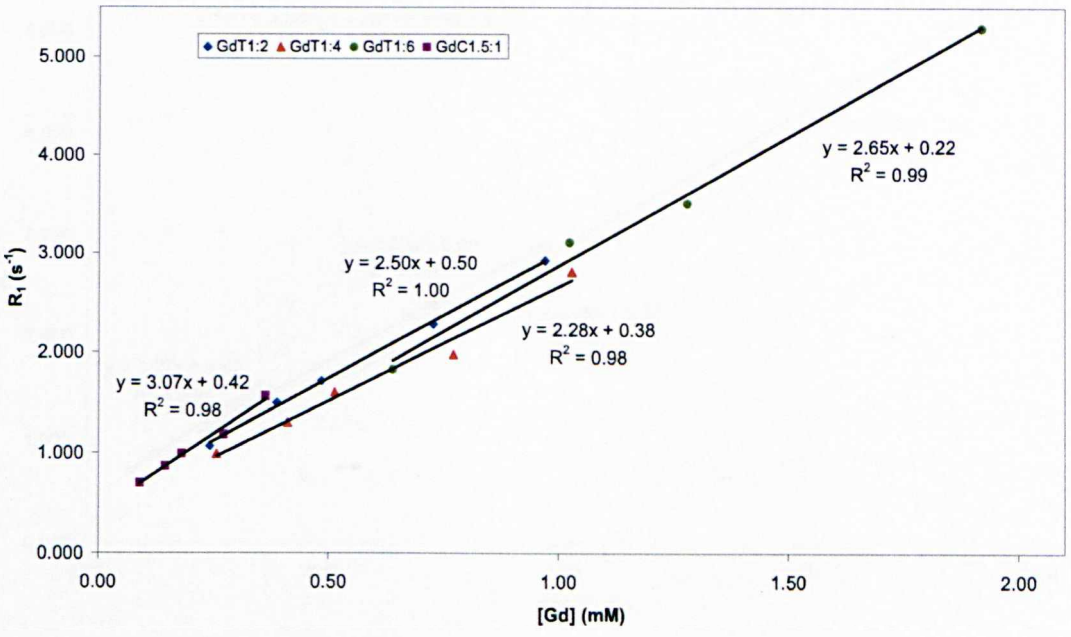



**Figure 4.7** $R_1$ *vs.* [Gd] plots and relative linear fits for some products of the cycloaddition reactions between **85** and **81**. Data are reported in Table 4.5 and discussed in the text.

**Table 4.5** Longitudinal and transversal relaxation times ($T_1$, $T_2$), rates ($R_1$, $R_2$) and relaxivities ($r_1$, $r_2$) for some of the products obtained by cycloaddition reactions between **85** and **81**.

| Product | [Gd] (mM) | $T_1$ (s) | $R_1$ ($s^{-1}$) | $r_1$ ($mM^{-1}$ $s^{-1}$) | $T_2$ (s) | $R_2$ ($s^{-1}$) | $r_2$ ($mM^{-1}$ $s^{-1}$) |
|---|---|---|---|---|---|---|---|
| **$GdC_{1.5:1}$** | 0.36 | 0.636 | 1.572 | 3.07 | 0.409 | 2.445 | 3.97 |
| | 0.27 | 0.845 | 1.184 | | 0.478 | 2.091 | |
| | 0.18 | 1.005 | 0.995 | | 0.653 | 1.532 | |
| | 0.15 | 1.152 | 0.868 | | 0.603 | 1.659 | |
| | 0.09 | 1.424 | 0.702 | | 0.730 | 1.370 | |
| **$GdT_{1:2}$** | 0.97 | 0.341 | 2.929 | 2.50 | 0.265 | 3.770 | 2.73 |
| | 0.73 | 0.438 | 2.285 | | 0.326 | 3.070 | |
| | 0.49 | 0.581 | 1.722 | | 0.397 | 2.521 | |
| | 0.39 | 0.664 | 1.506 | | 0.471 | 2.121 | |
| | 0.24 | 0.933 | 1.072 | | 0.561 | 1.782 | |
| **$GdT_{1:4}$** | 1.03 | 0.355 | 2.814 | 2.28 | 0.281 | 3.563 | 2.43 |
| | 0.77 | 0.505 | 1.982 | | 0.345 | 2.896 | |
| | 0.51 | 0.621 | 1.610 | | 0.450 | 2.222 | |
| | 0.41 | 0.766 | 1.305 | | 0.499 | 2.006 | |
| | 0.26 | 1.009 | 0.991 | | 0.580 | 1.726 | |
| **$GdT_{1:6}$** | 2.56 | - | - | 2.65 | 0.117 | 8.545 | 3.07 |
| | 1.92 | 0.189 | 5.298 | | 0.146 | 6.862 | |
| | 1.28 | 0.284 | 3.516 | | 0.198 | 5.044 | |
| | 1.02 | 0.321 | 3.116 | | 0.263 | 3.797 | |
| | 0.64 | 0.547 | 1.830 | | 0.370 | 2.704 | |

Although the transversal relaxivities (2.43-3.97 $mM^{-1}$ $s^{-1}$) show different variations in respect to that calculated for **85** (2.53 $mM^{-1}$ $s^{-1}$, Table 4.4) and are not easy

to explain, a clear improvement is noticed by comparing the obtained longitudinal relaxivity values for the cycloaddition products (2.28-3.07 $mM^{-1}$ $s^{-1}$) with the average value determined for monomer **85** (1.65 $mM^{-1}$ $s^{-1}$). That is in accordance with the prediction that polymeric derivatives of **85** would be endowed with an improved (i.e. faster) relaxation process, which is at the base of this whole project. The fact that oligomers were achieved instead of the target polymers explains why the increase in the $r_1$ values is not particularly large. However, the improvement is still significant, especially when compared with the relatively low molecular weight of the species which formed. When comparing the outcomes from the relaxation measurements in respect to the oligomers composition (as obtained by GPC, reported in Tables 3.3 and 3.4, and summarised again in Table 4.6) the 3.07 $mM^{-1}$ $s^{-1}$ value determined for $\mathbf{GdC_{1.5:1}}$ might surprise compared with those (lower) for $\mathbf{GdT_{1:2}}$, $\mathbf{GdT_{1:4}}$ and $\mathbf{GdT_{1:6}}$. According to GPC, $\mathbf{GdC_{1.5:1}}$ is formed by a 56.6% "1.9 kDa oligomer" and a 43.6% "1.0 kDa oligomer"; there is no trace of the "3.1 kDa oligomer" detected for thermal cycloaddition products (and correlated with a higher relaxivity on the basis of its MW, hypothetically reflecting its size).

**Table 4.6** Summary of the properties of some the products obtained by cycloaddition reactions between **85** and **81** and used in relaxation measurements (see Tables 3.3, 3.4 and 4.6.

| Product | $r_1$ ($mM^{-1}$ $s^{-1}$) | $M_w^1$ (kDa) [area%] | $M_w^2$ (kDa) [area%] | $M_w^3$ (kDa) [area%] | $M_w^4$ (kDa) [area%] |
|---|---|---|---|---|---|
| $\mathbf{GdC_{1.5:1}}$ | 3.07 | - | 1.9 [56.6] | | 1.0 [43.4] |
| $\mathbf{GdT_{1:2}}$ | 2.50 | 3.2 [9.6] | 1.8 [73.8] | | 0.9 [16.6] |
| $\mathbf{GdT_{1:4}}$ | 2.28 | 3.1 [1.4] | 2.1 [32.1] | 1.5 [44.9] | 0.9 [21.6] |
| $\mathbf{GdT_{1:6}}$ | 2.65 | 3.0 [2.7] | 2.0 [37.0] | 1.5 [40.1] | 0.9 [20.2] |

Since the sole difference between the **GdC** and the **GdT** species consists in the synthetic procedures through which they were prepared (click chemistry and thermal cycloaddition, respectively), a correlation between relaxivities and molecular structures seems to be possible. In particular, the stereoselectivity of click chemistry (leading to 1,4-triazoles only) might imply a more regular structure for the resulting oligomers, whilst the mix of 1,4- and 1,5-isomers obtained *via* thermal cycloaddition could take a higher irregularity in the products structure, where the "chain-folding" effect by the 1,5-triazole units leads to hindering the metal centre with consequent obstacle to the water exchange therein.

When comparing the products from thermal cycloadditions, it looks clear that the samples where the percentage of oligomers with the highest MW is bigger are also those with the highest relaxivity values, in accordance with the general concept that a structure with higher MW (and then hypothetically a bigger size) causes a higher relaxivity. For **GdT$_{1:4}$**, where the percentage of "3.1 kDa oligomer" is just 1.4%, the relaxivity is 2.28 $mM^{-1}$ $s^{-1}$. Instead for **GdT$_{1:2}$** and **GdT$_{1:6}$**, where the percentage of the same oligomer is 9.6% and 2.7% respectively, relaxivities of 2.50 and 2.65 $mM^{-1}$ $s^{-1}$ respectively were calculated. Although the product with the higher "3.1 kDa oligomer" percentage is not the one with the higher relaxivity between the two, also the distribution of the other oligomers is to be considered: **GdT$_{1:6}$** contains a 37% "2.0 kDa oligomer", which is missing in **GdT$_{1:2}$**.

In a comparison with analogous systems (e.g. PANAM and PAMAM dendrimers[155, 470]) the absolute values of the relaxivities calculated for the GdT species are clearly lower, but it has to be highlighted that also their molecular weights are lower. However, if a reasonable average number of 3-5 Gd-complexes are hypothesised for the GdT species (based on the MW values from GPC), an average increase in relaxivity of about 0.5 $mM^{-1}$ $s^{-1}$ per unit can be calculated with respect to the monomer Gd-complex **85**. The average increase in relaxivity for the dendrimeric systems is about 0.1-0.2 $mM^{-1}$ $s^{-1}$ $unit^{-1}$ with respect to the relative Gd-complex. Although these calculations must be taken with caution, they nonetheless seem to be very encouraging.

Thus, when considering the positive results achieved with the relatively low molecular weight of the obtained products and in view of the much higher aimed ones, the obtained data seem to confirm that the type of planned polymeric architecture and the molecular structure of the monomers designed to obtain it would lead to an MRI agent endowed with a high relaxivity.

## 4.3 Viability tests

The toxicity of the synthesised Gd-complexes was tested by incubating ST14A stem cells[471] (a type of cells from an immortalised cell line derived from embryonic striatum E14) in solutions containing different concentrations of each complex, at 37 °C and 5% $CO_2$ atmosphere for 24 hours. Solutions of **83-86** ranging from 0.01 to 10 mM were prepared in DMEM, whose typical formulation[91] is reported in Table 4.7.

Gd-DOTA-tetra-styryl-amide **86** precipitated quantitatively at all concentrations as a purple insoluble solid, leaving the supernatant solutions colourless. On the basis of the initial pink colour of the solution, it was deduced that an interaction had taken place between **86** and the pH indicator contained in DMEM, i.e. Phenol Red (Figure 4.8).

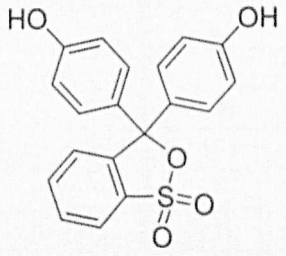



**Figure 4.8** Molecular structure of the pH indicator Phenol Red, among the components of DMEM.

Because of the presence of multiple aromatic rings in both **86** and Phenol Red, a possibility was that strong π-π interactions had formed between the two species, leading to insoluble aggregates and clusters that eventually precipitated. However, both the aromatic ring types in **86** and Phenol Red are electron rich, and π-π interactions appear unlikely from this point of view. Alternatively, it was hypothesised that bridges between two complexes might have formed through the phenol groups of the indicator, or that more complicated reactions had taken place mediated by or involving other components of the medium. However, it was not possible to verify any hypothesis because the precipitate was insoluble in all tried solvents, including acidic solutions and aromatic compounds.

**Table 4.7** Typical Dulbecco's modified Eagle's medium (DMEM) formulation.

| Component | MW (Da) | Concentration | |
|---|---|---|---|
| | | mg/l | mM |
| **Amino Acids** | | | |
| Glycine | 75 | 30 | 0.400 |
| L-Arginine hydrochloride | 211 | 84 | 0.398 |
| L-Cystine·2HCl | 313 | 63 | 0.201 |
| L-Glutamine | 146 | 580 | 3.97 |
| L-Histidine hydrochloride·$H_2O$ | 210 | 42 | 0.200 |
| L-Isoleucine | 131 | 105 | 0.802 |
| L-Leucine | 131 | 105 | 0.802 |
| L-Lysine hydrochloride | 183 | 146 | 0.798 |
| L-Methionine | 149 | 30 | 0.201 |
| L-Phenylalanine | 165 | 66 | 0.400 |
| L-Serine | 105 | 42 | 0.400 |
| L-Threonine | 119 | 95 | 0.798 |
| L-Tryptophan | 204 | 16 | 0.0784 |
| L-Tyrosine | 181 | 72 | 0.398 |
| L-Valine | 117 | 94 | 0.803 |
| **Vitamins** | | | |
| Choline chloride | 140 | 4 | 0.0286 |
| D-Calcium pantothenate | 477 | 4 | 0.00839 |
| Folic Acid | 441 | 4 | 0.00907 |
| i-Inositol | 180 | 7.2 | 0.0400 |
| Niacinamide | 122 | 4 | 0.0328 |
| Pyridoxine hydrochloride | 204 | 4 | 0.0196 |
| Riboflavin | 376 | 0.4 | 0.00106 |
| Thiamine hydrochloride | 337 | 4 | 0.0119 |
| **Inorganic Salts** | | | |
| Calcium Chloride ($CaCl_2·2H_2O$) | 147 | 264 | 1.80 |
| Ferric Nitrate ($Fe(NO_3)_3·9H_2O$) | 404 | 0.1 | 0.000248 |
| Magnesium Sulfate ($MgSO_4·7H_2O$) | 246 | 200 | 0.813 |
| Potassium Chloride (KCl) | 75 | 400 | 5.33 |
| Sodium Bicarbonate ($NaHCO_3$) | 84 | 3700 | 44.05 |
| Sodium Chloride (NaCl) | 58 | 6400 | 110.34 |
| Sodium Phosphate monobasic ($NaH_2PO_4·2H_2O$) | 154 | 141 | 0.916 |
| **Other Components** | | | |
| D-Glucose (Dextrose) | 180 | 4500 | 25.00 |
| Sodium Pyruvate | 110 | 110 | 1.000 |
| Phenol Red | 376.4 | 15 | 0.0399 |

Incubation was then carried out with the solutions of complexes **83-85**, after which the cells were washed with EBSS and tested for viability. Cells were first checked under an inverted microscope to assess morphological changes as possible occurrence of cell death. As shown in Figure 4.9, healthy cells (picture on the right),

unless undergoing mitosis, were attached to the plastic, well spread and devoid of large vacuoles, and it was observed that they had become in contact to each other; in contrast, dead cells (picture on the left) had a round morphology and were either loosely attached to the dish or floating in the medium.

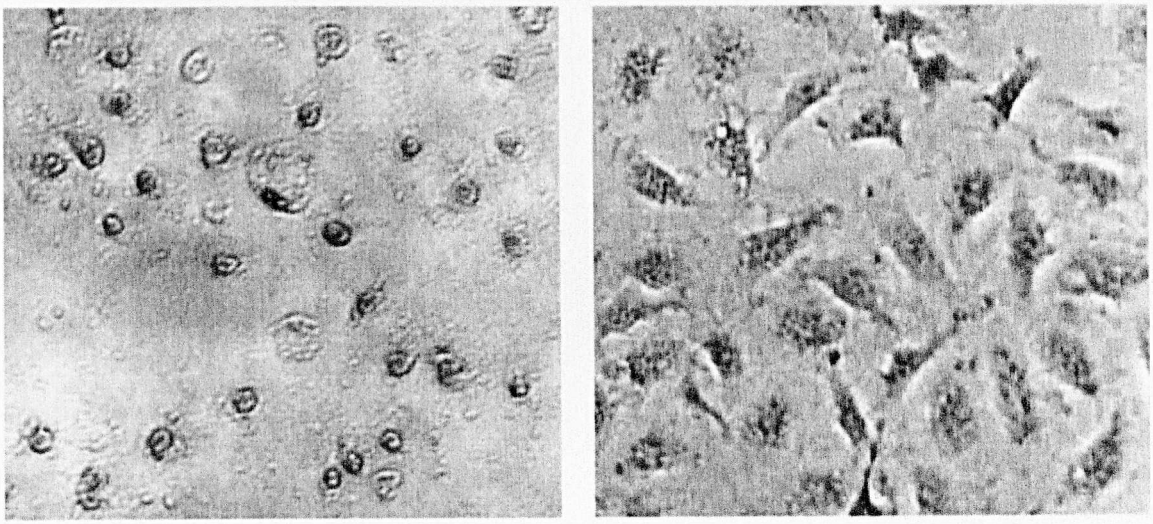


**Figure 4.9** Left: dead or dying cells, with the typical round morphology, as a consequence of incubation in the presence of a 10 mM toxic concentration of **84**. Right: healthy cells (irregularly-shaped), which survived incubation with a 1 mM concentration of **84**.

For a quantitative analysis of the effect of compounds **83-85** on cell survival, change in cell number was assessed using the Alamar Blue assay[472, 473] which utilizes a dye that detects changes in the redox state of the culture medium resulting from cell growth. The redox state of the medium determines whether the indicator assumes its oxidised (non-fluorescent, blue) or reduced (fluorescent, red) form, and this is usually assessed by UV-VIS spectroscopic analysis at 570 nm. Herein, the metabolic activity of the cells after incubation with **83-85** showed that at several concentrations the metabolism had increased when increasing the concentration of the solution in which the cells had been incubated (as shown in Figure 4.10).

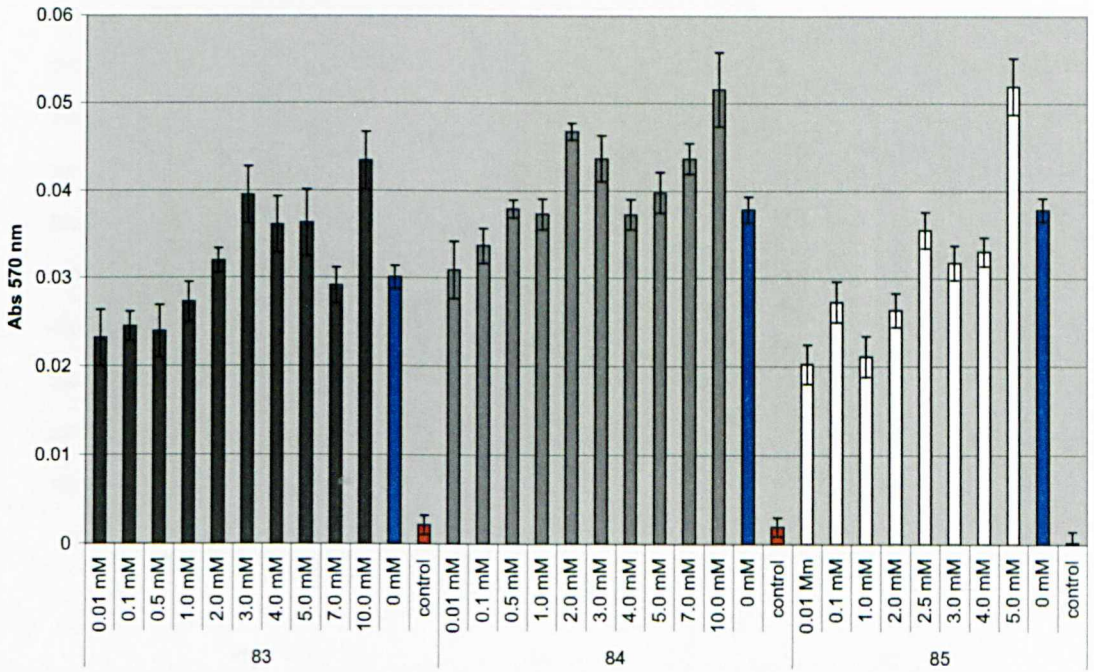



**Figure 4.10** Results of the Alamar Blue assay on cell cultures of **83-85**.

In particular, in experiments where cells were incubated with **83** and **84** at concentrations above 0.5-1 mM, absorbance values similar or higher than those measured in cells incubated without contrast agents ("0 mM") were obtained . That was unexpected, because the increase of a potentially toxic species should in theory lead to a decrease in the metabolic activity and eventually to cell death.

In order to clarify this issue, a different viability test, the Methylene Blue assay[474] was carried out using a limited range of concentrations. This colorimetric assay is considered to reflect more accurately the number of cells rather than their metabolic activity. The results obtained from this test are shown in Figure 4.11.

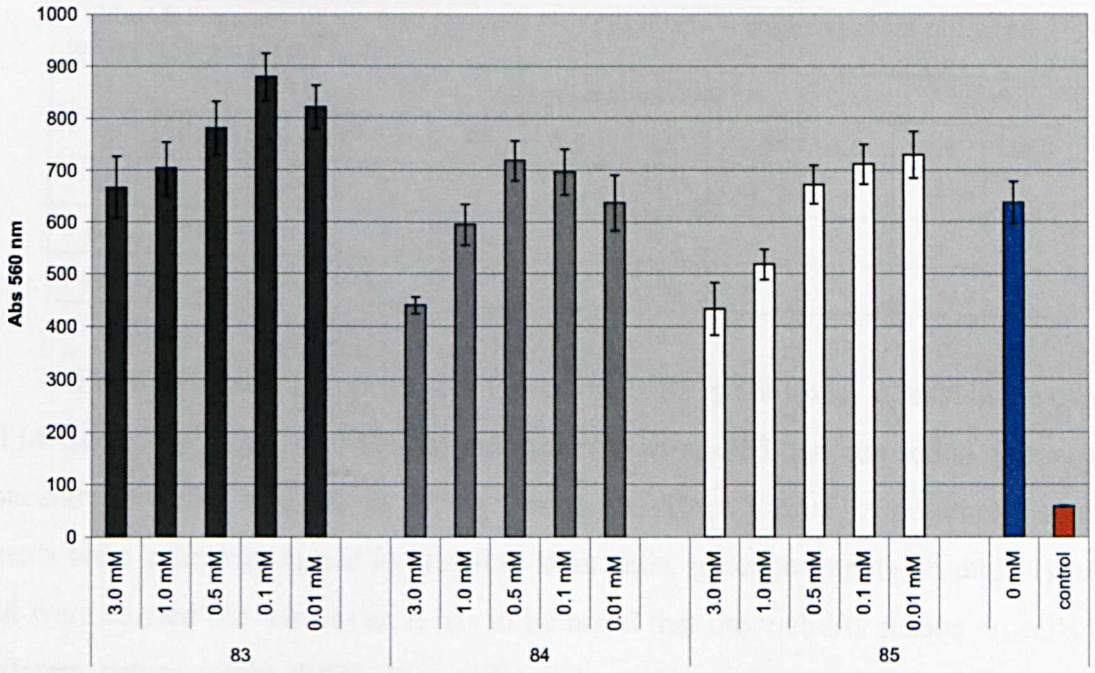



**Figure 4.11** Results of the Methylene Blue assay on cell cultures of **83-85**.

Interestingly, similar results were observed using the Methylene Blue assay to those obtained with the Alamar Blue test. All cells treated with **83** at concentrations between 0.01-3.0 mM, exhibit a higher absorbance (and therefore a higher number of cells due to their survival/proliferation) than controls incubated without any contrast agent (blue bar in Figure 4.12), although the number of cells appears to decrease with increasing the concentration. The same is true for concentrations of **84** and **85** up to 0.5 mM. This is unusual for the reasons explained above (the cellular activity and proliferation, and therefore the cell number, should decrease in the presence of toxic agents [as **83-85** are supposed to be, since they contain Gd], not *vice versa*). It was then hypothesised that the type of contrast agents used combined with the presence of gadolinium produced some effect promoting cell proliferation. To the best of our knowledge such a behaviour has not been reported in the literature. By combining the results of the growth assays (visual, Alamar Blue and Methylene Blue) the toxicity data summarised in Table 4.8 were obtained.

**Table 4.8** Summary of the final response (+ = positive; – = negative) about cell viability towards Gd-complexes **83-85**.

| | Concentration (mM) | | | | | | | | | |
|---|---|---|---|---|---|---|---|---|---|---|
| | **0.01** | **0.1** | **0.5** | **1.0** | **2.0** | **3.0** | **4.0** | **5.0** | **7.0** | **10.0** |
| **83** | + | + | + | + | + | + | + | + | + | – |
| **84** | + | + | + | + | + | + | + | – | – | – |
| **85** | + | + | + | + | + | + | + | – | – | – |

From this study it appears that Gd-complex **83** is not toxic, at least in the case of ST14A cells, up to a 7 mM concentration, while **84** and **85** can be used at a maximum concentration of 4 mM for *in vitro* experiments. Since the target polymeric contrast agents were primarily aimed at labelling stem cells, no experiments on other types of cell were carried out. However, it has to be noted that the viability results on cells of a different nature might differ. It is difficult to compare the results obtained with the toxicity evaluations reported for other contrast agents (first of all Gd-DOTA, and $Gd^{3+}$ ion itself)[122] because the latter are normally expressed in terms of their $LD_{50}$ values, and then referred to *in vivo* experiments carried out on animals rather than on cell cultures. However, the concentration range for which cell survival was observed in the presence of **83-85** appears remarkable considering that typical viable concentrations for *in vitro* experiments with Gd-based contrast agents lay in a range of 1-100 μM.

After establishing the substantial safety of **83-85** as contrast agents for *in vitro* experiments (*in vivo* outcomes might differ), it was tried to conduct the same tests also using cycloaddition products $\mathbf{GdC_{1.5:1}}$, $\mathbf{GdT_{1:2}}$, $\mathbf{GdT_{1:4}}$ and $\mathbf{GdT_{1:6}}$, whose relaxivity values were previously determined (Section 4.2). When these compounds were added to DMEM, a purple insoluble precipitate was observed, as with **86**. The reason is probably the presence of strong intermolecular interactions leading to the formation of insoluble aggregates and clusters that eventually precipitate, or side-reactions involving the Gd-complexes, the indicator and possibly some of the substances dissolved in DMEM. Also in this case as for **86**, the precipitated solids could not be solubilised in any of the solvents tested (aqueous hydrochloric acid, dimethyl sulfoxide, DMF, NMP, water, methanol, ethanol, isopropanol, ethyl acetate, acetone, DCM, chloroform, diethyl ether, chlorobenzene, toluene, hexane) and analysed. Therefore, viability tests could not be carried out. However, some experiments with products $\mathbf{LigT_{1:2}}$, $\mathbf{LigT_{1.165:1}}$ and $\mathbf{LigT_{1.33:1}}$ partially loaded (50%) with $Gd^{III}$ led to no solubility problems and relatively

good results in terms of cell viability, being **LigT$_{1:2}$** safe at 0.01 mM concentration, and **LigT$_{1.165:1}$** and **LigT$_{1.33:1}$** safe up to at least 0.1 mM.[475]

It was not possible to establish the correlation between the contrast enhancement obtained with the oligomers and their actual size, since the latter could not be calculated because of technical problems with the light-scattering detector of the GPC instrument. However, these results and especially the significant measured relaxivities of the oligomeric species **GdC$_{1.5:1}$**, **GdT$_{1:2}$**, **GdT$_{1:4}$** and **GdT$_{1:6}$**, together with the positive response from viability tests for the starting Gd-complexes suggest that future hyperbranched polymeric contrast agents with good contrast performance and low toxicity could indeed be prepared according to the methodologies that were followed throughout the present project.

See also the Conclusions section at the end of the thesis.

# 5. Conclusions and future perspectives

## 5.1 Conclusions

The synthetic work, the analyses and the properties assessments described in the previous chapters permit some interesting conclusions about the present project, which was aimed at an exploration of the possibility to produce MRI contrast agents for stem cell labelling with a polymeric molecular architecture endowing them with high relaxivity performance and lack of toxicity.

A rationally planned molecular structure pointed us towards the possibility of optimising the several parameters (size, hydrophilicity/-phobicity, stability, toxicity, solubility, etc.) which generally decide the efficacy of an MRI contrast agent. In particular, from the comprehensive literature review we carried out it emerged that the topic of the size has to be read in a very different way with respect to how it was done in the past and keeps on being done: it revealed to be not very effective to link magnetic complexes to big (and then slowly rotating) macromolecules solely, because a high freedom of rotation can still remain locally and negatively affect the improvement from the linkage itself.

A Gd-DOTA-based hyperbranched polymer seemed to fulfil the requirements of an ideal MRI contrast agent. The rigid structure with no possibility of independent rotational freedom for the Gd-complexes would ensure the desired slow tumbling time for the Gd-$H_2O$ vector. In addition, hydrophilicity favours a relatively rapid water exchange rate at the metal centre. The use of DOTA-derivatives as ligands would assure a high stability for the Gd-complexes, and the biological safety should be further enforced by the role of the whole macromolecule as a cage to trap toxic $Gd^{3+}$ ions in case of their improbable release

With this in mind, a number of synthetic routes were identified to achieve the target polymeric product, on the basis of suitable retrosynthetic analyses. Many unexpected difficulties were encountered during the synthesis of the tetrasubstituted macrocycles, both for their formation and purification. These problems were ascribed to the structure of the target DOTA-derivatives and in particular to their ability of forming a variety of intermolecular interactions. Despite this, several intermediates were successfully prepared and characterised, many for the first time. In particular (in addition to many functionalised compounds such as bromo- and chloroacetamides,

amines, alcohols, azides etc.) it has to be mentioned: tetra-ethyl ester **31** and tetra-butylamide **32** of DOTA, novel model compounds and ligands for the preparation of Gd-complexes to use as a comparison; DOTA **2** itself, for attempts of divergent synthesis of more complicated derivatives; DOTA-tetra-allylamide **52**, DOTA-tetra-propargylamide **53** and DOTA-tetra-styrylamide **54**, used as both monomers for polymerisation or co-polymerisation attempts and ligands to prepare the corresponding Gd-complexes which are themselves novel MRI contrast agents; tetra-styryl-derivative **63**, an interesting monomer for radical [co-]polymerisation; Zn-complex **73**, to be used in cycloaddition reactions to avoid the complexation and subsequent deactivation of $Cu^{I}$-catalyst (click chemistry) and to allow monitoring of the reaction progress and outcome by NMR spectroscopy without line-broadening problems. In addition, it is to be mentioned that several DOTA-derivatives were successfully formed but it was not possible to isolate them as pure compounds. Among them: DOTA-tetra-methyl ester **30**; DOTA-tetra-vinylbenzylamide **62**; Zn-DOTA-tetra-vinylbenzyltriazole **74**; DOTA-tetra-vinylbenzyltriazole **71**. Although these products could not be used as monomers, their syntheses were useful to explore the procedures for tetra-substitution on cylen and for click chemistry. Furthermore, their characterisation provided interesting information, for example about conformational equilibria in these types of derivatives.

The polymerisation attempts *via* metathesis or radical reactions did not lead to the desired products either because of a lack or an excess of reactivity by the monomers. On the other hand, cycloaddition reactions (either $Cu^{I}$-mediated or thermally activated) between **53**, **73** or **85** and a PEG-diazide led to oligomeric products that were characterised in terms of their molecular weight distribution, stereochemistry, conversion rate etc. The fact that low molecular weight products were obtained in place of the expected polymers, and the low calculated conversion rates (unusual, especially for $Cu^{I}$-catalysed additions) could be explained by different hypotheses, involving either the molecular geometry, or the coordinative inactivation of the catalyst (when used), or the formation of macrocycle structures. In spite of their limited molecular weight, the obtained products represent nonetheless interesting outcomes, since very few examples of synthesis of hyperbranched polymers *via* alkyne-azide cycloaddition reactions are reported in the literature.[476] In fact, the polymerisations described herein are the first attempted $A_4+B_2$ syntheses of hyperbranched polymers through this type of reaction, to the best of our knowledge.

The oligomers obtained were tested (thanks to Rachael Dobson, Developmental Biology Unit, Institute of Child Health, University College London) for MRI performance and toxicity, together with the Gd-complexes of some of the monomers and model compounds previously prepared. First, a synthetic protocol was set up for the efficient synthesis of Gd-complexes. Then, complexes **83-86** were prepared and fully characterised, which are also novel MRI contrast agents. Measurements of longitudinal and transversal relaxation rate were carried out for compounds **83-85** (**86** exhibited limited water solubility), allowing the calculation of the corresponding relaxivities. The average $r_1$ values (more significant for $T_1$-agents such as Gd-complexes) obtained for **84** and **85** (1.90 and 1.65 $mM^{-1}s^{-1}$, respectively) were close to those (few) reported in the literature for other DOTA-tetra-amides (2.5 $mM^{-1}s^{-1}$ for both DOTMA and DTMA;[284] 1.88 $mM^{-1}s^{-1}$ for DOTA-tetra-benzylamide[273]). The value calculated for **83** (average 4.35 $mM^{-1}s^{-1}$) was almost double. Relaxation enhancement tests were also carried out for some of the cycloaddition products (**GdC**$_{1.5:1}$, **GdT**$_{1:2}$, **GdT**$_{1:4}$ and **GdT**$_{1:6}$), selected on the basis of their water solubility and molecular weight distribution. Despite their relatively low molecular weights, the oligomers showed a significant increase in relaxivity (3.07, 2.50, 2.28, 2.65 $mM^{-1}s^{-1}$ respectively) in respect to the corresponding monomer (**85**, 1.65 $mM^{-1}s^{-1}$), which is one of the aims of the present project.

The other main target, i.e. low or ideally lack of toxicity, was first tested for complexes **83-85** by incubating stem cells with solutions at different concentration of each species. The cell viability was tested first by qualitative visual check of the health conditions of cells, and then quantitatively by Alamar Blue and Methylene Blue assays, which evaluate the cell survival from different parameters (metabolic activity or cell number). For complexes **83-85** the global assessment was very satisfactory: **83** was shown to be safe for ST14A cells up to 7 mM concentration, while cells survived in solutions of **84** and **85** up to 4 mM concentration, as compared to the usual 1-100 μM concentration range for viable *in vitro* experiments. Similar evaluations for the oligomers were affected by their ability to interact/react with some components of the culture medium (DMEM) by forming insoluble aggregates/products. However, preliminary studies[475] on the oligomers from cycloadditions of ligand **53** partially loaded with $Gd^{III}$ led to promising outcomes, such products being safe at least in a range of 0.01-0.1 mM.

Therefore, both the relaxivity determinations and the toxicity tests for the products obtained through the planned methodology are compatible and encouraging for the application of these and next species as MRI contrast agents for stem cells labelling.

## 5.2 Perspectives and future work

As an explorative work, the achievements discussed in the present thesis have to be seen also as preliminary results to be used as a basis for future applications in the synthesis of hyperbranched polymeric contrast agents and the monomers necessary to obtain them.

The obtained Gd-complexes (both from ligands and oligomeric species) could be further characterised: for instance, the former in terms of their stability constant, water exchange rate etc.; the latter in their size.

A variety of DOTA-derivatives can be designed to prepare a library and test the effectiveness of the corresponding Gd-complexes as both contrast agents and monomers for the formation of polymeric species. The protocols which have been optimised should allow (when run in parallel) the aimed tetra-substitution on cyclen. The characterisation and the properties exhibited by the compounds reported herein can address the choice on what functionalities it is preferable to add onto the monomers/ligands.

Different polymerisation reactions can be planned with either the monomers already synthesised (for example, DOTA-propargylamide **53** might be used in Sonogashira couplings) or with newly-synthesised monomers (maybe preferring mildly reactive moieties to highly reactive ones such as styryl groups). In the latter case, the choice would be between either trying to solve some of the difficulties encountered with the attempted polymerisations reported herein (e.g., a DOTA-tetra-azide might solve the problem of the possible coordinative saturation of the $Cu^{I}$-catalyst by tetra-propargylamides **53, 73** or **85**) or planning different procedures (e.g. polyesterifications, ROMPs etc.).

Relaxivity tests would allow determination of a trend between the molecular weight of the obtained polymers and the observed relaxation enhancements.

Finally, the toxicity screenings would ensure that stem cells can be safely cultured with the novel agents for labelling.

# 6. Experimental Part

## 6.1 Synthetic Chemistry

### 6.1.1 General

All reactions requiring anhydrous conditions or involving moisture sensitive reactants were performed under an atmosphere of dry nitrogen using oven dried (80 °C) and/or flame dried glassware.

Reactants, reagents and special solvents were obtained from commercial suppliers and were used without further purification: europium(III) chloride hexahydrate (99.99%), methylthymol blue tetrasodium salt (MTB) from Acros Organics; allylamine (98+%), 4-aminostyrene (97%), L-ascorbic acid disodium salt (99%), bromoacetic acid (98+%), 1,2-bis(chloroethoxy)ethane (97%), *tert*-butanol (99+%), cesium carbonate (99+%), chloroacetyl chloride (98%), di-*tert*-butyl dicarbonate (97+%), ethyl bromoacetate (98%), gadolinium(III) chloride hexahydrate (99.9%), *N*-hydroxysuccinimide (NHS, 98+%), potassium hydrogen sulphate (97%) from Alfa Aesar Lancaster; benzotriazol-1-yloxytris(dimethylamino)phosphonium hexafluorophosphate (BOP), deuterium oxide (99.92%), *N*,*N*-dimethylformamide-$d_7$ (99.5%) from Apollo; 1,2-diaminoethane (99%), 1-(3-dimethylaminopropyl)-3-ethylcarbodiimide hydrochloride (EDC·HCl, 98+%), 4-dimethylaminopyridine (DMAP, 99%), 2-mercaptoethylamine hydrochloride (98+%), triethylamine (99%) from Avocado; ammonium acetate, ammonium hydroxide (25% aqueous solution), copper(II) sulphate pentahydrate (98%), ethylenediaminetetraacetic acid disodium salt dihydrate (EDTA), hydrochloric acid (35%), magnesium sulphate, potassium carbonate, potassium iodide, sodium carbonate, sodium chloride, sodium hydrogen carbonate, sodium hydroxide, sodium sulphate from BDH; bromoacetyl bromide (98+%), 4-vinylbenzyl chloride (90%) from Fisher; benzylamine (95+%) from Fluka; *O*-(Benzotriazol-1-yl)-*N*,*N*,*N*′,*N*′-tetramethyluronium tetrafluoroborate (TBTU, 97%), benzyl bromide (98%), *n*-butylamine (99.5%), 2-[2-(2-chloroethoxy)ethoxy]ethanol (96%), *N*,*N*-diisopropylethylamine (99%), anhydrous *N*,*N*-dimethylformamide (99.8%), fluorescein isothiocyanate isomer I (FITC, 90%), Grubbs catalyst 2$^{nd}$ generation, hexamethylenetetramine (urotropine, 99+%), 1-hydroxybenzotriazole (HOBt, less than 5% water), 2-mercaptoethanol (99%), methyl bromoacetate (97%), propargylamine (98%), sodium azide (99%), trifluoroacetic acid (99+%), zinc perchlorate hexahydrate

from Sigma-Aldrich; 1,4,7,10-tetraazacyclododecane (cyclen, 98%) from Strem; chloroform-$d_1$, dimethyl sulphoxide-$d_6$ from VWR.

All common solvents were of AnalaR® grade from BDH and were dried in accordance with known protocols.[477, 478]

All reaction temperatures reported indicate the temperature of the bath in contact with the reaction vessel.

The presence of free (i.e. unreacted) gadolinium(III) ions during complexation reactions was checked by adding a small volume (approximately 0.2 ml) of reaction mixture to a sample tube containing 0.2 ml of a 0.2% aqueous solution of methylthymol blue[461, 462] and 2 ml of a pH 6 buffer, chosen indifferently among the following: a urotropine buffer (prepared from a 1 M solution of urotropine and by dropwise addition of 0.1 M HCl until a pH value of 6 was reached); an acetate buffer (prepared by mixing 10.4 ml of a 0.1 M solution of acetic acid and 189.6 ml of a 0.1 M solution of sodium acetate); a phosphate buffer (prepared by mixing 100 ml of a 0.1 M solution of $KH_2PO_4$ and 11.2 ml of a 0.1 M solution of NaOH). In a few cases the same test was repeated using different buffers, and the same results were obtained. The change of the solution colour from yellow into blue indicates the presence of free $Gd^{III}$ ions, whilst its persistence confirms the absence of such ions.

Flash column chromatography was performed using Merck-Kieselgel BDH $F_{254}$ (230-400 mesh). Either anhydrous or non-anhydrous solvents were used.

Routine monitoring of reactions were performed using analytical thin layer chromatography on pre-coated Merck Kieselgel 60 $F_{254}$ aluminium-backed plates, using potassium permanganate or iodine as visualisation reagents.

Samples were sonicated in a VWR USC600T ultrasonic bath (5.40 l, 260 W).

Dialyses were performed using Spectra/Por 7 regenerated cellulose dialysis membranes with molecular weight cut-off values of 500, 2000 and 25000 Da. The membranes were stored at 4 °C immersed in 0.1% solution of sodium azide. Before use, tubing of the needed length was cut and washed with distilled water, then soaked in 1 litre of distilled water for 30 minutes and rinsed again thoroughly. Dialyses were carried out by loading the bag with the amount of product dissolved in the minimum volume of distilled water necessary to dissolve it. The bag was sealed and placed in a beaker with 1 litre of distilled water, which was stirred for 14 hours. The external solution was replaced with the same volume of distilled water and evaporated under reduced pressure

or by lyophilisation. The residue (if any) was analysed by the suitable analytical techniques. The procedure was repeated 2-3 times.

Lyophilisation was achieved by using a Christ Alpha 1-2 LD lyophiliser.

"Aqueous GPC" analyses were performed by Smithers Rapra on a Viscotek "Evolve" Integrated GPC System fitted with an Aquagel guard plus 2 x mixed-OH (30 cm, 8 μm) columns, a Viscotek TDA301 (Triple Detector Array) detector unit, a Viscotek VE 7510 De-gasser, a Viscotek 1121 Solvent Pump and a Viscotek 5200 Autosampler. 0.3 M $NaNO_3$ + 0.01 M $NaH_2PO_4$ (pH 3) was used as mobile phase at a flow rate of 1.0 ml/min at 30 °C. Poly(ethylene oxide) standards were used for calibration. The data were collected and analysed using Polymer Laboratories Cirrus Multi Online GPC/SEC software v.2.0. Solutions for each sample were prepared by adding 10 ml of eluent to 20 mg of sample and leaving overnight to dissolve. The solutions were thoroughly mixed and then filtered through a Whatman Mini Uniprep Filter 0.45 μm PVDF membrane (Scientific Laboratory Supplies Ltd).

"DMF-GPC" analyses were performed by using a Viscotek 4 capillary bridge viscometer, PLgel 5μm MIXED-D 300x7.5mm column (styrene-divinylbenzene co-polymer). DMF + 1 v% $Et_3N$ + 1 v% AcOH was used as mobile phase at a flow rate of 0.5 ml/min at 40 °C. The DMF was Sigma Aldrich HPLC grade, AcOH and $Et_3N$ were Fisher HPLC grade. Poly(methyl methacrylate) standards ($M_n$ 2680, 5200, 10260, 30650, 60150, 138500, 300300 Da) were used for calibration. The data were acquired *via* a PL DataStream 24 bit high resolution, ultra low noise external interface and analysed using Polymer Laboratories Cirrus Multi Online GPC/SEC software v.2.0. Solutions for each sample were prepared by adding 1 ml of eluent to 2 mg of sample and leaving overnight to dissolve. The solutions were thoroughly mixed and then filtered through a Whatman Mini Uniprep Filter 0.2 μm PTFE membrane (Scientific Laboratory Supplies Ltd).

Elemental analyses were performed by the Elemental Analysis Service at London Metropolitan University. The figures reported are the average of two separate measurements.

All $^1H$ NMR spectra were recorded as solutions in specified deuterated solvents on a Bruker 2 channel DRX-400 spectrometer at Imperial College London, Department of Chemistry, NMR Service Facility, using the residual protic solvent signal as internal reference. Chemical shifts are expressed in parts per million (ppm, δ) using TMS as internal standard and are referenced to the indicated solvent. Coupling constants were

measured in Hz. Splitting patterns are designated as *s* for singlet, *d* for doublet, *t* for triplet, *q* for quartet, *m* for multiplet and *br* for broad. $^{13}C$ NMR spectra were recorded on a Bruker 2 channel DRX-400 spectrometer as solutions in specified deuterated solvents. Chemical shifts are reported in parts per million (ppm, δ) downfield from TMS and are referenced to the centre line of the specified solvent as internal standard.

FT-IR spectra were recorded on a Perkin-Elmer Spectrum RX FT-IR spectrometer with built-in internal calibration. The compound to analyse was either pressed together with fine anhydrous potassium bromide to obtain a disk, or added as a thin layer between KBr pellets. Results are reported in wave numbers ($cm^{-1}$).

Mass spectra were recorded under $CI^+$ or $FAB^+$ conditions on a Micromass AutoSpec Premier instrument, or $ESI^+$ conditions using a Micromass LCT Premier instrument at Imperial College London, Department of Chemistry, Mass Spectrometry Service Facility.

Melting points were obtained using a GallenKamp melting point apparatus and are uncorrected.

### 6.1.2 Experimental details

**1,4,7,10-Tetrakis(methoxycarbonylmethyl)-1,4,7,10-tetraazacyclododecane 30**

***Method I***

Cyclen (0.136 g, 0.792 mmol) and anhydrous $K_2CO_3$ (1.00 g) were suspended in dry MeCN (50 ml) and stirred for 15 min. Methyl bromoacetate (0.38 ml, 4.0 mmol) was added and the mixture heated at reflux for 48 hours. After cooling, the inorganic solids were filtered off and the solvent removed from the filtrate under reduced pressure. The yellow coloured crude product was partially purified by column chromatography ($SiO_2$, $CHCl_3$/EtOH 90:10 v/v, $R_f$ 0.29). The white solid obtained was characterised without further purification (crude yield: 0.219 g, 0.477 mmol, 60%).

M.p.: 155-157 °C. $CI^+$ MS, m/z: 461 ($[M+H]^+$; calculated 461.2611, found 461.2614). $FAB^+$ MS, m/z: 483 ($[M+Na]^+$; calculated 483.2431, found 483.2451), 461 ($[M+H]^+$; calculated 461.2611, found 461.2633). IR (KBr disk), $cm^{-1}$: 2966, 2852, 1721, 1460, 1385, 1355, 1312, 1290, 1258, 1213, 1155, 1087, 1010, 978, 911, 829, 776, 689, 622. $^1H$ NMR (400 MHz, 25 °C, $CDCl_3$), δ (ppm): 3.74 (s, 12H, $OCH_3$), 3.19 (br s, 8H,

$NCH_2CO$), 2.35 (br s, 16H, $NCH_2CH_2N$). $^{13}C$ NMR (100 MHz, 25 °C, $CDCl_3$), δ (ppm): 174.1 (CO), 55.0 ($OCH_3$), 52.2 ($N\underline{C}H_2CO$), 51.4 (br, $NCH_2CH_2N$).

***Method II***

Cyclen (0.100 g, 0.580 mmol), anhydrous $Cs_2CO_3$ (0.945 g, 2.90 mmol) and anhydrous KI (0.481 g, 2.90 mmol) were suspended in dry DMF (40 ml) and stirred for 15 min. Methyl bromoacetate (0.27 ml, 2.9 mmol) was added and the mixture was heated at 80 °C for 18 h. After cooling, undissolved solids were filtered, and the solvent removed from the filtrate under reduced pressure. The yellow coloured crude product was partially purified by column chromatography ($SiO_2$, $CHCl_3$/EtOH 90:10 v/v, $R_f$ 0.37) and recrystallised from MeOH with $Et_2O$. The white solid obtained was characterised without further purification (crude yield: 0.128 g , 0.279 mmol, 48%).

M.p.: 154-156 °C. $CI^+$ MS, m/z: 461 ($[M+H]^+$; calculated 461.2611, found 461.2605). $FAB^+$ MS, m/z: 483 ($[M+Na]^+$). IR (KBr disk), $cm^{-1}$: 2957, 2826, 1725, 1453, 1379, 1307, 1266, 1214, 1180, 1118, 1104, 1015, 968, 958, 887, 848, 806, 778, 715, 600. $^1H$ NMR (400 MHz, 25 °C, $CDCl_3$), δ (ppm): 3.75 (s, 12H, $CH_3$), 3.26 (br s, 16H, $NCH_2CH_2N$), 2.35 (br s, 8H, $NCH_2CO$). $^{13}C$ NMR (100 MHz, 25 °C, $CDCl_3$), δ (ppm): 174.1 (CO), 55.0 ($N\underline{C}H_2CO$), 52.3 ($CH_3$), 51.1 (br, $NCH_2CH_2N$).

**1,4,7,10-Tetrakis(ethoxycarbonylmethyl)-1,4,7,10-tetraazacyclododecane 31**

***Method I***

Cyclen (0.119 g, 0.6890 mmol) and anhydrous $K_2CO_3$ (1 g) were suspended in dry MeCN (50 ml) and stirred for 15 min. Ethyl bromoacetate (0.38 ml, 3.5 mmol) was added and the mixture was heated at reflux for 17 h. After cooling, undissolved solids were filtered, and the solvent removed from the filtrate under reduced pressure. The yellow coloured crude product was purified by column chromatography ($SiO_2$, $CHCl_3$/EtOH 90:10 v/v, $R_f$ 0.39) and recrystallised from EtOH with $Et_2O$. Yield: 0.185 g (0.359 mmol, 52%).

M.p.: 207-208 °C. Elemental analysis: calculated ($C_{24}H_{44}N_4O_8 \cdot K_2CO_3$) C 45.85%, H 6.77%, N 8.56%; found C 45.65%, H 6.82%, N 8.37%. $CI^+$ MS, m/z: 517 ($[M+H]^+$; calculated 517.3237, found 517.3244). IR (KBr disk), $cm^{-1}$: 2974, 2843, 1723, 1459, 1383, 1308, 1252, 1215, 1176, 1112, 1102, 1020, 973, 921, 894, 860, 773, 603. $^1H$ NMR (400 MHz, 25 °C, $CDCl_3$), δ (ppm): 4.16 (q, $^3J_{HH}$ = 7.2 Hz, 8H, $OCH_2$), 3.18

(br s, 8H, $NCH_2CO$), 2.34 (br s, 16H, $NCH_2CH_2N$), 1.25 (t, $^3J_{HH}$ = 7.2 Hz, 12H, $CH_3$). $^{13}C$ NMR (100 MHz, 25 °C, $CDCl_3$), δ (ppm): 173.6 (CO), 61.2 ($OCH_2$), 55.2 ($N\underline{C}H_2CO$), 51.5 (br, $NCH_2CH_2N$), 14.1 ($CH_3$).

***Method II***

Cyclen (0.107 g, 0.620 mmol), anhydrous $Cs_2CO_3$ (1.131 g, 3.472 mmol) and anhydrous KI (0.576 g, 3.47 mmol) were suspended in dry DMF (40 ml) and stirred for 15 min. Ethyl bromoacetate (0.28 ml, 2.5 mmol) was added and the mixture was heated at 80 °C for 18 h. After cooling, undissolved solids were filtered, and the solvent removed from the filtrate under reduced pressure. The yellow coloured crude product was purified by column chromatography ($SiO_2$, $CHCl_3$/EtOH 90:10 v/v, $R_f$ 0.37) and recrystallised from EtOH with $Et_2O$. Yield: 0.250 g (0.484 mmol, 78%).

M.p.: 207-209 °C. Elemental analysis: calculated ($C_{24}H_{44}N_4O_8 \cdot CsHCO_3$) C 42.26%, H 6.38%, N 7.88%; found C 42.54%, H 5.28%, N 7.97%. $CI^+$ MS, m/z: 517 ($[M+H]^+$; calculated 517.3237, found 517.3228). $FAB^+$ MS, m/z: 539 ($[M+Na]^+$). IR (KBr disk), $cm^{-1}$: 2974, 2843, 1723, 1459, 1383, 1308, 1252, 1215, 1176, 1112, 1102, 1020, 973, 921, 894, 860, 773, 603. $^1H$ NMR (400 MHz, 25 °C, $CDCl_3$), δ (ppm): 4.18 (q, $^3J_{HH}$ = 7.2 Hz, 8H, $OCH_2$), 3.22 (br s, 8H, $NCH_2CO$), 2.37 (br s, 16H, $NCH_2CH_2N$), 1.27 (t, $^3J_{HH}$ = 7.2 Hz, 12H, $CH_3$). $^{13}C$ NMR (100 MHz, 25 °C, $CDCl_3$), δ (ppm): 173.7 (CO), 61.2 ($OCH_2$), 55.2 ($N\underline{C}H_2CO$), 51.5 (br, $NCH_2CH_2N$), 14.1 ($CH_3$).

**1,4,7,10-Tetraazacyclododecane-1,4,7,10-tetraacetic acid (DOTA) 2**[124, 205]

Cyclen (0.364 g, 2.114 mmol) and bromoacetic acid (1.264 g, 9.098 mmol) were stirred in distilled water (25 ml) for 10 min. The pH of the solution was adjusted to 10 by dropwise addition of 5 M NaOH solution, and the resulting mixture was heated at 70 °C. The pH of the solution was maintained at approximately 10 throughout the reaction time (8 h). After cooling, the pH of the reaction mixture was brought down to 2 using concentrated HCl, and the solution was concentrated to dryness under reduced pressure. The white solid residue was purified by recrystallisation from $H_2O$ with acetone. Yield: 0.623 g (1.54 mmol, 73%).

Mp: 245 °C. Elemental analysis: calculated ($C_{16}H_{28}N_4O_8 \cdot HBr$) C 39.60%, H 6.02%, N 11.54%; found C 38.60%, H 6.78%, N 10.74%. $FAB^+$ MS, m/z: 853 ($[2M+2Na-H]^+$), 831 ($[2M+Na]^+$), 449 ($[M+2Na-H]^+$), 427 ($[M+Na]^+$), 405 ($[M+H]^+$). IR (KBr disk), $cm^{-1}$: 3099, 2853, 1682, 1460, 1354, 1313, 1291, 1250, 1155, 1087,

1011, 980, 911, 829, 776, 767, 689, 621. $^{1}$H NMR (400 MHz, 25 °C, $D_2O$), δ (ppm): 3.73 (br s, 8H, $NCH_2CO$), 3.26 (br s, 16H, $NCH_2CH_2N$). $^{13}$C NMR (100 MHz, 25 °C, $D_2O$), δ (ppm): 174.4 (CO), 57.5 (br, 8H, $NCH_2CO$), 52.8 (br, $NCH_2CH_2N$). $^{1}$H NMR (400 MHz, 25 °C, DMSO-$d_6$), δ (ppm): 12.88 (br s, 4H), 7.41 (br s, 2H), 3.68 (br s, 8H, $NCH_2CO$), 3.01 (br s, 16H, $NCH_2CH_2N$).

**_N_-Butyl-2-chloroacetamide 39[289]**

Chloroacetyl chloride (0.80 ml, 10 mmol) in dry THF (2 ml) was cooled to -10 °C on an ice bath. A solution of dry *n*-butylamine (1.00 ml, 10.0 mmol) and dry $Et_3N$ (1.39 ml, 10.0 mmol) in dry THF (2 ml) was added dropwise over 1 hour at -10 °C. The mixture was left stirring for 1 h. After removal of the solvent under reduced pressure, 0.1 M HCl (15 ml) was added, and the product was extracted with $CHCl_3$ (3x5 ml). The organic phase was dried over anhydrous $MgSO_4$. After evaporation of the solvent under reduced pressure, the resulting yellow oil was distilled under reduced pressure, and the pure product was obtained as a colourless oil in 84% yield (1.260 g, 8.424 mmol).

Elemental analysis: calculated C 48.17%, H 8.08%, N 9.36%; found C 48.12%, H 7.95%, N 9.26%. $CI^+$ MS, m/z: 167 ($[M+NH_4]^+$), 150 ($[M+H]^+$; calculated 150.0686, found 150.0682). IR (film on KBr pellets), $cm^{-1}$: 3296, 3088, 2960, 2934, 2874, 1660, 1548, 1465, 1439, 1259, 1237, 1156, 786, 692, 573. $^{1}$H NMR (400 MHz, 25 °C, $CDCl_3$), δ (ppm): 6.57 (br s, 1H, NH), 4.04 (s, 2H, $ClCH_2CO$), 3.31 (m, 2H, $CONHC\underline{H}_2$), 1.53 (m, 2H, $C\underline{H}_2CH_2CH_3$), 1.37 (m, 2H, $C\underline{H}_2CH_3$), 0.93 (t, $^{3}J_{HH}$ = 7.3 Hz, 3H, $CH_3$). $^{13}$C NMR (100 MHz, 25 °C, $CDCl_3$), δ (ppm): 165.7 (CO), 42.7 ($ClCH_2$), 39.6 ($\underline{C}H_2NH$), 31.3 ($\underline{C}H_2CH_2CH_3$), 20.0 ($\underline{C}H_2CH_3$), 13.7 ($CH_3$).

**1,4,7,10-Tetrakis(butylcarbamoylmethyl)-1,4,7,10-tetraazacyclododecane 32**

***Method I***

1,4,7,10-Tetrakis(ethoxycarbonylmethyl)-1,4,7,10-tetraazacyclododecane (0.100 g, 0.194 mmol) was dissolved in dry DCM (2 ml) and added dropwise to dry *n*-butylamine (10 ml). The solution was stirred at 80 °C for 18 h. After removal of the solvent under reduced pressure, the yellow solid was suspended in distilled water (30 ml) and extracted with $CHCl_3$ (3x10 ml). The organic phase was dried over anhydrous $Na_2CO_3$ and the solvent removed under reduced pressure. The residue was purified by

recrystallisation from hot dry MeCN, yielding 0.109 g of white solid (0.179 mmol, 92%).

M.p.: 158 °C. Elemental analysis: calculated C 61.50%, H 10.32%, N 17.93%; found C 61.61%, H 10.20%, N 17.81%. $FAB^+$ MS, m/z: 625 ($[M+H]^+$; calculated 625.5129, found 625.5143), 647 ($[M+Na]^+$). IR (KBr disk), $cm^{-1}$: 3298, 3078, 2958, 2932, 2874, 2817, 1659, 1553, 1465, 1361, 1299, 1275, 1234, 1142, 1099, 1001, 981, 720, 569. $^1H$ NMR (400 MHz, 25 °C, $CDCl_3$), δ (ppm): 7.14 (br s, 4H, NH), 3.22 (m, 8H, $NHC\underline{H}_2CH_2CH_2CH_3$), 3.07 (br s, 8H, $NCH_2CO$), 2.70 (br s, 16H, $NCH_2CH_2N$), 1.47 (m, 8H, $NHCH_2C\underline{H}_2CH_2CH_3$), 1.33 (m, 8H, $NHCH_2CH_2C\underline{H}_2CH_3$), 0.92 (t, $^3J_{HH}$ = 7.3 Hz, 12H, $CH_3$). $^{13}C$ NMR (100 MHz, 25 °C, $CDCl_3$,), δ (ppm): 170.6 (CO), 59.3 ($N\underline{C}H_2CO$), 53.3 (br, $NCH_2CH_2N$), 39.1 ($NH\underline{C}H_2CH_2CH_2CH_3$), 31.8 ($NHCH_2\underline{C}H_2CH_2CH_3$), 20.2 ($NHCH_2CH_2\underline{C}H_2CH_3$), 13.7 ($CH_3$).

***Method II***

DOTA (0.100 g, 0.247 mmol) and dry $Et_3N$ (0.28 ml, 2.0 mmol) were dissolved in a 1:1 v/v mixture of dry DMF and $CHCl_3$ (10 ml). Dry *n*-butylamine (0.11 ml, 1.1 mmol) and BOP (0.486 g, 1.10 mmol) were added, and the mixture was stirred at room temperature for 24 h. After removal of the solvent under reduced pressure, the yellow solid was suspended in distilled water (30 ml) and extracted with $CHCl_3$ (3x10 ml). The organic phase was dried over anhydrous $Na_2SO_4$ and the solvent evaporated under vacuum, yielding a pale yellow solid with a crude yield of 0.112 g (0.178 mmol, 72%). Further attempts of purification were unsuccessful.

$^1H$ NMR (400 MHz, 25 °C, $CDCl_3$), δ (ppm): 6.71 (br s, 4H, NH), 3.19 (m, 8H, $NHC\underline{H}_2CH_2CH_2CH_3$), 3.00 (br s, 8H, $NCH_2CO$), 2.56 (br s, 8H, $NC\underline{H}_2CH_2N$), 2.37 (br s, 8H, $NCH_2C\underline{H}_2N$), 1.47 (m, 8H, $NHCH_2C\underline{H}_2CH_2CH_3$), 1.30 (m, 8H, $NHCH_2CH_2C\underline{H}_2CH_3$), 0.88 (t, $^3J_{HH}$ = 7.4 Hz, 12H, $CH_3$). $^{13}C$ NMR (100 MHz, 25 °C, $CDCl_3$), δ (ppm): 170.9 (CO), 57.3 ($N\underline{C}H_2CO$), 50.3 (br, $NCH_2CH_2N$), 39.3 ($NH\underline{C}H_2CH_2CH_2CH_3$), 31.4 ($NHCH_2\underline{C}H_2CH_2CH_3$), 20.0 ($NHCH_2CH_2\underline{C}H_2CH_3$), 13.7 ($CH_3$).

***Method III***[289]

Cyclen (0.100 g, 0.580 mmol), $Cs_2CO_3$ (0.945 g, 2.90 mmol), KI (0.481 g, 2.90 mmol) and *N*-butyl-2-chloroacetamide **39** (0.434 g, 2.91 mmol) were suspended in dry DMF (20 ml) and heated at 70 °C for 15 h. After removal of the solvent under reduced

pressure, the residue was suspended in distilled water (20 ml) and the product extracted with $CHCl_3$ (5x10 ml). The organic phase was dried over anhydrous $Na_2CO_3$ and the solvent was evaporated under reduced pressure. The brown residue was purified by recrystallisation from hot dry MeCN, yielding the desired product in 69% yield (0.250 g, 0.401 mmol).

M.p.: 159 °C. Elemental analysis: calculated C 61.50%, H 10.32%, N 17.93%; found C 61.54%, H 10.30%, N 17.88%. $FAB^+$ MS, m/z: 625 ($[M+H]^+$; calculated 625.5129, found 625.5145), 647 ($[M+Na]^+$). IR (KBr disk), $cm^{-1}$: 3298, 2958, 2932, 2872, 2819, 1657, 1552, 1450, 1370, 1308, 1272, 1235, 1106, 1000, 714, 594. $^1H$ NMR (400 MHz, 25 °C, $CDCl_3$), δ (ppm): 7.11 (br s, 4H, NH), 3.25 (m, 8H, $NHC\underline{H}_2CH_2CH_2CH_3$), 3.07 (br s, 8H, $NCH_2CO$), 2.59 (br s, 16H, $NCH_2CH_2N$), 1.49 (m, 8H, $NHCH_2C\underline{H}_2CH_2CH_3$), 1.34 (m, 8H, $NHCH_2CH_2C\underline{H}_2CH_3$), 0.92 (t, $^3J_{HH}$ = 7.4 Hz, 12H, $CH_3$). $^{13}C$ NMR (100 MHz, 25 °C, $CDCl_3$), δ (ppm): 170.5 (CO), 58.4 ($N\underline{C}H_2CO$), 50.7 (br, $NCH_2CH_2N$), 39.2 ($NH\underline{C}H_2CH_2CH_2CH_3$), 31.6 ($NHCH_2\underline{C}H_2CH_2CH_3$), 20.1 ($NHCH_2CH_2\underline{C}H_2CH_3$), 13.7 ($CH_3$).

**_N_-(*Tert*-butoxycarbonyl)-1,2-diaminoethane 40**

***Method I*[327]**

A solution of di-*tert*-butyl-dicarbonate (0.500 g, 2.29 mmol) in dry dioxane (20 ml) was added over a period of 1 hour to a solution of 1,2-diaminoethane (1.22 ml, 18.3 mmol) in dry dioxane (20 ml). After addition, the mixture was allowed to stir for 15 h at room temperature and then the solvent was evaporated to dryness. The residue was suspended in water (30 ml) and filtered. The filtrate was extracted with DCM (3x10 ml) and the organic phase was dried over anhydrous $Na_2SO_4$. The solvent was removed under reduced pressure, leading to the desired product as a colourless oil in 62% yield (0.227 g, 1.42 mmol).

Elemental analysis: calculated C 52.48%, H 10.07%, N 17.48%; found C 52.38%, H 9.95%, N 17.36%. $CI^+$ MS, m/z: 161 ($[M+H]^+$; calculated 161.1290, found 161.1287). IR (film on KBr pellets), $cm^{-1}$: 3359, 2976, 2932, 2869, 1703, 1526, 1391, 1365, 1275, 1251, 1173, 1043, 954, 873, 781. $^1H$ NMR (400 MHz, 25 °C, $CDCl_3$), δ (ppm): 4.97 (br s, 1H, NH), 3.15 (q, $^3J_{HH}$ = 5.8 Hz, 2H, $C\underline{H}_2NH$), 2.78 (t, $^3J_{HH}$ = 5.8 Hz, 2H, $C\underline{H}_2NH_2$), 1.67 (br s, 2H, $NH_2$), 1.42 (s, 9H, $CH_3$). $^{13}C$ NMR (100 MHz, 25 °C,

$CDCl_3$), δ (ppm): 156.2 (CO), 79.2 ($\underline{C}(CH_3)_3$), 43.3 ($CH_2NH$), 41.8 ($CH_2NH_2$), 28.4 ($CH_3$).

***Method II*[328-330]**

A solution of di-*tert*-butyl-dicarbonate (0.500 g, 2.29 mmol) in dry DCM (20 ml) was added at 0 °C over a period of 1 hour to a solution of 1,2-diaminoethane (1.22 ml, 18.3 mmol) in dry DCM (20 ml). After addition, the mixture was allowed to stir for 24 h at room temperature and then washed with brine (1x15 ml) and water (2x15 ml). The organic phase was dried over anhydrous $Na_2SO_4$ and filtered. The solvent was removed from the filtrate under reduced pressure, leading to the desired product as a colourless oil in 89% yield (0.328 g, 2.04 mmol).

Elemental analysis: calculated C 52.48%, H 10.07%, N 17.48%; found C 52.46%, H 9.99%, N 17.42%. $CI^+$ MS, m/z: 161 ($[M+H]^+$; calculated 161.1290, found 161.1287). $^1H$ NMR (400 MHz, 25 °C, $CDCl_3$), δ (ppm): 5.15 (br s, 1H, NH), 3.16 (m, 2H, $C\underline{H}_2NH$), 2.79 (t, $^3J_{HH}$ = 5.9 Hz, 2H, $C\underline{H}_2NH_2$), 2.58 (br s, 2H, $NH_2$), 1.41 (s, 9H, $CH_3$). $^{13}C$ NMR (100 MHz, 25 °C, $CDCl_3$), δ (ppm): 156.2 (CO), 79.2 ($\underline{C}(CH_3)_3$), 42.8 ($CH_2NH$), 41.5 ($CH_2NH_2$), 28.4 ($CH_3$).

**2-[(Phenylmethyl)thio]ethanamine 42[331]**

2-Aminoethanethiol hydrochloride (0.200 g, 1.77 mmol) and anhydrous $K_2CO_3$ (0.486 g, 3.52 mmol) were suspended in dry methanol (10 ml). The mixture was heated to 80 °C. Benzyl bromide (0.21 ml, 1.8 mmol) in dry methanol (5 ml) was added dropwise, and the mixture was stirred at 80 °C for 15 h. The solvent was removed under reduced pressure, and the residue was suspended in 30 ml of 10% $NaHCO_3$ and extracted with $CHCl_3$ (3x10 ml). The organic phase was dried over anhydrous $Na_2CO_3$ and the solvent was evaporated, yielding a colourless oil. After chromatography ($SiO_2$, $CHCl_3$/EtOH 90:10 v/v) the desired product was obtained in 54% yield (0.158 g, 0.946 mmol).

Elemental analysis: calculated C 64.62%, H 7.83%, N 8.37%; found C 64.80%, H 7.84%, N 8.31%. $CI^+$ MS, m/z: 168 ($[M+H]^+$), 335 ($[2M+H]^+$). IR (film on KBr pellets), $cm^{-1}$: 3366, 3288, 3060, 3027, 2916, 2857, 1601, 1493, 1453, 1240, 1071, 1027, 848, 753, 702, 564, 471. $^1H$ NMR (400 MHz, 25 °C, $CDCl_3$), δ (ppm): 7.30 (m, 4H, $H^o$+$H^m$), 7.24 (m, 1H, $H^p$), 3.71 (s, 2H, $PhC\underline{H}_2S$), 2.84 (br t, $^3J_{HH}$ = 6.3 Hz, 2H, $SC\underline{H}_2CH_2NH_2$), 2.55 (t, $^3J_{HH}$ = 6.3 Hz, 2H, $SCH_2C\underline{H}_2NH_2$), 2.09 (s, 2H, $NH_2$). $^{13}C$ NMR

(100 MHz, 25 °C, $CDCl_3$,), δ (ppm): 138.2 ($C^{ipso}$), 128.8 ($C^o$), 128.5 ($C^m$), 127.0 ($C^p$), 40.6 ($PhCH_2S$), 35.9 ($SCH_2CH_2NH_2$), 34.9 ($SCH_2CH_2NH_2$).

**_N,N'_-Ethylenebis(2-chloro-acetamide) 43**[333]

A solution of chloroacetyl chloride (2.00 ml, 25.1 mmol) in 5 ml of toluene was added dropwise to a solution of ethylenediamine (0.80 ml, 12.0 mmol) in 10 ml of 5 M NaOH on an ice-salt bath under vigorous stirring. After 3 hours the white precipitate was filtered and washed several times with water, then recrystallised from MeOH yielding 1.474 g (6.916 mmol, 58%) of pure product as a white solid.

Mp: 173 °C. Elemental analysis: calculated C 33.82%, H 4.73%, N 13.15%; found C 33.74%, H 4.81%, N 13.01%. $CI^+$ MS: m/z 213 ($[M]^+$), 230 ($[M+NH_4]^+$). IR (KBr disk), $cm^{-1}$: 3301, 2952, 1654, 1540, 1428, 1405, 1380, 1316, 1264, 1230, 1130, 1084, 948, 782, 751, 574, 459, 416. $^1H$ NMR (400 MHz, 25 °C, DMSO-$d_6$), δ (ppm): 8.26 (br s, 2H, NH), 4.04 (s, 4H, $ClCH_2$), 3.17 (m, 4H, $NHCH_2$). $^{13}C$ NMR (100 MHz, 25 °C, DMSO-$d_6$), δ (ppm): 166.0 (CO), 42.5 ($ClCH_2$), 38.4 ($NHCH_2$).

**_N,N'_-Ethylenebis(2-bromoacetamide) 44**[334]

A solution of bromoacetyl bromide (2.73 ml, 31.4 mmol) in 5 ml of toluene was added dropwise to a solution of ethylenediamine (1.00 ml, 15.0 mmol) in 13.5 ml of 5 M NaOH on an ice-salt bath under vigorous stirring. After 2 hours the white precipitate was filtered and washed with water (1x10 ml), then recrystallised from EtOH yielding 2.456 g (8.133 mmol, 54%) of **44** as a white solid..

$CI^+$ MS: m/z 303 ($[M+H]^+$), 320 ($[M+NH_4]^+$). IR (KBr disk), $cm^{-1}$: 3286, 2922, 1652, 1559, 1539, 1304, 1225, 701, 656, 552. $^1H$ NMR (400 MHz, 25 °C, DMSO-$d_6$), δ (ppm): 8.31 (br s, 2H, NH), 3.84 (s, 4H, $BrCH_2$), 3.15 (m, 4H, $NHCH_2$). $^{13}C$ NMR (100 MHz, 25 °C, DMSO-$d_6$), δ (ppm): 166.1 (CO), 38.4 ($ClCH_2$), 29.4 ($NHCH_2$).

**_N_-Allyl-2-chloroacetamide 47**

Chloroacetyl chloride (0.80 ml, 10.0 mmol) in dry THF (2 ml) was cooled to -10 °C on an ice bath. A solution of dry allylamine (0.75 ml, 10.0 mmol) and dry $Et_3N$ (1.39 ml, 10.0 mmol) in dry THF (2 ml) was added dropwise over 1 hour at -10 °C. The mixture was left stirring for 1 h. After removal of the solvent under reduced pressure, 0.1 M HCl (15 ml) was added, and the product was extracted with $CHCl_3$. The organic phase was dried over anhydrous $K_2CO_3$. After evaporation of the solvent under reduced

pressure, the resulting brown oil was distilled under reduced pressure at 100 °C, and the pure product was collected as a colourless oil in 67% yield (0.898 g, 6.72 mmol).

Elemental analysis: calculated C 44.96%, H 6.04%, N 10.49%; found C 45.01%, H 6.11%, N 10.51%. $CI^+$ MS, m/z: 151 ($[M+NH_4]^+$), 134 ($[M+H]^+$; calculated 134.0373, found 134.0375). IR (film on KBr pellets), $cm^{-1}$: 3296, 3083, 1664, 1545, 1419, 1324, 1261, 1240, 1154, 990, 923, 788, 696, 651, 565. $^1H$ NMR (400 MHz, 25 °C, $CDCl_3$), δ (ppm): 6.71 (br s, 1H, NH), 5.82 (m, 1H, $NHCH_2C\underline{H}$), 5.18 (m, 2H, $NHCH_2CHC\underline{H}_2$), 4.05 (s, 2H, $ClCH_2CO$), 3.92 (m, 2H, $NHC\underline{H}_2$). $^{13}C$ NMR (100 MHz, 25 °C, $CDCl_3$), δ (ppm): 165.7 (CO), 133.2 ($NHCH_2\underline{C}H$), 116.9 ($NHCH_2CH\underline{C}H_2$), 42.5 ($ClCH_2$), 42.0 ($NHCH_2$).

**_N_-Allyl-2-bromoacetamide 48**

Bromoacetyl bromide (2.00 ml, 23.0 mmol) in dry THF (10 ml) was cooled to -10 °C on an ice bath. A solution of dry allylamine (1.73 ml, 23.0 mmol) and dry $Et_3N$ (3.21 ml, 23.0 mmol) in dry THF (10 ml) was added dropwise over 1 hour at -10 °C. The mixture was left stirring for 1 h. After removal of the solvent under reduced pressure, 0.1 M HCl (30 ml) was added, and the product was extracted with $CHCl_3$ (3x10 ml). The organic phase was dried over anhydrous $K_2CO_3$. After evaporation of the solvent under reduced pressure, the resulting brown oil was distilled under reduced pressure at 100 °C, and the pure product was collected as a colourless oil in 69% yield (2.813 g, 15.80 mmol).

Elemental analysis: calculated C 33.73%, H 4.53%, N 7.87%; found C 33.62%, H 4.50%, N 7.94%. $CI^+$ MS, m/z: 178-180 ($[M+H]^+$; calculated 177.9868-179.9847 , found 177.9816-179.9834), 195-197 ($[M+NH_4]^+$). IR (film on KBr pellets), $cm^{-1}$: 3284, 3083, 1654, 1550, 1429, 1309, 1212, 1134, 990, 923, 845, 693, 641, 561. $^1H$ NMR (400 MHz, 25 °C, $CDCl_3$), δ (ppm): 6.57 (br s, 1H, NH), 5.86 (m, 1H, $NHCH_2C\underline{H}$), 5.21 (m, 2H, $NHCH_2CHC\underline{H}_2$), 3.93 (m, 2H, $NHC\underline{H}_2$), 3.91 (s, 2H, $BrCH_2CO$). $^{13}C$ NMR (100 MHz, 25 °C, $CDCl_3$), δ (ppm): 165.2 (CO), 133.2 ($NHCH_2\underline{C}H$), 116.9 ($NHCH_2CH\underline{C}H_2$), 42.5 ($NHCH_2$), 29.2 ($BrCH_2$).

**_N_-(2-Propargyl)-2-chloroacetamide 49**

Chloroacetyl chloride (4.03 ml, 50.6 mmol) in dry THF (30 ml) was cooled to -5 °C on an ice bath. A solution of dry propargylamine (3.47 ml, 50.6 mmol) and dry $Et_3N$ (7.05 ml, 50.6 mmol) in dry THF (30 ml) was added dropwise over 1 hour at -5 °C. The

mixture was left stirring for 1 h. After removal of the solvent under reduced pressure, 0.1 M HCl (40 ml) was added, and the product was extracted with $CHCl_3$ (3x20 ml). The organic phase was dried over anhydrous $K_2CO_3$. After evaporation of the solvent under reduced pressure, the resulting beige solid was purified by flash chromatography ($SiO_2$, EtOAc/*c*-Hex 50:50 v/v, $R_f$ 0.40), leading to the desired product as a white solid in 49% yield (3.268 g, 24.84 mmol).

Mp: 68 °C. Elemental analysis: calculated C 45.65%, H 4.60%, N 10.65%; found C 45.76%, H 4.68%, N 10.73%. $CI^+$ MS, m/z: 149 ($[M+NH_4]^+$), 132 ($[M+H]^+$; calculated 132.0216, found 132.0219), 280 ($[2M+NH_4]^+$), 263 ($[2M+H]^+$). IR (KBr disk), $cm^{-1}$: 3417, 3277, 3057, 2997, 2953, 2122, 1677, 1639, 1618, 1544, 1447, 1414, 1384, 1318, 1236, 1077, 1004, 931, 783, 696, 659. $^1H$ NMR (400 MHz, 25 °C, $CDCl_3$), δ (ppm): 6.77 (br s, 1H, NH), 4.11 (m, 2H, $NHC\underline{H}_2$), 4.07 (s, 2H, $ClCH_2CO$), 2.28 (t, $^3J_{HH}$ = 2.6 Hz, 1H, C≡CH). $^{13}C$ NMR (100 MHz, 25 °C, $CDCl_3$), δ (ppm): 165.6 (CO), 78.5 (C≡$\underline{C}$H), 72.2 ($\underline{C}$≡CH), 42.3 ($ClCH_2$), 29.6 ($NH\underline{C}H_2$).

**_N_-(2-Propargyl)-2-bromoacetamide 50**

Bromoacetyl bromide (2.00 ml, 23.0 mmol) in dry THF (12 ml) was cooled to -5 °C on an ice bath. A solution of dry propargylamine (1.58 ml, 23.0 mmol) and dry $Et_3N$ (3.21 ml, 23.0 mmol) in dry THF (12 ml) was added dropwise over 1 hour at -5 °C. The mixture was left stirring for 1 h. After removal of the solvent under reduced pressure, 0.1 M HCl (20 ml) was added, and the product was extracted with $CHCl_3$ (3x10 ml). The organic phase was dried over anhydrous $K_2CO_3$. After evaporation of the solvent under reduced pressure, the resulting beige solid was purified by flash chromatography ($SiO_2$, EtOAc/*c*-Hex 50:50 v/v, $R_f$ 0.46), leading to the desired product as a white solid in 59% yield (2.371 g, 13.47 mmol).

Mp (°C): 76 °C. Elemental analysis: calculated C 34.12%, H 3.44%, N 7.96%; found C 34.03%, H 3.40%, N 7.94%. $CI^+$ MS, m/z: 176-178 ($[M+H]^+$), 193-195 ($[M+NH_4]^+$; calculated 192.9976-194.9956, found 192.9976-194.9957), 370 ($[2M+NH_4]^+$). IR (KBr disk), $cm^{-1}$: 3287, 3232, 3047, 3006, 2956, 2841, 2125, 1670, 1637, 1540, 1446, 1406, 1307, 1278, 1215, 1072, 1004, 918, 890, 713, 691, 666, 639, 560, 510. $^1H$ NMR (400 MHz, 25 °C, $CDCl_3$), δ (ppm): 6.71 (br s, 1H, NH), 4.08 (dd, $^4J_{HH}$ = 2.5 Hz, $^3J_{HH}$ = 5.3 Hz, 2H, $NHC\underline{H}_2$), 3.89 (s, 2H, $BrCH_2CO$), 2.28 (t, $^4J_{HH}$ = 2.5 Hz, 1H, C≡CH). $^{13}C$ NMR (100 MHz, 25 °C, $CDCl_3$), δ (ppm): 165.1 (CO), 78.5 (C≡$\underline{C}$H), 72.2 ($\underline{C}$≡CH), 29.9 ($BrCH_2$), 28.6 ($NH\underline{C}H_2$).

**N-Styryl-2-chloroacetamide 51**

Chloroacetyl chloride (2.00 ml, 25.1 mmol) in dry THF (15 ml) was cooled to -5 °C on an ice bath. A solution of 4-aminostyrene (2.94 ml, 25.1 mmol) and dry $Et_3N$ (3.50 ml, 25.1 mmol) in dry THF (15 ml) was added dropwise over 1 hour at -5 °C. The mixture was left stirring for 1 h. After removal of the solvent under reduced pressure, 0.1 M HCl (30 ml) was added, and the product was extracted with chloroform (3x15 ml). The organic phase was dried over anhydrous $K_2CO_3$. After evaporation of the solvent under reduced pressure, the resulting beige solid was purified by flash chromatography ($SiO_2$, EtOAc/*c*-Hex 40:60 v/v, $R_f$ 0.49), leading to the desired product as a white solid in 55% yield (2.702 g, 13.81 mmol).

Mp: 138 °C. Elemental analysis: calculated C 61.39%, H 5.15%, N 7.16%; found C 61.38%, H 5.07%, N 7.14%. $FAB^+$ MS, m/z: 196 ($[M+H]^+$). IR (KBr disk), $cm^{-1}$: 3474, 3123, 1670, 1615, 1546, 1511, 1403, 1343, 1297, 1255, 1195, 986, 964, 898, 865, 838, 792, 737, 691. $^1H$ NMR (400 MHz, 25 °C, $CDCl_3$), δ (ppm): 8.24 (br s, 1H, NH), 7.52 (d, $^3J_{HH}$ = 8.6 Hz, 2H, $H^o$), 7.40 (d, $^3J_{HH}$ = 8.6 Hz, 2H, $H^m$), 6.68 (dd, $^3J_{HH}$ = 17.6, $^3J_{HH}$ = 10.9 Hz, 1H, C<u>H</u>=$CH_2$), 5.71 (d, $^3J_{HH}$ = 17.6 Hz, 1H, CH=CH<u>H</u>$^{cis}$), 5.23 (d, $^3J_{HH}$ = 10.9 Hz, 1H, CH=CH<u>H</u>$^{trans}$), 4.19 (s, 2H, $ClCH_2$). $^{13}C$ NMR (100 MHz, 25 °C, $CDCl_3$,), δ (ppm): 163.6 (CO), 136.1 (CONH<u>C</u>$^{ipso}$), 135.9 (<u>C</u>H=$CH_2$), 134.6 ($C^p$), 126.9 ($C^m$), 120.0 ($C^o$), 113.6 (CH=<u>C</u>$H_2$), 42.8 ($ClCH_2$).

**1,4,7,10-Tetrakis(allylcarbamoylmethyl)-1,4,7,10-tetraazacyclo-dodecane 52**

Cyclen (0.100 g, 0.580 mmol), $K_2CO_3$ (0.401 g, 2.90 mmol) and *N*-allyl-2-chloroacetamide **47** (0.388 g, 2.90 mmol) were suspended in dry MeCN (20 ml) and heated at reflux (85 °C) for 18 h. After removal of the solvent under reduced pressure, the residue was suspended in distilled water (20 ml) and the product extracted with $CHCl_3$ (5x10 ml). The organic phase was dried over anhydrous $K_2CO_3$ and the solvent was evaporated under reduced pressure. The beige solid residue was purified by double precipitation from DCM with cyclohexane, yielding the desired product in 58% yield (0.189 g, 0.336 mmol).

M.p.: 167 °C. Elemental analysis: calculated C 59.98%, H 8.63%, N 19.98%; found C 60.02%, H 8.57%, N 19.99%. $FAB^+$ MS, m/z: 561 ($[M+H]^+$; calculated 561.3877, found 561.3871), 583 ($[M+Na]^+$). IR (KBr disk), $cm^{-1}$: 3242, 2954, 2822, 1666, 1541, 1452, 1427, 1368, 1308, 1263, 1227, 1109, 993, 972, 926, 807, 780, 722, 647, 584, 557. $^1H$ NMR (400 MHz, 25 °C, $CDCl_3$), δ (ppm): 7.06 (br s, 4H, NH), 5.82

(m, 4H, $NHCH_2C\underline{H}$), 5.15 (m, 8H, $NHCH_2CHC\underline{H_2}$), 3.88 (m, 8H, $NHC\underline{H_2}$), 3.08 (s, 8H, $NCH_2CO$), 2.70 (s, 16H, $NCH_2CH_2N$). $^{13}C$ NMR (100 MHz, 25 °C, $CDCl_3$), δ (ppm): 41.6 ($NHCH_2$), 53.6 ($NCH_2CH_2N$), 59.2 ($N\underline{C}H_2CO$), 116.4 ($NHCH_2CH\underline{C}H_2$), 134.3 ($NHCH_2\underline{C}H$), 170.4 (CO).

**1,4,7,10-Tetrakis(2-propynylcarbamoylmethyl)-1,4,7,10-tetraazacyclododecane 53**

***Method I***

*N*-Propargyl-2-chloroacetamide **49** (2.000 g, 15.27 mmol) and dry $Et_3N$ (2.13 ml, 15.3 mmol) were dissolved in dry DMF (2 ml). A solution of cyclen (0.641 g, 3.72 mmol) in distilled water (6 ml) was added dropwise in 1 hour at 50 °C. After 2 hours, the white solid precipitate was filtered and washed with distilled water. After drying under reduced pressure and in a freeze dryer, the desired product was obtained in 52% yield (1.065 g, 1.928 mmol).

Mp (°C): 203. Elemental analysis: calculated C 60.85%, H 7.30%, N 20.27%; found C 60.93%, H 7.31%, N 20.17%. ESI MS, m/z: 553 ($[M+H]^+$; calculated 553.3251, found 553.3257), 575 ($[M+Na]^+$), 277 ($[M+2H]^{2+}$). IR (KBr disk), $cm^{-1}$: 3283, 3069, 2948, 2825, 2122, 1657, 1532, 1450, 1424, 1360, 1326, 1300, 1259, 1224, 1143, 1105, 1081, 1044, 1021, 996, 978, 917, 890, 803, 759, 685, 595, 575, 536, 312. $^1H$ NMR (400 MHz, 25 °C, DMSO-$d_6$), δ (ppm): 8.41 (t, $^3J_{HH}$ = 5.5 Hz, 4H, NH), 3.87 (m, 8H, $NHC\underline{H_2}$), 3.05 (t, $^3J_{HH}$ = 2.4 Hz, 4H, C≡CH), 3.04 (s, 8H, $NCH_2CO$), 2.61 (s, 16H, $NCH_2CH_2N$). $^{13}C$ NMR (100 MHz, 25 °C, DMSO-$d_6$), δ (ppm): 170.4 (CO), 81.2 (C≡$\underline{C}$H), 72.8 ($\underline{C}$≡CH), 57.4 ($N\underline{C}H_2CO$), 53.2 ($NCH_2CH_2N$), 27.8 ($NHCH_2$).

***Method II***

*N*-Propargyl-2-bromoacetamide **50** (0.838 g, 4.76 mmol) and dry $Et_3N$ (0.66 ml, 4.8 mmol) were dissolved in dry DMF (2 ml). A solution of cyclen (0.200 g, 1.16 mmol) in distilled water (4 ml) was added dropwise in 1 hour at 50 °C. After 4 days, the white solid precipitate was filtered and washed with distilled water. After drying under reduced pressure and in a freeze dryer, the desired product was obtained in 1% yield (7.4 mg, 0.013 mmol).

$^1H$ NMR (400 MHz, 25 °C, DMSO-$d_6$), δ (ppm): 8.41 (t, $^3J_{HH}$ = 5.3 Hz, 4H, NH), 3.87 (m, 8H, $NHC\underline{H_2}$), 3.05 (t, $^3J_{HH}$ = 2.4 Hz, 4H, C≡CH), 3.04 (s, 8H, $NCH_2CO$),

2.62 (s, 16H, $NCH_2CH_2N$). $^{13}C$ NMR (100 MHz, 25 °C, DMSO-$d_6$), δ (ppm): 170.3 (CO), 81.2 (C≡CH), 72.8 (C≡CH), 57.4 ($NCH_2CO$), 53.2 ($NCH_2CH_2N$), 27.7 ($NHCH_2$).

***Method III***

Cyclen (1.664 g, 9.661 mmol), $Cs_2CO_3$ (13.850 g, 42.509 mmol) and KI (7.056 g, 42.51 mmol), all anhydrous, were suspended in dry DMF (100 ml). *N*-Propargyl-2-chloroacetamide **49** (5.592 g, 42.51 mmol) was added, and the suspension was stirred at 50 °C for 2 days. After removing the solvent under reduced pressure, the brown coloured solid was suspended in $H_2O$ (100 ml) and filtered under vacuum. The solid residue was washed with $H_2O$ until the filtrate was colourless (80 ml). The white solid was purified by recrystallisation from a 95:5 v/v mixture of DMF/$H_2O$, yielding 3.951 g (7.149 mmol, 74%) of the desired product.

Mp (°C): 204. Elemental analysis: calculated C 60.85%, H 7.30%, N 20.27%; found C 60.98%, H 7.21%, N 20.19%. ESI MS, m/z: 553 ($[M+H]^+$; calculated 553.3251, found 553.3257), 575 ($[M+Na]^+$), 277 ($[M+2H]^{2+}$). IR (KBr disk), $cm^{-1}$: 3283, 3069, 2948, 2825, 2122, 1657, 1532, 1450, 1424, 1360, 1326, 1300, 1259, 1224, 1143, 1105, 1081, 1044, 1021, 996, 978, 917, 890, 803, 759, 685, 595, 575, 536, 312. $^1H$ NMR (400 MHz, 25 °C DMSO-$d_6$), δ (ppm): 8.41 (t, $^3J_{HH}$ = 5.5 Hz, 4H, NH), 3.87 (m, 8H, $NHCH_2$), 3.05 (t, $^3J_{HH}$ = 2.4 Hz, 4H, C≡CH), 3.04 (s, 8H, $NCH_2CO$), 2.61 (s, 16H, $NCH_2CH_2N$). $^{13}C$ NMR (100 MHz, 25 °C, DMSO-$d_6$), δ (ppm): 170.4 (CO), 81.2 (C≡CH), 72.8 (C≡CH), 57.4 ($NCH_2CO$), 53.2 ($NCH_2CH_2N$), 27.8 ($NHCH_2$).

**1,4,7,10-Tetrakis(2-styrylcarbamoylmethyl)-1,4,7,10-tetraazacyclododecane 54**

*N*-Styryl-2-chloroacetamide **51** (0.931 g, 4.76 mmol) and dry $Et_3N$ (0.66 ml, 4.8 mmol) were dissolved in dry DMF (2 ml). A solution of cyclen (0.200 g, 1.16 mmol) in distilled water (4 ml) was added dropwise in 1 hour at 50 °C. After 2 hours, the white solid precipitate was filtered and washed with distilled water. After drying under reduced pressure and in a freeze dryer, the desired product was obtained in 63% yield (0.596 g, 0.737 mmol).

Mp: decomposes. Elemental analysis: calculated C 71.26%, H 6.98%, N 13.85%; found C 71.27%, H 7.07%, N 13.76%. $FAB^+$ MS, m/z: 809 ($[M+H]^+$), 831 ($[M+Na]^+$), 847 ($[M+K]^+$). IR (KBr disk), $cm^{-1}$: 3239, 3085, 3039, 2976, 2811, 1901, 1674, 1627, 1605, 1514, 1421, 1403, 1317, 1250, 1180, 1103, 1068, 991, 955, 902, 839, 717, 495. $^1H$ NMR (400 MHz, 25 °C, DMSO-$d_6$), δ (ppm): 9.97 (s, 4H, NH), 7.55 (d,

$^3J_{HH}$ = 8.6 Hz, 4H, $H^o$), 7.33 (d, $^3J_{HH}$ = 8.6 Hz, 4H, $H^m$), 6.63 (dd, $^3J_{HH}$ = 17.6 Hz, $^3J_{HH}$ = 11.0 Hz, 4H, C<u>H</u>=$CH_2$), 5.67 (d, $^3J_{HH}$ = 17.6 Hz, 4H, CH=CH$H^{cis}$), 5.14 (d, $^3J_{HH}$ = 11.0 Hz, 4H, CH=CH$H^{trans}$), 3.27 (s, 8H, $NCH_2CO$), 2.87 (s, 16H, $NCH_2CH_2N$). $^{13}$C NMR (100 MHz, 25 °C, DMSO-$d_6$), δ (ppm): 169.5 (CO), 138.4 (CONH<u>$C^{ipso}$</u>), 136.2 (<u>C</u>H=$CH_2$), 132.1 ($C^p$), 126.5 ($C^m$), 119.2 ($C^o$), 112.7 (CH=<u>C</u>$H_2$), 58.0 (N<u>C</u>$H_2$CO), 52.7 ($NCH_2CH_2N$).

**4-Vinylbenzylamine 55**

Ammonium acetate (0.545 g, 7.07 mmol) was suspended in THF (10 ml). 25% $NH_4OH$ (200 ml) was added, followed by dropwise addition of 4-vinylbenzyl chloride (1.00 ml, 7.07 mmol). The mixture was stirred at room temperature for 2 days, then it was extracted with $CHCl_3$ (3x30 ml). The organic phase was washed with brine (3x20 ml) and dried over anhydrous $Na_2SO_4$. The yellow coloured oil was purified by column chromatography ($SiO_2$, MeCN/MeOH/25%-$NH_4OH$ 80:19.9:0.1 v/v, $R_f$ 0.37), yielding 0.320 g (2.40 mmol, 34%) of **55** as a slightly yellow coloured oil. A complete characterisation was not possible, because the product tends to polymerise easily.

$CI^+$ MS, m/z: 134 ($[M+H]^+$), 151 ($[M+NH_4]^+$). $^1$H NMR (400 MHz, 25 °C, $CDCl_3$), δ (ppm): 7.40 (d, $^3J_{HH}$ = 8.1 Hz, 2H, $H^o$), 7.29 (d, $^3J_{HH}$ = 8.1 Hz, 2H, $H^m$), 6.78 (dd, $^3J_{HH}$ = 17.6 Hz, $^3J_{HH}$ = 10.9 Hz, 1H, C<u>H</u>=$CH_2$), 5.75 (d, $^3J_{HH}$ = 17.6 Hz, 1H, CH=CH<u>$H^{cis}$</u>), 5.24 (d, $^3J_{HH}$ = 10.9 Hz, 1H, CH=CH<u>$H^{trans}$</u>), 3.88 (s, 2H, C<u>$H_2$</u>$NH_2$), 1.77 (br s, 2H, $NH_2$). $^{13}$C NMR (100 MHz, 25 °C, $CDCl_3$), δ (ppm): 142.7 ($C^p$), 136.5 (<u>C</u>H=$CH_2$), 136.2 ($NH_2CH_2$<u>$C^{ipso}$</u>), 127.3 ($C^m$), 126.4 ($C^o$), 113.5 (CH=<u>C</u>$H_2$), 46.1 ($CH_2NH_2$).

**4-Vinylbenzylamine hydrochloride 56**

Ammonium acetate (0.545 g, 7.07 mmol) was suspended in THF (10 ml). 25% $NH_4OH$ (200 ml) was added, followed by dropwise addition of 4-vinylbenzyl chloride (1.00 ml, 7.07 mmol). The mixture was stirred at room temperature for 2 days, then it was extracted with $CHCl_3$ (3x30 ml). The organic phase was washed with brine (3x20 ml) and dried over anhydrous $Na_2SO_4$. After removal of the solvent under reduced pressure, the oil obtained was treated with 0.1 M HCl (50 ml). The water was removed by freeze-drying, and the residue was suspended in $CHCl_3$ and filtered. The desired product was obtained as a white solid in 83% yield (1.001 g, 5.903 mmol)

Mp: decomposes. Elemental analysis: calculated C 63.72%, H 7.13%, N 8.26%; found C 63.74%, H 7.21%, N 8.36%. $FAB^+$ MS, m/z: 134 ($[M\text{-}Cl]^+$), 117 ($[M\text{-}H\text{-}NH_2\text{-}HCl]^+$). IR (KBr disk), $cm^{-1}$: 3449, 3005, 2788, 2599, 2391, 2346, 2048, 1920, 1815, 1628, 1595, 1570, 1514, 1479, 1465, 1426, 1410, 1384, 1219, 1118, 1083, 989, 903, 847, 735. $^1H$ NMR (400 MHz, 25 °C, $D_2O$), δ (ppm): 7.53 (d, $^3J_{HH}$ = 8.2 Hz, 2H, $H^o$), 7.40 (d, $^3J_{HH}$ = 8.2 Hz, 2H, $H^m$), 6.78 (dd, $^3J_{HH}$ = 17.7 Hz, $^3J_{HH}$ = 11.0 Hz, 1H, $C\underline{H}=CH_2$), 5.87 (d, $^3J_{HH}$ = 17.7 Hz, 1H, $CH=CH\underline{H^{cis}}$), 5.33 (d, $^3J_{HH}$ = 11.0 Hz, 1H, $CH=CH\underline{H^{trans}}$), 4.14 (s, 2H, $C\underline{H_2}NH_2$). $^{13}C$ NMR (100 MHz, 25 °C, $D_2O$), δ (ppm): 138.2 ($C^p$), 135.9 ($\underline{C}H=CH_2$), 132.0 ($NH_2CH_2\underline{C^{ipso}}$), 129.1 ($C^m$), 126.7 ($C^o$), 115.3 ($CH=\underline{C}H_2$), 42.7 ($CH_2NH_2$).

**_N_-(4-vinylbenzyl)-2-chloroacetamide 57**

4-Vinylbenzylamine hydrochloride **56** (0.882 g, 5.20 mmol) was suspended in a solution of chloroacetyl chloride (0.42 ml, 5.2 mmol) in dry THF (10 ml). A solution of dry $Et_3N$ (1.45 ml, 10.4 mmol) in dry THF (10 ml) was added dropwise over a period of 1 h at 0 °C. The mixture was stirred for a further 1 h at room temperature, then filtered. The filtrate was evaporated under reduced pressure, and the brown coloured solid residue was suspended in $H_2O$ (20 ml) and extracted with DCM (3x10 ml). The organic phase was dried over anhydrous $MgSO_4$ and filtered. The filtrate was evaporated under reduced pressure, leading to the desired compound as a white solid in 91% yield (0.991 g, 4.73 mmol).

Mp: 115 °C. Elemental analysis: calculated C 63.01%, H 5.77%, N 6.68%; found C 63.06%, H 5.81%, N 6.60%. $CI^+$ MS, m/z: 227 ($[M+NH_4]^+$), 210 ($[M+H]^+$), 174 ($[M\text{-}Cl]^+$). IR (KBr disk), $cm^{-1}$: 3449, 3005, 2788, 2599, 2391, 2346, 2048, 1920, 1815, 1628, 1595, 1570, 1514, 1479, 1465, 1426, 1410, 1384, 1219, 1118, 1083, 989, 903, 847, 735. $^1H$ NMR (400 MHz, 25 °C, $CDCl_3$), δ (ppm): 7.42 (d, $^3J_{HH}$ = 8.1 Hz, 2H, $H^o$), 7.27 (d, $^3J_{HH}$ = 8.1 Hz, 2H, $H^m$), 6.86 (br s, 1H, NH), 6.70 (dd, $^3J_{HH}$ = 17.6 Hz, $^3J_{HH}$ = 10.9 Hz, 1H, $C\underline{H}=CH_2$), 5.75 (d, $^3J_{HH}$ = 17.6 Hz, 1H, $CH=CH\underline{H^{cis}}$), 5.26 (d, $^3J_{HH}$ = 10.9 Hz, 1H, $CH=CH\underline{H^{trans}}$), 4.48 (d, $^3J_{HH}$ = 5.8 Hz, 2H, $C\underline{H_2}NH$), 4.10 (s, 2H, $ClCH_2$). $^{13}C$ NMR (100 MHz, 25 °C, $CDCl_3$), δ (ppm): 165.8 (CO), 137.2 ($NHCH_2\underline{C^{ipso}}$), 136.7 ($C^p$), 136.2 ($\underline{C}H=CH_2$), 128.0 ($C^m$), 126.6 ($C^o$), 114.2 ($CH=\underline{C}H_2$), 43.6 ($C\underline{H_2}NH$), 42.6 ($ClCH_2$).

**N-(4-Vinylbenzyl)ethane-1,2-diamine 59**

4-Vinylbenzyl chloride (5.00 ml, 35.5 mmol) was added dropwise over 1 hour to ethylenediamine (25 ml) at 0 °C. After 4 hours the solvent was removed under reduced pressure, and the yellow coloured residue was suspended in 0.1 M NaOH (30 ml) and extracted with $CHCl_3$ (3x15 ml). The organic phase was dried over anhydrous $K_2CO_3$ and filtered. After evaporation of the solvent under reduced pressure a yellow oil was obtained (4.216 g; crude yield 23.92 mmol, 67%), whose NMR spectra looked rather clean. The compound polymerised quickly, and no further purification could be carried out.

$CI^+$ MS, m/z: 177 ($[M+H]^+$), 194 ($[M+NH_4]^+$). $^1H$ NMR (400 MHz, 25 °C, $CDCl_3$), δ (ppm): 7.38 (d, $^3J_{HH}$ = 8.7 Hz, 2H, $H^o$), 7.29 (d, $^3J_{HH}$ = 8.7 Hz, 2H, $H^m$), 6.72 (dd, $^3J_{HH}$ = 17.6, $^3J_{HH}$ = 10.9 Hz, 1H, C<u>H</u>=$CH_2$), 5.74 (d, $^3J_{HH}$ = 17.6 Hz, 1H, CH=CH<u>H</u>$^{cis}$), 5.23 (d, $^3J_{HH}$ = 10.9 Hz, 1H, CH=CH<u>H</u>$^{trans}$), 3.80 (s, 2H, ArC<u>H</u>$_2$NH), 2.82 (t, $^3J_{HH}$ = 5.8 Hz, 2H, C<u>H</u>$_2CH_2NH_2$), 2.70 (t, $^3J_{HH}$ = 5.8 Hz, 2H, $CH_2$C<u>H</u>$_2NH_2$), 1.54 (br s, 3H, NH+$NH_2$). $^{13}C$ NMR (100 MHz, 25 °C, $CDCl_3$,), δ (ppm): 140.3 (NHC$H_2$<u>C</u>$^{ipso}$), 136.7 (<u>C</u>H=$CH_2$), 136.5 ($C^p$), 128.4 ($C^m$), 126.4 ($C^o$), 113.6 (CH=<u>C</u>$H_2$), 53.7 (Ar$CH_2$NH), 52.0 (<u>C</u>$H_2CH_2NH_2$), 41.9 ($CH_2$<u>C</u>$H_2NH_2$).

**2-(4-Vinylbenzylthio)ethanol 60**

2-Mercaptoethanol (2.49 ml, 35.5 mmol) and $Na_2CO_3$ (7.521 g, 70.96 mmol) were suspended in dry MeOH (100 ml). 4-Vinylbenzyl chloride (5.00 ml, 35.5 mmol) was added dropwise, and the mixture was stirred at room temperature for 15 hours. After removal of the solvent under reduced pressure, the residue was suspended in $H_2O$ (100 ml) and extracted with $CHCl_3$ (3x30 ml). The organic phase was washed with brine (2x30 ml) and dried over anhydrous $Na_2SO_4$. After filtration and removal of the solvent under reduced pressure, the residue was purified by chromatography ($Al_2O_3$, $CHCl_3$, $R_f$ 0.35). The desired product was obtained as a white solid in 81% yield (5.564 g, 28.64 mmol).

Elemental analysis: calculated C 68.00%, H 7.26%; found C 67.86%, H 7.28%. $CI^+$ MS, m/z: 195 ($[M+H]^+$), 212 ($[M+NH_4]^+$). $^1H$ NMR (400 MHz, 25 °C, $CDCl_3$), δ (ppm): 7.36 (d, $^3J_{HH}$ = 8.5 Hz, 2H, $H^o$), 7.27 (d, $^3J_{HH}$ = 8.5 Hz, 2H, $H^m$), 6.69 (dd, $^3J_{HH}$ = 17.6 Hz, $^3J_{HH}$ = 10.9 Hz, 1H, C<u>H</u>=$CH_2$), 5.74 (d, $^3J_{HH}$ = 17.6 Hz, 1H, CH=CH<u>H</u>$^{cis}$), 5.24 (d, $^3J_{HH}$ = 10.9 Hz, 1H, CH=CH<u>H</u>$^{trans}$), 3.71 (s, 2H, $CCH_2S$), 3.67 (t, $^3J_{HH}$ = 6.0 Hz, 2H, $SCH_2$C<u>H</u>$_2$OH), 2.63 (t, $^3J_{HH}$ = 6.0 Hz, 2H, SC<u>H</u>$_2CH_2$OH), 2.09 (br s, 1H, OH). $^{13}C$

NMR (100 MHz, 25 °C, $CDCl_3$), δ (ppm): 137.6 ($SCH_2\underline{C}^{ipso}$), 136.5 ($C^p$), 136.3 ($\underline{C}H{=}CH_2$), 129.0 ($C^m$), 126.4 ($C^o$), 113.8 ($CH{=}\underline{C}H_2$), 60.2 ($CH_2OH$), 35.4 ($C\underline{C}H_2S$), 34.3 ($S\underline{C}H_2CH_2OH$).

**2-(4-Vinylbenzylthio)ethyl 2-chloroacetate 61**

Chloroacetyl chloride (2.05 ml, 25.7 mmol) in dry THF (20 ml) was cooled down to -5 °C on an ice bath. A solution of 2-(4-vinylbenzylthio)ethanol **60** (1.000 g, 5.147 mmol) and dry $Et_3N$ (0.72 ml, 5.1 mmol) in dry THF (10 ml) was added dropwise over 1 hour at -5 °C. The mixture was left stirring for 1 h, then it was filtered. The filtrate was evaporated under reduced pressure, and the residue was suspended in DCM (15 ml) and stirred with $Al_2O_3$ (10 g) for 2 h. After filtration through Celite, the filtrate was evaporated under vacuum, leading to the desired product as a slightly yellow coloured oil in 53% yield (0.739 mg, 2.73 mmol).

Elemental analysis: calculated C 57.66%, H 5.58%; found C 57.75%, H 5.44%. $CI^+$ MS, m/z: 270 ($M^+$), 288 ($[M+NH_4]^+$; calculated 288.0825, found 288.0826), 541 ($[2M+H]^+$), 558 ($[2M+NH_4]^+$),. IR (KBr disk), $cm^{-1}$: 3083, 3004, 2955, 2358, 2337, 1758, 1629, 1510, 1407, 1310, 1285, 1222, 1060, 991, 912, 845, 775, 697. $^1H$ NMR (400 MHz, 25 °C, $CDCl_3$), δ (ppm): 7.36 (d, $^3J_{HH}$ = 8.2 Hz, 2H, $H^o$), 7.27 (d, $^3J_{HH}$ = 8.2 Hz, 2H, $H^m$), 6.69 (dd, $^3J_{HH}$ = 17.6 Hz, $^3J_{HH}$ = 10.9 Hz, 1H, $C\underline{H}{=}CH_2$), 5.74 (d, $^3J_{HH}$ = 17.6 Hz, 1H, $CH{=}CH\underline{H}^{cis}$), 5.24 (d, $^3J_{HH}$ = 10.9 Hz, 1H, $CH{=}CH\underline{H}^{trans}$), 4.28 (t, $^3J_{HH}$ = 6.8 Hz, 2H, $CH_2O$), 4.06 (s, 2H, $ClCH_2$), 3.74 (s, 2H, $CCH_2S$), 2.66 (t, $^3J_{HH}$ = 6.8 Hz, 2H, $SC\underline{H}_2CH_2O$). $^{13}C$ NMR (100 MHz, 25 °C, $CDCl_3$), δ (ppm): 167.1 (C=O), 137.3 ($SCH_2\underline{C}^{ipso}$), 136.6 ($C^p$), 136.3 ($\underline{C}H{=}CH_2$), 129.1 ($C^m$), 126.4 ($C^o$), 113.9 ($CH{=}\underline{C}H_2$), 64.7 ($CH_2O$), 40.7 ($ClCH_2$), 36.0 ($C\underline{C}H_2S$), 29.2 ($S\underline{C}H_2CH_2O$).

**1,4,7,10-Tetrakis(4-vinylbenzylcarbamoylmethyl)-1,4,7,10-tetraazacyclododecane 62**

Cyclen (0.100 g, 0.580 mmol), $Cs_2CO_3$ (0.832 g, 2.55 mmol) and KI (0.424 g, 2.55 mmol) were suspended in DMF (8 ml). *N*-(4-Vinylbenzyl)-2-chloroacetamide **57** (0.535 g, 2.55 mmol) was added, and the mixture was stirred at 50 °C for 2 days. After removal of the solvents under reduced pressure, the obtained brown solid was suspended in water, sonicated for 10 minutes and then filtered. A brown coloured insoluble solid remained, which was not possible to purify any further. The solid was then characterised as it was.

ESI MS, m/z: 887 ($[M+Na]^+$), 865 ($[M+H]^+$), 452 ($[M+2Na]^{2+}$), 433 ($[M+2H]^{2+}$). $^1$H NMR (400 MHz, 25 °C, DMSO-$d_6$), δ (ppm): 8.48 (br s, 4H, NH), 7.35 (br d, $^3J_{HH}$ = 7.7 Hz, 8H, $H^o$), 7.19 (br d, $^3J_{HH}$ = 7.7 Hz, 8H, $H^m$), 6.65 (br dd, $^3J_{HH}$ = 17.5 Hz, $^3J_{HH}$ = 10.8 Hz, C<u>H</u>=$CH_2$), 5.74 (br d, $^3J_{HH}$ = 17.5 Hz, 4H, CH=CH<u>H</u>$^{cis}$), 5.19 (br d, $^3J_{HH}$ = 10.8 Hz, 4H, CH=CH<u>H</u>$^{trans}$), 4.24 (br d, $^3J_{HH}$ = 2.5 Hz, 8H, NHC<u>H</u>$_2$), 2.98 (br s, 8H, $NCH_2CO$), 2.50 (br s, 16H, $NCH_2CH_2N$). $^{13}$C NMR (100 MHz, 25 °C, DMSO-$d_6$), δ (ppm): 170.7 (CO), 139.2 ($NHCH_2$<u>C</u>$^{ipso}$), 136.4 (<u>C</u>H=$CH_2$), 135.7 ($C^p$), 128.7 ($C^m$), 126.0 ($C^o$), 113.8 (CH=C<u>H</u>$_2$), 57.0 (br, N<u>C</u>$H_2CO$), 52.7 (br, $NCH_2CH_2N$), 41.6 ($NHCH_2$).

**1,4,7,10-Tetrakis[2-(4-vinylbenzylthio)ethoxycarbonylmethyl]-1,4,7,10-tetraazacyclododecane 63**

***Method I***

Cyclen (0.168 g, 0.978 mmol), $Cs_2CO_3$ (1.402 g, 4.303 mmol) and KI (0.714 g, 4.30 mmol) were suspended in DMF (15 ml). 2-(4-Vinylbenzylthio)ethyl 2-chloroacetate **61** (1.165 g, 4.303 mmol) was added, and the mixture was stirred at 50 °C for 14 hours. After removal of the solvents under reduced pressure, the obtained brown solid was suspended in water, filtered and washed with water (5x20 ml). A brown coloured insoluble solid remained, which was not possible to purify any further. The solid was then characterised as obtained.

ESI MS, m/z: 555 ($[M+2H]^{2+}$), 1109 ($[M+H]^+$), 1131 ($[M+Na]^+$), 1153 ($[M-H+2Na]^+$), 1175 ($[M-2H+3Na]^+$). $^1$H NMR (400 MHz, 25 °C, DMSO-$d_6$), δ (ppm): 7.39 (d, $^3J_{HH}$ = 8.2 Hz, 8H, $H^o$), 7.22 (d, $^3J_{HH}$ = 8.2 Hz, 8H, $H^m$), 6.69 (dd, $^3J_{HH}$ = 17.6 Hz, $^3J_{HH}$ = 10.9 Hz, C<u>H</u>=$CH_2$), 5.78 (d, $^3J_{HH}$ = 17.6 Hz, 4H, CH=CH<u>H</u>$^{cis}$), 5.23 (d, $^3J_{HH}$ = 10.9 Hz, 4H, CH=CH<u>H</u>$^{trans}$), 4.16 (t, $^3J_{HH}$ = 6.8 Hz, 2H, $CH_2O$), 3.68 (s, 8H, $NCH_2CO$), 2.60 (br s, 16H, $NCH_2CH_2N$), 2.58 (t, $^3J_{HH}$ = 6.8 Hz, 2H, $SCH_2$<u>C</u>$H_2O$). $^{13}$C NMR (100 MHz, 25 °C, DMSO-$d_6$), δ (ppm): 173.4 (CO), 138.0 ($SCH_2$<u>C</u>$^{ipso}$), 136.3 (<u>C</u>H=$CH_2$), 135.8 ($C^p$), 129.1 ($C^m$), 126.2 ($C^o$), 114.1 (CH=C<u>H</u>$_2$), 63.3 ($CH_2O$), 54.7 (br, N<u>C</u>$H_2CO$), 50.0 (br, $NCH_2CH_2N$), 34.8 (C<u>C</u>$H_2S$), 29.0 (S<u>C</u>$H_2CH_2O$).

***Method II***

2-(4-Vinylbenzylthio)ethyl 2-chloroacetate **61** (0.692 g, 2.55 mmol) and TBMP (6.9 mg, 0.031 mmol) were stirred for 5 minutes in DMF (15 ml). Cyclen (0.100 g,

0.580 mmol), $Cs_2CO_3$ (0.842 g, 2.58 mmol) and KI (0.424 g, 2.55 mmol) were added, and the mixture was 50 °C for 2 days. After removal of the solvents under reduced pressure, a sticky brown oil was obtained, which was not possible to purify any further and was then characterised as obtained.

ESI MS, m/z: 555 ($[M+2H]^{2+}$), 1109 ($[M+H]^+$), 1131 ($[M+Na]^+$), 1153 ($[M-H+2Na]^+$), 1175 ($[M-2H+3Na]^+$). $^1$H NMR (400 MHz, 25 °C, DMSO-$d_6$), δ (ppm): 7.39 (d, $^3J_{HH}$ = 8.2 Hz, 8H, $H^o$), 7.27 (d, $^3J_{HH}$ = 8.2 Hz, 8H, $H^m$), 6.68 (dd, $^3J_{HH}$ = 17.6 Hz, $^3J_{HH}$ = 10.9 Hz, C<u>H</u>=$CH_2$), 5.78 (br d, $^3J_{HH}$ = 17.6 Hz, 4H, CH=CH<u>H</u>$^{cis}$), 5.21 (br d, $^3J_{HH}$ = 10.9 Hz, 4H, CH=CH<u>H</u>$^{trans}$), 4.17 (t, $^3J_{HH}$ = 6.8 Hz, 2H, $CH_2O$), 3.5 (br s, 8H, $NCH_2CO$), 2.62 (t, $^3J_{HH}$ = 6.8 Hz, 2H, $SC\underline{H}_2CH_2O$), 2.5 (br s, 16H, $NCH_2CH_2N$). $^{13}$C NMR (100 MHz, 25 °C, DMSO-$d_6$), δ (ppm): 171.9 (CO), 138.0 ($SCH_2C^{ipso}$), 136.2 (<u>C</u>H=$CH_2$), 135.7 ($C^p$), 129.0 ($C^m$), 126.1 ($C^o$), 114.0 (CH=C<u>H</u>$_2$), 63.0 ($CH_2O$), 55.1 (br, N<u>C</u>$H_2$CO), 50 (br, $NCH_2CH_2N$), 34.8 (C<u>C</u>$H_2$S), 29.1 (S<u>C</u>$H_2CH_2O$).

**2-[2-(2-Azidoethoxy)ethoxy]ethanol 64**[373]

2-[2-(2-Chloroethoxy)ethoxy]ethanol (0.50 ml, 3.4 mmol) was dissolved in dry DMF (15 ml). Sodium azide (0.447 g, 6.88 mmol) was added, and the suspension was heated to 100 °C. After 24 hours, the mixture was cooled to room temperature and the solvent was removed under reduced pressure. The residue was suspended in DCM and filtered through Celite. The filtrate was evaporated to give the product as a slightly yellow coloured oil in quantitative yield (0.640 g, 3.65 mmol).

Elemental analysis: calculated C 41.14%, H 7.48%, N 23.99%N; found C 41.28%, H 7.41%, N 23.94%. $CI^+$ MS, m/z: 193 ($[M+NH_4]^+$), 368 ($[2M+NH_4]^+$), 176 ($[M+H]^+$; calculated 176.1035, found 176.1031), 350 ($[2M]^+$). IR (film on KBr pellets), $cm^{-1}$: 3420, 2921, 2873, 2109, 1667, 1452, 1347, 1287, 1123, 1071, 934, 887, 640, 556. $^1$H NMR (400 MHz, 25 °C, $CDCl_3$), δ (ppm): 3.73 (m, 2H, C<u>H</u>$_2$OH), 3.68 (m, 6H, $N_3CH_2C\underline{H}_2OC\underline{H}_2C\underline{H}_2O$), 3.61 (m, 2H, $HOCH_2C\underline{H}_2O$), 3.38 (t, $^3J_{HH}$ = 5.0 Hz, 2H, $CH_2N_3$), 2.34 (br s, 1H, OH). $^{13}$C NMR (100 MHz, 25 °C, $CDCl_3$), δ (ppm): 72.4 ($HOCH_2\underline{C}H_2$), 70.0+70.4+70.6 ($N_3CH_2\underline{C}H_2O\underline{C}H_2\underline{C}H_2O$), 61.7 ($CH_2OH$), 50.8 ($CH_2N_3$).

**2-Chloro-*N*-((1-(2-(2-(2-hydroxyethoxy)ethoxy)ethyl)-*1H*-1,2,3-triazol-4-yl)methyl)acetamide 65**

2-[2-(2-Azidoethoxy)ethoxy]ethanol **64** (0.146 g, 0.836 mmol) was dissolved in *tert*-BuOH (5 ml). *N*-Propargyl-2-chloroacetamide (0.100 g, 0.760 mmol) was added,

followed by $CuSO_4 \cdot 5H_2O$ (0.019 g, 0.076 mmol), sodium ascorbate (0.030 g, 0.15 mmol) and distilled $H_2O$ (5 ml). The mixture was heated to 50 °C for 5 hours. After removal of the solvents under reduced pressure, the residue was purified by chromatography ($SiO_2$, $CHCl_3$/MeOH 90:10 v/v, $R_f$ 0.32). The desired product was obtained as a slightly yellow coloured oil in 98% yield (451 mg, 1.47 mmol).

Elemental analysis: calculated C 43.07%, H 6.24%, N 18.26%; found C 42.92%, H 6.22%, N 18.11%. ESI MS, m/z: 307/309 ($[M+H]^+$; calculated 307.1173, found 307.1164), 329/331 ($[M+Na]^+$). IR (film on KBr pellets), $cm^{-1}$: 3300, 2874, 1671, 1542, 1459, 1431, 1352, 1282, 1121, 1061, 929, 758, 666, 561. $^1H$ NMR (400 MHz, 25 °C, $CDCl_3$), δ (ppm): 7.95 (br s, 1H, NH), 7.43 (br s, 1H, CH ring), 4.58 (br s, 2H, $NHC\underline{H}_2$), 4.54 (t, $^3J_{HH}$ = 4.8 Hz, 2H, $NC\underline{H}_2CH_2O$), 4.04 (s, 2H, $ClCH_2$), 3.87 (t, $^3J_{HH}$ = 4.8 Hz, 2H, $NCH_2C\underline{H}_2O$), 3.75 (t, $^3J_{HH}$ = 4.5 Hz, 2H, $C\underline{H}_2OH$), 3.62 (s, 4H, $OC\underline{H}_2C\underline{H}_2O$), 3.57 (t, $^3J_{HH}$ = 4.5 Hz, 2H, $OC\underline{H}_2CH_2OH$), 2.86 (br s, 1H, OH). $^{13}C$ NMR (100 MHz, 25 °C, $CDCl_3$), δ (ppm): 166.3 (C=O), 72.4 ($OCH_2\underline{C}H_2OH$), 70.4 + 70.1 ($O\underline{C}H_2\underline{C}H_2O$), 69.1 ($NCH_2\underline{C}H_2O$), 61.6 ($CH_2OH$), 50.3 ($N\underline{C}H_2CH_2O$), 42.4 ($ClCH_2$), 35.1 ($NHCH_2$); the 2 carbons of the triazole ring were too broad to be observed.

**4-Vinylbenzyl azide 66**

4-Vinylbenzyl chloride (1.00 ml, 7.10 mmol) was dissolved in distilled $H_2O$ (1 ml) and EtOH (7 ml). $NaN_3$ (0.494 g, 7.60 mmol) was added, and the mixture was heated to reflux (100 °C) for 14 hours. After cooling to room temperature, the mixture was added to 100 ml of water and extracted with $Et_2O$ (3x30 ml). The organic phase was washed with water (2x15 ml) and dried over anhydrous $Na_2SO_4$. After filtration, the solvent was removed under reduced pressure. The yellow coloured oil obtained was purified by chromatography ($SiO_2$, *c*-Hex/DCM 70:30 v/v, $R_f$ 0.37), and the product was obtained as a colourless oil in 60% yield (679 mg, 4.27 mmol).

Elemental analysis: calculated C 67.91%, H 5.70%, N 26.40%; found C 67.73%, H 5.61%, N 26.33%. $CI^+$ MS, m/z: 159 ($[M+H]^+$), peaks coming from combinations between vinylbenzyl-fragments and $N_2$ (117, 151, 248, 263, 277, 291, 319, 338). IR (film on KBr pellets), $cm^{-1}$: 3361, 3087, 3024, 3008, 2928, 2875, 2100, 1630, 1511, 1406, 1344, 1252, 1207, 991, 912, 847, 824. $^1H$ NMR (400 MHz, 25 °C, $CDCl_3$), δ (ppm): 7.43 (d, $^3J_{HH}$ = 8.1 Hz, 2H, $H^o$), 7.28 (d, $^3J_{HH}$ = 8.1 Hz, 2H, $H^m$), 6.72 (dd, $^3J_{HH}$ = 17.6 Hz, $^3J_{HH}$ = 10.9 Hz, 1H, $C\underline{H}=CH_2$), 5.77 (d, $^3J_{HH}$ = 17.6 Hz, 1H, $CH=CH\underline{H}^{cis}$), 5.28 (d, $^3J_{HH}$ = 10.9 Hz, 1H, $CH=CH\underline{H}^{trans}$), 4.33 (s, 2H, $CH_2N_3$). $^{13}C$ NMR (100 MHz, 25

°C, $CDCl_3$), δ (ppm): 137.6 ($N_3CH_2\underline{C}^{ipso}$), 136.2 ($\underline{C}H=CH_2$), 134.8 ($C^p$), 128.4 ($C^m$), 126.6 ($C^o$), 114.4 ($CH=\underline{C}H_2$), 54.5 ($CH_2N_3$).

**_N_-((1-(4-Vinylbenzyl)-_1H_-1,2,3-triazol-4-yl)methyl)-2-chloroacetamide 67**

4-Vinylbenzyl azide **66** (0.133 g, 0.836 mmol) was dissolved in *tert*-BuOH (5 ml). *N*-Propargyl-2-chloroacetamide **49** (0.100 g, 0.760 mmol) was added, followed by $CuSO_4 \cdot 5H_2O$ (19.0 mg, 0.0760 mmol), sodium ascorbate (30.1 mg, 0.152 mmol) and distilled $H_2O$ (5 ml). The mixture was heated to reflux (100 °C) for 15 hours. After cooling to room temperature a white solid precipitated and was filtered under vacuum, resulting in a final yield of 55% (0.121 g, 0.416 mmol)

Elemental analysis: calculated C 57.83%, H 5.20%, N 19.27%; found C 57.68%, H 5.13%, N 19.15%. ESI MS, m/z: 603 ([2M+Na]+), 313 ([M+Na]+), 291 ([M+H]+; calculated 291.1013, found 291.1031). $^1$H NMR (400 MHz, 25 °C, $CDCl_3$), δ (ppm): 7.53 (br t, 1H, NH), 7.49 (s, 1H, CH triazole), 7.38 (d, $^3J_{HH}$ = 8.1 Hz, 2H, $H^o$), 7.21 (d, $^3J_{HH}$ = 8.1 Hz, 2H, $H^m$), 6.68 (dd, $^3J_{HH}$ = 17.6 Hz, $^3J_{HH}$ = 10.9 Hz, 1H, $C\underline{H}=CH_2$), 5.74 (d, $^3J_{HH}$ = 17.6 Hz, 1H, $CH=CH\underline{H}^{cis}$), 5.46 (s, 2H, $NCH_2$), 5.27 (d, $^3J_{HH}$ = 10.9 Hz, 1H, $CH=CH\underline{H}^{trans}$), 4.52 (d, $^3J_{HH}$ = 5.8 Hz, 2H, $NHC\underline{H}_2$), 4.00 (s, 2H, $ClCH_2$). $^{13}$C NMR (100 MHz, 25 °C, $CDCl_3$), δ (ppm): 166.2 (CO), 144.3 (C triazole), 138.2 ($NCH_2\underline{C}^{ipso}$), 135.8 ($\underline{C}H=CH_2$), 133.4 ($C^p$), 128.4 ($C^m$), 126.8 ($C^o$), 122.4 (CH triazole), 114.9 ($CH=\underline{C}H_2$), 54.0 ($NCH_2$), 42.4 ($ClCH_2$), 35.0 ($NHCH_2$).

**Fluorescein-5-(2-(2-(2-azidoethoxy)ethoxy)ethyl)thiocarbammate 68**

To a solution of FITC (90.0 mg, 0.231 mmol) and 2-[2-(2-azidoethoxy)ethoxy]ethanol **64** (45.0 mg, 0.257 mmol) in dry DMF (1 ml) was added dry $Et_3N$ (72 µl, 0.51 mmol). After stirring for 24 h at 60 °C, the solvent was removed under reduced pressure, and the residue was purified by chromatography ($SiO_2$, $CHCl_3$/MeOH 85:15 v/v, $R_f$ 0.32). The desired product was obtained as an orange solid in 77% yield (100 mg, 0.178 mmol).

Elemental analysis: calculated C 57.44%, H 4.28%, N 9.92%; found C 57.29%, H 4.39%, N 9.78%. ESI MS, m/z: 565 ($[M+H]^+$; calculated 565.1393, found 565.1389). $^1$H NMR (400 MHz, 25 °C, MeOH-$d_4$), δ (ppm): 8.21 (d, $^4J_{HH}$ = 1.8 Hz, 1H, NHCC$\underline{H}$CCO), 7.88 (dd, $^4J_{HH}$ = 1.8 Hz, $^3J_{HH}$ = 8.3 Hz, 1H, NHCC$\underline{H}$CH), 7.17 (d, $^3J_{HH}$ = 8.3 Hz, 1H, NHCCHC$\underline{H}$), 6.68 (d, $^4J_{HH}$ = 2.3 Hz, 2H, HOCC$\underline{H}$CO), 6.62 (d, $^3J_{HH}$ = 8.7 Hz, 2H, HOCCHC$\underline{H}$), 6.54 (dd, $^4J_{HH}$ = 2.3 Hz, $^3J_{HH}$ = 8.7 Hz, 2H, HOCC$\underline{H}$CH), 4.69 (br

s, 2H, $CSOCH_2$), 3.87 (br t, $^3J_{HH}$ = 4.1 Hz, 2H, $CSOCH_2CH_2$), 3.69 (m, 4H, $OCH_2CH_2OCH_2CH_2N_3$), 3.63 (t, $^3J_{HH}$ = 4.9 Hz, 2H, $OCH_2CH_2N_3$), 3.34 (t, $^3J_{HH}$ = 4.9 Hz, 2H, $CH_2N_3$). $^{13}C$ NMR (100 MHz, 25 °C, MeOH-$d_4$), δ (ppm): 213.6 (CS), 171.1 (C=O), 164.9 (NCCHCH), 161.3 (COH), 154.2 (CHCHCOH), 142.4 (HOCCHCO), 132.7 (NCCHCHC), 130.3 (SCNC), 130.2 (NCCHCH), 129.0 (NCCHCCOO), 125.7 (HOCCHCHC), 113.6 (NCCHC), 111.4 (HOCCHCH), 103.6 (HOCCHCO), 73.7 ($CSOCH_2CH_2$), 71.7-71.6 ($OCH_2CH_2OCH_2CH_2N_3$), 71.1 ($CH_2CH_2N_3$), 62.3 ($CSOCH_2$), 51.8 ($CH_2N_3$).

**1,4,7,10-Tetrakis{[1-(2-(2-(2-hydroxyethoxy)ethoxy)ethyl)-*1H*-1,2,3-triazol-4-yl]methylcarbamoylmethyl}-1,4,7,10-tetraazacyclododecane 70**

***Method I***

DOTA-tetra-propargyl-amide **53** (0.100 g, 0.181 mmol) and hydroxy-azide **64** (0.130 g, 0.742 mmol) were dissolved in DMF (15 ml) and water (15 ml). $CuSO_4.5H_2O$ (18.1 mg, 0.0724 mmol) and Na-ascorbate (28.7 mg, 0.145 mmol) were added, and the mixture was stirred at 50 °C for 20 hours. After removal of the solvents under reduced pressure, the obtained yellow coloured solid was suspended in DMF, stirred for 30 minutes at 50 °C and filtered. The filtrate was dried under vacuum, yielding 0.219 g of yellow coloured solid which was analysed without further purification.

Calculated conversion: 41%. $^1H$ NMR (400 MHz, 25 °C, DMSO-$d_6$), δ (ppm): 8.56 (br m, $NH^{cis}$), 8.43 (br m, $NH^{trans}$), 7.89 (br s, CH triazole), 4.61 (br s, OH), 4.48 (br m, $NCH_2CH_2O$), 4.33 (br m, $NHCH_2$-triazole), 3.89 (br m, $NHCH_2C{\equiv}CH$), 3.79 (br m, $NCH_2CH_2O$), 3.7-3.3 (br m, $OCH_2CH_2OCH_2CH_2OH$ + $NCH_2CO$), 3.05 (br m, $NCH_2CO$ + $NCH_2CH_2N$ + C≡CH), 2.58 (br s, $NCH_2CH_2N$). $^{13}C$ NMR (100 MHz, 25 °C, DMSO-$d_6$), δ (ppm): 171.2 ($CO^{cis}$), 170.5 ($CO^{trans}$), 144.7 (C triazole), 123.1 (CH triazole), 81.2 (C≡CH), 72.8 (C≡CH), 72.3 ($OCH_2CH_2OH$), 69.7 + 69.3 ($OCH_2CH_2O$), 68.8 ($NCH_2CH_2O$), 60.2 ($CH_2OH$), 56.6 ($NCH_2CO$), 53.4 ($NCH_2CH_2N$), 49.3 ($NCH_2CH_2O$), 34.1 ($NHCH_2$-triazole), 27.8 ($NHCH_2C{\equiv}CH$).

***Method II***

DOTA-tetra-propargyl-amide **53** (0.100 g, 0.181 mmol) and hydroxy-azide **64** (0.130 g, 0.742 mmol) were dissolved in DMF (15 ml) and water (15 ml). $Et_3N$ (0.10 ml, 0.74 mmol) was added, followed by $CuSO_4.5H_2O$ (18.1 mg, 0.0724 mmol) and Na-

ascorbate (28.7 mg, 0.145 mmol). The mixture was stirred at 50 °C for 20 hours. After removal of the solvents under reduced pressure, the obtained yellow coloured solid was suspended in DMF, stirred for 30 minutes at 50 °C and filtered. The filtrate was dried under vacuum, leading to 0.221 g of yellow coloured solid which was analysed without further purification.

Calculated conversion: 43%. $^{1}$H NMR (400 MHz, 25 °C, DMSO-$d_6$), δ (ppm): 8.56 (br m, $NH^{cis}$), 8.43 (br m, $NH^{trans}$), 7.88 (br s, CH triazole), 4.60 (br s, OH), 4.48 (br m, $NC\underline{H}_2CH_2O$), 4.34 (br m, $NHC\underline{H}_2$-triazole), 3.89 (br m, $NHC\underline{H}_2C{\equiv}CH$), 3.78 (br m, $NCH_2C\underline{H}_2O$), 3.7-3.3 (br m, $OC\underline{H}_2C\underline{H}_2OC\underline{H}_2C\underline{H}_2OH$ + $NCH_2CO$), 3.04 (br m, $NCH_2CO$ + $NC\underline{H}_2CH_2N$ + C≡CH), 2.62 (br s, $NCH_2C\underline{H}_2N$). $^{13}$C NMR (100 MHz, 25 °C, DMSO-$d_6$), δ (ppm): 171.0 ($CO^{cis}$), 170.4 ($CO^{trans}$), 144.7 (C triazole), 123.1 (CH triazole), 81.2 ($\underline{C}{\equiv}CH$), 72.6 ($C{\equiv}\underline{C}H$), 72.4 ($O\underline{C}H_2CH_2OH$), 69.8 + 69.3 ($O\underline{C}H_2\underline{C}H_2O$), 68.8 ($NCH_2\underline{C}H_2O$), 60.2 ($CH_2OH$), 56.5 ($N\underline{C}H_2CO$), 53.3 ($N\underline{C}H_2\underline{C}H_2N$), 50.0 ($N\underline{C}H_2CH_2O$), 34.0 ($NHCH_2$-triazole), 27.8 ($NH\underline{C}H_2C{\equiv}CH$).

**1,4,7,10-Tetrakis{[1-(4-vinylbenzyl)-*1H*-1,2,3-triazol-4-yl]methylcarbamoylmethyl}-1,4,7,10-tetraazacyclododecane 71**

***Method I***

DOTA-tetra-propargyl-amide **53** (0.100 g, 0.181 mmol) and 4-vinylbenzylazide **66** (0.115 g, 0.724 mmol) were dissolved in DMF (15 ml) and water (15ml). $CuSO_4.5H_2O$ (18.1 mg, 0.0724 mmol) and Na-ascorbate (28.7 mg, 0.145 mmol) were added, and the mixture was stirred at 50 °C for 2 days. After removal of the solvents under reduced pressure, the obtained yellow coloured solid was suspended in DMF, stirred for 30 minutes at 50 °C and filtered. The filtrate was dried under vacuum, leading to 0.209 g of yellow coloured solid which was analysed without further purification.

Calculated conversion: 19%. $^{1}$H NMR (400 MHz, 25 °C, DMSO-$d_6$), δ (ppm): 8.51 (br m, $NH^{cis}$), 8.41 (br m, $NH^{trans}$), 7.95 (s, CH triazole), 7.50 (d, $^{3}J_{HH}$ = 8.1 Hz, $H^{o}$), 7.35 (d, $^{3}J_{HH}$ = 8.1 Hz, $H^{m}$), 6.74 (dd, $^{3}J_{HH}$ = 17.6 Hz, $^{3}J_{HH}$ = 10.9 Hz, $C\underline{H}{=}CH_2$), 5.86 (d, $^{3}J_{HH}$ = 17.6 Hz, $CH{=}CH\underline{H}^{cis}$), 5.55 (s, $NCH_2$), 5.29 (d, $^{3}J_{HH}$ = 10.9 Hz, $CH{=}CH\underline{H}^{trans}$), 4.37 (s, $NHC\underline{H}_2$-triazole), 3.90 (br m, $NHC\underline{H}_2C{\equiv}CH$), 3.36 (br s, $NCH_2CO$), 3.10 (br s, C≡CH), 3.05 ($NCH_2CO$ + $NC\underline{H}_2CH_2N$), 2.58 ($NCH_2C\underline{H}_2N$). $^{13}$C NMR (100 MHz, 25 °C, DMSO-$d_6$), δ (ppm): 171.4 ($CO^{cis}$), 170.7 ($CO^{trans}$), 144.3 (C

triazole), 137.4 ($NCH_2\underline{C}^{ipso}$), 136.6 ($\underline{C}H{=}CH_2$), 135.6 ($C^p$), 129.2 ($C^m$), 126.9 ($C^o$), 122.4 (CH triazole), 115.2 ($CH{=}\underline{C}H_2$), 83.2 ($\underline{C}{\equiv}CH$), 73.4 ($C{\equiv}\underline{C}H$), 57.1 ($N\underline{C}H_2CO$), 53.8 ($N\underline{C}H_2C^{Ar}$), 51.1 ($N\underline{C}H_2\underline{C}H_2N$), 36.2 ($NHCH_2$-triazole), 28.3 ($NH\underline{C}H_2C{\equiv}CH$).

***Method II***

DOTA-tetra-propargyl-amide **53** (0.0500 g, 0.0905 mmol) and 4-vinylbenzylazide **66** (0.0634 g, 0.398 mmol) were dissolved in DMF (15 ml) and water (15ml). $CuSO_4.5H_2O$ (31.6 mg, 0.127 mmol) and Na-ascorbate (32.3 mg, 0.163 mmol) were added, and the mixture was stirred at 50 °C for 2 days. After removal of the solvents under reduced pressure, the obtained lightly green coloured solid was suspended in DMF, stirred for 30 minutes at 50 °C and filtered. The filtrate was dried under vacuum, leading to 0.102 g of yellow coloured solid which was analysed without further purification.

Conversion impossible to estimate. $^1$H NMR (400 MHz, 25 °C, DMSO-$d_6$) and $^{13}$C NMR (100 MHz, 25 °C, DMSO-$d_6$) spectra were too broad to be assigned properly (see discussion in Section 2.3.3).

***Method III***

Cyclen (13.3 mg, 0.0774 mmol), $Cs_2CO_3$ (101 mg, 0.309 mmol) and KI (51.4 m g, 0.310 mmol) were suspended in DMF (1 ml). *N*-((1-(4-Vinylbenzyl)-*1H*-1,2,3-triazol-4-yl)methyl)-2-chloroacetamide **67** (90.0 mg, 0.310 mmol) was added, and the mixture was stirred at 60 °C for 2 days. After removal of the solvents under reduced pressure a brown coloured solid was obtained, which was characterised without further purification.

ESI MS, m/z: 1211 ($[M+Na]^+$), 1189 ($[M+H]^+$), 617 ($[M+2Na]^{2+}$), 595 ($[M+2H]^{2+}$). $^1$H NMR (400 MHz, 25 °C, DMSO-$d_6$), δ (ppm): 8.41 (br s, 4H, NH), 7.90 (s, 4H, H triazole), 7.42 (d, $^3J_{HH}$ = 7.6 Hz, 8H, $H^m$ Ar), 7.25 (d, $^3J_{HH}$ = 7.6 Hz, 8H, $H^o$ Ar), 6.68 (dd, $^3J_{HH}$ = 17.5 Hz, $^3J_{HH}$ = 10.9 Hz, $C\underline{H}{=}CH_2$), 5.80 (d, $^3J_{HH}$ = 17.5 Hz, 4H, $CH{=}CH\underline{H}^{cis}$), 5.51 (s, 4H, $NCH_2Ar$), 5.25 (d, $^3J_{HH}$ = 10.9 Hz, 4H, $CH{=}CH\underline{H}^{trans}$), 4.27 (d, $^3J_{HH}$ = 3.8 Hz, 8H, $NHC\underline{H}_2$), 2.88 (br s, 8H, $NCH_2CO$), 2.38 (br s, 16H, $NCH_2CH_2N$). $^{13}$C NMR (100 MHz, 25 °C, DMSO-$d_6$), δ (ppm): 170.2 (C=O), 145.1 (C triazole), 136.9 ($C^p$), 136.0 ($\underline{C}H{=}CH_2$), 135.5 ($NCH_2\underline{C}^{ipso}$), 128.2 ($C^o$), 126.4 ($C^m$), 122.7 (CH triazole), 114.8 ($CH{=}C\underline{H}_2$), 57.5 ($N\underline{C}H_2CO$), 53.4 ($NCH_2CH_2N$), 52.4 ($NCH_2Ar$), 33.9 ($NHCH_2$).

**Zn-1,4,7,10-tetrakis(2-propynylcarbamoylmethyl)-1,4,7,10-tetraazacyclododecane 73**

Compound **53** (0.500 g, 0.905 mmol) was suspended in 80% MeOH (50 ml), and the suspension was heated to reflux (80 °C). A solution of $Zn(ClO_4)_2 \cdot 6H_2O$ (0.337 g, 0.905 mmol) in MeOH (10 ml) was added dropwise, and the mixture was refluxed for further 2 hours. After removal of the solvents under reduced pressure, a white solid was obtained, that was suspended in distilled $H_2O$ and heated to 50 °C for 1 hour. The suspension was cooled down to room temperature and filtered. The filtrate was dried and purified by precipitation from MeOH with $Et_2O$, leading to a white solid in 87% yield (0.643 g, 0.787 mmol).

Elemental analysis: calculated C 41.17%, H 4.94%, N 13.72%; found C 41.28%, H 4.91%, N 13.62%. ESI MS, m/z: 308 ($[L+Zn]^{2+}$), 615 ($[L+Zn-H]^+$; calculated 615.2386, found 615.2397), 715 ($[L+Zn+ClO_4]^+$). IR (KBr disk), $cm^{-1}$: 3411, 3270, 3079, 2930, 2123, 2025, 1631, 1560, 1463, 1431, 1384, 1365, 1311, 1247, 1145, 1117, 1086, 998, 973, 926. $^1H$ NMR (400 MHz, 25 °C, $D_2O$), δ (ppm): 4.00 (d, $^3J_{HH}$ = 2.4 Hz, 8H, $NHC\underline{H}_2$), 3.43 (br s, 4H, $NCH_2CO$), 2.95 (br m, 8H, $NC\underline{H}_2CH_2N$), 2.70 (br m, 8H, $NCH_2C\underline{H}_2N$), 2.56 (t, $^3J_{HH}$ = 2.4 Hz, 4H, C≡CH). $^{13}C$ NMR (100 MHz, 25 °C, $D_2O$), δ (ppm): 171.7 (C=O), 79.2 (C≡$\underline{C}$H), 72.2 ($\underline{C}$≡CH), 55.6 ($N\underline{C}H_2CO$), 50.3 ($NCH_2CH_2N$), 29.0 ($NHCH_2$).

Crystals for X-ray analysis were grown[407] in MeOH and di-*tert*-butyl ether. Crystallographic data are reported in Table 6.1.

**Table 6.1** Crystallographic data and experimental details for **73** (numbers in parentheses are estimated standard deviations in the least significant digits).[407]

| | |
|---|---|
| Empirical formula | $[C_{28}H_{40}N_8O_4Zn](ClO_4)_2$ |
| Formula weight | 816.96 |
| Temperature | 173(2) K |
| Crystal system, space group | Orthorhombic, Pbcn |
| Unit cell dimensions | a = 21.0127(3) Å, α = 90° |
| | b = 9.02337(13) Å, β = 90° |
| | c = 18.5258(2) Å, γ = 90° |
| Volume, Z | 3512.59(13) $Å^3$, 4 |
| Density (calculated) | 1.579 $g/cm^3$ |
| Absorption coefficient | 0.927 $mm^{-1}$ |
| F(000) | 1736 |
| Crystal colour / morphology | Colourless blocks |
| Crystal size | 0.23 x 0.09 x 0.06 $mm^3$ |
| θ range for data collection | 3.70 to 32.16° |
| Index ranges | -30<=h<=31, -12<=k<=13, -26<=l<=26 |
| Reflns collected / unique | 48325 / 5945 [R(int) = 0.0564] |
| Reflns observed [F>4s(F)] | 3960 |
| Absorption correction | Semi-empirical from equivalents |
| Max. and min. transmission | 1.00000 and 0.81808 |
| Refinement method | Full-matrix least-squares on $F^2$ |
| Data / restraints / parameters | 5945 / 132 / 260 |
| Goodness-of-fit on F2 | 1.067 |
| Final R indices [F>4s(F)] | R1 = 0.0552, wR2 = 0.1417 |
| R indices (all data) | R1 = 0.0916, wR2 = 0.1589 |
| Mean and maximum shift/error | 0.000 and 0.000 |

**Zn-1,4,7,10-tetrakis{[1-(4-vinylbenzyl)-*1H*-1,2,3-triazol-4-yl]methylcarbamoylmethyl}-1,4,7,10-tetraazacyclododecane 74**

Vinylbenzyl azide **66** (85.7 mg, 0.539 mmol) was suspended in *tert*-BuOH (4 ml). Zn-complex **73** (100 mg, 0.122 mmol) was added, followed by $CuSO_4 \cdot 5H_2O$ (12.2 mg, 0.0490 mmol), sodium ascorbate (19.4 mg, 0.0979 mmol) and water (4 ml). The mixture was heated to 50 °C and stirred for 24 hours. The solvents were removed under reduced pressure yielding a yellow coloured solid, which was characterised without further purification.

ESI MS, m/z: 626 ($[L+Zn-H]^{2+}$), 1252 ($[L+Zn-H]^+$), 1274 ($[L+Zn+Na-H]^+$), 1353 ($[L+Zn+ClO_4]^+$). $^1H$ NMR (400 MHz, 25 °C, DMSO-$d_6$), δ (ppm): 9.14 (br s, 4H, NH), 8.01 (s, 4H, H triazole), 7.41 (d, $^3J_{HH}$ = 7.7 Hz, 8H, $H^o$), 7.21 (d, $^3J_{HH}$ = 7.7 Hz, 8H, $H^m$), 6.69 (dd, $^3J_{HH}$ = 17.5 Hz, $^3J_{HH}$ = 10.8 Hz, C<u>H</u>=$CH_2$), 5.81 (d, $^3J_{HH}$ = 17.5 Hz, 4H, CH=CH<u>H</u>$^{cis}$), 5.49 (s, 8H, $NCH_2Ar$), 5.27 (d, $^3J_{HH}$ = 10.8 Hz, 4H, CH=CH<u>H</u>$^{trans}$), 4.32 (s, 8H, NHC<u>H</u>$_2$), 3.39 (br s, 8H, $NCH_2CO$), 2.99 (br m, 8H, NC<u>H</u>$_2$$CH_2N$), 2.66 (br m, 8H, $NCH_2$C<u>H</u>$_2$N). $^{13}C$ NMR (100 MHz, 25 °C, DMSO-$d_6$), δ (ppm): 171.3 (CO), 144.2 ($C^q$ triazole), 137.5 ($NCH_2$<u>C</u>$^{ipso}$), 136.4 (<u>C</u>H=$CH_2$), 135.8 ($C^p$), 128.7 ($C^m$), 126.9

($C^o$), 123.9 (CH triazole), 115.4 ($CH=C\underline{H}_2$), 56.3 ($N\underline{C}H_2CO$), 53.0 ($NCH_2Ar$), 51.1 ($NCH_2CH_2N$), 35.0 ($NHCH_2$).

**1,2-Bis(2-azidoethoxy)ethane 81**

1,2-Bis(chloroethoxy)ethane (1.00 ml, 6.40 mmol) was dissolved in dry DMF (40 ml). Sodium azide (8.320 g, 128.0 mmol) was added, and the suspension was stirred at 60 °C for 15 hours. The mixture was let cool down to room temperature and the solvent was removed under reduced pressure. The residue was suspended in DCM and filtered through Celite, and the filtrate was evaporated under reduced pressure. The slightly yellow coloured oil obtained was purified by chromatography ($SiO_2$, *n*-Hex/DCM 70:30 v/v, Rf 0.25). The product was obtained as a colourless oil in 91% yield (1.166 g, 5.824 mmol).

Elemental analysis: calculated C 36.00%, H 6.04%, N 41.98%; found C 35.89%, H 6.12%, N 41.85%. $CI^+$ MS, m/z: 201 ($[M+H]^+$), 218 ($[M+NH_4]^+$; calculated 218.1365, found 218.1366). IR (film on KBr pellets), $cm^{-1}$: 2924, 2870, 2112, 1443, 1345, 1287, 1125, 934, 853, 825, 646, 557. $^1H$ NMR (400 MHz, 25 °C, $CDCl_3$), δ (ppm): 3.67 (t, $^3J_{HH}$ = 4.9 Hz, 4H, $N_3CH_2C\underline{H}_2$), 3.66 (s, 4H, $N_3CH_2CH_2OC\underline{H}_2$), 3.37 (t, $^3J_{HH}$ = 4.9 Hz, 4H, $N_3CH_2$). $^{13}C$ NMR (100 MHz, 25 °C, $CDCl_3$), δ (ppm): 70.6 ($N_3CH_2CH_2O\underline{C}H_2$), 70.0 ($N_3CH_2\underline{C}H_2$), 50.6 ($N_3CH_2$).

**General procedure for the polymerisation of Zn-complex 73 and diazide 81 by click-chemistry**

Compound **73** (1 mol equiv; see Table 6.2) was suspended in dry DMF (see Table 6.2). Compound **81** (amount depending on the molar ratio required for the reaction; see Table 6.2) was added, and the suspension was degassed with $N_2$ for 10 min. $CuSO_4 \cdot 5H_2O$ (10 mol% per functionality in defect; see Table 6.2) and sodium ascorbate (20 mol% per functionality in defect; see Table 6.2) were added, and the suspension was heated to 50 °C. After 15 h the reaction was cooled to room temperature and filtered, and the filtrate was dried under reduced pressure and analysed.

For some ratios, the residue from the filtrate was dissolved in 10 ml of 0.1 M EDTA by stirring for 12 h. The solution was then placed in a dialysis tubing with reported MWCO of 25 kDa, which in turn was placed in a dialysis tubing with reported MWCO of 2 kDa and dialysed against water.

| Table 6.2 Reaction conditions for click chemistry experiments between **73** and **81**. | | | | | | |
|---|---|---|---|---|---|---|
| **Product** | **[73]/ [81]** | **73 (mg)** | **81 (mg)** | **$CuSO_4$ (mg)** | **Na-ASC (mg)** | **DMF (ml)** |
| **$ZnC_{1.5:1}$** | 1.5:1 | 612 | 100 | 24.9 | 39.6 | 30 |
| **$ZnC_{1:1}$** | 1:1 | 408 | 100 | 24.9 | 39.6 | 20 |
| **$ZnC_{1:2}$** | 1:2 | 200 | 98.0 | 24.4 | 38.8 | 10 |
| **$ZnC_{1:4}$** | 1:4 | 200 | 196 | 24.4 | 38.8 | 10 |

Typical $^{1}H$ NMR set of signals (400 MHz, 25 °C, $D_2O$), δ (ppm): 7.9 (H triazole), 4.5 ($NC\underline{H_2}CH_2O$), 4.4 ($NHC\underline{H_2}$), 3.7 ($NCH_2C\underline{H_2}O$), 3.5 ($OC\underline{H_2}C\underline{H_2}O$), 3.4 ($NCH_2CO$), 3.0 + 2.7 ($NC\underline{H_2}C\underline{H_2}N$), 2.6 (C≡CH).

Typical $^{13}C$ NMR set of signals (100 MHz, 25 °C, $D_2O$), δ (ppm): 171 (C=O), 143 (Cq triazole), 124 (CH triazole), 80 (C≡CH), 73 ($\underline{C}$≡CH), 70-68 ($NCH_2\underline{C}H_2O\underline{C}H_2\underline{C}H_2O$), 56 ($N\underline{C}H_2CO$), 51-49 ($N\underline{C}H_2CH_2O$ + $N\underline{C}H_2\underline{C}H_2N$ + $CH_2N_3$), 30 ($NHCH_2$).

**General procedure for the polymerisation of Gd-complex 85 and diazide 81 by click-chemistry**

Compound **85** (1 mol equiv; see Table 6.3) was suspended in dry DMF (see Table 6.3). Compound **81** (amount depending on the molar ratio required for the reaction; see Table 6.3) was added, and the suspension was degassed with $N_2$ for 10 min. $CuSO_4 \cdot 5H_2O$ (10 mol% per functionality in defect; see Table 6.3) and sodium ascorbate (20 mol% per functionality in defect; see Table 6.3) were added, and the suspension was heated to 50 °C. After 15 h the reaction was cooled to room temperature and filtered, and the filtrate was dried under reduced pressure and analysed.

For some ratios, the residue from the filtrate was dissolved in 10 ml of 0.1 M EDTA by stirring for 12 h. The solution was then placed in a dialysis tubing with reported MWCO of 25 kDa, which in turn was placed in a dialysis tubing with reported MWCO of 2 kDa and dialysed against water.

| Table 6.3 Reaction conditions for click chemistry experiments between **85** and **81**. | | | | | | |
|---|---|---|---|---|---|---|
| **Product** | **[85]/ [81]** | **85 (mg)** | **81 (mg)** | **$CuSO_4$ (mg)** | **Na-ASC (mg)** | **DMF (ml)** |
| **$GdC_{1.5:1}$** | 1.5:1 | 625 | 100 | 24.9 | 39.6 | 30 |
| **$GdC_{1:1}$** | 1:1 | 417 | 100 | 24.9 | 39.6 | 20 |
| **$GdC_{1:1.33}$** | 1:1.33 | 313 | 100 | 24.9 | 39.6 | 15 |
| **$GdC_{1:2}$** | 1:2 | 200 | 96.0 | 23.9 | 38.0 | 10 |
| **$GdC_{1:4}$** | 1:4 | 200 | 192 | 23.9 | 38.0 | 10 |

Signals in the $^{1}H$ NMR and $^{13}C$ NMR spectra were too broad to identify and assign sure peaks.

**General procedure for the polymerisation of ligand 53 and diazide 81 by thermal cycloaddition**

Compound **53** (1 mol equiv; see Table 6.4) was suspended in dry DMF (see Table 6.4). Compound **81** (amount depending on the molar ratio required for the reaction; see Table 6.4) was added, the suspension was degassed with $N_2$ for 10 min and then heated to 100 °C. After 15 h the reaction was cooled to room temperature and filtered, and the filtrate was dried under reduced pressure and analysed.

For some ratios, the residue from the filtrate was dissolved in 10 ml of distilled water by stirring for 12 h. The solution was then placed in a dialysis tubing with reported MWCO of 25 kDa, which in turn was placed in a dialysis tubing with reported MWCO of 2 kDa and dialysed against water.

**Table 6.4** Reaction conditions for thermal cycloaddition experiments between **53** and **81**.

| Product | [53]/ [81] | 53 (mg) | 81 (mg) | $CuSO_4$ (mg) | Na-ASC (mg) | DMF (ml) |
|---|---|---|---|---|---|---|
| **$LigT_{1.33:1}$** | 1.33:1 | 367 | 100 | - | - | 15 |
| **$LigT_{1.165:1}$** | 1.165:1 | 322 | 100 | - | - | 15 |
| **$LigT_{1:1}$** | 1:1 | 276 | 100 | - | - | 10 |
| **$LigT_{1:2}$** | 1:2 | 200 | 145 | - | - | 10 |
| **$LigT_{1:4}$** | 1:4 | 200 | 290 | - | - | 10 |

Typical $^{1}H$ NMR set of signals (400 MHz, 25 °C, DMF-$d_7$), δ (ppm): 8.5 (NH), 8.0 (H 1,4-triazole), 7.6 (H 1,5-triazole), 4.6 ($NC\underline{H_2}CH_2O$), 4.5 ($NHC\underline{H_2}$), 3.8 ($NCH_2C\underline{H_2}O$), 3.6 ($OC\underline{H_2}C\underline{H_2}O$), 3.2 ($NCH_2CO$), 3.0 (C≡CH), 2.7 ($NC\underline{H_2}C\underline{H_2}N$).

Typical $^{13}C$ NMR set of signals (100 MHz, 25 °C, DMF-$d_7$) , δ (ppm): 171 (C=O), 146 (Cq 1,4-triazole), 137 (Cq 1,5-triazole), 133 (CH 1,5-triazole), 124 (CH 1,4-triazole), 81 (C≡CH), 73 ($\underline{C}$≡CH), 70-68 ($NCH_2\underline{C}H_2O\underline{C}H_2\underline{C}H_2O$), 56 ($N\underline{C}H_2CO$), 51-49 ($N\underline{C}H_2CH_2O + N\underline{C}H_2\underline{C}H_2N + CH_2N_3$), 32 ($NHCH_2$-triazole), 28 ($NH\underline{C}H_2C$≡CH).

**General procedure for the polymerisation of Gd-complex 85 and diazide 81 by thermal cycloaddition**

Compound **85** (1 mol equiv; see Table 6.5) was suspended in dry DMF (see Table 6.5). Compound **81** (amount depending on the molar ratio required for the

reaction; see Table 6.5) was added, the suspension was degassed with $N_2$ for 10 min and then heated to 100 °C. After 15 h the reaction was cooled to room temperature and filtered, and the filtrate was dried under reduced pressure and analysed.

For some ratios, the residue from the filtrate was dissolved in 10 ml of distilled water by stirring for 12 h. The solution was then placed in a dialysis tubing with reported MWCO of 25 kDa, which in turn was placed in a dialysis tubing with reported MWCO of 2 kDa and dialysed against water.

**Table 6.5** Reaction conditions for thermal cycloaddition experiments between **85** and **81**.

| Product | [85]/ [81] | 85 (mg) | 81 (mg) | $CuSO_4$ (mg) | Na-ASC (mg) | DMF (ml) |
|---|---|---|---|---|---|---|
| $GdT_{1:1}$ | 1:1 | 417 | 100 | - | - | 20 |
| $GdT_{1:2}$ | 1:2 | 200 | 96.0 | - | - | 10 |
| $GdT_{1:4}$ | 1:4 | 200 | 192 | - | - | 10 |
| $GdT_{1:6}$ | 1:6 | 200 | 288 | - | - | 10 |

Typical $^1$H NMR set of broad signals (400 MHz, 25 °C, $D_2O$), δ (ppm): 7.8 (H 1,4-triazole), 7.5 (H 1,5-triazole), 4.4 ($NC\underline{H_2}CH_2O$ + $NHC\underline{H_2}$), 3.8 ($NCH_2C\underline{H_2}O$), 3.5 ($OC\underline{H_2}C\underline{H_2}O$), 3.0-2.7 ($NC\underline{H_2}C\underline{H_2}N$ + $NCH_2CO$), 2.6 (C≡CH).

No signals observable in the $^{13}$C NMR spectrum.

**Gd-1,4,7,10-tetrakis(ethoxycarbonylmethyl)-1,4,7,10-tetraazacyclododecane 82**

Compound **31** (200 mg, 0.387 mmol) was dissolved in 40 ml of distilled water. $GdCl_3 \cdot 6H_2O$ (96.0 mg, 0.258 mmol) was added, and the mixture was heated at 50 °C. After 4 days the test with MTB (see General) for the presence of free $Gd^{III}$ ions was negative. The solvent was removed under reduced pressure, and the residue was suspended in dry DCM, refluxed for 1 h and filtered, yielding 173 mg (0.217 mmol) of white solid (yield: 84% with respect to the $GdCl_3 \cdot H_2O$).

Mp: >374 °C. Elemental analysis: calculated ($C_{24}H_{44}N_4O_8 \cdot GdCl_3 \cdot H_2O$) C 36.11%, H 5.81%, N 7.02%; found C 36.49%, H 6.00%, N 7.07%. $FAB^+$ MS, m/z: 774 ($[C_{24}H_{44}N_4O_8GdCl_2]^+$). IR (KBr disk), $cm^{-1}$: 2861, 2362, 1615, 1392, 1331, 1275, 1244, 1083, 1018, 976, 938, 906, 613. $^1$H NMR (400 MHz, 25 °C, $D_2O$), δ (ppm): 71.00 (br s), 51.00 (br s), 4.07 (br s), 3.81 (br s), 3.73 (br s), 3.55 (br s), 3.34 (br s), 2.95 (br m), 2.10 (br s), 1.13 (br m), 0.80 (br s). $^{13}$C NMR (100 MHz, 25 °C, $D_2O$): no signal observable after >10000 scans.

**Gd-1,4,7,10-tetrakis(butylcarbamoylmethyl)-1,4,7,10-tetraazacyclododecane 83**

Compound **32** (159 mg, 0.254 mmol) was dissolved in 20 ml of distilled water. $GdCl_3 \cdot 6H_2O$ (62.9 mg, 0.169 mmol) was added, and the mixture was heated at 50 °C. After 5 hours the test with MTB (see General) for the presence of free $Gd^{III}$ ions was negative. The solvent was removed under reduced pressure, and the residue was suspended in dry DCM, refluxed for 2 h and filtered, yielding 110 mg (0.121 mmol) of white solid (yield: 72% with respect to the $GdCl_3 \cdot 6H_2O$).

Mp: >270 °C (decomposes). Elemental analysis: calculated ($C_{32}H_{64}N_8O_4 \cdot GdCl_3 \cdot H_2O$) C 42.40%, H 7.34%, N 12.36%; found C 42.46%, H 7.45%, N 12.37%. $FAB^+$ MS, m/z: 780 ($[C_{32}H_{64}GdN_8O_4]^+$), 815 ($[C_{32}H_{64}ClGdN_8O_4]^+$), 854 ($[C_{32}H_{64}Cl_2GdN_8O_4]^+$). IR (KBr disk), $cm^{-1}$: 3417, 2959, 1627, 1464, 1412, 1384, 1368, 1325, 1298, 1243, 1156, 1080, 997, 959, 898, 834, 719. $^1H$ NMR (500 MHz, 27 °C, $D_2O$), δ (ppm): 3.37 (br s), 3.12 (br s), 2.83 (br s), 1.40 (br s), 1.24 (br s), 0.81 (br s). $^{13}C$ NMR (125 MHz, 27 °C, $D_2O$), δ (ppm): 171.1 (br, CO), 57.2 (br, $N\underline{C}H_2CO$), 50.7 (br, $N\underline{C}H_2\underline{C}H_2N$), 39.7, 34.8, 31.1, 20.0, 13.4 (br, $CH_3$).

**Gd-1,4,7,10-tetrakis(allylcarbamoylmethyl)-1,4,7,10-tetraazacyclododecane 84**

Compound **52** (0.408 g, 0.727 mmol) was dissolved in 30 ml of distilled water. $GdCl_3 \cdot 6H_2O$ (0.180 g, 0.485 mmol) was added, and the mixture was heated at 50 °C. After 5 hours the test with MTB (see General) for the presence of free $Gd^{III}$ ions was negative. The solvent was removed under reduced pressure, and the residue was suspended in dry DCM, refluxed for 2 h and filtered, yielding 0.327 g of white solid (0.388 mmol, 80% with respect to the $GdCl_3 \cdot 6H_2O$).

Mp: >270 °C (decomposes). Elemental analysis: calculated ($C_{28}H_{48}N_8O_4 \cdot GdCl_3 \cdot H_2O$) C 39.92%, H 5.98%, N 13.30%; found C 39.79%, H 6.01%, N 13.36%. $FAB^+$ MS, m/z: 716 ($[C_{28}H_{48}GdN_8O_4]^+$). IR (KBr disk), $cm^{-1}$: 1627, 1485, 1462, 1433, 1412, 1388, 1363, 1324, 1297, 1268, 1243, 1156, 1083, 996, 972, 952, 918, 882, 831, 796, 721, 666, 566, 486. $^1H$ NMR (500 MHz, 27 °C, $D_2O$), δ (ppm): 5.77 (br s), 5.32 (br s), 3.73 (br s), 3.49 (br s), 3.24 (br s), 3.09 (br s), 2.95 (br s), 2.67 (br s), 2.60 (br s), 2.10 (br s), 1.15 (br s). $^{13}C$ NMR (125 MHz, 27 °C, $D_2O$): no signal observable after 10000 scans.

**Gd-1,4,7,10-tetrakis(2-propynylcarbamoylmethyl)-1,4,7,10-tetraazacyclododecane 85**

Compound **53** (200 mg, 0.362 mmol) was suspended in distilled water (30 ml). $GdCl_3 \cdot 6H_2O$ (89.7 mg, 0.241 mmol) was added, and the mixture was heated at 50 °C. After 4 hours the test with MTB (see General) for the presence of free $Gd^{III}$ ions was negative. The solvent was removed under reduced pressure, and the residue was washed in a Soxhlet with dry DCM for 2 days, resulting in 172 mg (0.206 mmol) of white solid (yield: 86% with respect to the $GdCl_3 \cdot 6H_2O$).

Mp: decomposes. Elemental analysis: calculated ($C_{28}H_{40}N_8O_4 \cdot GdCl_3 \cdot H_2O$) C 40.31%, H 5.07%, N 13.43%; found C 40.41%, H 5.15%, N 13.34%. ESI MS, m/z: 708.2290 ($[C_{28}H_{38}GdN_8O_4]^+$; calculated 708.2257). IR (KBr disk), $cm^{-1}$: 3450, 3227, 3085, 2951, 2865, 2109, 1621, 1567, 1462, 1426, 1358, 1324, 1292, 1276, 1085, 1029, 976, 931, 832, 723, 689.

Crystals for X-ray analysis were grown[407] in MeOH and di-*tert*-butyl ether. Crystallographic data are reported in Table 6.6.

**Table 6.6** Crystallographic data and experimental details for **85** (numbers in parentheses are estimated standard deviations in the least significant digits).[407]

| | |
|---|---|
| Empirical formula | $[C_{28}H_{40}N_8O_4Gd]Cl_3(H_2O)$ |
| Formula weight | 834.29 |
| Temperature | 173(2) K |
| Crystal system, space group | Triclinic, P-1 |
| Unit cell dimensions | a = 11.0647(11) Å, α = 111.544(9)<br>b = 13.9522(15) Å, β = 102.872(8)<br>c = 15.2655(13) Å, γ = 100.013(9) |
| Volume, Z | 2050.2(3) $Å^3$, 2 |
| Density (calculated) | 1.562 $g/cm^3$ |
| Absorption coefficient | 12.776 $mm^{-1}$ |
| F(000) | 986 |
| Crystal colour / morphology | Colourless plates |
| Crystal size | 0.18 x 0.12 x 0.05 $mm^3$ |
| θ range for data collection | 3.28 to 74.49° |
| Index ranges | -13<=h<=13, -16<=k<=17, -18<=l<=18 |
| Reflns collected / unique | 28742 / 7883 [R(int) = 0.1045] |
| Reflns observed [F>4s(F)] | 5498 |
| Absorption correction | Semi-empirical from equivalents |
| Max. and min. transmission | 1.00000 and 0.37247 |
| Refinement method | Full-matrix least-squares on $F^2$ |
| Data / restraints / parameters | 7883 / 0 / 480 |
| Goodness-of-fit on F2 | 1.634 |
| Final R indices [F>4s(F)] | R1 = 0.0877, wR2 = 0.2238 |
| R indices (all data) | R1 = 0.1226, wR2 = 0.2593 |
| Mean and maximum shift/error | 0.000 and 0.000 |

**Gd-1,4,7,10-tetrakis(2-styrylcarbamoylmethyl)-1,4,7,10-tetraazacyclododecane 86**

Compound **54** (300 mg, 0.371 mmol) was suspended in a 1:1 v/v mixture of distilled water and DMF (60 ml). $GdCl_3 \cdot 6H_2O$ (91.9 mg, 0.247 mmol) was added, and the mixture was heated at 50 °C. After 3 hours the test with MTB (see General) for the presence of free $Gd^{III}$ ions was negative. The solvent was removed under reduced pressure, and the residue was washed in a Soxhlet with dry THF for 2 days, resulting in 231 mg (0.211 mmol) of white solid (yield: 86% with respect to the $GdCl_3 \cdot 6H_2O$).

Mp: decomposes. Elemental analysis: calculated ($C_{48}H_{56}N_8O_4 \cdot GdCl_3 \cdot H_2O$) C 52.86%, H 5.36%, N 10.27%; found C 52.95%, H 5.48%, N 10.23%. ESI MS, m/z: 1000 ($[C_{48}H_{55}ClGdN_8O_4]^+$), 964 ($[C_{48}H_{54}GdN_8O_4]^+$; calculated 964.3509, found 964.3472). IR (KBr disk), $cm^{-1}$: 3416, 2976, 1631, 1553, 1511, 1458, 1426, 1407, 1384, 1364, 1323, 1247, 1081, 991, 963, 908, 844, 714.

## 6.2 MRI measurements and biological assays

### 6.2.1 Determination of relaxivity

Longitudinal water proton relaxation rates were measured (thanks to Rachael Dobson, Developmental Biology Unit, Institute of Child Health, University College London; and Jack Wells, Radiology and Physics Unit, Institute of Child Health, University College London) at 25 °C by a $T_1$-weighted spin-echo pulse sequence with an echo-time *TE* of 28 ms and an array of repetition-times *TR* of 100, 110, 130, 150, 180, 200, 250, 300, 400, 500, 600, 700, 800, 1000, 1200, 1500, 1800 and 2500 ms on two MRI spectrometers operating at a magnetic field strength of either 2.35 T (corresponding to a proton Larmor frequency of 100 MHz) or 9.4 T (400 MHz). 300 μl solutions of each contrast agent in a 0.1-2.5 mM concentration range in double distilled water were prepared and scanned. Alternatively, longitudinal water proton relaxation rates were also measured at 2.35 T and 25 °C by mean of an inversion-recovery technique using an array of inversion-times τ of 100, 200, 300, 400, 500, 600, 700, 800, 900, 1000, 1200, 1400, 1800, 2200 and 2800 ms.

Results are shown in Table 6.7.

**Table 6.7** Longitudinal and transversal relaxation times ($T_1$, $T_2$), rates ($R_1$, $R_2$) and relaxivities ($r_1$, $r_2$) for Gd-complexes **83-85** and selected cycloaddition products. T = 25 °C.

| Product | [Gd] (mM) | $T_1$ (s) | $R_1$ ($s^{-1}$) | $r_1$ ($mM^{-1}\ s^{-1}$) | [Gd] (mM) | $T_2$ (s) | $R_2$ ($s^{-1}$) | $r_2$ ($mM^{-1}\ s^{-1}$) |
|---|---|---|---|---|---|---|---|---|
| **83** SE, 2.35 T | 0 | 2.761 | 0.362 | 4.21 | 0 | 0.887 | 1.127 | 2.80 |
| | 0.1 | 1.469 | 0.681 | | 0.4 | 0.364 | 2.751 | |
| | 0.2 | 1.056 | 0.947 | | 0.7 | 0.321 | 3.120 | |
| | 0.5 | 0.525 | 1.905 | | 1.0 | 0.260 | 3.843 | |
| | 0.8 | 0.339 | 2.950 | | 1.3 | 0.225 | 4.444 | |
| | 1.0 | 0.225 | 4.444 | | 2.5 | 0.120 | 8.339 | |
| | 1.2 | 0.219 | 4.566 | | | | | |
| | 1.5 | 0.154 | 6.494 | | | | | |
| | 2.0 | 0.113 | 8.850 | | | | | |
| **83** IR, 2.35 T | 0 | 2.480 | 0.403 | 4.49 | Not measured | | | |
| | 0.1 | 1.331 | 0.751 | | | | | |
| | 0.2 | 0.932 | 1.072 | | | | | |
| | 0.4 | 0.480 | 2.082 | | | | | |
| | 0.7 | 0.321 | 3.112 | | | | | |
| | 0.8 | 0.279 | 3.576 | | | | | |
| | 1 | 0.241 | 4.146 | | | | | |
| | 1.3 | 0.194 | 5.142 | | | | | |
| | 1.7 | 0.142 | 7.031 | | | | | |
| | 2.5 | 0.082 | 12.247 | | | | | |
| **83** SE, 9.4 T | Data not available | | | 4.38 | Data not available | | | 4.77 |
| **84** SE, 2.35 T | 0 | 3.105 | 0.322 | 1.88 | | | | 3.73 |
| | 0.1 | 1.753 | 0.570 | | | | | |
| | 0.2 | 1.463 | 0.684 | | | | | |
| | 0.5 | 0.757 | 1.321 | | | | | |
| | 0.8 | 0.539 | 1.855 | | | | | |
| | 1.0 | 0.424 | 2.358 | | | | | |
| | 1.2 | 0.429 | 2.331 | | | | | |
| | 1.5 | 0.319 | 3.135 | | | | | |
| | 2.0 | 0.238 | 4.202 | | | | | |
| **84** IR, 2.35 T | 0.0 | 3.105 | 0.322 | 1.92 | Not measured | | | |
| | 0.1 | 1.753 | 0.571 | | | | | |
| | 0.2 | 1.463 | 0.683 | | | | | |
| | 0.5 | 0.757 | 1.320 | | | | | |
| | 0.8 | 0.539 | 1.854 | | | | | |
| | 1.0 | 0.424 | 2.360 | | | | | |
| | 1.2 | 0.429 | 2.330 | | | | | |
| | 1.5 | 0.319 | 3.136 | | | | | |
| | 2.0 | 0.238 | 4.207 | | | | | |
| **84** SE, 9.4 T | 0 | 1.393 | 0.718 | 2.83 | 0 | 1.018 | 0.982 | 2.60 |
| | 0.4 | 0.513 | 1.949 | | 0.4 | 0.222 | 4.505 | |
| | 0.7 | 0.438 | 2.283 | | 0.7 | 0.256 | 3.906 | |
| | 1.0 | 0.405 | 2.469 | | 1.0 | 0.184 | 5.435 | |
| | 1.3 | 0.326 | 3.067 | | 1.3 | 0.153 | 6.536 | |

| | | | | | | | | |
|---|---|---|---|---|---|---|---|---|
| | 2.5 | 0.199 | 5.025 | | 2.5 | 0.093 | 10.753 | |
| **85** SE, 2.35 T | 0 | 2.761 | 0.362 | 1.59 | | | | 2.53 |
| | 0.1 | 1.913 | 0.523 | | | | | |
| | 0.2 | 1.577 | 0.634 | | | | | |
| | 0.5 | 0.785 | 1.274 | | | | | |
| | 0.8 | 0.593 | 1.686 | | | | | |
| | 1.0 | 0.558 | 1.792 | | | | | |
| | 1.2 | 0.409 | 2.445 | | | | | |
| | 1.5 | 0.382 | 2.618 | | | | | |
| | 2.0 | 0.279 | 3.584 | | | | | |
| **85** IR, 2.35 T | 0.0 | 2.761 | 0.362 | 1.71 | Not measured | | | |
| | 0.1 | 1.753 | 0.571 | | | | | |
| | 0.2 | 1.463 | 0.683 | | | | | |
| | 0.5 | 0.757 | 1.320 | | | | | |
| | 0.8 | 0.539 | 1.854 | | | | | |
| | 1.0 | 0.424 | 2.360 | | | | | |
| | 1.2 | 0.429 | 2.330 | | | | | |
| | 1.5 | 0.319 | 3.136 | | | | | |
| | 2.0 | 0.238 | 4.207 | | | | | |
| | 3.0 | 0.186 | 5.366 | | | | | |
| **85** SE, 9.4 T | | | | 1.62 | | | | 3.63 |
| **$GdC_{1.5:1}$** | 0.36 | 0.636 | 1.572 | 3.07 | 0.36 | 0.409 | 2.445 | 3.97 |
| | 0.27 | 0.845 | 1.184 | | 0.27 | 0.478 | 2.091 | |
| | 0.18 | 1.005 | 0.995 | | 0.18 | 0.653 | 1.532 | |
| | 0.15 | 1.152 | 0.868 | | 0.15 | 0.603 | 1.659 | |
| | 0.09 | 1.424 | 0.702 | | 0.09 | 0.730 | 1.370 | |
| **$GdT_{1:2}$** | 0.97 | 0.341 | 2.929 | 2.50 | 0.97 | 0.265 | 3.770 | 2.73 |
| | 0.73 | 0.438 | 2.285 | | 0.73 | 0.326 | 3.070 | |
| | 0.49 | 0.581 | 1.722 | | 0.49 | 0.397 | 2.521 | |
| | 0.39 | 0.664 | 1.506 | | 0.39 | 0.471 | 2.121 | |
| | 0.24 | 0.933 | 1.072 | | 0.24 | 0.561 | 1.782 | |
| **$GdT_{1:4}$** | 1.03 | 0.355 | 2.814 | 2.28 | 1.03 | 0.281 | 3.563 | 2.43 |
| | 0.77 | 0.505 | 1.982 | | 0.77 | 0.345 | 2.896 | |
| | 0.51 | 0.621 | 1.610 | | 0.51 | 0.450 | 2.222 | |
| | 0.41 | 0.766 | 1.305 | | 0.41 | 0.499 | 2.006 | |
| | 0.26 | 1.009 | 0.991 | | 0.26 | 0.580 | 1.726 | |
| **$GdT_{1:6}$** | 2.56 | - | - | 2.65 | 2.56 | 0.117 | 8.545 | 3.07 |
| | 1.92 | 0.189 | 5.298 | | 1.92 | 0.146 | 6.862 | |
| | 1.28 | 0.284 | 3.516 | | 1.28 | 0.198 | 5.044 | |
| | 1.02 | 0.321 | 3.116 | | 1.02 | 0.263 | 3.797 | |
| | 0.64 | 0.547 | 1.830 | | 0.64 | 0.370 | 2.704 | |

### 6.2.2 Incubation for cell viability tests

ST14A stem cells[471] were kindly provided by Prof. Elena Cattaneo (Laboratory of Stem Cell Biology and Pharmacology of Neurodegenerative Diseases, Department of Pharmacological Sciences and Centre for Stem Cell Research, University of Milano, via Balzaretti 9, 20133 Milano, Italy), and they were derived from the embryonic day 14 (E14) rat Striatum through retroviral transduction of a temperature sensitive SV40 Large TAg oncogene.

Cells (10000 cells/well, as counted with a Fuchs–Rosenthal hemacytometer) were cultured (thanks to Rachael Dobson, Developmental Biology Unit, Institute of Child Health, University College London) in 96-well dishes with solutions of each compound in DMEM as culture medium (8x100 µl wells/solution). Each solution was prepared from a 20 mM stock solution of agent. 8 wells on each dish were used for cell culturing with DMEM only. The dishes were incubated at standard conditions of 5% $CO_2$ in air, 37 °C and 100% humidity. After 24 hours the medium was removed and the cells were washed with EBSS.

**Alamar Blue assay[472, 473]**

After washing with EBSS, cells were seeded into the wells of a 96-well plate (100 µl/well) with culture medium containing 10% w/v Alamar Blue, 10% w/v FCS and 1% penicillin-streptomycin in DMEM. Incubation was carried out at standard conditions of 5% $CO_2$ in air, 37 °C and 100% humidity. As negative control, wells with Alamar Blue solution were also prepared with no cells and with cells previously incubated without a contrast agent. After 24 hours, 3 absorbance values for each dish were measured at 570 nm with an ELISA plate reader (Revelation). The data was analysed by taking the average across the dishes for each compound and subtracted from the control (wells with no cells). Results are reported in Table 6.8.

**Table 6.8** Results of the Alamar Blue assay on cell cultures of **83-85**

| 83 | | | 84 | | | 85 | | |
|---|---|---|---|---|---|---|---|---|
| **Conc. (mM)** | **Abs (570 nm)** | **Std. Err.** | **Conc. (mM)** | **Abs (570 nm)** | **Std. Err.** | **Conc. (mM)** | **Abs (570 nm)** | **Std. Err.** |
| 0.01 mM | 0.0232 | 0.00317 | 0.01 mM | 0.0309 | 0.00328 | 0.01 Mm | 0.0203 | 0.00224 |
| 0.1 mM | 0.0245 | 0.00162 | 0.1 mM | 0.0337 | 0.00196 | 0.1 mM | 0.0273 | 0.00233 |
| 0.5 mM | 0.0239 | 0.00295 | 0.5 mM | 0.0379 | 0.00102 | 1.0 mM | 0.0212 | 0.00229 |
| 1.0 mM | 0.0273 | 0.00225 | 1.0 mM | 0.0374 | 0.00177 | 2.0 mM | 0.0264 | 0.00191 |
| 2.0 mM | 0.0320 | 0.00137 | 2.0 mM | 0.0468 | 0.00095 | 2.5 mM | 0.0356 | 0.00209 |
| 3.0 mM | 0.0395 | 0.00328 | 3.0 mM | 0.0437 | 0.00263 | 3.0 mM | 0.0318 | 0.00200 |
| 4.0 mM | 0.0361 | 0.00322 | 4.0 mM | 0.0373 | 0.00172 | 4.0 mM | 0.0331 | 0.00164 |
| 5.0 mM | 0.0363 | 0.00381 | 5.0 mM | 0.0398 | 0.00231 | 5.0 mM | 0.0519 | 0.00323 |
| 7.0 mM | 0.0291 | 0.00208 | 7.0 mM | 0.0437 | 0.00174 | 0 mM | 0.0379 | 0.00134 |
| 10.0 mM | 0.0434 | 0.00327 | 10.0 mM | 0.0516 | 0.00423 | control | 0.0002 | 0.00122 |
| 0 mM | 0.0301 | 0.00132 | 0 mM | 0.0379 | 0.00149 | | | |
| control | 0.0021 | 0.00109 | control | 0.0019 | 0.00107 | | | |

## Methylene Blue assay[474]

Cells were washed with EBSS and fixed onto a 96-well plate. 100 µl of 1% w/v Methylene Blue in 0.01 M borate buffer (pH 8.4) was added to each well. After 30 minutes the plates were washed with borate buffer and dried at room temperature. The dye was solubilised adding 100 µl of 0.1 M HCl to each well, and the absorbance at 650 nm was measured for each well with an ELISA plate reader (Revelation). Results are reported in Table 6.9.

**Table 6.9** Results of the Methylene Blue assay on cell cultures of **83-85**

| **Conc. (mM)** | 83 | | 84 | | 85 | |
|---|---|---|---|---|---|---|
| | **Abs (560 nm)** | **Std. Err.** | **Abs (560 nm)** | **Std. Err.** | **Abs (560 nm)** | **Std. Err.** |
| 0.01 mM | 0.821 | 0.0413 | 0.637 | 0.0535 | 0.730 | 0.0448 |
| 0.1 mM | 0.879 | 0.0458 | 0.697 | 0.0434 | 0.712 | 0.0379 |
| 0.5 mM | 0.781 | 0.0513 | 0.718 | 0.0375 | 0.673 | 0.0365 |
| 1.0 mM | 0.703 | 0.0504 | 0.595 | 0.0394 | 0.518 | 0.0289 |
| 3.0 mM | 0.667 | 0.0594 | 0.440 | 0.0157 | 0.433 | 0.0497 |

| 0 mM | | control | |
|---|---|---|---|
| **Abs (560 nm)** | **Std. Err.** | **Abs (560 nm)** | **Std. Err.** |
| 0.638 | 0.0591 | 0.0404 | 0.00152 |

## References


(1) Lauffer, R. B. *Chem. Rev.* **1987**, *87(5)*, 901-927.
(2) Caravan, P.; Ellison, J. J.; McMurry, T. J.; Lauffer, R. B. *Chem. Rev.* **1999**, *99(9)*, 2293-2352.
(3) Aime, S.; Dastru, W.; Crich Simonetta, G.; Gianolio, E.; Mainero, V. *Biopolymers* **2002**, *66(6)*, 419-428.
(4) Stiriba, S.-E.; Frey, H.; Haag, R. *Angew. Chem., Int. Ed.* **2002**, *41(8)*, 1329-1334.
(5)
(6) Bloch, F.; Hansen, W. W.; Packard, M. *Phys. Rev.* **1946**, *70*, 474-485.
(7) Purcell, E. M.; Pound, R. V.; Bloembergen, N. *Phys. Rev.* **1946**, *70*, 980-987.
(8) Damadian, R. *Science* **1971**, *171(976)*, 1151-1153.
(9) Lauterbur, P. C. *Nature* **1973**, *242(5394)*, 190-191.
(10) Kumar, A.; Welti, D.; Ernst, R. R. *J. Magn. Reson., Ser A* **1975**, *18(1)*, 69-83.
(11) Mansfield, P. *J. Phys. C* **1977**, *10(3)*, L55-L58.
(12) Wiener, S. N.; Flynn, M. J.; Edelstein, J. *Radiology* **1980**, *136(1)*, 181-185.
(13) Chapman, B.; Turner, R.; Ordidge, R. J.; Doyle, M.; Cawley, M.; Coxon, R.; Glover, P.; Mansfield, P. *Magn. Reson. Med.* **1987**, *5(3)*, 246-254.
(14) Dumoulin, C. L.; Souza, S. P.; Hart, H. R. *Magn. Reson. Med.* **1987**, *5(3)*, 238-245.
(15) Bandettini, P. A.; Wong, E. C.; Hinks, R. S.; Tikofsky, R. S.; Hyde, J. S. *Magn. Reson. Med.* **1992**, *25(2)*, 390-397.
(16) Kwong, K. K.; Belliveau, J. W.; Chesler, D. A.; Goldberg, I. E.; Weisskoff, R. M.; Poncelet, B. P.; Kennedy, D. N.; Hoppel, B. E.; Cohen, M. S.; Turner, R. *Proc. Natl. Acad. Sci. USA* **1992**, *89(12)*, 5675-5679.
(17)
(18) Aime, S.; Botta, M.; Fasano, M.; Terreno, E. *Acc. Chem. Res.* **1999**, *32(11)*, 941-949.
(19) Aime, S.; Fasano, M.; Terreno, E. *Chem. Soc. Rev.* **1998**, *27(1)*, 19-29.
(20) Bianchi, A.; Calabi, L.; Corana, F.; Fontana, S.; Losi, P.; Maiocchi, A.; Paleari, L.; Valtancoli, B. *Coord. Chem. Rev.* **2000**, *204*, 309-393.
(21) Botta, M. *Eur. J. Inorg. Chem.* **2000**, *(3)*, 399-407.
(22) Comblin, V.; Gilsoul, D.; Hermann, M.; Humblet, V.; Jacques, V.; Mesbahi, M.; Sauvage, C.; Desreux, J. F. *Coord. Chem. Rev.* **1999**, *185-186*, 451-470.
(23) Parker, D. *Coord. Chem. Rev.* **2000**, *205*, 109-130.
(24) Parker, D.; Dickins, R. S.; Puschmann, H.; Crossland, C.; Howard, J. A. K. *Chem. Rev.* **2002**, *102(6)*, 1977-2010.
(25) Parker, D.; Williams, J. A. G. *J. Chem. Soc., Dalton Trans.* **1996**, *(18)*, 3613-3628.
(26) Toth, E.; Burai, L.; Merbach, A. E. *Coord. Chem. Rev.* **2001**, *216-217*, 363-382.
(27) Bloembergen, N. *J. Chem. Phys.* **1957**, *27*, 572-573.
(28) Bloembergen, N.; Purcell, E. M.; Pound, R. V. *Phys. Rev.* **1948**, *73*, 679-712.
(29) Solomon, I. *Phys. Rev.* **1955**, *99*, 559-565.
(30) Eisinger, J.; Shulman, R. G.; Blumberg, W. E. *Nature* **1961**, *192*, 963-964.
(31) Andrew, E. R.; Bottomley, P. A.; Hinshaw, W. S.; Holland, G. N.; Moore, W. S.; Simaroj, C. *Phys. Med. Biol.* **1977**, *22(5)*, 971-974.
(32) Damadian, R.; Goldsmith, M.; Minkoff, L. *Physiol. Chem. Phys. Med. NMR* **1977**, *9(1)*, 97-100, 108.
(33) Hinshaw, W. S.; Bottomley, P. A.; Holland, G. N. *Nature* **1977**, *270(5639)*, 722-723.
(34) Lauterbur, P. C.; Dias, M. H. M.; Rudin, A. M. *Front. Biol. Energ.* **1978**, *1*, 752-759.
(35) Brady, T. J.; Goldman, M. R.; Pykett, I. L.; Buonanno, F. S.; Kistler, J. P.; Newhouse, J. H.; Burt, C. T.; Hinshaw, W. S.; Pohost, G. M. *Radiology* **1982**, *144(2)*, 343-347.
(36) Goldman, M. R.; Brady, T. J.; Pykett, I. L.; Burt, C. T.; Buonanno, F. S.; Kistler, J. P.; Newhouse, J. H.; Hinshaw, W. S.; Pohost, G. M. *Circulation* **1982**, *66(5)*, 1012-1016.
(37) Young, I. R.; Clarke, G. J.; Bailes, D. R.; Pennock, J. M.; Doyle, F. H.; Bydder, G. M. *J. Comput. Tomogr.* **1981**, *5(6)*, 543-547.
(38) Carr, D. H.; Brown, J.; Bydder, G. M.; Weinmann, H. J.; Speck, U.; Thomas, D. J.; Young, I. R. *Lancet* **1984**, *1(8375)*, 484-486.
(39) Lin, S.-P.; Brown Jeffrey, J. *J. Magn. Reson. Imaging* **2007**, *25(5)*, 884-899.
(40) Dawson, P. *Eur. J. Radiol.* **1996**, *23(3)*, 201-204.
(41) Okuhata, Y. *Adv. Drug Delivery Rev.* **1999**, *37(1-3)*, 121-137.
(42) Toth, E. *Compr. Coord. Chem. II* **2003**, *9*, 841-881.
(43) Koenig, S. H.; Brown, R. D., III *Magn. Reson. Med.* **1984**, *1(4)*, 478-495.

(44) Louie, A. Y.; Huber, M. M.; Ahrens, E. T.; Rothbacher, U.; Moats, R.; Jacobs, R. E.; Fraser, S. E.; Meade, T. J. *Nat. Biotech.* **2000**, *18(3)*, 321-325.
(45) Mahfouz, A. E.; Hamm, B.; Taupitz, M. *Eur. Radiol.* **1997**, *7(4)*, 507-513.
(46) Hwang, L.-P.; Freed, J. H. *J. Chem. Phys.* **1975**, *63(1)*, 118-130.
(47) Hwang, L.-P.; Freed, J. H. *J. Chem. Phys.* **1975**, *63(9)*, 4017-4025.
(48) Freed, J. H. *J. Chem. Phys.* **1978**, *68(9)*, 4034-4037.
(49) Iton, L. E.; Turkevich, J. *J. Phys. Chem.* **1977**, *81(5)*, 435-449.
(50) Luz, Z.; Shulman, R. G. *J. Chem. Phys.* **1965**, *43(10)*, 3750-3756.
(51) Sur, S. K.; Bryant, R. G. *J. Phys. Chem.* **1995**, *99(17)*, 6301-6308.
(52) Caravan, P.; Amedio, J. C., Jr.; Dunham, S. U.; Greenfield, M. T.; Cloutier, N. J.; McDermid, S. A.; Spiller, M.; Zech, S. G.; Looby, R. J.; Raitsimring, A. M.; McMurry, T. J.; Lauffer, R. B. *Chem.--Eur. J.* **2005**, *11(20)*, 5866-5874.
(53) Brinkley, M. *Bioconjugate Chem.* **1992**, *3(1)*, 2-13.
(54) Parker, D. *Chem. Soc. Rev.* **2004**, *33(3)*, 156-165.
(55) Woods, M.; Kiefer, G. E.; Bott, S.; Castillo-Muzquiz, A.; Eshelbrenner, C.; Michaudet, L.; McMillan, K.; Mudigunda, S. D. K.; Ogrin, D.; Tircso, G.; Zhang, S.; Zhao, P.; Sherry, A. D. *J. Am. Chem. Soc.* **2004**, *126(30)*, 9248-9256.
(56) Gschneidner, K. A., Jr.; Eyring, L.; Editors *Handbook on the Physics and Chemistry of Rare Earths, Vol. 4: Nonmetallic Compounds*, 1979.
(57) Jacques, V.; Desreux, J. F. *Top. Curr. Chem.* **2002**, *221(Contrast Agents I)*, 123-164.
(58) Kobayashi, H.; Sato, N.; Hiraga, A.; Saga, T.; Nakamoto, Y.; Ueda, H.; Konishi, J.; Togashi, K.; Brechbiel, M. W. *Magn. Reson. Med.* **2001**, *45(3)*, 454-460.
(59) Runge, V. M. *J. Magn. Reson. Imaging* **2000**, *12(2)*, 205-213.
(60) Venkatachalam, M. A.; Rennke, H. G. *Circ. Res.* **1978**, *43(3)*, 337-347.
(61) Klaassen, C. D.; Watkins, J. B., III *Pharm. Rev.* **1984**, *36(1)*, 1-67.
(62) Aime, S.; Botta, M.; Dastru, W.; Fasano, M.; Panero, M.; Arnelli, A. *Inorg. Chem.* **1993**, *32(10)*, 2068-2071.
(63) De Jong, M.; Bakker, W. H.; Bernard, B. F.; Valkema, R.; Kwekkeboom, D. J.; Reubi, J.-C.; Srinivasan, A.; Schmidt, M.; Krenning, E. P. *J. Nucl. Med.* **1999**, *40(12)*, 2081-2087.
(64) Lemieux, G. A.; Yarema, K. J.; Jacobs, C. L.; Bertozzi, C. R. *J. Am. Chem. Soc.* **1999**, *121(17)*, 4278-4279.
(65) Nunn, A. D.; Linder, K. E.; Tweedle, M. F. *Q. J. Nucl. Med.* **1997**, *41(2)*, 155-162.
(66) Tilcock, C. *Adv. Drug Delivery Rev.* **1999**, *37(1-3)*, 33-51.
(67) Lauffer, R. B.; Brady, T. J. *Magn. Reson. Imaging* **1985**, *3(1)*, 11-16.
(68) Spanoghe, M.; Lanens, D.; Dommisse, R.; Van der Linden, A.; Alder Weireldt, F. *Magn. Reson. Imaging* **1992**, *10(6)*, 913-917.
(69) Lowe, M. P. *Aust. J. Chem.* **2002**, *55(9)*, 551-556.
(70) Aime, S.; Crich, S. G.; Botta, M.; Giovenzana, G.; Palmisano, G.; Sisti, M. *Chem. Commun.* **1999**, *(16)*, 1577-1578.
(71) Aime, S.; Barge, A.; Botta, M.; Howard, J. A. K.; Kataky, R.; Lowe, M. P.; Moloney, J. M.; Parker, D.; de Sousa, A. S. *Chem. Commun.* **1999**, *(11)*, 1047-1048.
(72) Blair, S.; Lowe, M. P.; Mathieu, C. E.; Parker, D.; Senanayake, P. K.; Kataky, R. *Inorg. Chem.* **2001**, *40(23)*, 5860-5867.
(73) Bruce, J. I.; Dickins, R. S.; Govenlock, L. J.; Gunnlaugsson, T.; Lopinski, S.; Lowe, M. P.; Parker, D.; Peacock, R. D.; Perry, J. J. B.; Aime, S.; Botta, M. *J. Am. Chem. Soc.* **2000**, *122(40)*, 9674-9684.
(74) Hovland, R.; Glogard, C.; Aasen, A. J.; Klaveness, J. *J. Chem. Soc., Perkin Trans. 2* **2001**, *(6)*, 929-933.
(75) Lokling, K. E.; Fossheim, S. L.; Skurtveit, R.; Bjornerud, A.; Klaveness, J. *Magn. Reson. Imaging* **2001**, *19(5)*, 731-738.
(76) Lowe, M. P.; Parker, D. *Chem. Commun.* **2000**, *(8)*, 707-708.
(77) Lowe, M. P.; Parker, D. *Inorg. Chim. Acta* **2001**, *317(1,2)*, 163-173.
(78) Lowe, M. P.; Parker, D.; Reany, O.; Aime, S.; Botta, M.; Castellano, G.; Gianolio, E.; Pagliarin, R. *J. Am. Chem. Soc.* **2001**, *123(31)*, 7601-7609.
(79) Zhang, S.; Wu, K.; Sherry, A. D. *Angew. Chem. Int. Ed.* **1999**, *38(21)*, 3192-3194.
(80) Tannock, I. F.; Rotin, D. *Cancer Res.* **1989**, *49(16)*, 4373-4384.
(81) Wike-Hooley, J. L.; Haveman, J.; Reinhold, H. S. *Radiotherapy and oncology* **1984**, *2(4)*, 343-366.
(82) Aime, S.; Botta, M.; Gianolio, E.; Terreno, E. *Angew. Chem. Int. Ed.* **2000**, *39(4)*, 747-750.
(83) Aime, S.; Ascenzi, P.; Comoglio, E.; Fasano, M.; Paoletti, S. *J. Am. Chem. Soc.* **1995**, *117(36)*, 9365-9366.

(84) Burai, L.; Toth, E.; Seibig, S.; Scopelliti, R.; Merbach, A. E. *Chem.--Eur. J.* **2000**, *6(20)*, 3761-3770.
(85) Seibig, S.; Toth, E.; Merbach, A. E. *J. Am. Chem. Soc.* **2000**, *122(24)*, 5822-5830.
(86) Kendrick, M. J. *Metals in biological systems* Ellis Horwood: London, 1992.
(87) Li, W. H.; Fraser, S. E.; Meade, T. J. *J. Am. Chem. Soc.* **1999**, *121(6)*, 1413-1414.
(88) De Leon-Rodriguez, L. M.; Ortiz, A.; Weiner, A. L.; Zhang, S. R.; Kovacs, Z.; Kodadek, T.; Sherry, A. D. *J. Am. Chem. Soc.* **2002**, *124(14)*, 3514-3515.
(89) Nivorozhkin, A. L.; Kolodziej, A. F.; Caravan, P.; Greenfield, M. T.; Lauffer, R. B.; McMurry, T. J. *Angew. Chem. Int. Ed.* **2001**, *40(15)*, 2903-2906.
(90) Bottenstein, J. E. S., G. *Cell culture in the neurosciences*; Plenum Press: New York 1985.
(91) Freshney, R. I. *Culture of animal cells: a manual of basic technique*, 5th ed.; Wiley-Liss: Hoboken, 2005.
(92) Dousset, V.; Tourdias, T.; Brochet, B.; Boiziau, C.; Petry, K. G. *J. Neurol. Sci.* **2008**, *265(1-2)*, 122-126.
(93) Heyn, C.; Bowen, C. V.; Rutt, B. K.; Foster, P. J. *Magn. Reson. Med.* **2005**, *53(2)*, 312-320.
(94) Lewin, M.; Carlesso, N.; Tung, C. H.; Tang, X. W.; Cory, D.; Scadden, D. T.; Weissleder, R. *Nat. Biotech.* **2000**, *18(4)*, 410-414.
(95) Morawski, A. M.; Lanza, G. A.; Wickline, S. A. *Curr. Opin. Biotechnol.* **2005**, *16(1)*, 89-92.
(96) Shapiro, E. M.; Sharer, K.; Skrtic, S.; Koretsky, A. P. *Magn. Reson. Med.* **2006**, *55(2)*, 242-249.
(97) Wilhelm, C.; Cebers, A.; Bacri, J. C.; Gazeau, F. *Eur. Biophys. J. Biophys. Lett.* **2003**, *32(7)*, 655-660.
(98) Taupitz, M.; Schnorr, J.; Abramjuk, C.; Wagner, S.; Pilgrimm, H.; Hunigen, H.; Hamm, B. *J. Magn. Reson. Imaging* **2000**, *12(6)*, 905-911.
(99) Crich, S. G.; Biancone, L.; Cantaluppi, V.; Esposito, D. D. G.; Russo, S.; Camussi, G.; Aime, S. *Magn. Reson. Med.* **2004**, *51(5)*, 938-944.
(100) Daldrup-Link, H. E.; Rudelius, M.; Metz, S.; Piontek, G.; Pichler, B.; Settles, M.; Heinzmann, U.; Schlegel, J.; Oostendorp, R. A. J.; Rummeny, E. J. *Eur. J. Nucl. Med. Mol. Imaging* **2004**, *31(9)*, 1312-1321.
(101) Modo, M.; Cash, D.; Mellodew, K.; Williams, S. C. R.; Fraser, S. E.; Meade, T. J.; Price, J.; Hodges, H. *Neuroimage* **2002**, *17(2)*, 803-811.
(102) Franano, F. N.; Edwards, W. B.; Welch, M. J.; Brechbiel, M. W.; Gansow, O. A.; Duncan, J. R. *Magn. Reson. Imaging* **1995**, *13(2)*, 201-214.
(103) Ohara, P. B.; Koenig, S. H. *Biochemistry* **1986**, *25(6)*, 1445-1450.
(104) Parker, D. *Chem. Soc. Rev.* **1990**, *19(3)*, 271-291.
(105) Zak, O.; Aisen, P. *Biochemistry* **1988**, *27(3)*, 1075-1080.
(106) Abu-Alfa, A. *J. Am. Coll. Radiol.* **2008**, *5(1)*, 45-52.
(107) Bellin, M.-F.; Van Der Molen Aart, J. *Eur. J. Radiol.* **2008**, *66(2)*, 160-167.
(108) Broome Dale, R. *Eur. J. Radiol.* **2008**, *66(2)*, 230-234.
(109) Cowper Shawn, E. *J. Am. Coll. Radiol.* **2008**, *5(1)*, 23-28.
(110) Kallen Alexander, J.; Jhung Michael, A.; Cheng, S.; Hess, T.; Turabelidze, G.; Abramova, L.; Arduino, M.; Guarner, J.; Pollack, B.; Saab, G.; Patel Priti, R. *Am. J. Kidney Dis.* **2008**, *51(6)*, 966-975.
(111) Kuo Phillip, H. *J. Am. Coll. Radiol.* **2008**, *5(1)*, 29-35.
(112) Alexander, V. *Chem. Rev.* **1995**, *95(2)*, 273-342.
(113) Lauffer, R. B. *Chem. Rev.* **1987**, *87(5)*, 901-927.
(114) Toth, E.; Helm, L.; Merbach, A. E. in *Comprehensive Coordination Chemistry II*, 2003; Vol. 9, pp 841-881.
(115) Raymond, K. N.; Pierre, V. C. *Bioconjugate Chem.* **2005**, *16(1)*, 3-8.
(116) Graif, M.; Steiner, R. E. *Br. J. Radiol.* **1986**, *59(705)*, 865-873.
(117) Johnston, D. L.; Liu, P.; Lauffer, R. B.; Newell, J. B.; Wedeen, V. J.; Rosen, B. R.; Brady, T. J.; Okada, R. D. *J. Nucl. Med.* **1987**, *28(5)*, 871-877.
(118) Konings, M. S.; Dow, W. C.; Love, D. B.; Raymond, K. N.; Quay, S. C.; Rocklage, S. M. *Inorg. Chem.* **1990**, *29(8)*, 1488-1491.
(119) McNamara, M. T.; Higgins, C. B.; Ehman, R. L.; Revel, D.; Sievers, R.; Brasch, R. C. *Radiology* **1984**, *153(1)*, 157-163.
(120) Runge, V. M.; Schoerner, W.; Niendorf, H. P.; Laniado, M.; Koehler, D.; Claussen, C.; Felix, R.; James, A. E., Jr. *Magn. Reson. Imaging* **1985**, *3(1)*, 27-35.
(121) Wenzel, T. J.; Ashley, M. E.; Sievers, R. E. *Anal. Chem.* **1982**, *54(4)*, 615-621.
(122) Bousquet, J. C.; Saini, S.; Stark, D. D.; Hahn, P. F.; Nigam, M.; Wittenberg, J.; Ferrucci, J. T. *Radiology* **1988**, *166(3)*, 693-698.
(123) Cacheris, W. P.; Nickle, S. K.; Sherry, A. D. *Inorg. Chem.* **1987**, *26(6)*, 958-960.
(124) Desreux, J. F. *Inorg. Chem.* **1980**, *19(5)*, 1319-1324.

(125) Loncin, M. F.; Desreux, J. F.; Merciny, E. *Inorg. Chem.* **1986**, *25(15)*, 2646-2648.
(126) Paulroth, C.; Raymond, K. N. *Inorg. Chem.* **1995**, *34(6)*, 1408-1412.
(127) Powell, D. H.; NiDhubhghaill, O. M.; Pubanz, D.; Helm, L.; Lebedev, Y. S.; Schlaepfer, W.; Merbach, A. E. *J. Am. Chem. Soc.* **1996**, *118(39)*, 9333-9346.
(128) Rizkalla, E. N.; Choppin, G. R.; Cacheris, W. *Inorg. Chem.* **1993**, *32(5)*, 582-586.
(129) Bianchi, A.; Calabi, L.; Giorgi, C.; Losi, P.; Mariani, P.; Paoli, P.; Rossi, P.; Valtancoli, B.; Virtuani, M. *J. Chem. Soc., Dalton Trans.* **2000**, *(5)*, 697-705.
(130) Fossheim, S. L.; Fahlvik, A. K.; Klaveness, J.; Muller, R. N. *Magn. Reson. Imaging* **1999**, *17(1)*, 83-89.
(131) Kang, S. I.; Ranganathan, R. S.; Emswiler, J. E.; Kumar, K.; Gougoutas, J. Z.; Malley, M. F.; Tweedle, M. F. *Inorg. Chem.* **1993**, *32(13)*, 2912-2918.
(132) Aime, S.; Botta, M.; Frullano, L.; Crich, S. G.; Giovenzana, G. B.; Pagliarin, R.; Palmisano, G.; Sisti, M. *Chem. Eur. J.* **1999**, *5(4)*, 1253-1260.
(133) Aime, S.; Gianolio, E.; Corpillo, D.; Cavallotti, C.; Palmisano, G.; Sisti, M.; Giovenzana, G. B.; Pagliarin, R. *Helv. Chim. Acta* **2003**, *86(3)*, 615-632.
(134) Aime, S.; Botta, M.; Crich, S. G.; Giovenzana, G. B.; Jommi, G.; Pagliarin, R.; Sisti, M. *Inorg. Chem.* **1997**, *36(14)*, 2992-3000.
(135) Aime, S.; Botta, M.; Crich, S. G.; Giovenzana, G. B.; Pagliarin, R.; Piccinini, M.; Sisti, M.; Terreno, E. *J. Biol. Inorg. Chem.* **1997**, *2(4)*, 470-479.
(136) Aime, S.; Botta, M.; Frullano, L.; Crich, S. G.; Giovenzana, G.; Pagliarin, R.; Palmisano, G.; Sirtori, F. R.; Sisti, M. *J. Med. Chem.* **2000**, *43(21)*, 4017-4024.
(137) Bogdanov, A. A., Jr.; Weissleder, R.; Brady, T. J. *Adv. Drug Delivery Rev.* **1995**, *16(2,3)*, 335-348.
(138) Aime, S.; Botta, M.; Crich, S. G.; Giovenzana, G.; Palmisano, G.; Sisti, M. *Bioconjugate Chem.* **1999**, *10(2)*, 192-199.
(139) Bogdanov, A. A.; Weissleder, R.; Frank, H. W.; Bogdanova, A. V.; Nossif, N.; Schaffer, B. K.; Tsai, E.; Papisov, M. I.; Brady, T. J. *Radiology* **1993**, *187(3)*, 701-706.
(140) Kayyem, J. F.; Kumar, R. M.; Fraser, S. E.; Meade, T. J. *Chem. Biol.* **1995**, *2(9)*, 615-620.
(141) Sieving, P. F.; Watson, A. D.; Rocklage, S. M. *Bioconjugate Chem.* **1990**, *1(1)*, 65-71.
(142) Tacke, J.; Adam, G.; Classen, H.; Muhler, A.; Prescher, A.; Gunther, R. W. *J. Magn. Reson. Imaging* **1997**, *7(4)*, 678-682.
(143) Armitage, F. E.; Richardson, D. E.; Li, K. C. P. *Bioconjugate Chem.* **1990**, *1(6)*, 365-374.
(144) Jacobs, R. E.; Fraser, S. E. *Science* **1994**, *263(5147)*, 681-684.
(145) Penzol, G.; Armisen, P.; Fernandez-Lafuente, R.; Rodes, L.; Guisan, J. M. *Biotechnol. Bioeng.* **1998**, *60(4)*, 518-523.
(146) Rebizak, R.; Schaefer, M.; Dellacherie, E. *Bioconjugate Chem.* **1997**, *8(4)*, 605-610.
(147) Rebizak, R.; Schaefer, M.; Dellacherie, E. *Bioconjugate Chem.* **1998**, *9(1)*, 94-99.
(148) Rebizak, R.; Schaefer, M.; Dellacherie, E. *Eur. J. Pharm. Sci.* **1999**, *7(3)*, 243-248.
(149) Siauve, N.; Clement, O.; Cuenod, C. A.; Benderbous, S.; Frija, G. *Magn. Reson. Imaging* **1996**, *14(4)*, 381-390.
(150) Wang, S. C.; Wikstrom, M. G.; White, D. L.; Klaveness, J.; Holtz, E.; Rongved, P.; Moseley, M. E.; Brasch, R. C. *Radiology* **1990**, *175(2)*, 483-488.
(151) Corsi, D. M.; Vander Elst, L.; Muller, R. N.; van Bekkum, H.; Peters, J. A. *Chem.--Eur. J.* **2001**, *7(1)*, 64-71.
(152) Rongved, P.; Klaveness, J. *Carbohydr. Res.* **1991**, *214(2)*, 315-323.
(153) Bryant, L. H., Jr.; Brechbiel, M. W.; Wu, C.; Bulte, J. W.; Herynek, V.; Frank, J. A. *J. Magn. Reson. Imaging* **1999**, *9(2)*, 348-352.
(154) Li, D. B.; Zheng, J.; Weinmann, H. J. *Radiology* **2001**, *218(3)*, 670-678.
(155) Margerum, L. D.; Campion, B. K.; Koo, M.; Shargill, N.; Lai, J. J.; Marumoto, A.; Sontum, P. C. *J. Alloys Compd.* **1997**, *249(1-2)*, 185-190.
(156) Peters, J. A.; Huskens, J.; Raber, D. J. *Prog. Nucl. Magn. Reson. Spectrosc.* **1996**, *28*, 283-350.
(157) Roberts, H. C.; Saeed, M.; Roberts, T. P. L.; Muhler, A.; Shames, D. M.; Mann, J. S.; Stiskal, M.; Demsar, F.; Brasch, R. C. *J. Magn. Reson. Imaging* **1997**, *7(2)*, 331-338.
(158) Roberts, H. C.; Saeed, M.; Roberts, T. P. L.; Muhler, A.; Brasch, R. C. *J. Magn. Reson. Imaging* **1999**, *9(2)*, 204-208.
(159) Schwickert, H. C.; Roberts, T. P. L.; Muhler, A.; Stiskal, M.; Demsar, F.; Brasch, R. C. *Eur. J. Radiol.* **1995**, *20(2)*, 144-150.
(160) Sherry, A. D. *J. Alloys Compd.* **1997**, *249(1-2)*, 153-157.
(161) Takahashi, M.; Hara, Y.; Aoshima, K.; Kurihara, H.; Oshikawa, T.; Yamashita, M. *Tetrahedron Lett.* **2000**, *41(44)*, 8485-8488.
(162) Wiener, E. C.; Auteri, F. P.; Chen, J. W.; Brechbiel, M. W.; Gansow, O. A.; Schneider, D. S.; Belford, R. L.; Clarkson, R. B.; Lauterbur, P. C. *J. Am. Chem. Soc.* **1996**, *118(33)*, 7774-7782.

(163) Wu, C. C.; Brechbiel, M. W.; Kozak, R. W.; Gansow, O. A. *Bioorg. Med. Chem. Lett.* **1994**, *4(3)*, 449-454.
(164) Nicolle, G. M.; Toth, E.; Schmitt-Willich, H.; Raduchel, B.; Merbach, A. E. *Chem.--Eur. J.* **2002**, *8(5)*, 1040-1048.
(165) Schmiedl, U.; Ogan, M.; Paajanen, H.; Marotti, M.; Crooks, L. E.; Brito, A. C.; Brasch, R. C. *Radiology* **1987**, *162(1)*, 205-210.
(166) Lauffer, R. B.; Parmelee, D. J.; Dunham, S. U.; Ouellet, H. S.; Dolan, R. P.; Witte, S.; McMurry, T. J.; Walovitch, R. C. *Radiology* **1998**, *207(2)*, 529-538.
(167) Manning, H. C.; Goebel, T.; Marx, J. N.; Bornhop, D. J. *Org. Lett.* **2002**, *4(7)*, 1075-1078.
(168) Stuber, M.; Botnar, R. M.; Danias, P. G.; McConnell, M. V.; Kissinger, K. V.; Yucel, E. K.; Manning, W. J. *J. Magn. Reson. Imaging* **1999**, *10(5)*, 790-799.
(169) Aime, S.; Batsanov, A. S.; Botta, M.; Howard, J. A. K.; Parker, D.; Senanayake, K.; Williams, G. *Inorg. Chem.* **1994**, *33(21)*, 4696-4706.
(170) Aime, S.; Botta, M.; Fasano, M.; Crich, S. G.; Terreno, E. *J. Biol. Inorg. Chem.* **1996**, *1(4)*, 312-319.
(171) Aime, S.; Chiaussa, M.; Digilio, G.; Gianolio, E.; Terreno, E. *J. Biol. Inorg. Chem.* **1999**, *4(6)*, 766-774.
(172) Anelli, P. L.; Calabi, L.; deHaen, C.; Fedeli, F.; Losi, P.; Murru, M.; Uggeri, F. *Gazz. Chim. Ital.* **1996**, *126(2)*, 89-97.
(173) Caravan, P.; Cloutier, N. J.; Greenfield, M. T.; McDermid, S. A.; Dunham, S. U.; Bulte, J. W. M.; Amedio, J. C., Jr.; Looby, R. J.; Supkowski, R. M.; Horrocks, W. D., Jr.; McMurry, T. J.; Lauffer, R. B. *J. Am. Chem. Soc.* **2002**, *124(12)*, 3152-3162.
(174) Muller, R. N.; Raduchel, B.; Laurent, S.; Platzek, J.; Pierart, C.; Mareski, P.; Vander Elst, L. *Eur. J. Inorg. Chem.* **1999**, *(11)*, 1949-1955.
(175) Toth, E.; Connac, F.; Helm, L.; Adzamli, K.; Merbach, A. E. *J. Biol. Inorg. Chem.* **1998**, *3(6)*, 606-613.
(176) Aime, S.; Botta, M.; Fedeli, F.; Gianolio, E.; Terreno, E.; Anelli, P. *Chem. Eur. J.* **2001**, *7(24)*, 5261-5269.
(177) Aime, S.; Crich, S. G.; Gianolio, E.; Terreno, E.; Beltrami, A.; Uggeri, F. *Eur. J. Inorg. Chem.* **1998**, *(9)*, 1283-1289.
(178) Aime, S.; Botta, M.; Ermondi, G.; Terreno, E.; Anelli, P. L.; Fedeli, F.; Uggeri, F. *Inorg. Chem.* **1996**, *35(10)*, 2726-2736.
(179) Aime, S.; Benetollo, F.; Bombieri, G.; Colla, S.; Fasano, M.; Paoletti, S. *Inorg. Chim. Acta* **1997**, *254(1)*, 63-70.
(180) Aime, S.; Botta, M.; Parker, D.; Williams, J. A. G. *J. Chem. Soc., Dalton Trans.* **1995**, *(13)*, 2259-2266.
(181) Aime, S.; Cabella, C.; Colombatto, S.; Geninatti Crich, S.; Gianolio, E.; Maggioni, F. *J. Magn. Reson. Imaging* **2002**, *16(4)*, 394-406.
(182) Aime, S.; Botta, M.; Crich, S. G.; Giovenzana, G.; Pagliarin, R.; Sisti, M.; Terreno, E. *Magn. Reson. Chem.* **1998**, *36(Spec. Issue)*, S200-S208.
(183) Aime, S.; Frullano, L.; Geninatti Crich, S. *Angew. Chem. Int. Ed.* **2002**, *41(6)*, 1017-1019.
(184) Webb, B.; Frame, J.; Zhao, Z.; Lee, M. L.; Watt, G. D. *Arch. Biochem. Biophys.* **1994**, *309(1)*, 178-183.
(185) Zhang, X.; Chang, C. A.; Brittain, H. G.; Garrison, J. M.; Telser, J.; Tweedle, M. F. *Inorg. Chem.* **1992**, *31(26)*, 5597-5600.
(186) Kwon, G.; Suwa, S.; Yokoyama, M.; Okano, T.; Sakurai, Y.; Kataoka, K. *J. Controlled Release* **1994**, *29(1-2)*, 17-23.
(187) Rolland, A.; Omullane, J.; Goddard, P.; Brookman, L.; Petrak, K. *J. Appl. Polym. Sci.* **1992**, *44(7)*, 1195-1203.
(188) Bogdanov, A. A., Jr.; Martin, C.; Weissleder, R.; Brady, T. J. *Biochim. Biophys. Acta* **1994**, *1193(1)*, 212-218.
(189) Glogard, C.; Stensrud, G.; Hovland, R.; Fossheim, S. L.; Klaveness, J. *Int. J. Pharm.* **2002**, *233(1-2)*, 131-140.
(190) Glogard, C.; Hovland, R.; Fossheim, S. L.; Aasen, A. J.; Klaveness, J. *J. Chem. Soc., Perkin Trans. 2* **2000**, *5*, 1047-1052.
(191) Kabalka, G. W.; Davis, M. A.; Holmberg, E.; Maruyama, K.; Huang, L. *Magn. Reson. Imaging* **1991**, *9(3)*, 373-377.
(192) Kim, S. K.; Pohost, G. M.; Elgavish, G. A. *Bioconjugate Chem.* **1992**, *3(1)*, 20-26.
(193) Leclercq, F.; Cohen-Ohana, M.; Mignet, N.; Sbarbati, A.; Herscovici, J.; Scherman, D.; Byk, G. *Bioconjugate Chem.* **2003**, *14(1)*, 112-119.
(194) Mulder, W. J. M.; Strijkers, G. J.; Griffioen, A. W.; van Bloois, L.; Molema, G.; Storm, G.; Koning, G. A.; Nicolay, K. *Bioconjugate Chem.* **2004**, *15(4)*, 799-806.

(195) Sipkins, D. A.; Gijbels, K.; Tropper, F. D.; Bednarski, M.; Li, K. C. P.; Steinman, L. *J. Neuroimmunol.* **2000**, *104(1)*, 1-9.
(196) Sipkins, D. A.; Cheresh, D. A.; Kazemi, M. R.; Nevin, L. M.; Bednarski, M. D.; Li, K. C. P. *Nat. Med.* **1998**, *4(5)*, 623-626.
(197) Viondury, J.; Masson, S.; Devoisselle, J. M.; Sciaky, M.; Desmoulin, F.; Confortgouny, S.; Coustaut, D.; Cozzone, P. J. *J. Pharmacol. Exp. Ther.* **1989**, *250(3)*, 1113-1118.
(198) Zhao, X.; Zhuo, R. X.; Lu, Z. G.; Liu, W. Y. *Polyhedron* **1997**, *16(16)*, 2755-2759.
(199) Atkins, T. J.; Richman, J. E.; Oettle, W. F. *Org. Synth.* **1978**, *58*, 86-98.
(200) Cox, J. P. L.; Craig, A. S.; Helps, I. M.; Jankowski, K. J.; Parker, D.; Eaton, M. A. W.; Millican, A. T.; Millar, K.; Beeley, N. R. A.; Boyce, B. A. *J. Chem. Soc., Perkin Trans. 1* **1990**, *(9)*, 2567-2576.
(201) Moi, M. K.; Meares, C. F.; Denardo, S. J. *J. Am. Chem. Soc.* **1988**, *110(18)*, 6266-6267.
(202) Renn, O.; Meares, C. F. *Bioconjugate Chem.* **1992**, *3(6)*, 563-569.
(203) Richman, J. E.; Atkins, T. J. *J. Am. Chem. Soc.* **1974**, *96(7)*, 2268-2270.
(204) Weisman, G. R.; Reed, D. P. *J. Org. Chem.* **1996**, *61(15)*, 5186-5187.
(205) Das, T.; Chakraborty, S.; Banerjee, S.; Samuel, G.; Sarma, H. D.; Venkatesh, M.; Pillai, M. R. A. *J. Labelled Compd. Radiopharm.* **2003**, *46(3)*, 197-209.
(206) Mease, R. C. M., L. F.; Srivastava, S. C.; Patent, U. S., Ed.; Associated Universities, Inc. (Washington, DC) U.S.A, 1995; Vol. 5428156.
(207) Stetter, H.; Frank, W.; Mertens, R. *Tetrahedron* **1981**, *37(4)*, 767-772.
(208) Garrity, M. L.; Brown, G. M.; Elbert, J. E.; Sachleben, R. A. *Tetrahedron Lett.* **1993**, *34(35)*, 5531-5534.
(209) Kline, S. J.; Betebenner, D. A.; Johnson, D. K. *Bioconjugate Chem.* **1991**, *2(1)*, 26-31.
(210) McMurry, T. J.; Brechbiel, M.; Kumar, K.; Gansow, O. A. *Bioconjugate Chem.* **1992**, *3(2)*, 108-117.
(211) Takenouchi, K.; Tabe, M.; Watanabe, K.; Hazato, A.; Kato, Y.; Shionoya, M.; Koike, T.; Kimura, E. *J. Org. Chem.* **1993**, *58(24)*, 6895-6899.
(212) Faulkner, S.; Matthews, J. L. in *Comprehensive Coordination Chemistry II*, 2003; Vol. 9, pp 913-944.
(213) Dumont, A.; Jacques, V.; Peng, Q. X.; Desreux, J. F. *Tetrahedron Lett.* **1994**, *35(22)*, 3707-3710.
(214) Corey, E. J.; Bailar, J. C., Jr. *J. Am. Chem. Soc.* **1959**, *81*, 2620-2629.
(215) Aime, S.; Barge, A.; Botta, M.; Parker, D.; De Sousa, A. S. *J. Am. Chem. Soc.* **1997**, *119(20)*, 4767-4768.
(216) Spirlet, M. R.; Rebizant, J.; Desreux, J. F.; Loncin, M. F. *Inorg. Chem.* **1984**, *23(3)*, 359-363.
(217) Kumar, K.; Tweedle, M. F. *Inorg. Chem.* **1993**, *32(20)*, 4193-4199.
(218) Wang, X. Y.; Jin, T. Z.; Comblin, V.; Lopezmut, A.; Merciny, E.; Desreux, J. F. *Inorg. Chem.* **1992**, *31(6)*, 1095-1099.
(219) Wu, S. L.; Horrocks, W. D. *Inorg. Chem.* **1995**, *34(14)*, 3724-3732.
(220) Burai, L.; Fabian, I.; Kiraly, R.; Szilagyi, E.; Brucher, E. *J. Chem. Soc., Dalton Trans.* **1998**, *(2)*, 243-248.
(221) Brucher, E.; Laurenczy, G.; Makra, Z. *Inorg. Chim. Acta* **1987**, *139(1-2)*, 141-142.
(222) Toth, E.; Brucher, E.; Lazar, I.; Toth, I. *Inorg. Chem.* **1994**, *33(18)*, 4070-4076.
(223) Jang, Y. H.; Blanco, M.; Dasgupta, S.; Keire, D. A.; Shively, J. E.; Goddard, W. A. *J. Am. Chem. Soc.* **1999**, *121(26)*, 6142-6151.
(224) Szilagyi, E.; Toth, E.; Kovacs, Z.; Platzek, J.; Raduchel, B.; Brucher, E. *Inorg. Chim. Acta* **2000**, *298(2)*, 226-234.
(225) Chang, C. A.; Liu, Y. L.; Chen, C. Y.; Chou, X. M. *Inorg. Chem.* **2001**, *40(14)*, 3448-3455.
(226) Aime, S.; Botta, M.; Crich, S. G.; Giovenzana, G. B.; Jommi, G.; Pagliarin, R.; Sisti, M. *J. Chem. Soc., Chem. Commun.* **1995**, *(18)*, 1885-1886.
(227) Bornhop, D. J.; Griffin, J. M. M.; Goebel, T. S.; Sudduth, M. R.; Bell, B.; Motamedi, M. *Appl. Spectrosc.* **2003**, *57(10)*, 1216-1222.
(228) Kim, W. D.; Kiefer, G. E.; Maton, F.; McMillan, K.; Muller, R. N.; Sherry, A. D. *Inorg. Chem.* **1995**, *34(8)*, 2233-2243.
(229) Kumar, K. *J. Alloys Compd.* **1997**, *249(1-2)*, 163-172.
(230) Kim, Y. H.; Webster, O. *J. Macromol. Sci., Polym. Rev.* **2002**, *C42(1)*, 55-89.
(231) Gao, C.; Yan, D. Y. *Chem. Commun.* **2001**, *(01)*, 107-108.
(232) Hanselmann, R.; Holter, D.; Frey, H. *Macromolecules* **1998**, *31(12)*, 3790-3801.
(233) Jikei, M.; Kakimoto, M. *Prog. Polym. Sci.* **2001**, *26(8)*, 1233-1285.
(234) Malmstrom, E.; Hult, A.; Gedde, U. W.; Liu, F.; Boyd, R. H. *Polymer* **1997**, *38(19)*, 4873-4879.
(235) Mulkern, T. J.; Tan, N. C. B. *Polymer* **2000**, *41(9)*, 3193-3203.
(236) Muscat, D.; Van Benthem, R. A. T. M. *Top. Curr. Chem.* **2001**, *212(Dendrimers III)*, 41-80.

(237) Yates, C. R.; Hayes, W. *Eur. Polym. J.* **2004**, *40(7)*, 1257-1281.
(238) Bianchi, A.; Calabi, L.; Giorgi, C.; Losi, P.; Mariani, P.; Paoli, P.; Rossi, P.; Valtancoli, B.; Virtuani, M. *J. Chem. Soc., Dalton Trans.* **2000**, *(5)*, 697-705.
(239) Beckwith, A. L. J. in *The Chemistry of Amides*; Zabicky, J., Ed.; Wiley: New York, 1970, pp 73-185.
(240) March, J. *Advanced Organic Chemistry: Reactions, Mechanisms, and Structure*, IV ed.; Wiley, 1992.
(241) Beeby, A.; Clarkson, I. M.; Dickins, R. S.; Faulkner, S.; Parker, D.; Royle, L.; de Sousa, A. S.; Williams, J. A. G.; Woods, M. *J. Chem. Soc., Perkin Trans. 2* **1999**, *(3)*, 493-503.
(242) Eisenwiener, K. P.; Powell, P.; Macke, H. R. *Bioorg. Med. Chem. Lett.* **2000**, *10(18)*, 2133-2135.
(243) Heppeler, A.; Froidevaux, S.; Macke, H. R.; Jermann, E.; Behe, M.; Powell, P.; Hennig, M. *Chem.--Eur. J.* **1999**, *5(7)*, 1974-1981.
(244) Roy, B. C.; Mallik, S. *Org. Lett.* **2001**, *3(12)*, 1877-1879.
(245) Tsukube, H.; Mizutani, Y.; Shinoda, S.; Okazaki, T.; Tadokoro, M.; Hori, K. *Inorg. Chem.* **1999**, *38(15)*, 3506-3512.
(246) Jones, J. R. *Surv. Prog. Chem.* **1973**, *6*, 83-112.
(247) Tournier, H.; Hyacinthe, R.; Schneider, M.; (Bracco Research SA, Switz.). Application: WO, 2005, pp 56 pp.
(248) Garrity, M.; Varadarajan, J.; Watson, A. D.; (Cockbain, Julian Roderick Michaelson, USA). Application: WO, 1996, pp 57 pp.
(249) Chen, J.; Linder, K. E.; Marinelli, E. R.; Metcalfe, E.; Nunn, A.; Swenson, R. E.; Tweedle, M.; (Bracco Imaging S.p.A., Italy). Application: WO, 2005, pp 117 pp.
(250) Margerum, L.; Campion, B.; Fellmann, J. D.; Garrity, M.; Varadarajan, J.; (Nycomed Imaging AS, Norway; Cockbain, Julian). Application: WO, 1995, pp 61 pp.
(251) Hovinen, J.; (Wallac Oy, Finland). Application: WO, 2007, pp 20pp.
(252) Jaakkola, L.; Ylikoski, A.; Hovinen, J. *Bioconjugate Chem.* **2006**, *17(4)*, 1105-1107.
(253) Andre, J. P.; Geraldes, C. F. G. C.; Martins, J. A.; Merbach, A. E.; Prata, M. I. M.; Santos, A. C.; de Lima, J. J. P.; Toth, E. *Chem.--Eur. J.* **2004**, *10(22)*, 5804-5816.
(254) Frullano, L.; Tejerina, B.; Meade, T. J. *Inorg. Chem.* **2006**, *45(21)*, 8489-8491.
(255) Li, C.; Winnard, P. T., Jr.; Takagi, T.; Artemov, D.; Bhujwalla, Z. M. *J. Am. Chem. Soc.* **2006**, *128(47)*, 15072-15073.
(256) Ansari, M. H.; Ahmad, M.; Dicke, K. A. *Bioorg. Med. Chem. Lett.* **1993**, *3(6)*, 1071-1072.
(257) Woods, M.; Botta, M.; Avedano, S.; Wang, J.; Sherry, A. D. *Dalton Trans.* **2005**, *(24)*, 3829-3837.
(258) Shinoda, S.; Nishimura, T.; Tadokoro, M.; Tsukube, H. *J. Org. Chem.* **2001**, *66(18)*, 6104-6108.
(259) Shinoda, S.; Okazaki, T.; Nishimura, T.; Tsukube, H.; Hori, K. *Chem. Commun. (Cambridge, U. K.)* **2001**, *(11)*, 976-977.
(260) Tsukube, H.; Mizutani, Y.; Shinoda, S.; Tadokoro, M.; Hori, K. *Tetrahedron Lett.* **1997**, *38(28)*, 5021-5024.
(261) Anelli, P. L.; Lattuada, L.; Gabellini, M.; Recanati, P. *Bioconjugate Chem.* **2001**, *12(6)*, 1081-1084.
(262) Collman, J. P.; Decreau, R. A.; Costanzo, S. *Org. Lett.* **2004**, *6(6)*, 1033-1036.
(263) Dunand, F. A.; Dickins, R. S.; Parker, D.; Merbach, A. E. *Chem.--Eur. J.* **2001**, *7(23)*, 5160-5167.
(264) Hovland, R.; Aasen, A. J.; Klaveness, J. *Org. Biomol. Chem.* **2003**, *1(10)*, 1707-1710.
(265) Kataky, R.; Matthes, K. E.; Nicholson, P. E.; Parker, D.; Buschmann, H. J. *J. Chem. Soc., Perkin Trans. 2* **1990**, *(8)*, 1425-1432.
(266) Plush, S. E.; Lincoln, S. F.; Wainwright, K. P. *Dalton Trans.* **2004**, *(9)*, 1410-1417.
(267) Ranganathan, R. S.; Pillai, R. K.; Raju, N.; Fan, H.; Nguyen, H.; Tweedle, M. F.; Desreux, J. F.; Jacques, V. *Inorg. Chem.* **2002**, *41(25)*, 6846-6855.
(268) Trokowski, R.; Zhang, S. R.; Sherry, A. D. *Bioconjugate Chem.* **2004**, *15(6)*, 1431-1440.
(269) Zhang, S. R.; Jiang, X. Y.; Sherry, A. D. *Helv. Chim. Acta* **2005**, *88(5)*, 923-935.
(270) Zhang, S. R.; Wu, K. C.; Biewer, M. C.; Sherry, A. D. *Inorg. Chem.* **2001**, *40(17)*, 4284-4290.
(271) Zucchi, G.; Ferrand, A. C.; Scopelliti, R.; Bunzli, J. C. G. *Inorg. Chem.* **2002**, *41(9)*, 2459-2465.
(272) Zucchi, G.; Scopelliti, R.; Bunzli, J. C. G. *J. Chem. Soc., Dalton Trans.* **2001**, *(13)*, 1975-1985.
(273) Zucchi, G.; Scopelliti, R.; Pittet, P. A.; Bunzli, J. C. G.; Rogers, R. D. *J. Chem. Soc., Dalton Trans.* **1999**, *(6)*, 931-938.
(274) Dickins, R. S.; Howard, J. A. K.; Moloney, J. M.; Parker, D.; Peacock, R. D.; Siligardi, G. *Chem. Commun.* **1997**, *(18)*, 1747-1748.
(275) Dickins, R. S.; Howard, J. A. K.; Maupin, C. L.; Moloney, J. M.; Parker, D.; Riehl, J. P.; Siligardi, G.; Williams, J. A. G. *Chem. Eur. J.* **1999**, *5(3)*, 1095-1105.
(276) Gunnlaugsson, T.; Parker, D. *Chem. Commun.* **1998**, *(4)*, 511-512.

(277) Gunnlaugsson, T.; Harte, A. J.; Leonard, J. P.; Nieuwenhuyzen, M. *Chem. Commun.* **2002**, *(18)*, 2134-2135.

(278) Gunnlaugsson, T.; Mac Donaill, D. A.; Parker, D. *J. Am. Chem. Soc.* **2001**, *123(51)*, 12866-12876.

(279) Gunnlaugsson, T.; Davies, R. J. H.; Nieuwenhuyzen, M.; O'Brien, J. E.; Stevenson, C. S.; Mulready, S. *Polyhedron* **2003**, *22(5)*, 711-724.

(280) Gunnlaugsson, T.; O'Brien, J. E.; Mulready, S. *Tetrahedron Lett.* **2002**, *43(47)*, 8493-8497.

(281) Gunnlaugsson, T.; Davies, R. J. H.; Kruger, P. E.; Jensen, P.; McCabe, T.; Mulready, S.; O'Brien, J. E.; Stevenson, C. S.; Fanning, A. M. *Tetrahedron Lett.* **2005**, *46(21)*, 3761-3766.

(282) Parker, D.; Williams, J. A. G. *J. Chem. Soc., Perkin Trans. 2* **1995**, *(7)*, 1305-1314.

(283) Tsukube, H.; Adachi, H.; Morosawa, S. *J. Org. Chem.* **1991**, *56(25)*, 7102-7108.

(284) Aime, S.; Barge, A.; Bruce, J. I.; Botta, M.; Howard, J. A. K.; Moloney, J. M.; Parker, D.; de Sousa, A. S.; Woods, M. *J. Am. Chem. Soc.* **1999**, *121(24)*, 5762-5771.

(285) Dijkstra, G.; Kruizinga, W. H.; Kellogg, R. M. *J. Org. Chem.* **1987**, *52(19)*, 4230-4234.

(286) Flessner, T.; Doye, S. *J. Prakt. Chem.* **1999**, *341(2)*, 186-190.

(287) Lehmann, F. *Synlett.* **2004**, *(13)*, 2447-2448.

(288) Gunnlaugsson, T. *Tetrahedron Lett.* **2001**, *42(50)*, 8901-8905.

(289) Gunnlaugsson, T.; Brougham, D. F.; Fanning, A. M.; Nieuwenhuyzen, M.; O'Brien, J. E.; Viguier, R. *Org. Lett.* **2004**, *6(26)*, 4805-4808.

(290) Caliendo, G.; Fiorino, F.; Perissutti, E.; Severino, B.; Gessi, S.; Cattabriga, E.; Borea, P. A.; Santagada, V. *Eur. J. Med. Chem.* **2001**, *36(11-12)*, 873-886.

(291) Corelli, F.; Botta, M.; Lossani, A.; Pasquini, S.; Spadari, S.; Focher, F. *Farmaco* **2004**, *59(12)*, 987-992.

(292) Ju, Y.; Varma, R. S. *Green Chem.* **2004**, *6(4)*, 219-221.

(293) Williams, L. *Chem. Commun. (Cambridge)* **2000**, *(6)*, 435-436.

(294) Ascenso, J. R.; Delgado, R.; Frausto da Silva, J. J. R. *J. Chem. Soc., Perkin Trans. 2* **1985**, *(6)*, 781-788.

(295) Delgado, R.; Frausto da Silva, J. J. R. *Talanta* **1982**, *29(10)*, 815-822.

(296) Desreux, J. F.; Merciny, E.; Loncin, M. F. *Inorg. Chem.* **1981**, *20(4)*, 987-991.

(297) Stetter, H.; Frank, W. *Angew. Chem., Int. Ed.* **1976**, *15(11)*, 686.

(298) Bordwell, F. G.; Algrim, D. *J. Org. Chem.* **1976**, *41(14)*, 2507-2508.

(299) Kolthoff, I. M.; Chantooni, M. K., Jr.; Bhowmik, S. *J. Am. Chem. Soc.* **1968**, *90(1)*, 23-28.

(300) Crampton, M. R.; Robotham, I. A. *J. Chem. Res., Synop.* **1997**, *(1)*, 22-23.

(301) Ansell, M. F. in *The Chemistry of Acyl Halides*; Patai, S., Ed.; Wiley: New York, 1972, pp 35-68.

(302) Albert, R.; Smith-Jones, P.; Stolz, B.; Simeon, C.; Knecht, H.; Bruns, C.; Pless, J. *Bioorg. Med. Chem. Lett.* **1998**, *8(10)*, 1207-1210.

(303) Schottelius, M.; Schwaiger, M.; Wester, H. J. *Tetrahedron Lett.* **2003**, *44(11)*, 2393-2396.

(304) Fazal, M. A.; Roy, B. C.; Sun, S. G.; Mallik, S.; Rodgers, K. R. *J. Am. Chem. Soc.* **2001**, *123(26)*, 6283-6290.

(305) Govenlock, L. J.; Howard, J. A. K.; Moloney, J. M.; Parker, D.; Peacock, R. D.; Siligardi, G. *J. Chem. Soc., Perkin Trans. 2* **1999**, *(11)*, 2415-2418.

(306) Beyermann, M.; Henklein, P.; Klose, A.; Sohr, R.; Bienert, M. *Int. J. Pept. Protein Res.* **1991**, *37(4)*, 252-256.

(307) Grayson, I. *Spec. Chem.* **2000**, *20(3)*, 86,88.

(308) Sheehan, J. C.; Hess, G. P. *J. Am. Chem. Soc.* **1955**, *77*, 1067-1068.

(309) Albericio, F.; Cases, M.; Alsina, J.; Triolo, S. A.; Carpino, L. A.; Kates, S. A. *Tetrahedron Lett.* **1997**, *38(27)*, 4853-4856.

(310) Coste, J.; Lenguyen, D.; Castro, B. *Tetrahedron Lett.* **1990**, *31(2)*, 205-208.

(311) Carpino, L. A. *J. Am. Chem. Soc.* **1993**, *115(10)*, 4397-4398.

(312) Dourtoglou, V.; Ziegler, J. C.; Gross, B. *Tetrahedron Lett.* **1978**, *(15)*, 1269-1272.

(313) Marder, O.; Shvo, Y.; Albericio, F. *Chim. Oggi* **2002**, *20(7-8)*, 37-41.

(314) Konig, W.; Geiger, R. *Chem. Ber. Recl.* **1970**, *103(7)*, 2034-&.

(315) Konig, W.; Geiger, R. *Chem. Ber. Recl.* **1970**, *103(3)*, 788-&.

(316) Rao, M. J.; Acharya, A. S. *J. Protein Chem.* **1991**, *10(1)*, 129-138.

(317) Sehgal, D.; Vijay, I. K. *Anal. Biochem.* **1994**, *218(1)*, 87-91.

(318) Staros, J. V.; Wright, R. W.; Swingle, D. M. *Anal. Biochem.* **1986**, *156(1)*, 220-222.

(319) Glasovac, Z.; Kovacevic, B.; Mestrovic, E.; Eckert-Maksic, M. *Tetrahedron Lett.* **2005**, *46(50)*, 8733-8736.

(320) Angelova, P.; Kostova, K.; Hinrichs, K.; Tsankov, D. *Cent. Eur. J. Chem.* **2005**, *3(4)*, 658-667.

(321) Es-Safi, N.-E.; Le Guerneve, C.; Kerhoas, L.; Ducrot, P.-H. *Tetrahedron* **2006**, *62(11)*, 2705-2714.

(322) Kislyi, V. P.; Danilova, E. B.; Semenov, V. V. *Russ. Chem. Bull.* **2003**, *52(8)*, 1770-1776.
(323) Singhal, N.; Johar, M.; Lown, J. W.; Sondhi, S. M. *Phosphorus, Sulfur Silicon Relat. Elem.* **2001**, *174*, 81-92.
(324) Song, Y.-H.; Hong, S.; Lim, H.; Seo, J.; Chung, S.; No, I.; Lee, K.; Yoon, M. *Chem. Pharm. Bull.* **2004**, *52(5)*, 597-601.
(325) Dickins, R. S.; Howard, J. A. K.; Maupin, C. L.; Moloney, J. M.; Parker, D.; Peacock, R. D.; Riehl, J. P.; Siligardi, G. *New J. Chem.* **1998**, *22(8)*, 891-899.
(326) Greene, T. W. W., P. G. M. *Protective groups in organic synthesis*, 2nd ed.; Wiley: Chichester 1991.
(327) Kim, I. H.; Morisseau, C.; Watanabe, T.; Hammock, B. D. *J. Med. Chem.* **2004**, *47(8)*, 2110-2122.
(328) Brana, M. F.; Dominguez, G.; Saez, B.; Romerdahl, C.; Robinson, S.; Barlozzari, T. *Eur. J. Med. Chem.* **2002**, *37(7)*, 541-551.
(329) Chhabra, S. R.; Mahajan, A.; Chan, W. C. *J. Org. Chem.* **2002**, *67(12)*, 4017-4029.
(330) Eisenfuhr, A.; Arora, P. S.; Sengle, G.; Takaoka, L. R.; Nowick, J. S.; Famulok, M. *Bioorg. Med. Chem.* **2003**, *11(2)*, 235-249.
(331) Nicolaou, K. C.; Hughes, R.; Pfefferkorn, J. A.; Barluenga, S. *Chem.--Eur. J.* **2001**, *7(19)*, 4296-4310.
(332) Fanning, A.-M.; Plush, S. E.; Gunnlaugsson, T. *Chem. Commun.* **2006**, *(36)*, 3791-3793.
(333) Goto, M.; Okubo, A.; Sawai, T.; Yoshikawa, S. *Inorg. Chem.* **1970**, *9(6)*, 1488-1496.
(334) Bonnans-Plaisance, C.; Levesque, G.; Toulin, V. *Phosphorus, Sulfur Silicon Relat. Elem.* **1998**, *143*, 231-244.
(335) Harries, C.; Petersen, I. *Ber. Dtsch. Chem. Ges.* **1910**, *43*, 634-639.
(336) Casadei, M. A.; Cesa, S.; Inesi, A. *Tetrahedron* **1995**, *51(20)*, 5891-5900.
(337) Farkas, V.; Toth, T.; Orosz, G.; Huszthy, P.; Hollosi, M. *Tetrahedron: Asymmetry* **2006**, *17(12)*, 1883-1889.
(338) Enholm, E.; Low, T. *J. Org. Chem.* **2006**, *71(6)*, 2272-2276.
(339) Pospisil, J.; Potacek, M. *Tetrahedron* **2006**, *63(2)*, 337-346.
(340) Viguier, R. F. H.; Hulme, A. N. *J. Am. Chem. Soc.* **2006**, *128(35)*, 11370-11371.
(341) Walter, H. *Heterocycles* **1995**, *41(11)*, 2427-2435.
(342) Pokorski, J. K.; Miller Jenkins, L. M.; Feng, H.; Durell, S. R.; Bai, Y.; Appella, D. H. *Org. Lett.* **2007**, *9(12)*, 2381-2383.
(343) Prasuhn, D. E., Jr.; Yeh, R. M.; Obenaus, A.; Manchester, M.; Finn, M. G. *Chem. Commun.* **2007**, *(12)*, 1269-1271.
(344) Kim, J. S.; Rieter, W. J.; Taylor, K. M. L.; An, H.; Lin, W.; Lin, W. *J. Am. Chem. Soc.* **2007**, *129(29)*, 8962-8963.
(345) Lu, Q.; Singh, A.; Deschamps, J. R.; Chang, E. L. *Inorg. Chim. Acta* **2000**, *309(1-2)*, 82-90.
(346) Inagaki, F.; Miyazawa, T. *Prog. Nucl. Magn. Reson. Spectrosc.* **1980**, *14(2)*, 67-111.
(347) Denisov, E. T.; Khudyakov, I. V. *Chem. Rev.* **1987**, *87(6)*, 1313-1357.
(348) Save, M.; Weaver, J. V. M.; Armes, S. P.; McKenna, P. *Macromolecules* **2002**, *35(4)*, 1152-1159.
(349) Robinson, K. L.; Khan, M. A.; de Banez, M. V.; Wang, X. S.; Armes, S. P. *Macromolecules* **2001**, *34(10)*, 3155-3158.
(350) Kolb, H. C.; Finn, M. G.; Sharpless, K. B. *Angew. Chem., Int. Ed.* **2001**, *40(11)*, 2004-2021.
(351) Kolb, H. C.; Sharpless, K. B. *Drug Discovery Today* **2003**, *8(24)*, 1128-1137.
(352) Huisgen, R. in *1,3-Dipolar Cycloaddition Chemistry*; Padwa, A., Ed.; Wiley: New York, 1984; Vol. 1, pp 1-176.
(353) Jorgensen, K. A. *Angew. Chem., Int. Ed.* **2000**, *39(20)*, 3558-3588.
(354) Tietze, L. F.; Kettschau, G. *Top. Curr. Chem.* **1997**, *189(Stereoselective Heterocyclic Synthesis I)*, 1-120.
(355) Adolfsson, H.; Converso, A.; Sharpless, K. B. *Tetrahedron Lett.* **1999**, *40(21)*, 3991-3994.
(356) Gontcharov, A. V.; Liu, H.; Sharpless, K. B. *Org. Lett.* **1999**, *1(5)*, 783-786.
(357) Kolb, H. C.; VanNieuwenhze, M. S.; Sharpless, K. B. *Chem. Rev.* **1994**, *94(8)*, 2483-2547.
(358) Huisgen, R.; Szeimies, G.; Moebius, L. *Chem. Ber.* **1967**, *100(8)*, 2494-2507.
(359) Huisgen, R. *Pure Appl. Chem.* **1989**, *61(4)*, 613-628.
(360) Lwowski, W. in *1,3-Dipolar Cycloaddition Chemistry*; Padwa, A., Ed.; Wiley: New York, 1984; Vol. 1, pp 559-651.
(361) Tornoe, C. W.; Christensen, C.; Meldal, M. *J. Org. Chem.* **2002**, *67(9)*, 3057-3064.
(362) Rostovtsev, V. V.; Green, L. G.; Fokin, V. V.; Sharpless, K. B. *Angew. Chem., Int. Ed.* **2002**, *41(14)*, 2596-2599.
(363) Sonogashira, K.; Tohda, Y.; Hagihara, N. *Tetrahedron Lett.* **1975**, *(50)*, 4467-4470.
(364) Bock, V. D.; Hiemstra, H.; van Maarseveen, J. H. *Eur. J. Org. Chem.* **2005**, *(1)*, 51-68.

(365) Himo, F.; Lovell, T.; Hilgraf, R.; Rostovtsev, V. V.; Noodleman, L.; Sharpless, K. B.; Fokin, V. V. *J. Am. Chem. Soc.* **2005**, *127(1)*, 210-216.
(366) Lipshutz, B. H.; Taft, B. R. *Angew. Chem., Int. Ed.* **2006**, *45(48)*, 8235-8238.
(367) Diez-Gonzalez, S.; Correa, A.; Cavallo, L.; Nolan, S. P. *Chem.--Eur. J.* **2006**, *12(29)*, 7558-7564.
(368) Binder, W. H.; Sachsenhofer, R. *Macromol. Rapid Commun.* **2007**, *28(1)*, 15-54.
(369) Voit, B. I. *Book of Abstracts, 219th ACS National Meeting, San Francisco, CA, March 26-30,* MACR-026.
(370) Voit, B. *J. Polym. Sci., Part A: Polym. Chem.* **2000**, *38(14)*, 2505-2525.
(371) Lu, G.; Burgess, K. *Bioorg. Med. Chem. Lett.* **2006**, *16(15)*, 3902-3905.
(372) Ruttens, B.; Kovac, P. *Helv. Chim. Acta* **2006**, *89(2)*, 320-332.
(373) Fernandez-Megia, E.; Correa, J.; Rodriguez-Meizoso, I.; Riguera, R. *Macromolecules* **2006**, *39(6)*, 2113-2120.
(374) Canaria, C. A.; Smith, J. O.; Yu, C. J.; Fraser, S. E.; Lansford, R. *Tetrahedron Lett.* **2005**, *46(28)*, 4813-4816.
(375) Rensen, P. C. N.; van Leeuwen, S. H.; Sliedregt, L. A. J. M.; Van Berkel, T. J. C.; Biessen, E. A. L. *J. Med. Chem.* **2004**, *47(23)*, 5798-5808.
(376) Iyer, S. S.; Anderson, A. S.; Reed, S.; Swanson, B.; Schmidt, J. G. *Tetrahedron Lett.* **2004**, *45(22)*, 4285-4288.
(377) Amvam-Zollo, P. H.; Sinay, P. *Carbohydr. Res.* **1986**, *150*, 199-212.
(378) Ramenda, T.; Bergmann, R.; Wuest, F. *Lett. Drug Des. Discovery* **2007**, *4(4)*, 279-285.
(379) Kosiova, I.; Kovackova, S.; Kois, P. *Tetrahedron* **2006**, *63(2)*, 312-320.
(380) Zhao, X. Z.; Semenova, E. A.; Liao, C.; Nicklaus, M.; Pommier, Y.; Burke, T. R. *Bioorg. Med. Chem.* **2006**, *14(23)*, 7816-7825.
(381) Wilkinson, B. L.; Bornaghi, L. F.; Houston, T. A.; Innocenti, A.; Supuran, C. T.; Poulsen, S.-A. *J. Med. Chem.* **2006**, *49(22)*, 6539-6548.
(382) Oh, K.; Guan, Z. *Chem. Commun. (Cambridge, U. K.)* **2006**, *(29)*, 3069-3071.
(383) Lee, B.-Y.; Park, S. R.; Jeon, H. B.; Kim, K. S. *Tetrahedron Lett.* **2006**, *47(29)*, 5105-5109.
(384) Blass, B. E.; Coburn, K. R.; Faulkner, A. L.; Hunn, C. L.; Natchus, M. G.; Parker, M. S.; Portlock, D. E.; Tullis, J. S.; Wood, R. *Tetrahedron Lett.* **2002**, *43(22)*, 4059-4061.
(385) Goeminne, A.; McNaughton, M.; Bal, G.; Surpateanu, G.; Van der Veken, P.; De Prol, S.; Versees, W.; Steyaert, J.; Apers, S.; Haemers, A.; Augustyns, K. *Bioorg. Med. Chem. Lett.* **2007**, *17(9)*, 2523-2526.
(386) Alonso, G.; Garcia-Lopez, M. T.; Garcia-Munoz, G.; Madronero, R.; Rico, M. *J. Heterocycl. Chem.* **1970**, *7(6)*, 1269-1272.
(387) Dondoni, A.; Marra, A. *J. Org. Chem.* **2006**, *71(20)*, 7546-7557.
(388) Theocharis, A. B.; Alexandrou, N. E.; Terzis, A. *J. Heterocycl. Chem.* **1990**, *27(6)*, 1741-1744.
(389) Josephson, L.; Kircher, M. F.; Mahmood, U.; Tang, Y.; Weissleder, R. *Bioconjugate Chem.* **2002**, *13(3)*, 554-560.
(390) Kircher, M. F.; Mahmood, U.; King, R. S.; Weissleder, R.; Josephson, L. *Cancer Res.* **2003**, *63(23)*, 8122-8125.
(391) Moore, A.; Medarova, Z.; Potthast, A.; Dai, G. P. *Cancer Res.* **2004**, *64(5)*, 1821-1827.
(392) Nitin, N.; LaConte, L. E. W.; Zurkiya, O.; Hu, X.; Bao, G. *J. Biol. Inorg. Chem.* **2004**, *9(6)*, 706-712.
(393) Schellenberger, E. A.; Sosnovik, D.; Weissleder, R.; Josephson, L. *Bioconjugate Chem.* **2004**, *15(5)*, 1062-1067.
(394) Huber, M. M.; Staubli, A. B.; Kustedjo, K.; Gray, M. H. B.; Shih, J.; Fraser, S. E.; Jacobs, R. E.; Meade, T. J. *Bioconjugate Chem.* **1998**, *9(2)*, 242-249.
(395) Moore, A.; Marecos, E.; Bogdanov, A.; Weissleder, R. *Radiology* **2000**, *214(2)*, 568-574.
(396) Schulze, E.; Ferrucci, J. T.; Poss, K.; Lapointe, L.; Bogdanova, A.; Weissleder, R. *Invest. Radiol.* **1995**, *30(10)*, 604-610.
(397) Liang, Z. P.; Lauterbur, P. C. *IEEE Trans. Med. Imaging* **1994**, *13(4)*, 677-686.
(398) Ladmiral, V.; Mantovani, G.; Clarkson, G. J.; Cauet, S.; Irwin, J. L.; Haddleton, D. M. *J. Am. Chem. Soc.* **2006**, *128(14)*, 4823-4830.
(399) Dirks, A. J.; Van Berkel, S. S.; Hatzakis, N. S.; Opsteen, J. A.; Van Delft, F. L.; Cornelissen, J. J. L. M.; Rowan, A. E.; Van Hest, J. C. M.; Rutjes, F. P. J. T.; Nolte, R. J. M. *Chem. Commun. (Cambridge, U. K.)* **2005**, *(33)*, 4172-4174.
(400) Yilmaz, M. D.; Bozdemir, O. A.; Akkaya, E. U. *Org. Lett.* **2006**, *8(13)*, 2871-2873.
(401) Deiters, A.; Cropp, T. A.; Mukherji, M.; Chin, J. W.; Anderson, J. C.; Schultz, P. G. *J. Am. Chem. Soc.* **2003**, *125(39)*, 11782-11783.
(402) Wang, Q.; Chan, T. R.; Hilgraf, R.; Fokin, V. V.; Sharpless, K. B.; Finn, M. G. *J. Am. Chem. Soc.* **2003**, *125(11)*, 3192-3193.

(403) Llauger-Bufi, L.; Felts, S. J.; Huezo, H.; Rosen, N.; Chiosis, G. *Bioorg. Med. Chem. Lett.* **2003**, *13(22)*, 3975-3978.
(404) Hoedl, C.; Strauss, W. S. L.; Sailer, R.; Seger, C.; Steiner, R.; Haslinger, E.; Schramm, H. W. *Bioconjugate Chem.* **2004**, *15(2)*, 359-365.
(405) Quintanilla-Licea, R.; Colunga-Valladares, J. F.; Caballero-Quintero, A.; Rodriguez-Padilla, C.; Tamez-Guerra, R.; Gomez-Flores, R.; Waksman, N. *Molecules* **2002**, *7(8)*, 662-673.
(406) Maumela, H.; Hancock, R. D.; Carlton, L.; Reibenspies, J. H.; Wainwright, K. P. *J. Am. Chem. Soc.* **1995**, *117(25)*, 6698-6707.
(407) Balali-Mood, B. *Transfer Report*, Imperial College London, London, 2008.
(408) Shannon, R. D. *Acta Crystallogr., Sect. A* **1976**, *A32(5)*, 751-767.
(409) Bielawski, C. W.; Grubbs, R. H. *Prog. Polym. Sci.* **2007**, *32(1)*, 1-29.
(410) Grubbs, R. H.; Khosravi, E. *Mater. Sci. Technol.* **1999**, *20(Synthesis of Polymers)*, 65-104.
(411) Grubbs, R. H.; Hillmyer, M.; Benedicto, A.; Wu, Z. *Polym. Prepr. (Am. Chem. Soc., Div. Polym. Chem.)* **1994**, *35(1)*, 688.
(412) Risse, W.; Grubbs, R. H. *J. Mol. Catal.* **1991**, *65(1-2)*, 211-217.
(413) Buchmeiser, M. R. *Adv. Polym. Sci.* **2006**, *197(Surface-Initiated Polymerization I)*, 137-171.
(414) Buchmeiser, M. R. *J. Chromatogr. Libr.* **2003**, *67(Monolithic Materials)*, 103-120.
(415) Armstrong, S. K. *J. Chem. Soc., Perkin Trans. 1* **1998**, *(2)*, 371-388.
(416) Furstner, A. *Top. Organomet. Chem.* **1998**, *1(Alkene Metathesis in Organic Synthesis)*, 37-72.
(417) Furstner, A. *Angew. Chem., Int. Ed.* **2000**, *39(17)*, 3012-3043.
(418) Grubbs, R. H.; Chang, S. *Tetrahedron* **1998**, *54(18)*, 4413-4450.
(419) Trnka, T. M.; Grubbs, R. H. *Acc. Chem. Res.* **2001**, *34(1)*, 18-29.
(420) Herisson, J. L.; Chauvin, Y. *Makromol. Chem.* **1971**, *141*, 161-176.
(421) Fischer, E. O.; Maasböl, A. *Angew. Chem., Int. Ed.* **1964**, *3(8)*, 580-581.
(422) Schrock, R. R. *J. Am. Chem. Soc.* **1974**, *96(21)*, 6796-6797.
(423) Leymet, I.; Siove, A.; Parlier, A.; Rudler, H.; Fontanille, M. *Makromol. Chem.* **1989**, *190(10)*, 2397-2405.
(424) Liaw, D. J. *J. Polym. Sci., Part A: Polym. Chem.* **1993**, *31(2)*, 309-316.
(425) Warwel, S.; Siekermann, V. *Makromol. Chem., Rapid Commun.* **1983**, *4(6)*, 423-427.
(426) Schrock, R. R.; Murdzek, J. S.; Bazan, G. C.; Robbins, J.; DiMare, M.; O'Regan, M. *J. Am. Chem. Soc.* **1990**, *112(10)*, 3875-3886.
(427) Kinderman, S. S.; van Maarseveen, J. H.; Schoemaker, H. E.; Hiemstra, H.; Rutjes, F. P. J. T. *Org. Lett.* **2001**, *3(13)*, 2045-2048.
(428) Nguyen, S. T.; Johnson, L. K.; Grubbs, R. H.; Ziller, J. W. *J. Am. Chem. Soc.* **1992**, *114(10)*, 3974-3975.
(429) Nguyen, S. T.; Grubbs, R. H.; Ziller, J. W. *J. Am. Chem. Soc.* **1993**, *115(21)*, 9858-9859.
(430) Scholl, M.; Trnka, T. M.; Morgan, J. P.; Grubbs, R. H. *Tetrahedron Lett.* **1999**, *40(12)*, 2247-2250.
(431) Wu, Z.; Nguyen, S. T.; Grubbs, R. H.; Ziller, J. W. *J. Am. Chem. Soc.* **1995**, *117(20)*, 5503-5511.
(432) Kingsbury, J. S.; Harrity, J. P. A.; Bonitatebus, P. J., Jr.; Hoveyda, A. H. *J. Am. Chem. Soc.* **1999**, *121(4)*, 791-799.
(433) Formentin, P.; Gimeno, N.; Steinke, J. H. G.; Vilar, R. *J. Org. Chem.* **2005**, *70(20)*, 8235-8238.
(434) Lehman, S. E.; Schwendeman, J. E.; O'Donnell, P. M.; Wagener, K. B. *Inorg. Chim. Acta* **2003**, *345*, 190-198.
(435) Pederson, R. L.; Fellows, I. M.; Ung, T. A.; Ishihara, H.; Hajela, S. P. *Adv. Synth. Catal.* **2002**, *344(6+7)*, 728-735.
(436) Schmidt, B. *Eur. J. Org. Chem.* **2004**, *(9)*, 1865-1880.
(437) Schmidt, B. *J. Mol. Catal. A: Chem.* **2006**, *254(1-2)*, 53-57.
(438) Sworen, J. C.; Pawlow, J. H.; Case, W.; Lever, J.; Wagener, K. B. *J. Mol. Catal. A: Chem.* **2003**, *194(1-2)*, 69-78.
(439) Hong, S. H.; Sanders, D. P.; Lee, C. W.; Grubbs, R. H. *J. Am. Chem. Soc.* **2005**, *127(49)*, 17160-17161.
(440) Buckley, D.; Dunstan, S.; Henbest, H. B. *J. Chem. Soc.* **1957**, 4880-4891.
(441) Inagaki, Y.; Osugi, J.; Sasaki, M. *J. Chem. Soc., Perkin Trans. 2* **1985**, *(1)*, 115-119.
(442) Koch, A. S.; Harbison, W. G.; Hubbard, J. M.; de Kort, M.; Roe, B. A. *J. Org. Chem.* **1996**, *61(17)*, 5959-5963.
(443) Smith, R. E.; Davis, W. R. *Anal. Chem.* **1984**, *56(13)*, 2345-2349.
(444) Bourgeois, D.; Pancrazi, A.; Nolan, S. P.; Prunet, J. *J. Organomet. Chem.* **2002**, *643-644*, 247-252.
(445) Forman, G. S.; McConnell, A. E.; Tooze, R. P.; Van Rensburg, W. J.; Meyer, W. H.; Kirk, M. M.; Dwyer, C. L.; Serfontein, D. W. *Organometallics* **2005**, *24(19)*, 4528-4542.

(446) Meyer, W. H.; McConnell, A. E.; Forman, G. S.; Dwyer, C. L.; Kirk, M. M.; Ngidi, E. L.; Blignaut, A.; Saku, D.; Slawin, A. M. Z. *Inorg. Chim. Acta* **2006**, *359(9)*, 2910-2917.
(447) Hong, S. H.; Grubbs, R. H. *J. Am. Chem. Soc.* **2006**, *128(11)*, 3508-3509.
(448) Bevington, J. C. *Radical polymerization*; Academic Press: London, 1961.
(449) Moad, G.; Solomon, D. H. *The chemistry of free radical polymerization*; Pergamon: Oxford, 1995.
(450) Davis, F. J. *Polymer chemistry: a practical approach*; Oxford University Press: Oxford, 2004.
(451) Slark, A. T.; Sherrington, D. C.; Titterton, A.; Martin, I. K. *J. Mater. Chem.* **2003**, *13(11)*, 2711-2720.
(452) Brandrup, J.; Immergut, E. H.; Editors *Polymer Handbook, Fourth Edition*, 1998.
(453) Das, S. K.; Chatterjee, S. R.; Palit, S. R. *Proc. Roy. Soc. (London)* **1955**, *A227*, 252-258.
(454) O'Brien, J. L.; Gornick, F. *J. Am. Chem. Soc.* **1955**, *77(18)*, 4757-4763.
(455) Dvornic, P. R.; Hu, J.; Meier, D. J.; Nowak, R. M.; Parham, P. L.; (USA). Application: US, 2002, pp 9 pp.
(456) Ryu, E.-H.; Zhao, Y. *Org. Lett.* **2005**, *7(6)*, 1035-1037.
(457) Anelli, P. L.; Bertini, I.; Fragai, M.; Lattuada, L.; Luchinat, C.; Parigi, G. *Eur. J. Inorg. Chem.* **2000**, *(4)*, 625-630.
(458) Yan, G. P.; Liu, M. L.; Li, L. Y. *Bioconjugate Chem.* **2005**, *16(4)*, 967-971.
(459) Aime, S.; Botta, M.; Crich, S. G.; Giovenzana, G.; Pagliarin, R.; Sisti, M.; Terreno, E. *Magn. Reson. Chem.* **1998**, *36*, S200-S208.
(460) Aime, S.; Botta, M.; Frullano, L.; Crich, S. G.; Giovenzana, G. B.; Pagliarin, R.; Palmisano, G.; Sisti, M. *Chem.--Eur. J.* **1999**, *5(4)*, 1253-1260.
(461) Brown, R. R.; Clarke, D. W.; Daffner, R. H. *Am. J. Roentgenol.* **2000**, *175(4)*, 1087-1090.
(462) Nayan, R. *J. Inorg. Nucl. Chem.* **1980**, *42(12)*, 1743-1747.
(463) Yoshino, T.; Okazaki, H.; Murakami, S.; Kagawa, M. *Talanta* **1974**, *21(6)*, 676-679.
(464) Lowe, M. P. *Curr. Pharm. Biotechnol.* **2004**, *5(6)*, 519-528.
(465) Livramento, J. B.; Sour, A.; Borel, A.; Merbach, A. E.; Toth, E. *Chem.--Eur. J.* **2006**, *12(4)*, 989-1003.
(466) Toth, E.; Helm, L.; Merbach, A. E. *Top. Curr. Chem.* **2002**, *221(Contrast Agents I)*, 61-101.
(467) Aime, S.; Botta, M.; Ermondi, G. *Inorg. Chem.* **1992**, *31(21)*, 4291-4299.
(468) Koenig, S. H. *Isr. J. Chem.* **1989**, *28(4)*, 345-353.
(469) Chapon, C.; Lemaire, L.; Franconi, F.; Marescaux, L.; Legras, P.; Denizot, B.; Le Jeune, J.-J. *Magn. Reson. Med.* **2004**, *52(4)*, 932-936.
(470) Wiener, E. C.; Brechbiel, M. W.; Brothers, H.; Magin, R. L.; Gansow, O. A.; Tomalia, D. A.; Lauterbur, P. C. *Magn. Reson. Med.* **1994**, *31(1)*, 1-8.
(471) Cattaneo, E.; Conti, L. *J. Neurosci. Res.* **1998**, *53(2)*, 223-234.
(472) Ahmed, S. A.; Gogal, R. M., Jr.; Walsh, J. E. *J. Immunol. Methods* **1994**, *170(2)*, 211-224.
(473) Fields, R. D.; Lancaster, M. V. *Am. Biotechnol. Lab.* **1993**, *11(4)*, 48-50.
(474) Pelletier, B.; Dhainaut, F.; Pauly, A.; Zahnd, J. P. *J. Biochem. Biophys. Methods* **1988**, *16(1)*, 63-73.
(475) Grignolo, C. *MRes Thesis*, Imperial College London, London, 2008.
(476) Li, C.; Finn, M. G. *J. Polym. Sci., Part A: Polym. Chem.* **2006**, *44(19)*, 5513-5518.
(477) Armarego, W. L. F. P., D. D. *Purification of laboratory chemicals*; Butterworth-Heinemann: Oxford, 2001.
(478) Vogel, A. I. *A text-book of practical organic chemistry, including qualitative organic analysis* Longman: London, 1986.